The synthesis of pyrimidine ketoamide molecules as EGFR inhibitors for cancer treatment.

Gciniwe Sindiswa Mathenjwa

A dissertation submitted to the Faculty of Science, University of the Witwatersrand, Johannesburg, in fulfilment of the requirements for the Degree of Master of Science

Supervisor: Dr Moira L. Bode

Co-supervisor: Dr Allan M. Prior

20 February 18

Declaration

I declare that the work presented in this thesis was carried out exclusively by me under the supervision of Dr M.L. Bode and Dr A.M. Prior. It is being submitted for the degree of Master of Science in the University of the Witwatersrand, Johannesburg. It has not been submitted before for any degree or examination in any other University.

_____

Gciniwe Sindiswa Mathenjwa

20 February 2018

TABLE OF CONTENTS

ABSTRACT

The epidermal growth factor receptor (EGFR) is a major tyrosine kinase that is responsible for cell growth, differentiation and proliferation in human bodies. EGFR overexpression has been detected in various cancer cell lines. Hence, EGFR has been validated as a potential target for anti-cancer treatment. Monoclonal antibodies (MAbs) and tyrosine kinase inhibitors (TKIs) have been developed for EGFR inhibition. EGFR-TKIs have been found to be the most promising inhibitors, and hence there have been major research efforts towards their development. Gefitinib and erlotinib are first generation reversible EGFR-TKIs, but their main drawback is the development of drug resistance due to the T790M mutation. Afatinib is a second generation covalent irreversible EGFR-TKI that is active against the T790M mutant, however, it has a narrow therapeutic window that introduces severe side effects. Recently, covalent reversible EGFR-TKIs have been developed using various strategies: the use of the cyanoacrylate group as the active warhead is one strategy that is currently under development.

In this project we aimed to synthesise anilino-pyrimidine ketoamides and ketoesters as a novel series of covalent reversible EGFR-TKIs. In the first part of this project eight anilino-pyrimidine ketoamides were synthesised. Starting from 4,6-dichloropyrimidine a nucleophilic displacement of one chloro group was performed using monoprotected diethylene glycol yielding 4-chloro-6-{2-[2-(tetrahydro-2*H*-pyran-2-yloxy)ethoxy]ethoxy}pyrimidine. As a key step, an acid catalysed amination reaction was used to couple the functionalised pyrimidine with eight different aniline substrates. Using 3-bromoaniline as an example, this reaction yielded 2-{2-[4-(3-bromophenylamino)pyrimidin-6-yloxy]ethoxy}ethanol as an intermediate. After successful synthesis of the key intermediate, the hydroxy group was oxidised using 2-iodoxybenzoic acid (IBX) to afford 2-{2-[4-(3-bromophenylamino)pyrimidin-6-yloxy]ethoxy}acetaldehyde. The Passerini reaction was then used to convert the aldehyde to an α-hydroxy amide functionality, thereby forming 2-hydroxy-*N*-isopropyl-3-{2-[4-(3-bromophenylamino)pyrimidin-6-yloxy]ethoxy}propanamide. Finally, the α-hydroxy amide system was oxidised using IBX to afford the desired α-ketoamide system, thereby completing the synthesis of 2-hydroxy-*N*-isopropyl-3-{2-[4-(3-bromophenylamino)pyrimidin-6-yloxy]ethoxy}propanamide and seven analogues.

In the second part of this project, a similar synthetic approach was utilised in an attempt to synthesise anilino-pyrimidine ketoesters. Starting from 2-{2-[4-(3-bromophenylamino)pyrimidin-6-yloxy]ethoxy}acetaldehyde; potassium cyanide was used to prepare 2-hydroxy-3-{2-[4-(3-bromophenylamino)pyrimidin-6-yloxy]ethoxy}propanenitrile. Functional group conversion from the cyanohydrin to α-hydroxy ester was attempted using

methanol in an acidic medium but, unfortunately, an unexpected product was obtained. Instead of affording an α-hydroxy ester system, from this reaction we isolated an acetal of the original aldehyde. Unfortunately, the unsuccessful attempt to synthesise methyl-3-{2-[4-(3-bromophenylamino)pyrimidin-6-yloxy]ethoxy}-2-hydroxypropanoate prevented further progress towards the synthesis of the targeted methyl-3-{2-[4-(3-bromophenylamino)pyrimidin-6-yloxy]ethoxy}-2-oxopropanoate.

A selection of the anilino-pyrimidine analogues were screened for anticancer activity in an *in vitro* MTT assay using five different cell lines. From the preliminary results, 2-{2-[4-(3-chloro-4-fluorophenylamino)pyrimidin-6-yloxy]ethoxy}acetaldehyde was the only active compound with an IC_{50} = 48.74 μM against the MCF7 breast cancer cell line and an IC_{50} = 30.75 μM against the SF268 glioblastoma cell line.

ACKNOWLEDGEMENTS

Throughout the two years of this project, I have been made aware of the ups and downs of scientific research. It's been a learning curve, but here I am at the "end" and there are a number of people to extend my gratitude to.

First and foremost, I would like to thank my supervisors, Dr Allan Prior and Dr Moira Bode for their endless advice, encouragement, guidance, support, patience and willingness to help throughout the course of this project.

I would also like to thank Dr Amanda Rousseau for her advice, support and encouragement; especially during the last months of this project.

To Prof Charles de Koning and Prof Jo Michael, thank you for the useful remarks and suggestions during the group presentations.

I also wish to thank Dr Izak Kotze and Mr Hendrik Henning for running the NMR spectra. My gratitude also goes to Miss Refilwe Moepya and Mr Thapelo Mbhele for their generous time performing the HRMS analysis.

Thank you to Dr Leone Harmse for conducting the anticancer screening.

To the WITS Organic Research group, thank you for making my experience in the organic research lab fun. Thank you for your assistance and intellectual contribution.

Thank you to the National Research Fund and the WITS Post Graduate Merit Award for funding; and thank you to the University of the Witwatersrand for providing the facilities to do my research.

To my friends thank you for brightening up my days when everything seemed to fall apart.

With love, this goes out to my source of strength, the reason why I keep pressing on, a huge appreciation to my family. Your prayers are what sustained me thus far. I cannot express how much your presence keeps me going, thank you!

A special love-filled thank you goes out to my shining star, Nkanyezi. You would not know it, but it is you who made it possible.

Last but not least, all glory to The Lord Jesus Christ for giving me the strength to endure not escape…"not by might nor by power, but by my Spirit," says the LORD Almighty.

LIST OF ABBREVIATIONS

ATP adenosine triphosphate

BINAP 2,2'-bis(diphenylphosphino)-1,1'-binaphthyl

cat. catalytic

d days

DCM dichloromethane

DMF *N*,*N*-dimethylformamide

DMSO dimethyl sulfoxide

EtOAc ethyl acetate

ERBB erythroblastosis oncogene B

FDA food and drug administration

h hour(s)

HER human epidermal growth factor receptor

Hex hexane

HRMS High resolution mass spectroscopy

Hz hertz, s^{-1}

IC_{50} 50% inhibitory concentration

IR infrared

KHMDS potassium bis(trimethylsilyl)amide

MCR multicomponent coupling reaction

MeOH methanol

min. minutes

m.p. melting point

MS mass spectroscopy

m/z	mass to charge ratio
NMR	nuclear magnetic resonance
ppm	parts per million
R_f	retardation factor
r.t.	room temperature
TLC	thin layer chromatography
WHO	world health organization

CHAPTER 1: Epidermal Growth Factor Receptor in Non-Small Cell Lung Cancer

1.1. Introduction

Enzymes are macromolecular catalysts for biochemical reactions. Enzymes regulate most of the biological processes that occur within living organisms. Most enzymes are proteins, although a few are catalytic RNA molecules.[1]

Kinases are enzymes that belong to the transferase class; these enzymes are responsible for a reversible covalent process in cells known as phosphorylation.[2] This process is a transfer of phosphate groups from phosphate donating molecules such as adenosine triphosphate (ATP) to individual substrates.[2] There are three types of substrates that kinases can act upon: protein substrates, carbohydrate substrates and lipid substrates; and they are classified depending on their specific substrates.[2] Protein kinases phosphorylate proteins on their histidine, tyrosine, threonine or serine amino acids. Protein kinases often act on more than one amino acid and the amino acid substrates can regulate activity for more than one kinase.[2] Hence, protein kinases are classified into two broad classes depending on what controls their activity: serine-threonine protein kinases and tyrosine-specific protein kinases.[2]

Tyrosine kinases (TKs) are one of the most important kinase families as regards to cancer biology.[3] There are 90 distinct tyrosine kinases found in humans, which have been broadly classified into 58 receptor tyrosine kinases (RTKs) and 32 non-receptor tyrosine kinases (NRTKs).[3] The main difference between RTKs and NRTKs is in their structural domain organisation. RTKs exist on the cell membrane as part of the cell surface while NRTKs are cytoplasmic enzymes, meaning that they are located inside the cell. The RTK structural domain is made up of two subdomains; the N-terminal and C-terminal subdomain. These two subdomains make up three regions of RTKs; the extracellular region, the transmembrane region and the intracellular region (Figure 1.1).[22] As suggested by the group name, NRTKs don't have receptor-like features and they lack the extracellular and the transmembrane regions. NRTKs are said to be intracellular since they are restricted to the cytoplasm (intracellular region) and don't have direct interaction with extracellular ligands.[2] Previous studies have demonstrated strong evidence regarding the involvement of TKs in cancer. Previous results have demonstrated an intimate relationship between abnormal cell signal transduction of the TKs and the initiation and progression of a variety of human cancers.[2,3,4] Hence, RTKs and NRTKs both present themselves as potential drug targets for the treatment of certain cancer types. Intensive research has focused on the development of

RTK inhibitors for cancer treatment, mainly because the evidence linking these receptors with certain types of human cancers is the most substantial.[2]

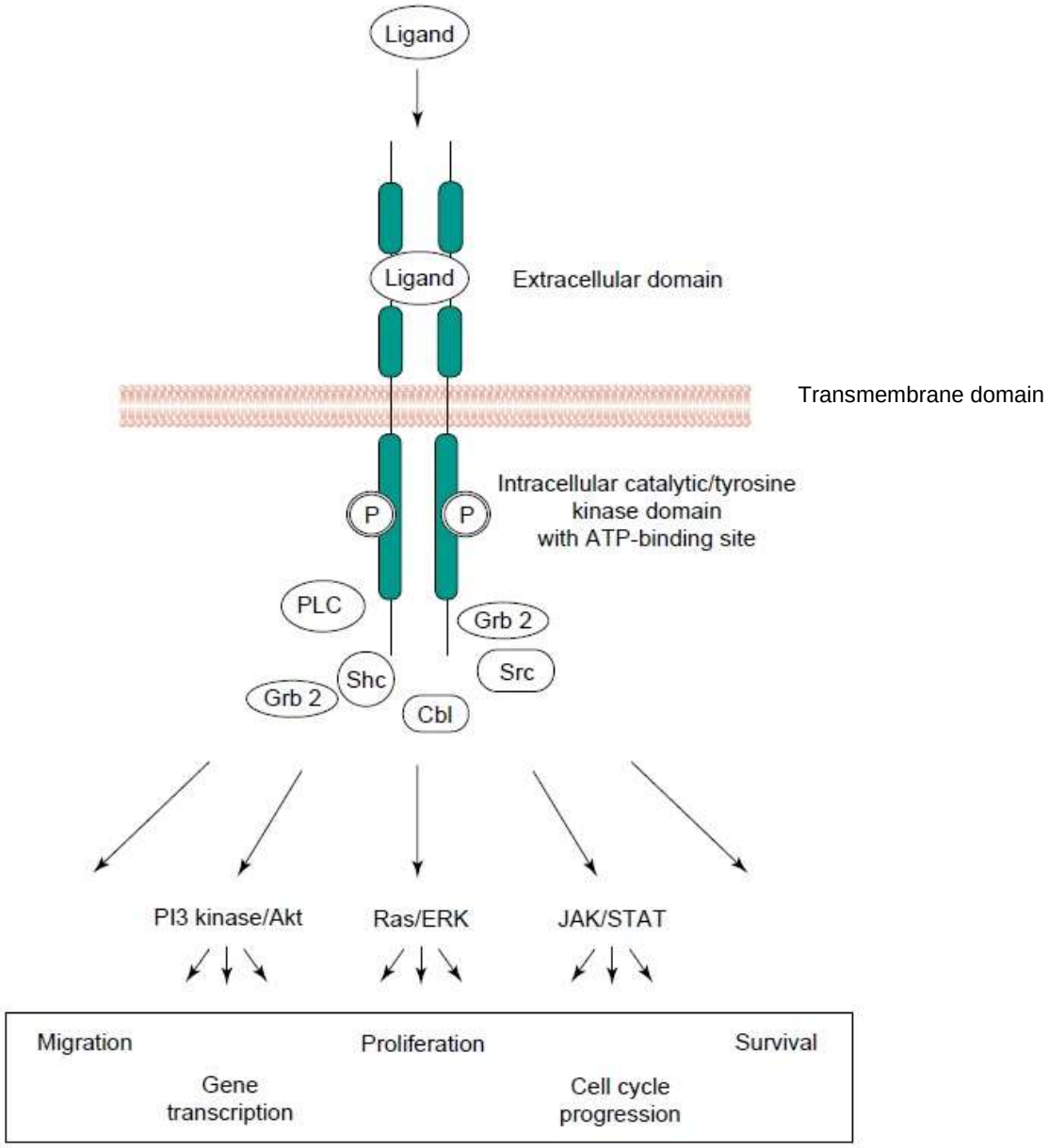

Figure 1.1: Structural domains of RTKs. Shown are the extracellular ligand binding domain, the transmembrane domain and the intracellular tyrosine kinase domain. The signalling pathways that are activated upon specific ligand binding are also indicated. Abbreviations: ERK: extracellular-regulated kinase; JAK: janus kinase; P: phosphorylated tyrosine residue; PI3 kinase: phosphatidylinositol-3 kinase; Grb 2: Growth factor receptor bound protein2; Src: rous sarcoma oncogene cellular homolog; Shc: SH2-containing collagen-related proteins; PLC: phospholipase C; STAT: signal transducer and activator of transcription .[22]

RTKs are cell-surface transmembrane receptors which have been widely studied, mainly because of their particular significance to cancer. The 58 RTKs have been classified into 20 subfamilies.[3,22] Platelet-derived growth factor (PDGFR), fibroblast growth factor receptor (FGFR), epidermal growth factor receptor (EGFR) and insulin receptor families are some of the 20 RTK subfamilies.[2] These receptors mediate critical functions in signal transduction processes, transducing signals from various ligands of the extracellular environment to different intracellular signalling pathways.[3,15] Epidermal growth factor (EGF), fibroblast growth factor (FGF), nerve growth factor (NGF) and vascular endothelial growth factor (VEGF) are some examples of the extracellular ligands that bind to the receptors.[2,3,12,15] The biological processes facilitated by RTKs include: cell proliferation, differentiation, migration, metabolism and apoptosis.[15] Extensive understanding of all parts of the signal transduction process is critical, mainly because it gives better understanding of the cause of cancer and its potential treatments.

The first RTK subfamily to be associated with cancer was the EGFR/ERBB family.[3] The EGFR/ERBB subfamily consists of four closely related RTKs, which include EGFR (ERBB1), HER2 (ERBB2), HER3 (ERBB3), and HER4 (ERBB4).[3,8] Although these RTKs have a similar basic structure they each have distinct properties, including the difference observed in their tyrosine kinase activity. EGFR is a 53 amino acid-containing RTK that acts primarily as a growth factor receptor and in downstream signalling from growth factor activation. As is the case for most RTKs, EGFR is a transmembrane protein that is activated by the binding of its specific growth factor ligand. EGFR inactive monomer consists of the extracellular ligand binding domain, the single transmembrane portion and the intracellular tyrosine kinase domain that resides within the cytoplasm and regulates signalling pathways to control cellular proliferation.[8]

Upon binding to the EGF ligand, EGFR transitions from an inactive monomer to an active homodimer or heterodimer with other EGFR/ERBB family members. As a result, autophosphorylation of the intracellular tyrosine domain occurs initiating several signal transduction pathways (Figure 1.1). The major pathways include the Ras-Raf-mitogen activated protein kinase (Ras-Ref-MEPK-ERK) pathway which controls cell growth, proliferation, apoptosis and cell survival; the phosphatidylinositol-3-kinase (PI3K/AKT) pathway which stimulates cell proliferation and growth and inhibition of apoptosis; and the janus kinase (JAK-STAT) pathway which induces gene transcription and protein translation.[2,3,8,22] In normal cells, activation of the EGFR signaling pathways is under regulated physiological control; however, irregular activation of these pathways can lead to uncontrollable cell growth, which leads to cancer.[3,8]

Irregular activation of EGFR can be a result of mutational activation of the receptor or receptor/ligand overexpression. As a result of the irregular EGFR activation, strongly enhanced signaling capacity of the kinase is observed which then leads to malignant transformation. This dysregulation has been observed in 43-89% of non-small cell lung cancer cases.[3,4,8] Since this discovery extensive research has focused on designing therapeutic strategies to inhibit EGFR. One such method is the use of epidermal growth factor receptor tyrosine kinase inhibitors (EGFR-TKIs). EGFR-TKIs are low molecular weight drugs that bind to the ATP binding site, thus inhibiting EGFR tyrosine phosphorylation and in turn inhibiting lung cancer.[15]

1.2. Lung cancer

Lung cancer is one of the deadliest types of cancer for both men and women worldwide. According to the WHO cancer fact sheet, in 2015 lung cancer was the most common cause of cancer deaths worldwide. Lung cancer was responsible for 1.7 million of the 8.8 million observed cancer deaths.[10] About 80% of lung cancer deaths are caused by tobacco smoking.[6,7,10] Although tobacco smoking is the major risk factor for lung cancer, not all smokers get lung cancer and not all lung cancer deaths are due to tobacco smoking. Other risk factors include passive smoking, ultraviolet and ionizing radiation, and chemical carcinogens such as asbestos and arsenic.[7]

The two types of primary lung cancer are the less common small-cell lung cancer (SCLC) and the most common non-small-cell lung cancer (NSCLC) which is made up of three subtypes; squamous cell carcinoma, adenocarcinoma and large-cell carcinoma. The major differences between the two types of lung cancer are in their biology, therapeutic approaches and outcomes. SCLC accounts for about 15% of the reported lung cancer cases and of all cancer patients, patients with SCLC express the most malignancy.[32] This type of lung cancer is broadly divided into two groups; the classic and the variant type. The variant subtype expresses poor chemotherapy response as compared to the classic subtype, hence it has shorter survival time.[28] SCLC generally spreads to other organs quicker than NSCLC. Additionally, the growth fraction and cell replication time of SCLC is much more rapid than that of NSCLC.[30]

NSCLC accounts for about 85% of the lung cancer cases diagnosed every year.[9] Studies of NSCLC cell lines have detected the overexpression of EGFR in 43-89% cases.[4,8] During a study of the *in vitro* biological behaviour of the NSCLC, a high concentration of EGFR was detected on the cell surfaces of the NSCLC cell lines.[4] The observed overexpression of EGFR in NSCLC suggested EGFR as a novel potential target for lung cancer treatment. As

previously stated, this observation then led to the development of EGFR-TKIs, amongst other cancer therapeutics, as potential drugs for the treatment of NSCLC.

1.3. EGFR as a drug target for NSCLC treatment

EGFR overexpression or deregulation in NSCLC has prompted the development of EGFR inhibitors for NSCLC treatment. Like any other RTK, EGFR can be viewed as a multisite drug target. The extracellular ligand binding domain, intracellular tyrosine kinase domain and the transmembrane domain have all been identified as potential targets for drug development, and they have been investigated in a number of experimental studies.[15,22] Monoclonal antibodies, small organic molecules, antisense oligonucleotides, and peptidomimetics are some of the strategies that have been explored for kinase inhibition.[3,15,22] Monoclonal antibodies and small organic molecules are two main approaches that have been used for cancer therapeutics.[3,16]

Monoclonal antibodies are employed for EGFR inhibition by targeting the extracellular domain, blocking ligand binding and/or receptor activation which consequently obstructs EGF dependent cell proliferation. Several EGFR antibodies have advanced in clinical studies and cetuximab is one of the FDA approved drugs.[3] Cetuximab directly binds to EGFR with high affinity and therefore blocks ligand-induced EGFR autophosphorylation. Cetuximab was approved by the FDA for the treatment of colorectal cancer and head and neck cancer.[3,16] Cetuximab has also been used in combination with other chemotherapeutic treatments against advanced NSCLC and increased anti-tumour effects were observed.[16] Despite the effectiveness observed with the use of cetuximab, a number of factors have been observed that make its development and use troublesome. Monoclonal antibodies such as cetuximab require relatively costly complex processes for their production while small organic molecules are produced by simpler organic synthesis methods. Furthermore, monoclonal antibodies are intravenously administered which is a more difficult administration process as compared to the orally available small organic molecules.[16] One particularly promising approach is the use of small organic molecules which are ATP-competitive inhibitors.

ATP-competitive EGFR-TKIs bind to the ATP binding site which is situated on the intracellular domain of EGFR and compete with ATP for binding. This attenuates the cell signalling pathway that would normally induce tumour cell proliferation and division. All of the currently used EGFR-TKIs are ATP-competitive inhibitors, meaning that they interfere with the intracellular EGFR kinase domain. Quinazolines, pyridopyrimidines and pyrrolopyrimidines are some of the most promising EGFR-TKIs. In addition to the already mentioned advantages of using small organic molecules, one hypothesised advantage of ATP-competitive EGFR-TKIs was the development of highly selective inhibitors; the high

selectivity was hypothesised to be due to the highly conserved ATP-binding site.[3] The ATP-binding site has been identified as a promising target for NSCLC treatment and this has been confirmed by the advanced widespread use of several ATP-competitive EGFR-TKIs. Gefitinib, erlotinib and afatinib are some examples of the ATP-competitive FDA approved EGFR-TKIs that are currently on the market for the treatment of NSCLC and these will be discussed in detail in subsequent sections.[23]

1.3.1. The ATP binding site

The ATP binding site is conserved within the intracellular tyrosine kinase domain (Figure 1.1). The structural features of the ATP binding cleft include the adenine region, the sugar region, the hydrophobic channel and the phosphate binding region (Figure 1.2).[3,15]

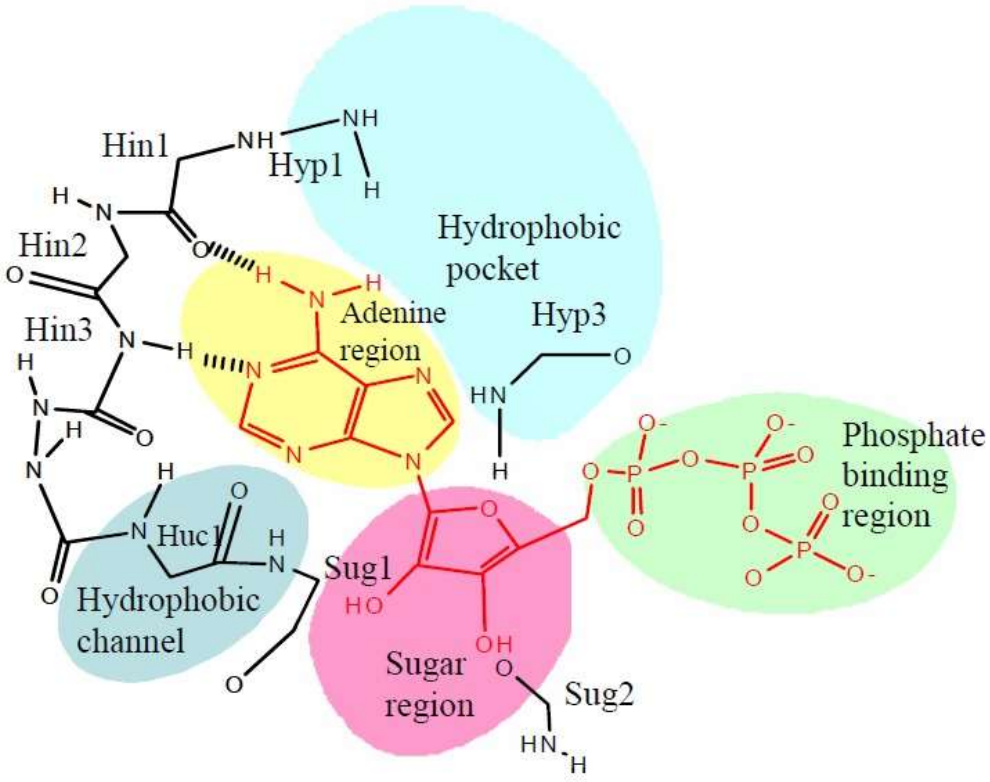

Figure 1.2: Overview of the ATP binding site of protein kinases.[15] The protein is shown in black and the ATP molecule is shown in red.

As seen in Figure 1.2, ATP has various interactions with the different regions of its binding pocket. The adenine region interacts with the backbone amides in the hinge region (NH and C=O functionalities) via hydrogen bonding. These hydrogen bond interactions have been observed as being the most important interactions as regards to the binding of ATP competitive inhibitors.[3,15] Directly attached to the adenine region is the sugar region and

although this region is not significantly used by ATP it does play a crucial role in inhibitor selectivity.[15] The phosphate binding region is also not particularly significant for ATP binding, but it can be used to improve inhibitor selectivity.[15] The last important structural region observed in the ATP binding cleft is the hydrophobic pocket. When ATP is bound to the active site, the hydrophobic region is blocked off. At the entrance of the hydrophobic pocket lies a gatekeeper residue. The gatekeeper residue is situated on the N-terminal side of the linker region, controlling access to the hydrophobic pocket.[3,34] The gatekeeper residue is the threonine 790 amino acid and its side chain is important in drug design as it helps with the specificity of the kinase towards inhibitors.[3,34]

1.3.2. First generation EGFR-TKIs

1.3.2.1. Erlotinib and gefitinib

First generation EGFR-TKIs are low molecular weight quinazoline derivatives that selectively and reversibly bind in the ATP binding pocket, competing with ATP (Figure 1.3).[18] These orally administered drugs have been shown to be effective against both the wild-type and some mutant EGFR.[23]

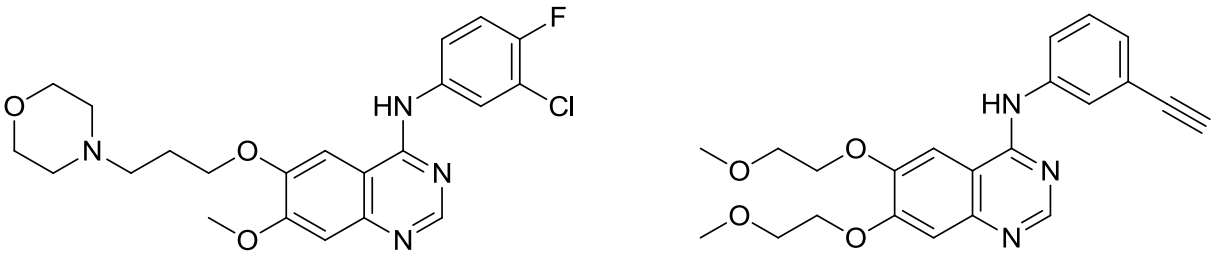

1. Gefitnib (Iressa) **2. Erlotinib (Tarceva)**

Figure 1.3: Chemical structures of the anilino-quinazoline based first generation EGFR-TKIs used for the treatment of NSCLC.

Upon successful binding of these drugs in the ATP pocket, autophosphorylation of EGFR is inhibited, which in turn inhibits the activation of the downstream signalling pathways of EGFR hence inhibiting the replication of malignant cells resulting in apoptosis.

During phase II clinical trials, both gefitinib (**1**) and erlotinib (**2**) showed antitumour activity.[23,24] Gefitinib was initially approved in May 2003 as monotherapy for locally advanced and metastatic NSCLC. After the approval, the FDA then requested post marketing studies to investigate the efficacy of gefitinib.[25] At that time, docetaxel was FDA approved as second-line treatment of advanced NSCLC for chemo-naïve patients. A study that evaluated the efficacy of gefitinib against docetaxel indicated that there was no significant difference in the survival benefit between the two drugs.[25,27] Results from another study that evaluated

gefitinib survival in lung cancer (ISEL) indicated that the drug showed no significant increase in the overall survival when compared to placebo.[26] Based on the ISEL trial results, in June 2005 the FDA approval was amended, limiting gefitinib distribution and application to patients who were currently benefiting, or had benefited from gefitinib monotherapy.[25]

Erlotinib was approved by the FDA in November 2004 as monotherapy for second or third-line treatment of chemotherapy resistant advanced NSCLC.[18] Phase I trial studies had recommended a daily dose of 150 mg/d on a continuous uninterrupted program.[31] To investigate whether erlotinib prolonged overall survival, a phase III clinical trial study was conducted that evaluated the recommended 150 mg/d dose of erlotinib against placebo in chemotherapy resistant NSCLC. The obtained results indicated that erlotinib increased the overall survival by 2 months; it was 6.7 months for the erlotinib group and 4.7 months for the placebo group.[28] Additionally, it was observed that patients with EGFR positive tumour cells had a higher rate of response.[28,31] Also, this trial study indicated superiority for erlotinib as compared to the results obtained for gefitinib in a similar study.[26,28] However, this might not directly mean that erlotinib is superior to gefitinib, it could possibly be an effect of different characteristics between the patients in the two trial studies.

Subsequent studies then reported that NSCLC patients with somatic EGFR mutations showed increased clinical response as compared to the wild-type EGFR when treated with both erlotinib and gefitinib.[18,24] Further studies then reported an interesting aspect that tumours with EGFR-activating mutations completely relied on EGFR for the activation of the downstream signalling pathways which regulates their survival.[8,23] This then meant that EGFR inhibition would result in apoptosis of the cancer cells. The most commonly observed EGFR mutations are the exon 19 deletion and the L858R point mutation.[23,24] The implications of the increased clinical response of EGFR-mutant NSCLC patients and the increased knowledge about EGFR mutations in NSCLC patients allowed for further developments in the use EGFR-TKIs for NSCLC treatment.[25]

New trial studies were done targeting NSCLC patients with somatic EGFR mutations. A phase III multicentre, open-label, randomised trial was done investigating the efficacy of erlotinib against platinum based chemotherapy in EGFR-mutant patients. The results indicated superiority for erlotinib as regards to the progression free survival; it was 9.7 months for the erlotinib treated patients and 5.2 months for the chemotherapy based patients.[23,33] The overall survival was 19.3 months for the erlotinib group and 19.5 months for the chemotherapy group, showing that no significant difference was observed. Based on this trial study, erlotinib was then FDA-approved in May 2013 as first-line treatment for EGFR-mutated NSCLC patients.[33] A similar phase III trial study was conducted for gefitinib and it

was then reapproved by the FDA in July 2015.[23,25] Gefitinib indicated increased progression free survival when compared to chemotherapy during the treatment of EGFR-mutated NSCLC patients, providing an additional first-line treatment option for this group of patients.[25] Despite the observed clinical activity of erlotinib and gefitinib, over time patients acquired resistance towards these drugs hence making them ineffective. The acquired resistance was normally observed after a median of 14 months.[23] For further developments in search for more effective NSCLC treatments a better understanding behind the observed resistance was required.

1.3.2.2. The binding mode of the first generation EGFR-TKIs

Erlotinib and gefitinib both have similar binding modes in the ATP binding pocket.[49] From Figure 1.3 it is important to note that the quinazoline core of the inhibitors mimics the adenine functionality of the natural ATP substrate. Thus, as the adenine ring forms hydrogen bonds with the back bone amides in the hinge region (Figure 1.2), the same interactions are observed between the quinazoline core of gefitinib and the main amide chain of M793 in the hinge region (Figure 1.4).[49]

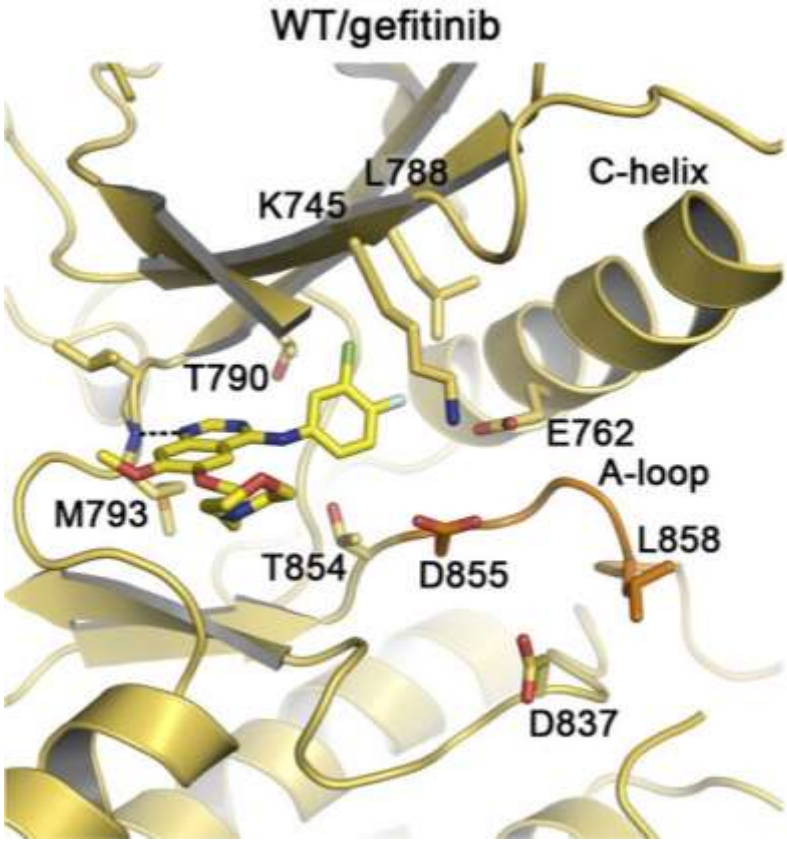

Figure 1.4: Gefitinib binding mode in ATP binding pocket of the wild type EGFR.[49]

One other important interaction between the inhibitor and the active site is that of the aniline moiety. As can be seen in Figure 1.4 the 3-chloro-4-fluoro aniline probes the hydrophobic pocket of the active site. Successful probing of the hydrophobic pocket is only possible when the amino acid side chain is small, for example threonine (T790 in this case), as this results in effective binding while a bulky methionine group would induce steric hindrance.[24,49]

1.3.2.3. Mechanism of acquired resistance to erlotinib and gefitinib

Of the multiple identified mechanisms that result in the observed erlotinib and gefitinib resistance, most mechanisms have been identified to be secondary mutations.[34] The T790M mutation is one of the most commonly identified secondary mutations that results in the ineffectiveness of the first generation EGFR-TKIs.[23] About 50-60% of tumours in patients that developed resistance to erlotinib and gefitinib were found to have the T790M mutation.[23]

Threonine 790 is an amino acid commonly known as the gatekeeper residue. It resides in the hydrophobic pocket of the ATP binding site and it has been thought of as a determinant of the specificity of ATP-competitive EGFR-TKIs.[3,34] The T790M mutation is a result of the substitution of the threonine amino acid by the bulky methionine amino acid. The bulky methionine was hypothesised to inhibit the activity of erlotinib and gefitinib by sterically hindering their binding into the ATP hydrophobic pocket.[24] The T790M mutation was shown to increase the affinity of EGFR to natural ATP, resulting in the loss of efficacy of the first generation drugs as they compete with ATP. Although the exact mechanism by which the T790M mutation results in the observed resistance is not fully understood, the inhibition through steric hindrance hypothesis doesn't quite make sense as structurally similar irreversible EGFR-TKIs remain active *in vitro* even when the T790M mutation is observed. It is thought that the irreversible EGFR-TKIs retain their anti-cancer activity through covalently binding in the ATP pocket. The covalent binding eliminates the competition of existing in reverse equilibrium with the natural ATP substrate, hence they remain active.[23,24] This class of irreversible inhibitors is known as the second generation EGFR-TKIs.

1.3.3. The way forward: second generation EGFR-TKIs

The next approach was to develop EGFR inhibitors that would exhibit activity against multiple targets and form irreversible covalent bonds with the targeted active site.[35] Second generation EGFR-TKIs are also anilino-quinazoline or quinolone derivatives like erlotinib and gefitinib. Chemical modification of erlotinib and gefitinib offered new drug discovery possibilities, the presence of a Michael acceptor in the second generation drugs allowed for the formation of an irreversible covalent bond in the active site. Various second generation drugs have been developed over the past years, but Afatinib (**3**, Figure 1.5) remains the most promising drug.[9] With the exception of the formation of a covalent bond, the binding

mode interactions between afatinib and the active site are similar to the ones observed for gefitinib.[34]

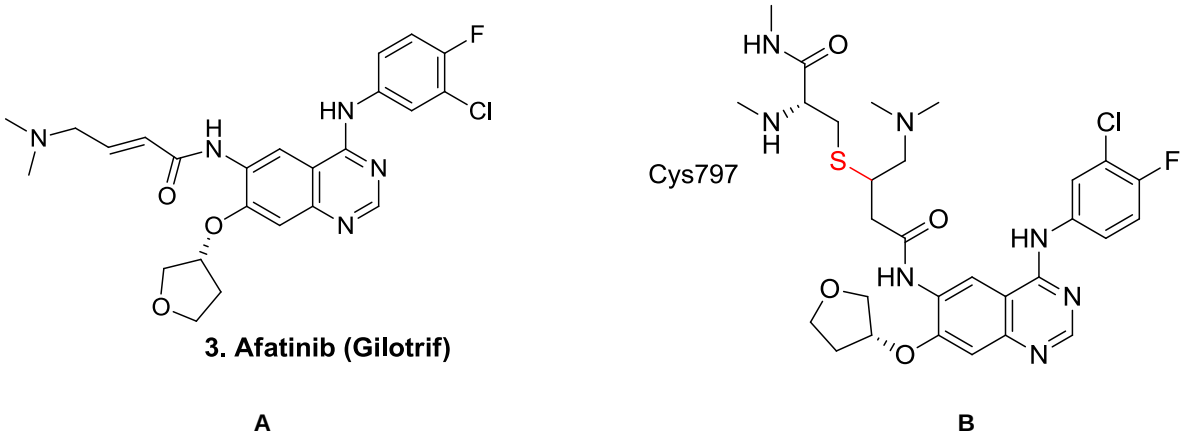

Figure 1.5: A. Chemical structure of the anilino-quinazoline based second generation EGFR-TKI, Afatinib, used for the treatment of NSCLC. **B.** The main covalent bond interaction (highlighted in red), between afatinib and the Cys797 residue in the ATP binding pocket of EGFR.[38]

The most prominent structural difference observed between the first generation EGFR-TKIs and afatinib is the presence of the reactive acrylamide group in afatinib (Figure 1.5A). The acrylamide functionality (Michael acceptor) allows for the formation of a covalent bond with the cysteine residue (Figure 1.5B). Afatinib is a dual EGFR/HER2 inhibitor that selectively, irreversibly and covalently binds to the Cys797 residue in the tyrosine kinase catalytic domain hence inhibiting its activity.[35,38] Since afatinib forms irreversible covalent bonds in the ATP binding site this allows for longer inhibition time of the EGFR tyrosine activity: afatinib completely inhibits EGFR until new receptors are synthesised.[35]

Initially, afatinib was considered as a potential candidate to overcome the T790M mutation since it had been confirmed to be a more potent inhibitor of mutant T790M EGFR *in vitro* than the first generation EGFR-TKIs.[9,23] Clinical studies revealed that afatinib was equally potent against the wild type and mutant T790M EGFR, and it was reported that there was significant inhibition observed with this drug towards the mutant T790M EGFR.[38] Toxicity was reported to be the main limitation of effective inhibition.[38] The recommended afatinib dosage for the inhibition of the wild type EGFR wasn't effective against the mutant T790M EGFR, the main drawback was that higher dosages were associated with side effects.[37,38] The most commonly observed side effects were gastrointestinal e.g. diarrhoea and vomiting; and cutaneous e.g. acne and rash.[9,23,38] Other second generation EGFR-TKIs include, dacomitinib, neratinib, carnetinib and pelitinib.[38] However, the main drawback of all the second generation drugs is that they contain the very reactive acrylamide functionality, which was believed to come with the toxicity burden. Hence new developments were still required

to find molecules that enhanced activity while limiting the observed toxicities.[38] Essentially the ideal drug would have to inhibit the mutant T790M EGFR and the wild type EGFR without severe toxicities.

1.3.4. Overcoming toxicity limitations: third generation EGFR-TKIs

Recently a new class of EGFR-TKIs has been under investigation and most compounds from this class are currently under clinical development. Like the second generation EGFR-TKIs, the third generation EGFR-TKIs bind covalently in the ATP binding pocket of EGFR. Research has shown that covalent binding of the tyrosine kinase inhibitors to the EGFR is required in order to overcome the observed T790M gatekeeper mutation, hence the third generation EGFR-TKIs still contain the Michael acceptor functionality which allows for the covalent binding of the Cys797 residue.[38] Interestingly, however, the third generation EGFR-TKIs seem to selectively inhibit the mutant T790M EGFR, while having much less activity against the wild type EGFR.[38] Since this generation of small molecule inhibitors have very low inhibitory effect against the wild type EGFR, that eliminates the toxicity limitation observed with the second generation EGFR-TKIs.[38,39]

Third generation EGFR-TKIs are orally available amino pyrimidine based derivatives (Figure 1.6). Several members of this class of EGFR-TKIs have been developed, but most of them have not yet progressed to clinical trials. Osimertinib (**4**), olmutinib (**5**) and rociletinib (**6**) are a few molecules that have been extensively studied and have even progressed to clinical trials.[38,39] WZ4002 (**7**) is one other small molecule inhibitor that has been widely studied although it hasn't progressed to human clinical trials.[39]

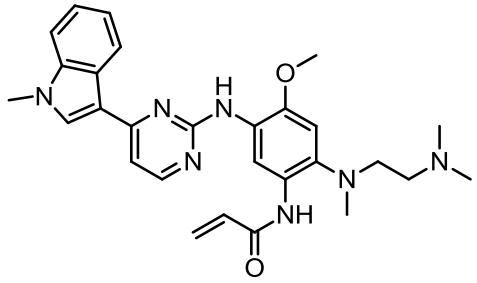

4. Osimertinib

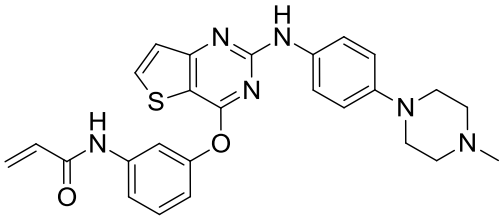

5. Olmutinib

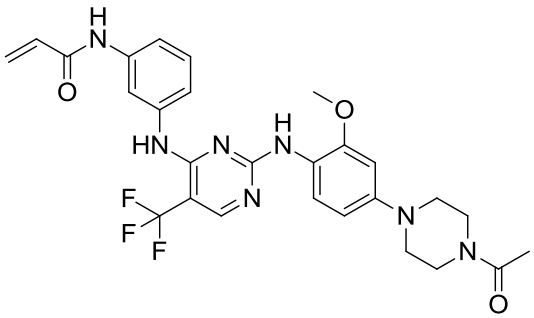

6. Rociletinib

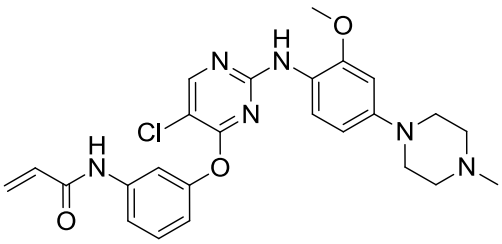

7. WZ4002

Figure 1.6: Chemical structures of the amino pyrimidine based third generation EGFR-TKIs. Osimertinib (**4**) is the only FDA approved molecule for the treatment of NSCLC patients with mutant T790M EGFR.[40]

1.3.4.1. Osimertinib

Osimertinib (**4**) is an orally available mono-anilino pyrimidine third generation EGFR-TKI. Osimertinib forms an irreversible covalent bond with the Cys797 residue in the ATP binding pocket.[40] Unlike the second generation EGFR-TKIs, osimertinib only selectively inhibits the mutant positive EGFR, having very low activity towards the wild type EGFR.[39,40] Osimertinib is characterized by the pyrimidine scaffold, different from the first and second generation quinazoline scaffold, thus it takes a different orientation in the active site.[52] Unlike the second generation EGFR-TKIs, osimertinib doesn't need to be inside the back hydrophobic pocket for effective inhibition (Figure 1.7). That is, the bulky methionine amino acid chain that is a result of the T790M mutation doesn't affect its activity.[38]

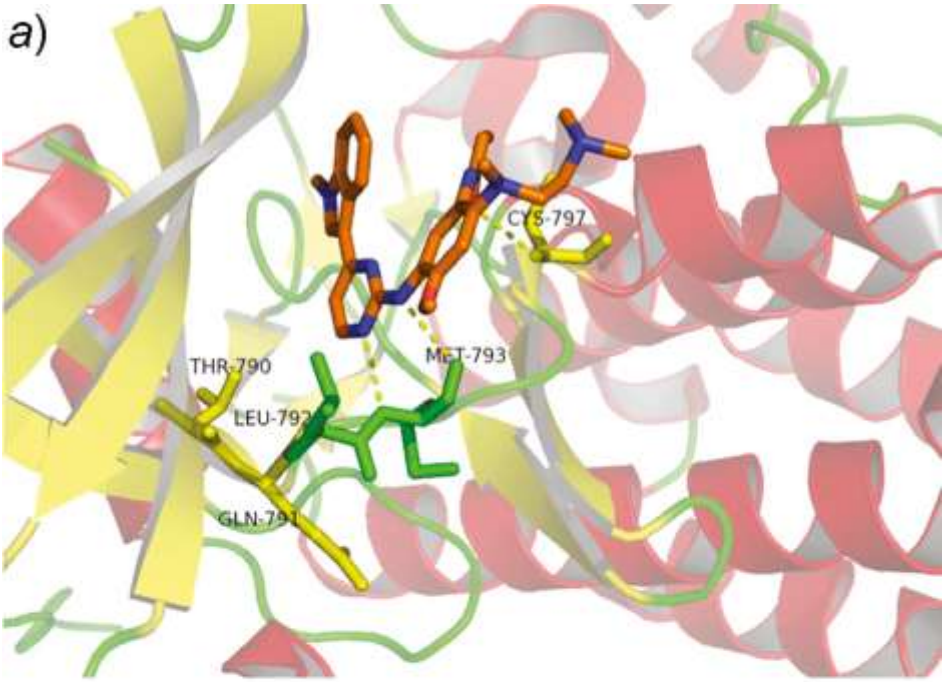

Figure 1.7: Osimertinib (**4**) binding mode in ATP binding pocket of EGFR.[38]

From Figure 1.7 above it is important to note the different binding mode of osimertinib as compared to the explained binding mode of the first and second generation drugs. In the binding mode of first and second generation drugs, the aniline moiety binds into the back hydrophobic pocket of the ATP binding site and the gatekeeper residue has been shown to have an effect on the observed resistance of mostly the first generation drugs.[24] However, osimertinib is observed to lack that aniline moiety that needs to probe the hydrophobic pocket. Instead it has an indole group that lies adjacent to the gatekeeper residue (THR-790).[38] Hence, even when the threonine is substituted with the bulky methionine as a result of the T790M mutation the activity of osimertinib is retained.

In November 2015 osimertinib was FDA approved for the treatment of metastatic NSCLC in patients with mutant T790M EGFR after failure of either the first or the second generation EGFR-TKIs.[39] Several pre-clinical trials were conducted that demonstrated effective activity and safety of osimertinib both *in vitro* and *in vivo* and these findings led to the approval of osimertinib.

During phase I studies in NSCLC patients with mutation positive EGFR, no dose limiting toxicities were observed. The most commonly observed toxicities were diarrhoea, nausea and rash.[40] At high dose levels between 160 and 240 mg/d the observed toxicities became more severe and frequent; this was thought to be as a result of the inhibition of the wild type EGFR at such high doses.[40] As a result, a recommended daily dose of 80 mg was adopted.[40] The observed response rate and progression free survival was superior for the EGFR

mutant positive patients as compared to the mutant negative patients. The response rate was 67% for mutant positive patients, and for mutant negative patients the response rate was as low as 21%.[39,40] Furthermore, the progression free survival was longer for mutant positive patients (9.6 months) as compared to the mutation negative patients (2.8 months).[40]

To assess the safety and efficacy of osimertinib, phase II studies were conducted using the recommended daily dose of 80 mg in NSCLC patients with mutant T790M EGFR.[40] Results confirmed that osimertinib provided good clinical efficacy with a good toxicity profile.[41] The observed overall response rate was 66% and the progression free survival was 11 months.[41] Osimertinib is currently undergoing phase III clinical trials. This particular study is investigating the efficacy of osimertinib as a first line treatment for NSCLC patients with either the primary mutations (exon 19 deletion and L858R point mutation) or the secondary acquired T790M mutation. The study also aims to investigate the efficacy of osimertinib as a second line treatment for NSCLC patients with specifically the acquired secondary T790M mutation.[42]

Despite the good clinical efficacy demonstrated by osimertinib for the treatment of NSCLC patients with mutant positive EGFR, acquired resistance develops after an average of 8-10 months of treatment, making the drug ineffective. Among a number of mutations that are thought to result in the observed resistance, the C797S mutation located within the EGFR tyrosine kinase domain was found to be the most prominent mechanism.[39,40]

1.3.4.2. Mechanism of acquired resistance to third generation EGFR-TKIs

As it has been previously noted that the formation of a covalent bond between third generation EGFR-TKIs and the Cys797 residue is required for growth inhibition of NSCLC cells with the T790M mutation, the mutation of this amino acid was considered as a feasible candidate for the observed resistance mutation.[40] The C797S mutation was found to be the most common mechanism leading to the observed resistance of EGFR to third generation inhibitors.[39,40] The C797S mutation is known to be a tertiary substitution mutation where the cysteine in the 797 position is substituted by a serine amino acid, resulting in an impaired target for the covalent bond formation with the third generation EGFR-TKIs, osimertinib to be specific.[39] Hence it hinders the formation of a covalent bond between the drug and the target.

Studies have demonstrated various ways in which the C797S mutation in EGFR harbouring the T790M mutation could potentially be inhibited. Since first generation EGFR-TKIs don't require the formation of a covalent bond with the Cys797 residue for effective inhibition activity, they could subsequently be used to inhibit EGFR in NSCLC patients that have acquired the C797S mutation.[43] To validate this hypothesis, erlotinib was found to be

effective in inhibiting EGFR with the C797S mutation *in vitro*.[43] These results opened new therapeutic strategies, demonstrating that for mutant T790M EGFR cells that have developed the C797S mutation upon treatment, combination or subsequent therapy of first and third generation EGFR-TKIs could be effectively explored.[39] That is because neither the T790M nor the C797S mutation alone would be effective in mediating resistance to the combined therapy of EGFR-TKIs; i.e. osimertinib would inhibit the secondary T790M mutation while erlotinib inhibits the tertiary C797S substitution mutation.[39,43]

Furthermore, studies have discovered an interesting effect of the configuration of the two mutations (the T790M and the C797S) in the tyrosine residue of EGFR to the combination therapy. Studies have shown that the allelic context in which the C797S mutations was developed may predict the efficacy of the EGFR-TKIs.[39,43] When the two mutations are *cis* to each other, then the NSCLC cells become completely resistant to all three generations of EGFR-TKIs and even to combination therapy.[39,43] However, when the mutations are *trans* to each other, then the combination therapy using first and third generation EGFR-TKIs becomes effective.[39,43] These results demonstrated that whether the C797S is *cis* or *trans* to the T790M potentially has an impact on drug response, and that it has useful clinical implications which should be prioritised going forward.[43]

The presence of the T790M mutation together with the C797S mutation was not the only biomarker that was observed during the study of NSCLC patients with T790M positive EGFR, who had developed resistance to the third generation EGFR-TKIs. Other subtypes included cells that had the T790M mutation without the C797S mutation and EGFR cells that were negative of both the T790M and C797S mutation.[38,39] New therapeutic strategies had to be explored going forward. Since all mutant selective EGFR-TKIs target the ATP binding site of EGFR, current research is exploring new therapeutic strategies by applying a different mechanism of action. One emerging strategy is the use of inhibitors targeting the allosteric sites in the tyrosine kinase domain of EGFR,[46] another emerging strategy is the development of drugs that covalently and reversibly bind into the ATP binding pocket.[45]

1.3.5. Recent developments: Overcoming the T790M and C797S drug resistance

There is a great limitation observed with the currently existing EGFR-TKIs that are designed to target NSCLC patients that have acquired resistance. First generation EGFR-TKIs are effective towards the wild type EGFR and against EGFR that has somatic mutations (exon 19 deletion and L858R point mutation); however patients develop resistance towards this drug after an average time of 14 months.[23] The resistance was found to be due to the secondary T790M acquired mutation. Second generation drugs were then developed with

the aim of targeting the T790M mutation. Although these drugs were effective towards both the wild and mutant EGFR *in vitro*, they didn't show any profound effectiveness towards the inhibition of the T790M mutation *in vivo*. Their limitation was found to be the narrow therapeutic window which precluded dosages that would be efficient for the inhibition of the T790M mutation.[37,38] The next strategy applied was the development of third generation EGFR-TKIs which were still targeted towards the T790M mutation. Although these drugs are effective against the targeted mutation, resistance arises rapidly.[39,40] The C797S mutation appears to be the most common mechanism of acquired resistance to third generation EGFR-TKIs.[39,40]

This highlights the need for new therapeutic strategies that will overcome both the T790M and C797S mutation in NSCLC patients. The two classes of compounds to be discussed below are still in their developing stages.

1.3.5.1. Fourth generation EGFR-TKIs

There is an emerging interest in therapeutic strategies with a different mechanism of action as compared to the already existing ATP-competitive inhibitors. Recent investigations have discovered fourth generation inhibitors that could potentially overcome the drug resistant T790M and C797S mutations.[39] Fourth generation EGFR-TKIs are allosteric inhibitors that bind to EGFR, but not in the ATP binding site (Figure 1.8).[46] EA1001 (**8**, Figure 1.9) was the lead compound that was discovered to have good efficacy and selectivity against mutant EGFR; i.e. at a concentration of 1mM ATP the IC_{50} for the inhibition of L858R/T790M mutant EGFR was 0.024 μM as compared to $>$ 50 μM required for the wild type EGFR inhibition.[46] However, compound **8** didn't show any exceptional inhibitory effect towards the individual L858R and T790M mutations.[46] A structure based optimisation strategy was done and the most active compound was EA1045 (**9**, Figure 1.9). The compound was a result of replacing the unsubstituted benzene group in EA1001 with a 4-fluorophenol group. EA1045 was found to have profound potency and selectivity for the inhibition of L858R/T790M mutant EGFR.[46] *In vitro* studies also indicated that EA1045 is effective and selective for the T790M mutant EGFR that is in its inactive monomer state.[46]

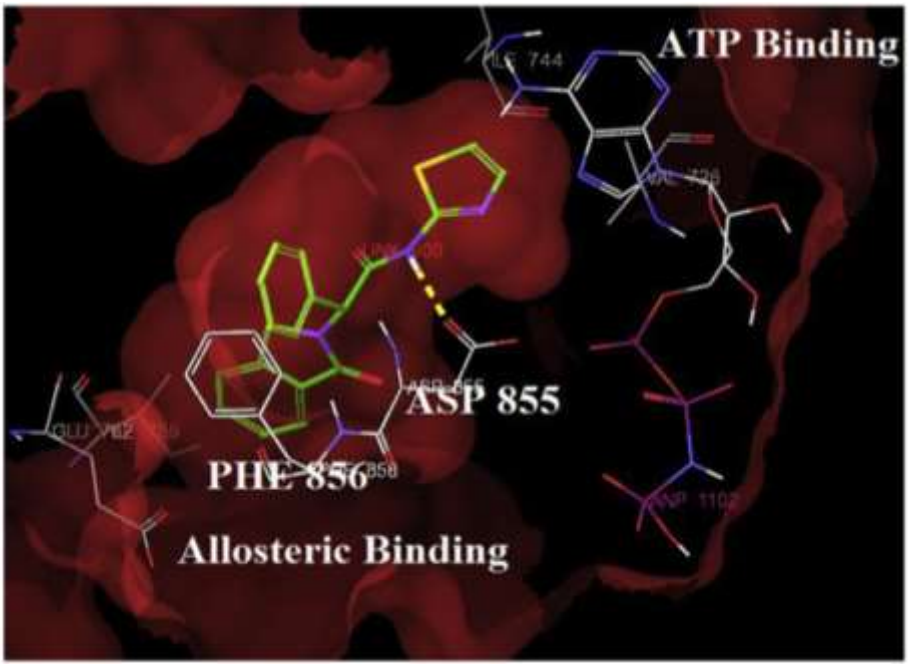

Figure 1.8: Allosteric binding of fourth generation inhibitor EA1001 (**8**) to EGFR kinase domain away from ATP binding cleft.[39] The yellow/green structure represents the EA1001 inhibitor and the grey/purple structure represents ATP still in its active site.

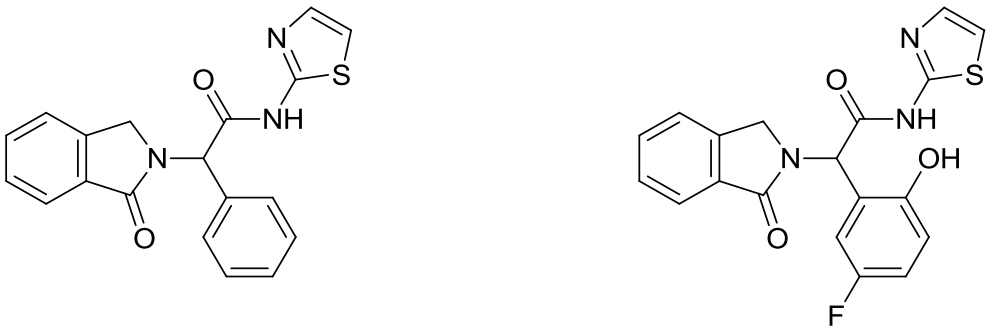

Figure 1.9: Chemical structures of the fourth generation EGFR-TKIs.

When EA1045 was used in mice containing the L858R/T790M/C797S mutant NSCLC tumour xenografts it wasn't effective alone. However, in combination with cetuximab high tumour regression was observed[39,46] thus indicating the importance of combination treatment as a potential key therapeutic strategy going forward. This study clearly revealed that EA1045 has the potential of overcoming the T790M and the C797S mutations, but only if EGFR dimerisation is inhibited.[39] This explains why the combination of EA1045 and cetuximab was effective. No human clinical trials have been done as yet to validate the efficacy and safety of this compound in NSCLC patients as it is still in its developing stages.

Given the diversity of the resistance mechanisms observed with each generation of EGFR-TKIs, combination therapy of EGFR-TKIs with other classes of inhibitors might be one of the most promising therapeutic strategies to be applied for the treatment of NSCLC patients.

1.3.5.2. Covalent reversible EGFR-TKIs

Although there has been great success observed with the covalent inhibitors, the progressive emergence of drug resistant mutations in the active site demonstrated the need for continuous development of new generations of EGFR-TKIs. Some recent developments are focused on an alternative innovative class of compounds: the covalent reversible inhibitors. That is, this class of compounds has a covalent yet reversible warhead instead of the covalent irreversible warhead observed with the second, third and fourth generation inhibitors.[45] Covalent reversible EGFR-TKIs are theoretically devoid of the drawbacks observed with the conventional covalent irreversible inhibitors, yet they still have the potential to combine their positive effects.[45,52] Investigations have indicated that irreversible binding is not required for effective inhibition of the mutant EGFR, a reversible inhibitor with sufficient affinity to outcompete ATP should work as well.[34]

One relevant determinant of any inhibitors' efficacy is its residence time towards its target active site.[54] For the development of inhibitors that outcompete the natural ATP in its active site it became of importance to develop inhibitors with optimised prolonged drug-target residence time and covalent binding nature afforded this characteristic.[52] The reversible nature was then introduced to eliminate toxicity and resistance issues often observed with irreversible covalent binding.[52,55] Taunton and co-workers showed that a rapid reversible bond can be formed between the target protein and an inhibitor containing electron deficient olefins (Scheme 1).[51,52,58]

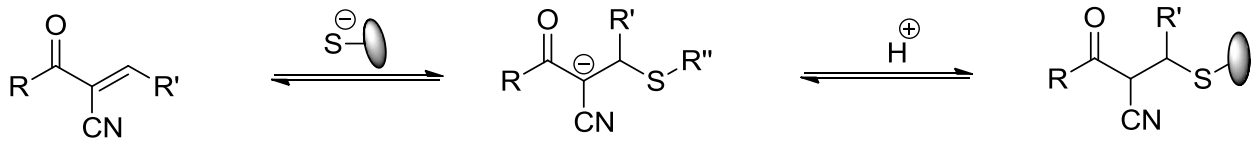

Scheme 1: Representation of the reversible covalent Michael addition of thiols to electron deficient Michael acceptors. Where, R = aromatic ring and R' = NH or O- alkyl.[58]

Based on this strategy several other studies have focused on designing compounds with the α-cyano-α,β-unsaturated carbonyl warhead to explore the concept of covalent reversible inhibition of drug resistant EGFR.[45,52] Although these compounds are still used as tool compounds, here we will briefly discuss the successes that have been achieved thus far.

A study by Basu and co-workers reported a structure based design of covalent reversible EGFR inhibitors,[45] wherein they designed and synthesised a library of compounds based on the WZ4002 (**7**) scaffold. To afford the covalent reversible characteristic, the Michael acceptor of compound **7** was chemically tuned by the introduction of electron withdrawing groups at R_1 resulting in an electron deficient olefin (**10**, Figure 1.10). The synthesised compounds were then biochemically evaluated.

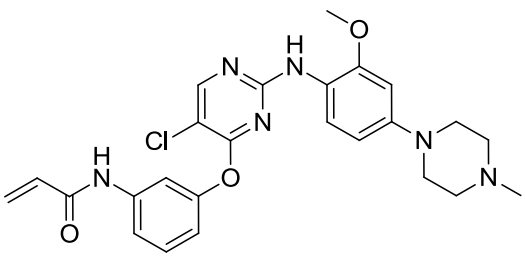

7. WZ4002

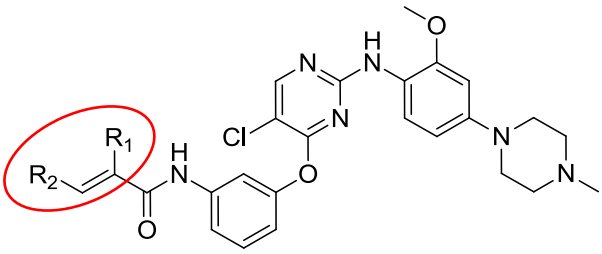

10. Covalent reversible inhibitors

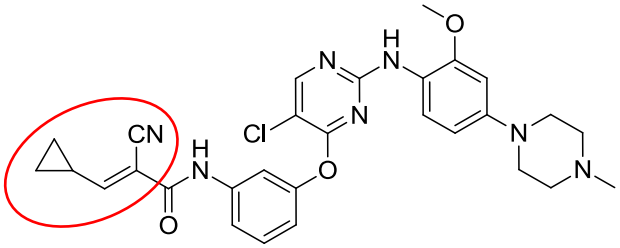

11

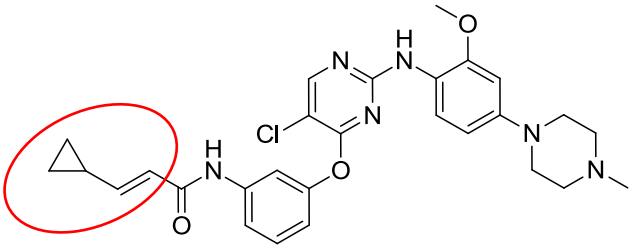

12

Figure 1.10: Chemical structure of the third generation EGFR-TKI WZ4002 (**7**), the design of covalent reversible inhibitors (**10 and 11**) and the control compound used to investigate the effect of the electron withdrawing group (**12**). Where, R_1 = electron withdrawing group and R_2 = aliphatic or aryl group.

A series of these compounds were found to be highly selective and displayed a strong inhibitory effect towards the mutant EGFR compared to the wild type EGFR *in vivo*.[45] Cyano and fluoro electron withdrawing groups were explored, and it was observed that the cyano containing compounds were generally more potent. To evaluate whether the electron withdrawing cyano group had any effect on the inhibitory activity of the compounds, compounds **11** and **12** were directly compared (Figure 1.10). Compound **11** was ten times more potent than compound **12**,[45] which indicated that the electron withdrawing group does indeed increase the inhibitory effect of this drug. This study indicated that α-cyano-α,β-unsaturated compounds are a promising class of compounds for mutant EGFR inhibition, however, further investigations are still required for their development.

1.4. An alternative approach to covalent reversible EGFR-TKIs

The search for covalent reversible inhibitors is not limited to compounds containing the cyanoacrylate functional group, several other functional groups can be chemically tuned such that they become covalent reversible warheads. One important aspect is for the reactive warhead to produce a labile cross-linked product upon attack by the serine or cysteine of the biological target.[51] Any functional group that has this characteristic serves as a potential moiety for the development of covalent reversible inhibitors. Reversibly reactive moieties include aldehydes, ketones, nitriles and boronic acids.[51] Boronic acids and aldehydes have been widely used as protease inhibitors.

Of interest to us are ketones or rather α-keto carbonyl/amide compounds. Activated ketones such as α-keto esters, α-keto acids and α-keto amides have been reported to reversibly inhibit cysteine proteases.[57] These functional groups form a short-lived reversible covalent bond with the cysteine thiol (Scheme 2).[57] This results in a reversible equilibrium between the inhibitor and the formed hemithioketal. The inhibition effect of these α-keto carbonyl compounds has, however, not been investigated in kinase enzymes.

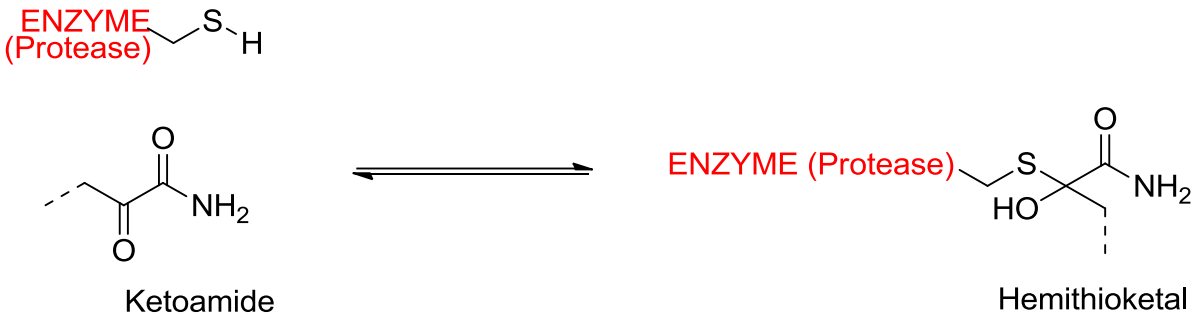

Scheme 2: Representation of the reversible inhibition of a protease enzyme by a compound containing the ketoamide warhead.

EGFR-TKIs containing the α-keto carbonyl warhead have, to date, not been studied in any research group. In this work, we set out to explore the covalent reversible inhibition of EGFR using α-ketoamide containing compounds. Ketoamides have been used to make protease inhibitors with some success. This current approach could be valuable since the cysteine nucleophile will still be used, just in a different enzyme. It is thus an intuitive hypothesis that the reversible nature of the bond formed between the two substrates will still be retained even in our systems. Such an approach might lead to compounds which can form reversible covalent bonds with the cysteine (Cys797) residue of EGFR and hopefully selectively inhibit the mutant type EGFR while sparing the wild type EGFR in order to avoid any undesired side effects.

1.5. Aims of this project

Given the potential that the activated ketone warhead approach could offer in drug discovery, it is therefore essential to study the effect of this warhead in EGFR inhibition. This project is based on literature results that have demonstrated that effective inhibition of EGFR is not restricted to irreversible binding. A reversible inhibitor that binds with sufficient affinity to surpass ATP should work as effectively. This current work will explore the concept of covalent reversible inhibitors for the inhibition of EGFR in NSCLC treatment, by specifically applying the α-ketoamide warhead. The α-ketoamide warhead may allow for reversible covalent bond formation with EGFR, through the formation of a hemithioketal similar to the one represented in Scheme 2. In this study we aim to design, synthesise and test the synthesised pyrimidine ketoamides for biological activity against EGFR.

Considering the progressive drug resistance and observed toxicities with current EGFR-TKIs, our objective will be to synthesise highly competitive or effective EGFR-TKIs that will not introduce any severe side effects. Since their binding will be reversible, these inhibitors will compete with ATP at the receptor catalytic domain to avoid autophosphorylation and the downstream intracellular signalling from occurring.

1.5.1. Design of target compounds

Computational molecular modelling was previously done in our laboratory by Dr Allan Prior to determine the optimal drug scaffold, predict preferred binding conformations and also calculate the binding energy of the designed molecules. A library of pyrimidine ketoamides was designed and modelled using Accelrys (Biovia) Discovery Studio 4.0. The pyrimidine core was designed to mimic the adenine base of ATP and an appropriate side-chain was added that would position the activated ketone in such a way that it could form covalent reversible bonds with the target cysteine thiol. Modelling of these pyrimidine ketoamides in the T790M mutated EGFR (PDB code: 4I24) showed that they preferred to dock with the *N*-aryl group pointing towards a hydrophobic pocket at the back of the active site near MET790 (Figure 1.11A). The pyrimidyl core bound to the hinge region and formed a hydrogen bond to MET793 (NH) via the pyrimidyl nitrogen with an average distance of 1.85 Å. Predominantly, the ethylene glycol linker was positioned near the edge of the pocket which placed the electrophilic ketoamide carbonyl close to thiol of CYS797 with a distance of 3.63 Å. This suggested that covalent bond formation between the bound ketoamide inhibitor and the thiol (CYS797) may be possible. Based on this model, a series of pyrimidine ketoamides bearing different aniline substrates was proposed for synthesis in this project (Figure 1.11B).

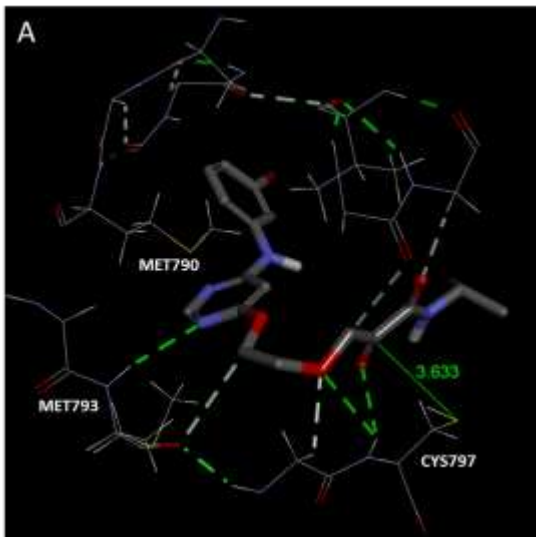

A

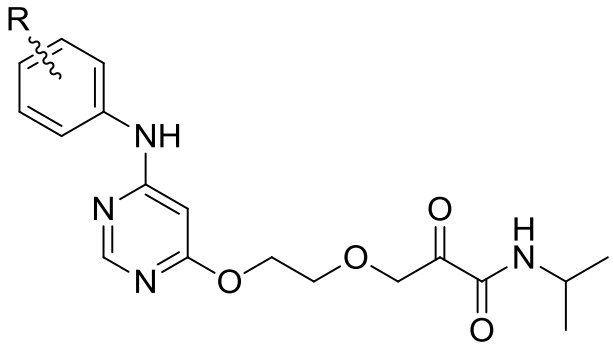

B

R = 3-bromo
= H
= 3-chloro-4-fluoro
= 3-ethynyl
= 3,5-dimethoxy
= 3,4-difluoro
= 2-chloro-4-((3-fluorobenzyl)oxy)
= 3-chloro-4-((3-fluorobenzyl)oxy)

Figure 1.11: A: Highest scored docked pose of the pyrimidine ketoamides with T790M mutated EGFR (PDB: 4I24). B. Chemical structure of the proposed anilino-pyrimidine ketoamide molecules.

1.5.2. Chemistry

Scheme 3 outlines the retrosynthetic strategy towards desired pyrimidine ketoamide molecules. We plan to synthesise the pyrimidine ketoamides **13a-h** by the oxidation of α-hydroxy amide intermediates **14a-h**, which can be accessed using isocyanide chemistry with isopropyl isocyanide and the aldehydes **15a-h**. Compounds **15a-h** can be accessed from the oxidation of compounds **16a-h** using IBX. We plan to synthesize **16a-h** from the monoprotected diethylene glycol **17**, 4,6-dichloropyrimidine **18** and various anilines **19a-h**.

Scheme 4 details the proposed step for the monoprotection of diethylene glycol to yield the desired precursor **17**.

Once this methodology has been successfully applied for the synthesis of pyrimidine ketoamide molecules, they will be screened for anti-cancer activities by Dr. Leonie Harmse, Department of Pharmacy and Pharmacology, University of the Witwatersrand. We also wish

to investigate a different activated ketone group that has the potential of forming a reversible covalent bond with the cysteine thiol. The anilino-pyrimidine scaffold will be retained, only changing the ketoamide warhead to a ketoester to afford compounds of the general chemical structure shown in Figure 1.12.

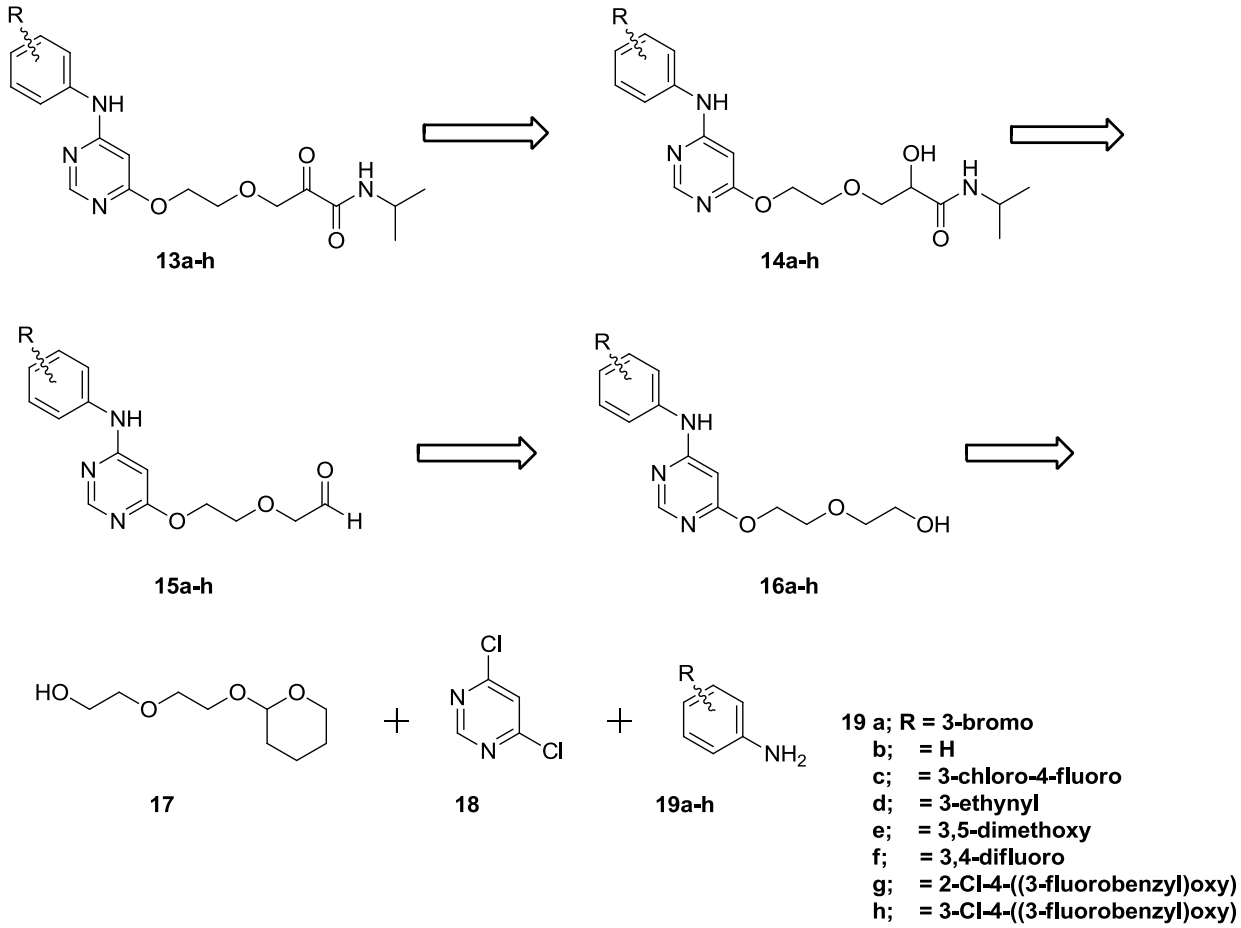

Scheme 3: Retrosynthetic strategy towards ketoamides.

Scheme 4: Reagents and conditions: *p*-TSA, 0 – 25°C, 24 h

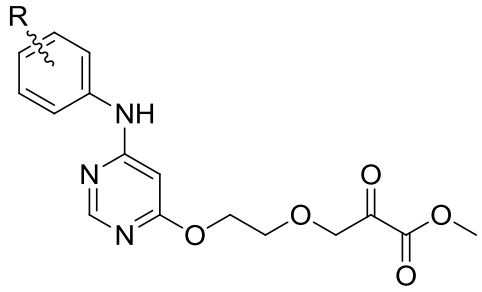

Figure 1.12: Chemical structure of the proposed anilino-pyrimidine ketoester molecules.

In a similar manner to ketoamides, we plan to access the ketoester **20** by the oxidation of α-hydroxy ester **21** (Scheme 5). Compound **21** can be accessed by sequential hydrolysis and esterification of cyanohydrin **22**, which we plan to synthesise by reaction of potassium cyanide (KCN) and aldehyde **15**.

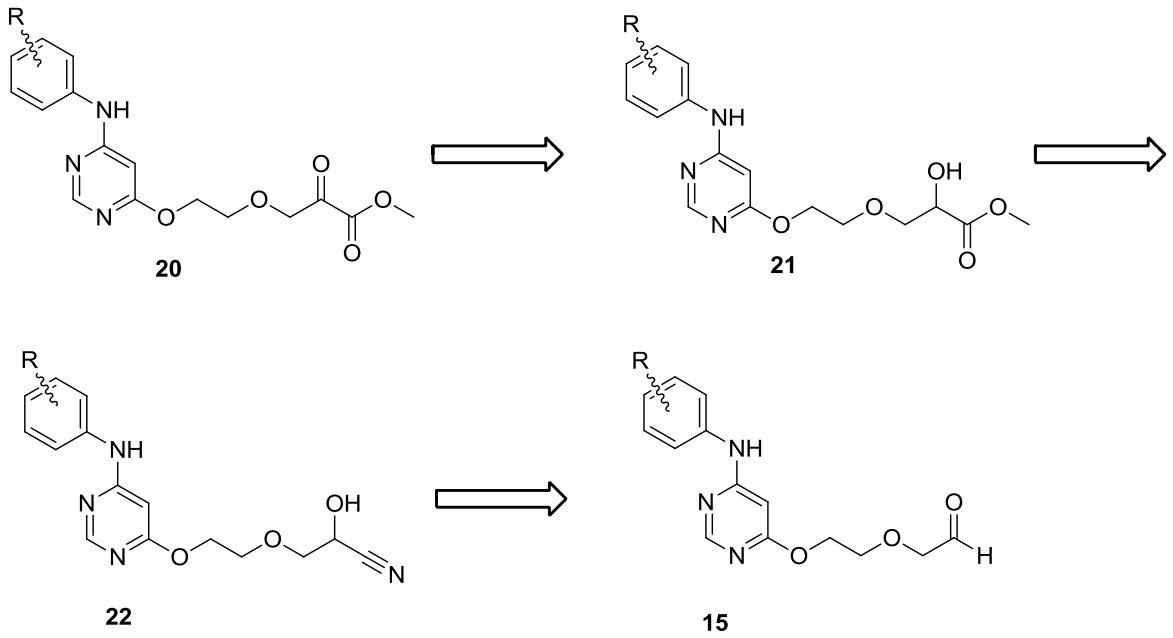

Scheme 5: Retrosynthetic strategy towards ketoesters.

Through this work, we hope to discover new α-ketoamide EGFR inhibitors with promising anti-cancer activities. We also hope that this project will identify the best anilino-pyrimidine scaffolds that can be used for T790M EGFR inhibition, and hence influence future developments in the search for covalent reversible EGFR-TKIs.

CHAPTER 2: RESULTS AND DISCUSSION

2.1. Synthesis of pyrimidine ketoamides as EGFR inhibitors

As per the aims discussed in Chapter 1, this project focused on the synthesis of anilino-pyrimidine molecules as potential EGFR-TKIs for cancer treatment. Scheme 3 outlined the retrosynthetic strategy towards the desired ketoamide molecules. Scheme 6 below outlines an overview of the proposed synthetic route towards the target compounds **13a-h**.

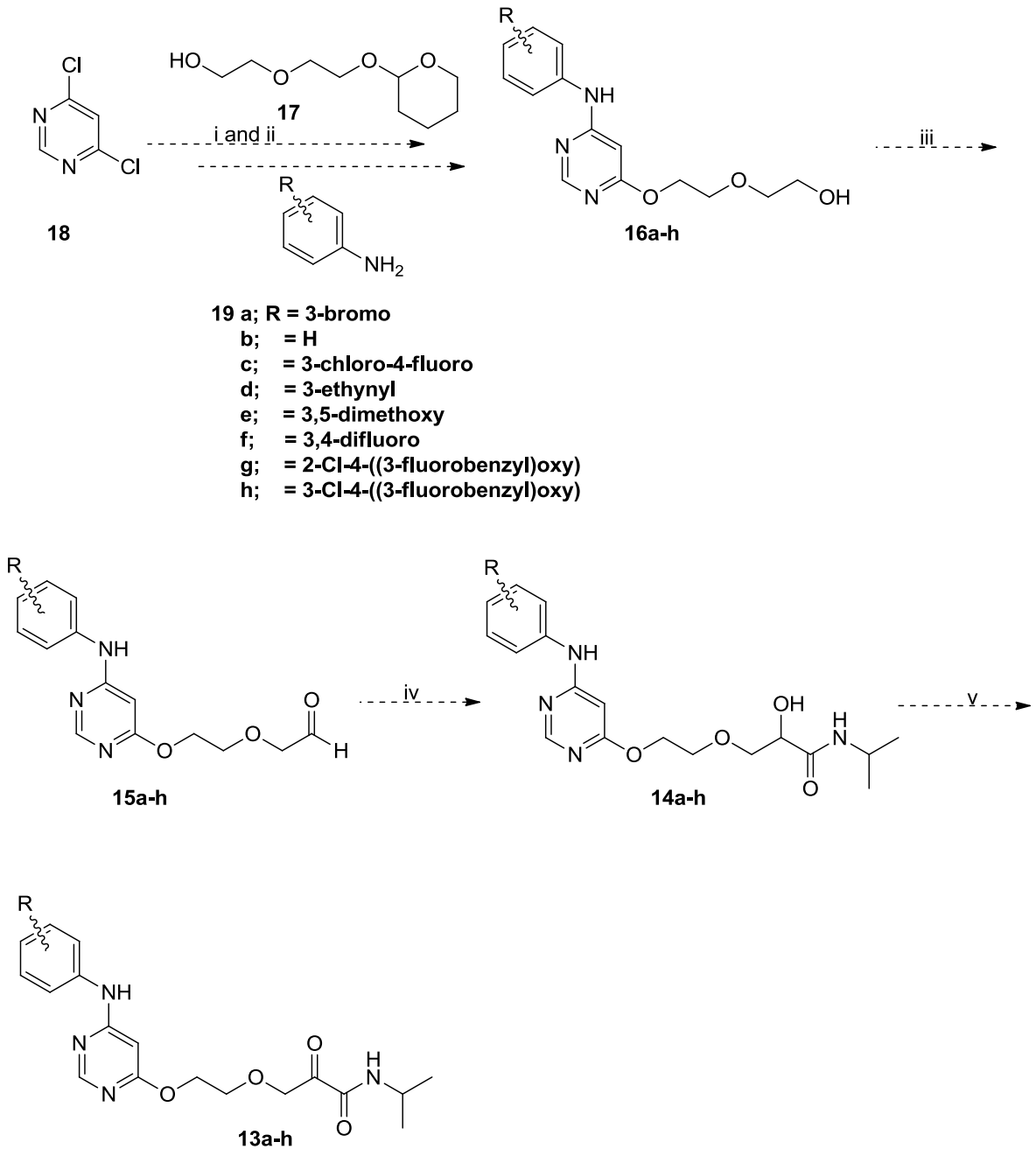

Scheme 6: Overview of the proposed synthetic route towards the pyrimidine ketoamides **13a-h**

Steps (i) and (ii) would involve two nucleophilic displacements of the chloro groups of compound **18**: one by the aniline derivatives **19a-h** and one by the monoprotected diethylene glycol chain **17**. In step (iii) compound **16** would then be oxidised to give the aldehyde **15**. Using isocyanide chemistry compound **15** would undergo functional group interconversion to give compound **14** in step (iv), which would be oxidised to give the target compound **13** in the final step.

The synthesis began with the preparation of the two general intermediates; 2-[2-(tetrahydro-2*H*-pyran-2-yloxy)ethoxy]ethanol **17** and 4,6-dichloropyrimidine **18**.

The atom numbering on compounds does not follow the official IUPAC rules. The atoms were numbered to simplify the discussion of assignments. The m/z values reported in the following sections are for compounds containing the ^{79}Br or ^{35}Cl isotopes.

2.1.1. The synthesis of 2-[2-(tetrahydro-2*H*-pyran-2-yloxy)ethoxy]ethanol 1

Compound **17** was synthesised from the commercially available diethylene glycol **23** (Scheme 7). Monoprotection of one hydroxyl group on diethylene glycol **23** was performed using 3,4-dihydro-2*H*-pyran **24** in the presence of *p*-toluenesulfonic acid (*p*-TSA). The desired compound **17** was obtained as a clear oil in 69% yield, which corresponded to the results obtained by Tian *et al.*[59]

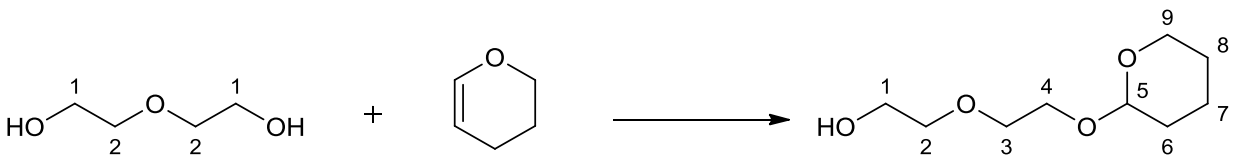

23 **24** **17**

Scheme 7: Reagents and conditions: *p*-TSA, 0 – 25°C, 24 h, 69%

Upon ^{1}H NMR spectroscopic analysis of compound **17**, a triplet characteristic of H-5 was observed at δ 4.64. Another characteristic peak was observed as a multiplet between δ 1.91 – 1.48 integrating for 6 protons; which was assigned to be overlapping signals for H-6, H-7 and H-8. Furthermore, five other multiplets were observed between δ 3.92 – 3.41, which in total integrated for 11 protons: corresponding to those protons attached to carbon atoms bearing oxygen (H-1, H-2, H-3, H-4, H-9) and OH. The ^{13}C NMR spectrum showed a total of nine signals which indicated that the molecule was no longer symmetrical and a new functional group had been introduced. The signal observed at δ 99.1 was characteristic of C-5 and that indeed confirmed that the diethylene glycol chain had been monoprotected.

2.1.2. The synthesis of 4,6-dichloropyrimidine 18

For many years the preparation of 4,6-dichloropyrimidines from their corresponding dihydroxypyrimidines has been carried out using excess phosphoryl chloride ($POCl_3$)[60] and we followed the same procedure for this synthesis. To synthesise compound **18** commercially available 4,6-dihydroxypyrimidine **25** was refluxed with $POCl_3$, resulting in the chlorinated compound **18** in 59% yield (Scheme 8). The obtained 59% yield was in agreement with the 58% yield obtained by McCluskey *et al.* when chlorinating structurally similar compounds.[60] Only two aromatic singlets integrating for one proton each were observed in the ^{1}H NMR spectrum of **18**, one at δ 8.97 assigned to H-1' and the other one at δ 8.11 assigned to H-3'. The absence of peaks corresponding to the hydroxyl groups was a clear indication that the reaction had taken place. Further confirmation was obtained from IR spectral analysis, no OH stretching peaks were observed between 3200 – 3600 cm^{-1}. From the ^{13}C NMR spectrum three signals were observed, one at δ 162.1 assigned to C-4' and C-2' and the others at δ 158.8 and 121.9 assigned to C-1' and C-3', respectively.

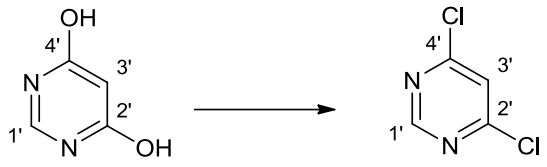

25 **18**

Scheme 8: Reagents and conditions: $POCl_3$, reflux, 3 h, 59%

2.1.3. The synthesis of 2-{2-[4-(3-bromophenylamino)pyrimidin-6-yloxy]ethoxy} ethanol 16a and analogues

With the two general intermediates **17** and **18** in hand, the amino pyrimidine ethanol compounds **16** could be accessed in one of two approaches (Scheme 9). In the first approach (a) the first chloro group of compound **18** is substituted by an aniline derivative **19** and the second chloro group is subsequently displaced by the monoprotected diethylene glycol chain **17**. In the second approach (b) the sequence of nucleophilic displacements is reversed.

The aniline derivates were commercially available. Three of the anilines **19c-d, h** have been used in FDA approved EGFR-TKIs, hence we chose them. The other aniline derivatives were chosen to investigate the effect of electron-withdrawing substituents against electron-donating substituents.

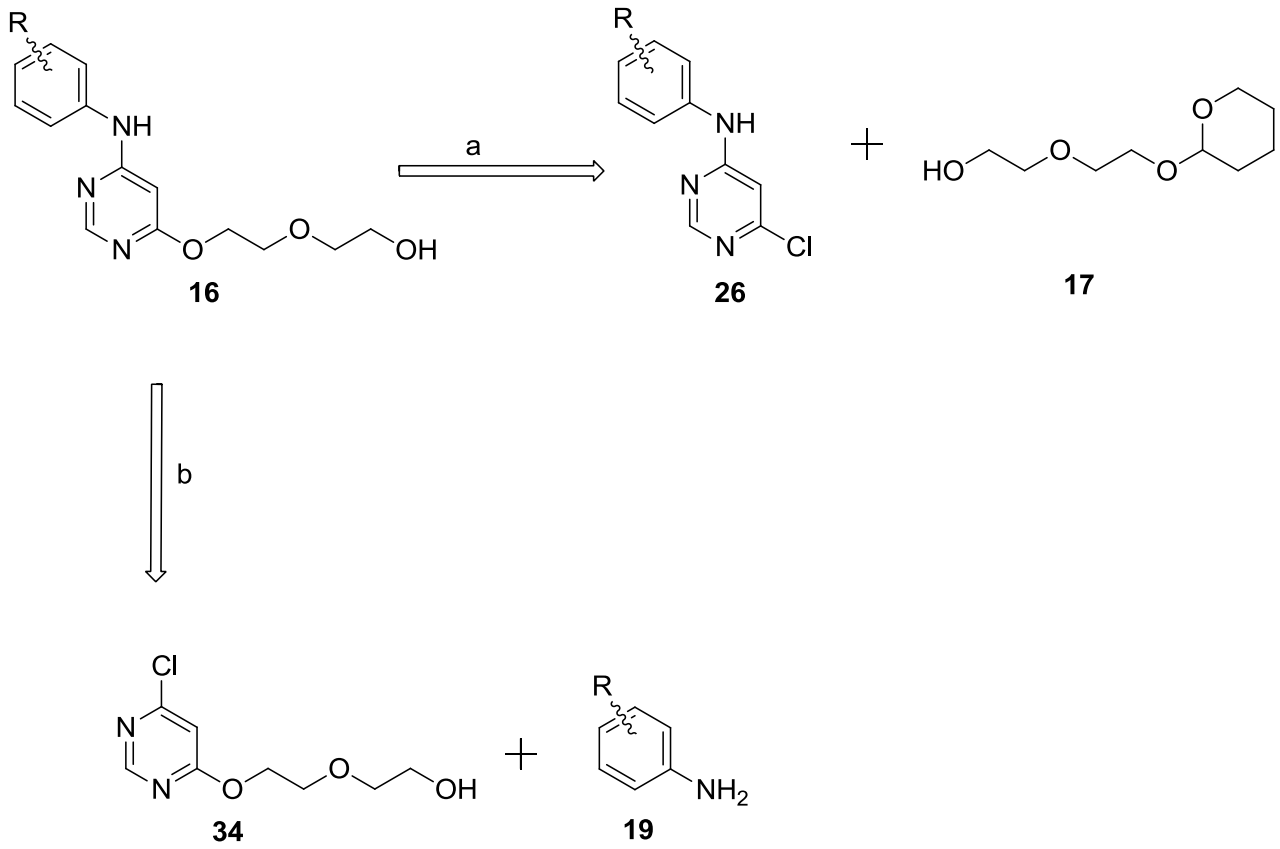

Scheme 9: Two possible approaches, a and b, for the synthesis of compounds **16**

2.1.3.1. The first approach (a) towards the synthesis of 2-{2-[4-(3-bromophenylamino) pyrimidin-6-yloxy]ethoxy}ethanol 16a

The synthesis began with the preparation of intermediate **26a** from the already synthesised compound **18**. The 3-bromoaniline **19a** group was installed by sequential addition of ethanol, 3-bromoaniline and triethylamine to a round bottomed flask containing 2,4-dichloropyrimidine **18** (Scheme 10(i)). The reaction was refluxed at 80ºC and monitored by thin layer chromatography (TLC). This step afforded the desired product **26a** (as confirmed by ^{1}H NMR spectroscopy and MS) in 16% yield.

In the ^{1}H NMR spectrum of compound **26a** five additional signals were observed accounting for the installed anilino moiety. The presence of a singlet integrating for one proton at δ 10.03 was characteristic of the amino group. Another characteristic feature was the upfield shift of the H-3' proton from δ 8.11 to δ 6.84. This indicated that chlorine had been substituted with the amino group which donates electron density to the ortho position (H-3') through resonance. Aromatic signals characteristic of the bromoaniline group were observed between δ 8.06 and 7.24. Further confirmation was obtained from the ^{13}C NMR spectrum where the C-2' and C-4' signals were no longer observed in the same environment indicating

that a new moiety had been installed resulting in the loss of symmetry of the pyrimidine scaffold. The signal at δ 160.9 was assigned to C-2' and that at δ 158.4 to C-4', the slight upfield shift observed with the C-2' signal was characteristic of the electron donating effect of the amino group. The upfield shift in the δ value of C-3' from δ 122.0 to δ 105.7 also confirmed that the aniline group had been installed. Six more signals were observed at δ 140.7, 130.7, 125.5, 122.2, 121.6 and 118.8 which were characteristic of the bromoaniline carbon atoms.

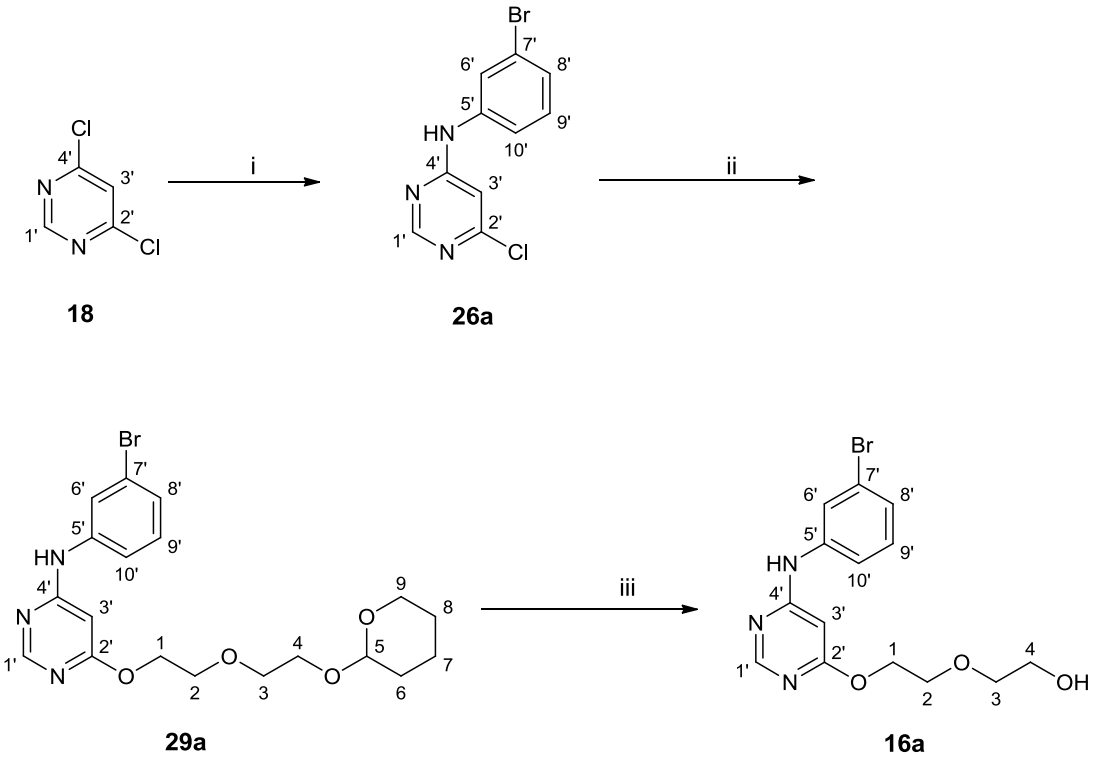

Scheme 10: Reagents and conditions: i. 3-$BrPhNH_2$ **19a**, Et_3N, EtOH, reflux, 18 h, 55%; ii. **17**, NaH, DMF, 150°C, 3.9% or NaH, DMSO, 150-160°C,16% ; iii. 4M HCl, r.t., overnight, 57%

Literature states that 4,6-dichloropyrimidines should undergo aminolysis quite easily.[62] The 16% isolated yield for compound **26a** was undesirable and we believed that the product was lost during the reaction workup. An alternative workup procedure had to be investigated to optimize both the yield and purity of the desired product. Thus the reaction was repeated as before but once all the starting material had reacted based on TLC analysis, a test workup procedure was performed on a 10 mL portion of the 100 mL reaction mixture. The 10 mL reaction mixture was first dissolved in ethyl acetate and consecutively washed with water, saturated ammonium chloride and finally saturated brine. This gave a yellow solid of mass 913 mg which, according to ^1H NMR spectroscopy, was a mixture of the desired product **26a** and both of the starting materials, **18** and 3-bromoaniline **19a**. The rest of the reaction, 90 mL, was refluxed for a further 48 h. After that period, starting material **18** had completely

reacted; however, a significant amount of 3-bromoaniline **19a** was still in the mixture (as confirmed by ^{1}H NMR spectroscopy). It was decided to add more starting material **18** to the reaction in proportion to the excess 3-bromoaniline that remained in the reaction. After refluxing for a further 18 h the reaction went to completion (as confirmed by ^{1}H NMR spectroscopy). The crude reaction mixture was purified by liquid-liquid extraction. Similar to the previous extraction, the reaction mixture was dissolved in EtOAc and consecutively washed once with water, twice with saturated ammonium chloride and finally once with saturated brine. The desired product **26a** was obtained as an orange solid in 55% yield.

Although the isolated yield had significantly improved, the yield was still not optimal considering that this step was towards the beginning of our synthesis. The reaction was repeated, but this time compound **18** was used in excess. The workup was also further simplified: during the workup diethyl ether was added to the reaction mixture to precipitate the triethylammonium chloride salt; the filtrate was then washed once with water and the collected organic layer was concentrated *in vacuo* to give a yellow solid which was washed with water (*via* sonication) to afford desired product **26a** (as confirmed by ^{1}H NMR spectroscopy and MS) in a much improved yield of 86%.

The next step was then the displacement of the second chlorine group in **26a** by 2-[2-(tetrahydro-2*H*-pyran-2-yloxy)ethoxy]ethanol **17** (Scheme 10(ii). This reaction was carried out by reacting a solution of **26a** in DMF with that of compound **17** and sodium hydride in DMF and heating at 150°C. Previous attempts to do this reaction at lower temperatures (80-110°C) had resulted in no reaction occurring, highlighting the need for much higher reaction temperatures for this nucleophilic substitution reaction. This procedure, however, produced the desired product as a minor product and a major undesired product as confirmed by NMR spectroscopy and MS. Under our reaction conditions, at high temperatures such as 150°C, it appeared that hydride (H^{-}) attacks the electrophilic carbon atom of DMF resulting in the formation of a *N,N*-dimethylamide anion ($^{-}N(Me)_2$) **28** (Scheme 11). The two anions, **17** and **28** then compete for chlorine substitution on **26a**, and in this case the major product was a result of **28** acting as a nucleophile instead of anion **17** (as confirmed by ^{1}H NMR spectroscopy and MS) (Scheme 11). From the ^{1}H NMR spectrum of **29a** it was evident that **17** had been installed, additional peaks were now observed in the aliphatic region. One significant signal integrating for one proton was observed at δ 4.63 which was characteristic of H-5. In addition to the expected aromatic signals, several multiplets were observed between δ 4.51 to 3.41 which in total integrated for 10 protons and they were assigned to H-1, H-2, H-3, H-4 and H-9. From the ^{1}H NMR spectrum of **30a** one significant singlet integrating for six protons was observed at δ 3.05 and that was assigned to H-11' (Scheme

11). The separation of the two compounds by silica gel column chromatography was difficult as they both had very similar R_f values.

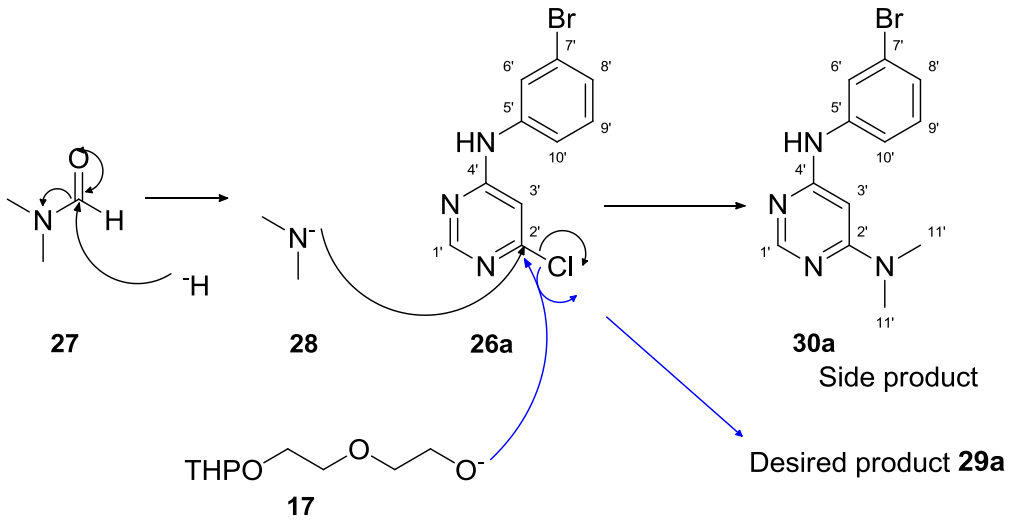

Scheme 11: Under our reaction conditions, at high temperatures (150°C) in the presence of hydride, it appeared that DMF decomposes into *N,N*-dimethylamide anion.

To solve the problem at hand the reaction was repeated, but this time using dimethyl sulfoxide (DMSO) as a solvent which would not be prone to decomposition by hydride. The reaction then produced an oil which contained both the starting material **26a** and the desired product **29a** (as confirmed by ^{1}H NMR spectroscopy and MS).The oil was then purified over a silica gel column to give **29a** in a very poor 16% yield and 4% of the starting material **26a** was recovered. The presence of the starting material was a result of the reaction stopping before 100% conversion of the starting material, but prolonged reaction time was ineffective in resolving this matter. To account for the very low yield, the probability is that the product decomposes during the reaction; however, no detailed analysis was carried out. Due to the observed yields being very low a second approach (b) was explored as an alternative method where the diethylene glycol chain **17** was attached prior to the amination reaction (Scheme 9).

2.1.3.2. The second approach (b) towards the synthesis of 2-{2-[4-(3-bromophenylamino)pyrimidin-6-yloxy]ethoxy}ethanol 16a

This second approach began with the synthesis of intermediate **31** (Scheme 12). Theoretically, the nucleophilic substitution of 4,6-dichloropyrimidine by an alkoxide ion should not be difficult. The pyrimidine ring is activated towards nucleophilic displacement by the electron withdrawing effect of the other chlorine atom.[62] As expected, no difficulties were observed with this reaction even though the isolated yield was moderate.

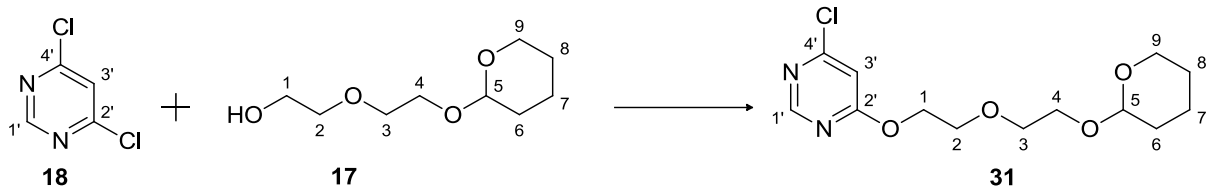

Scheme 12: Reagents and conditions: NaH, THF, 0 – 25°C, 48 h, 54%

The monoprotected diethylene glycol **17** was deprotonated using NaH in THF and reacted with 4,6-dichloropyrimidine **18** to afford the desired product **31**. The reaction was performed by stirring under nitrogen atmosphere at room temperature for 48 h. Any observed impurities (from TLC analysis) were removed by silica gel column chromatography to give compound **31** as a colourless oil in 54% yield.

Nine signals were observed from the ^{1}H NMR spectrum of **31**. Amongst the nine signals two singlets in the aromatic region were observed at δ 8.56 and δ 6.83, each integrating for one proton which were assigned to H-1' and H-3' respectively. The aliphatic region contained a triplet at δ 4.63 integrating for one proton, and a multiplet at δ 4.57 integrating for two protons, characteristic of H-5 and H-1 respectively. Furthermore, the presence of a multiplet at δ 3.76 – 3.69 integrating for two protons and a multiplet at δ 1.88 – 1.47 integrating for six protons confirmed that compound **31** was successfully synthesized. The first multiplet was characteristic of H-3 and the second multiplet was characteristic of H-6, H-7 and H-8. In the ^{13}C NMR spectrum, the presence of two quaternary carbon atoms attested to the fact that the substitution of one chlorine atom had indeed occurred as C-2' and C-4' were no longer in the same environment. In the ^{13}C NMR spectrum of the starting material **18**, C-2' and C-4' both appeared as one signal at δ 162.1; while for compound **31** we observed C-2' at δ 170.1 and C-4' at δ 160.6. Conclusive evidence was obtained from the high resolution mass spectrum (HRMS) of **31**. A molecular ion peak was observed at m/z 303.1106 which was in agreement with the calculated $[M+H]^{+}$ for $C_{13}H_{20}ClN_2O_4$ of 303.1103.

With compound **31** in hand we were now in a position to do the amination reaction to afford the anilino-pyrimidine alcohol compounds. Our first attempt was to try this reaction under basic conditions. Unfortunately, when **31** was coupled with 3-bromoaniline **19a** in the presence of sodium hydride (NaH) in tetrahydrofuran (THF) no reaction was observed (Scheme 13). The reaction was initially performed at room temperature overnight and upon TLC analysis, a spot in correspondence with starting material **19a** was observed R_f = 0.78 (50% EtOAc:Hex) and a spot corresponding to **31** with R_f = 0.55 (50% EtOAc:Hex) was observed. The temperature was raised to 70°C, and upon TLC analysis both starting materials had been consumed. Unfortunately, the ^{1}H NMR spectrum of the crude material

obtained from the reaction mixture did not indicate the presence of either the starting materials or the desired product. We then changed the solvent to DMSO and the reaction was heated at 150°C overnight, but no reaction occurred as confirmed by TLC analysis.

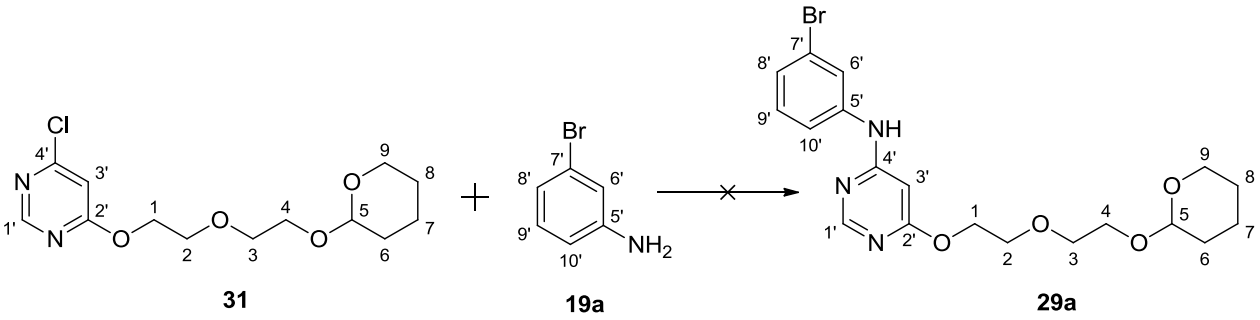

Scheme 13: Reagents and conditions: NaH, THF, r.t. – 70°C, overnight, no reaction

A strong base, potassium bis(trimethylsilyl)amide (KHMDS) was then used for the base catalysed amination reaction (Scheme 14). Initially 2-propanol was used as a solvent for this reaction and after stirring overnight at room temperature only the starting materials were present, as confirmed by TLC. The reaction mixture was then refluxed overnight and a new product had formed as seen by TLC. The observed new spot was less polar than both starting materials. This contradicted what was expected as the desired product was expected to be more polar than the starting materials. The mixture was purified using silica gel column chromatography and the new spot was submitted for characterization by ^{1}H NMR spectroscopy. ^{1}H NMR spectroscopic analysis showed the presence of a doublet integrating for six protons at δ 1.36, a septet at δ 5.39 integrating for one proton, and two singlets at δ 6.73 and 8.56. This suggested that KHMDS had deprotonated the hydroxyl group of 2-propanol instead of the amine of **19a**. 2-Propanol then acted as both a solvent and a nucleophile, substituting the diethylene glycol chain to give the undesired product **32**. The doublet and septet could then be assigned to H-2 and H-1, respectively.

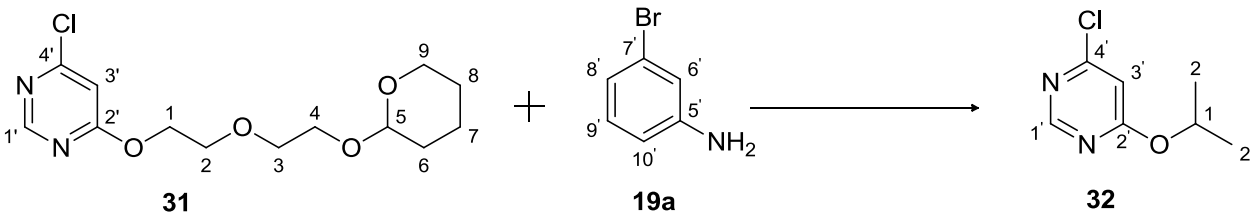

Scheme 14: Reagents and conditions: KHMDS, 2-propanol, 80°C.

Further attempts to carry out this transformation then involved varying the solvent and observing the results. The second solvent tried was DMF (Scheme 15); however, this solvent also didn't yield the desired product. Although DMF had proved to act as a nucleophile in our previous reactions (Scheme 11), that was only when the reaction temperature was raised to 120°C. At temperatures lower than 120°C DMF had not been observed to be a competing nucleophile. However, for the present reaction at 80°C instead of the nitrogen on **19b** acting as a nucleophile, ($^{-}N(Me)_2$) **28** acted as a nucleophile substituting the chlorine atom on compound **31** to give the undesired product **33**. As expected, the ^{1}H NMR spectrum of **33** was very similar to that of starting material **31** except that we now observed a prominent singlet at δ 3.06 integrating for six protons. The singlet was assigned to H-5' and that confirmed that **31** had undergone a nucleophilic substitution by **28**.

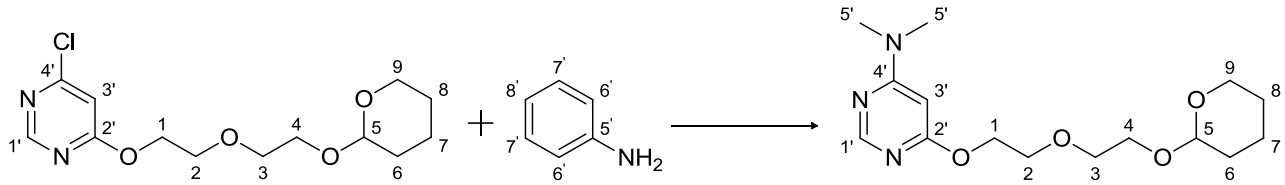

31 **19b** **33**

Scheme 15: Reagents and conditions: KHMDS, DMF, 80°C.

The next attempt was made using DMSO as a solvent. Little success was achieved for this reaction as the reaction rate was very slow. Prolonged reaction times or increasing the number mole equivalents of KHMDS proved ineffective; a small fraction of the starting material was converted into the product and the reaction would not proceed any further. In most cases more than 95% of the starting material was recovered.

After this failed attempt we then decided to try a palladium-catalysed cross-coupling reaction, employing tris-dibenzylideneacetone di-palladium [$Pd_2(dba)_3$] as a pre-catalyst and (*rac*)-BINAP as a supporting ligand (Scheme 16).

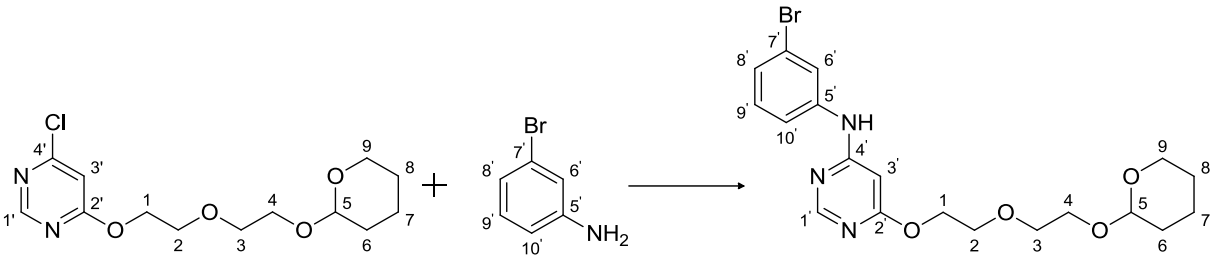

Scheme 16: Reagents and conditions: 2-4 mol% $Pd_2(dba)_3$, 6-12 mol% (*rac*)-BINAP, K_2CO_3, DMSO, 80°C, 24-96 h.

The choice of both the pre-catalyst and the supporting ligand was based on the findings of Changunda *et al.* that using $Pd_2(dba)_3$ as a palladium source and (*rac*)-BINAP as a supporting ligand was generally successful for C-N, C-O and C-S cross-coupling reactions.[61] In order to carry out the reaction, the catalyst was prepared in a round bottomed flask by adding $Pd_2(dba)_3$ and (*rac*)-BINAP in DMSO and stirred at 80°C for ten minutes under nitrogen purge. Compounds **31**, **19a** and K_2CO_3 were then consecutively added and the reaction was stirred at 80°C overnight. This afforded the desired product **29a** in 20% yield. The reaction was repeated and the isolated yield slightly increased to 22%. One of the problems with using bromoaniline **19a** is that it could participate in the cross-coupling reaction to give the homo-coupled product. Confirmation of the synthesis of compound **29a** was obtained from ^{1}H NMR spectroscopic analysis. The ^{1}H NMR spectra of compounds **29a** and **31** were very similar in the aliphatic region, however, the presence of two additional signals in the aromatic region confirmed that the amination reaction had occurred. Two singlets each integrating for one proton were observed at δ 8.35 and δ 6.16 and were assigned to H-1' and H-3', respectively. Additionally, a singlet integrating for one proton was observed at δ 7.51 and it could be assigned to H-6'. A multiplet integrating for three protons was also observed at δ 7.23 – 7.21 and it was assigned to H-8', H-9' and H-10'. To avoid the homo-coupling possibility we performed the reaction using aniline **19b**, the desired product was afforded in 25% yield. The isolated yield of 25% was undesirable. In all cases starting materials **31** and **19** were recovered. Other unidentified side products were also recovered. Analysis of the ^{1}H NMR spectrum of the side products did not give a clear indication of what they were. Prolonged reaction times and the scaling up of the catalyst loading proved ineffective for yield optimisation. To improve the yield of the metal-catalysed amination for our substrate various other factors like the choice of our supporting ligand and an alternative mediating metal would have to be investigated. However, we decided to pursue alternative reactions.

One other attempt investigated for this transformation was an acid catalysed amination (Scheme 17). It was observed that the acid played two roles: catalysing the amination reaction and deprotection of **31**. The deprotection of THP-protected alcohols under acidic conditions is a well-known reaction, but what was quite puzzling was the exact mechanism through which the acid catalysed the cross-coupling reaction. We imagined that the acid protonated the nitrogen atoms of compound **31** making the ring more electron deficient, thus activating it for nucleophilic substitution. This approach seemed to offer an advantage as two steps could be done as one. However, our initial results proved otherwise, with a lot of side products being formed which resulted in very low yields of the desired product **16a**. Upon TLC analysis, roughly six spots were observed. The crude material was purified by silica gel column chromatography and all the products that were collected in reasonable quantities were submitted for NMR spectroscopic characterisation, but only the desired product could be identified.

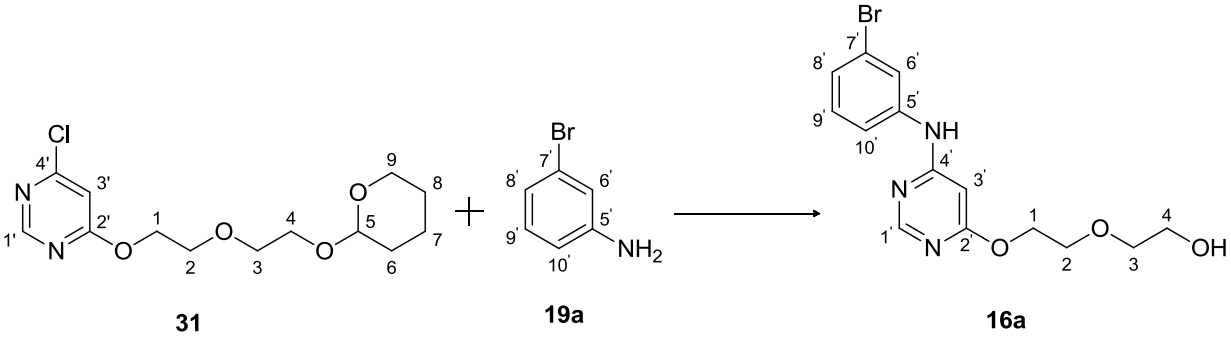

Scheme 17: Reagents and conditions: conc. HCl, 2-propanol, reflux, 24 h, 19%

The ^{1}H NMR spectrum of the product with R_f = 0.48 (94% DCM:MeOH) was confirmed to be the desired product. The ^{1}H NMR spectrum had seven signals in the aromatic region; three singlets were observed at δ 9.58, δ 8.42 and δ 6.10, each integrating for one proton and were assigned to NH, H-1' and H-3' respectively. The other four signals observed in the aromatic region were due to the 3-bromoaniline: two triplets at δ 8.02 and δ 7.26 each integrating for one proton were assigned to H-6' and H-9', and the two doublet of doublet of doublets observed at δ 7.50 and δ 7.16 which also integrated for one proton each were assigned to H-8' and H-10', respectively. The absence of the multiplet at δ 1.88 – 1.47 characteristic of H-6, H-7 and H-8 was enough proof that the deprotection had indeed taken place. Further confirmation that the amination reaction had occurred was obtained from ^{13}C NMR spectroscopy: four quaternary carbon signals were observed which indeed align with the desired compound **16a**. The IR spectrum of **16a** had a broad signal at 3378 cm^{-1}, which is characteristic of the OH group. The high resolution mass spectrum showed a molecular

ion peak at *m/z* 354.0448, consistent with the $[M+H]^+$ for $C_{14}H_{17}BrN_3O_3$ of 354.0440, further confirming the formation of product **16a**. Although the desired product **16a** had been successfully synthesised, the 19% isolated yield was undesirable and further investigations had to be carried out for improvement. To try and improve the yield the deprotection of **31** and the amination reaction were done as two separate steps.

The deprotection was carried out in the presence of hydrochloric acid catalyst in 2-propanol at room temperature to afford compound **34** as a pale yellow oil in 63% yield (Scheme 18).

31 **34**

Scheme 18: Reagents and conditions: conc. HCl, 2-propanol, r.t., overnight, 63%

As expected the ^{1}H NMR spectra of starting material **31** and product **34** were very similar; the absence of the triplet at δ 4.63 and the multiplet at δ1.88 – 1.47 in the spectrum of **34** confirmed that the deprotection had indeed taken place as these signals are characteristic of the protecting group. A new OH stretch was observed in the IR spectrum of **34** at 3406 cm^{-1}, which was further confirmation that the deprotection had occurred. Further confirmation was obtained from the HRMS spectrum of **34**, a molecular ion peak at m/z 219.0531 was observed which was in good agreement with the calculated $[M+H]^+$ for $C_8H_{12}ClN_2O_3$ of 219.0529.

The amination proceeded in the presence of HCl and afforded the desired compound **16a** in 41% yield as a pale yellow solid, as confirmed by NMR spectroscopic analysis (Scheme 19). The reaction failed to go to completion, as confirmed by TLC, but longer reaction times and addition of more of the acid catalyst seemed to be ineffective in improving the conversion.

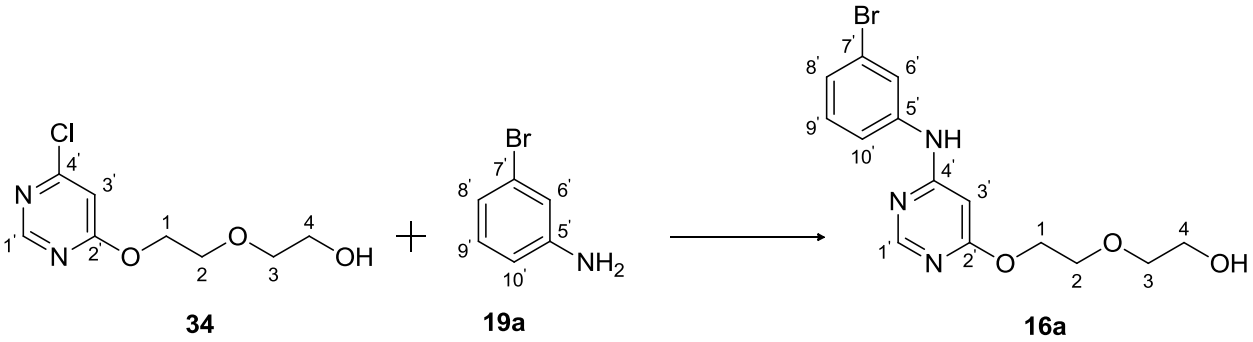

Scheme 19: Reagents and conditions: conc. HCl, 2-propanol, reflux, 48 h, 41%

A comparison of the yields obtained for the various attempts (Scheme 10 – 19) to perform the amination reaction indicated that the acid catalysed amination where we first deprotected the alcohol and then did the amination reaction gave the best yield. No further reaction conditions were investigated for the reaction.

Seven other analogues **16b-h** were then prepared through the acid catalysed amination of **34** and they all gave moderate yields of the desired compounds (Scheme 20). As expected, the ^{1}H and ^{13}C NMR spectra of the products were similar, with small changes arising depending on the aniline used for the amination reaction. Key signals of the compounds are described in Tables 1 and 2 below.

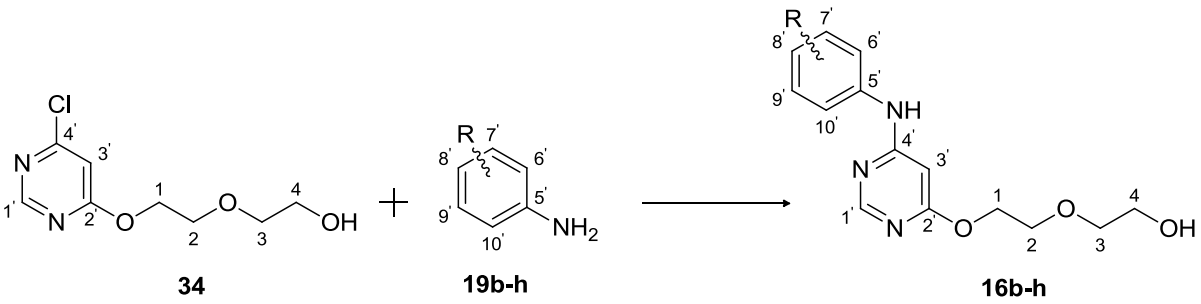

16b: R = H, 73%

16c: = 3-chloro-4-fluoro, 62%

16d: = 3-ethynyl, 29%

16e: = 3,5-dimethoxy, 54%

16f: = 3,4-difluoro, 52%

16g: = 2-chloro-4-((3-fluorobenzyl)oxy), 13%

16h: = 3-chloro-4-((3-fluorobenzyl)oxy), 9%

Scheme 20: Reagents and conditions: conc. HCl, 2-propanol, reflux, 48 h

The isolated yields were relatively good for all of the substituted anilines, with the exception of **16g & h**. This was hypothesised to be an effect of steric hindrance, as both the anilines **19g & h** are sterically more hindered than the other derivatives.

Table 1: Key signals in the ^{1}H NMR spectra of the anilino-pyrimidine alcohols **16a-h**

Compound	NH (ppm)	H-1' (ppm)	Aniline protons (ppm)	H-3' (ppm)	H-3 and H-4 (ppm)
16a	9.58 (s)	8.42 (s)	8.02 (t, H-6'), 7.50 (ddd, H-8'), 7.26 (t, H-9'), 7.16 (ddd, H-10')	6.10 (s)	3.55 – 3.44 (m)
16b	9.40 (s)	8.35 (s)	7.57 (d, H-6' and H-10'), 7.31 (t, H-7' and H-9'), 7.01 (t, H-8')	6.08 (s)	3.56 – 3.44 (m)
16c	9.91 (s)	8.43 (s)	8.01 (dd, H-6'), 7.50 (ddd, H-10'), 7.36 (t, H-9')	6.16 (s)	3.57 – 3.44 (m)
16d	9.95 (s)	8.44 (s)	7.87 – 7.83 (m, H-6'), 7.63 – 7.56 (m, H-10'), 7.33 (t, H-9'), 7.16 – 7.10 (m, H-8')	6.20 (s)	3.54 – 3.44 (m)
16e	9.36 (s)	8.37 (s)	6.84 (d, H-6' and H-10'), 6.19 (t, H-8')	6.09 (s)	3.54 – 3.46 (m)
16f	9.68 (s)	8.38 (s)	7.85 (ddd, H-6'), 7.39 – 7.30 (m, H-9'), 7.29 – 7.22 (m, H-10')	6.08 (s)	3.51 – 3.43 (m)
16g	9.36 (s)	8.35 (s)	7.81 (d, H-10'), 7.41 – 7.37 (m, H-9'), 7.21 – 7.15 (m, H-7')	6.00 (s)	3.54 – 3.46 (m)
16h	9.39 (s)	8.35 (s)	7.81 (d, H-6'), 7.38 (dd, H-10'), 7.22 – 7.13 (m, H-9')	5.99 (s)	3.52 – 3.46 (m)

Table 2: Key signals in the ^{13}C NMR spectra of the anilino-pyrimidine alcohols **16a-h**

Compound	C-4' (ppm)	C-1' (ppm)	Aniline carbon atoms (ppm)	C-3' (ppm)	C-3 (ppm)	C-4 (ppm)
16a	161.1	156.7	141.0 (C-5'), 130.1 (C-9'), 124.0 (C-8'), 121.0 (C-7'), 121.2 (C-6'), 117.7 (C-10')	88.1	71.8	59.6
16b	161.8	157.6	139.5 (C-5'), 128.7 (C-7' and C-9'), 122.5 (C-8'), 119.9 (C-6' and C-10')	87.7	72.1	60.0
16c	161.6	157.1	152.5 (d, *J* = 241.4 Hz, C-8'), 137.2 (d, *J* = 2.9 Hz, C-5'), 121.0 (C-6'), 119.9 (d, *J* = 6.7 Hz, C-10'), 119.0 (d, *J* = 20.0 Hz, C-7'), 116.8 (d, *J* = 21.8 Hz, C-9'),	88.4	72.3	60.2
16d	162.2	156.1	139.6 (C-5'), 129.9 (C-9'), 127.0 (C-8'), 123.6 (C-6'), 122.5 (C-7'), 121.6 (C-10')	88.2	72.6	60.5
16e	162.4	158.1	161.1 (C-7' and C-9'), 142.1 (C-5'), 98.6 (C-6' and C-10'), 94.6 (C-8')	88.8	72.9	60.7
16f	161.1	156.6	148.4 (dd, *J* = 243.3, 13.1 Hz, C-7'), 144.1 (dd, *J* = 240.8, 12.9 Hz, C-8'), 136.5 (dd, *J* = 9.2, 2.5 Hz, C-5'), 116.8 (d, *J* = 17.7 Hz, C-9'), 115.3 (dd, *J* = 5.7, 3.0 Hz, C-10'), 108.1 (d, *J* = 21.4 Hz, C-6')	87.8	71.8	59.6

16g	162.4	158.2	149.2 (C-8'), 134.7 (C-5'), 122.2 (C-10'), 122.0 (C-6'), 120.3 (C-9'), 115.4 (C-7')	88.2	72.9	60.7
16h	161.8	157.7	148.7 (C-8'), 134.2 (C-5'), 121.7 (C-10'), 121.5 (C-6'), 119.8 (C-9'), 114.9 (C-7')	87.7	72.3	60.2

As can be seen from Tables 1 and 2, the key signals only shifted slightly when varying the aniline substituents. Some interesting NMR spectral features were observed for the synthesised compounds. For compounds **16c** and **16f** (Figure 2.1), the expected fluorine coupling to the carbon atoms and protons was evident in their NMR spectra.

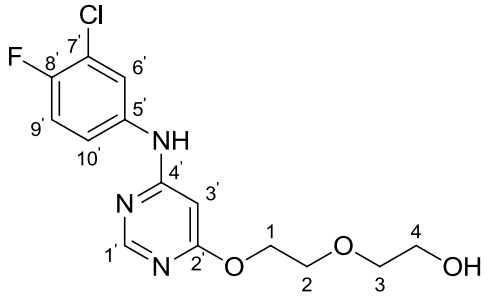

16c

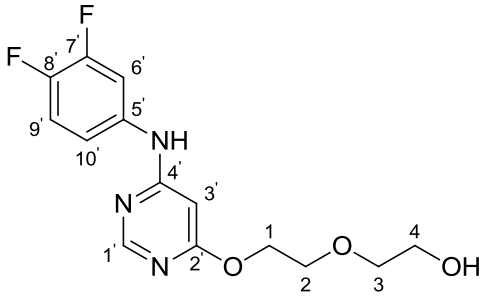

16f

Figure 2.1: Chemical structures of compounds **16c** and **16f**

Carbon-fluorine coupling constants ($J_{C\text{-}F}$) have been reported in literature; $^{1}J_{C\text{-}F} \sim 245$ Hz, $^{2}J_{C\text{-}F} \sim 21$ Hz, $^{3}J_{C\text{-}F} \sim 8$ Hz and $^{4}J_{C\text{-}F} \sim 3$ Hz. From the ^{13}C NMR spectrum of compound **16f** two similar doublet of doublet signals were observed at δ 148.4 and δ 144.1 with $J_{C\text{-}F}$ = 243.3 and 13.1 Hz and $J_{C\text{-}F}$ = 240.8 and 12.9 Hz, respectively. Comparing the observed $J_{C\text{-}F}$ to the known literature values, the observed $J_{C\text{-}F}$ values corresponded with $^{1}J_{C\text{-}F}$ and $^{2}J_{C\text{-}F}$. That then meant that each of the signals could either be assigned to C-7' or C-8'. Using the heteronuclear multiple bond correlation (HMBC) experiment, the signal at δ 144.1 had a long range correlation with H-10' but no correlation was observed with the signal at δ 148.4. Correlation between carbon atoms and protons separated by three bonds is more likely to be observed than the four bond correlation. Hence the signal at δ 144.1 was assigned to be C-8' and C-7' was assigned to the signal at δ 148.4. Assignment of the other carbon atoms was done with no difficulty: from the distortionless enhancement by polarization transfer (DEPT-

135) experiment, the doublet of doublets at ð 136.5 was the only other quaternary carbon atom with fluorine splitting ($J_{C\text{-}F}$ = 9.2, 2.5 Hz) and was assigned to C-5'. C-6', C-9' and C-10' were easily assigned using the heteronuclear single quantum correlation (HSQC) experiment. Interestingly C-6' which was expected to be a doublet of doublets was observed as a doublet with $J_{C\text{-}F}$ = 21.4 Hz. No plausible conclusion was reached as to why C-6' only coupled to the *ortho* fluorine and not to the *meta* one. The fluorine coupling to carbon atoms and protons was also seen for compounds **16g** and **16h**.

2.1.4. The synthesis of 2-{2-[4-(3-bromophenylamino)pyrimidin-6-yloxy]ethoxy}acetaldehyde 15a and analogues

The next step towards the synthesis of pyrimidine ketoamide molecules was the oxidation of an alcohol **16a** to an aldehyde **15a** (Scheme 21). Oxidation of the alcohol **16a** was initially attempted by stirring a solution of compound **16a** in DCM in the presence of Dess–Martin periodinane (DMP) **35** (Scheme 22B) at room temperature overnight.

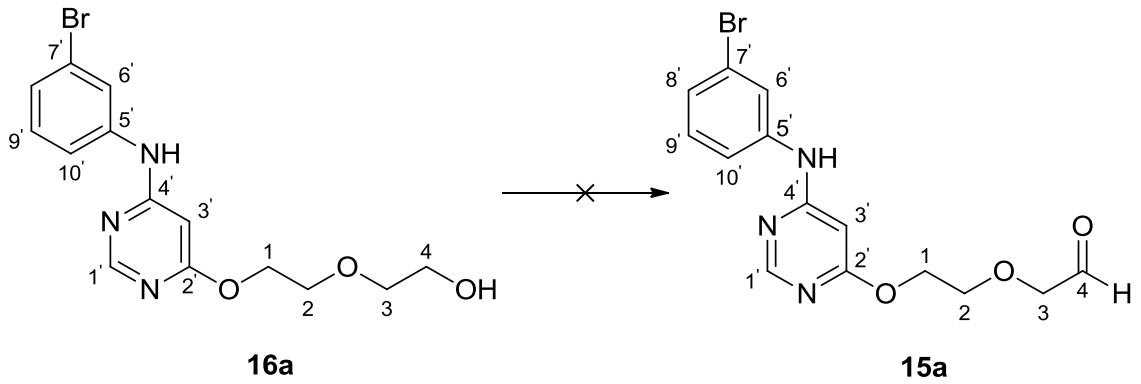

Scheme 21: Reagents and conditions: DMP, DCM, r.t., overnight, no reaction

DMP has been widely used for the oxidation of primary and secondary alcohols to aldehydes and ketones with no further oxidation of aldehydes to the carboxylic acid analogues being seen.[63,64] We chose DMP over other commonly used oxidants because it was relatively easy to prepare and store, and it was readily soluble in organic solvents. DMP can easily be prepared from 2-iodoxybenzoic acid (IBX) **36** (Scheme 22A).

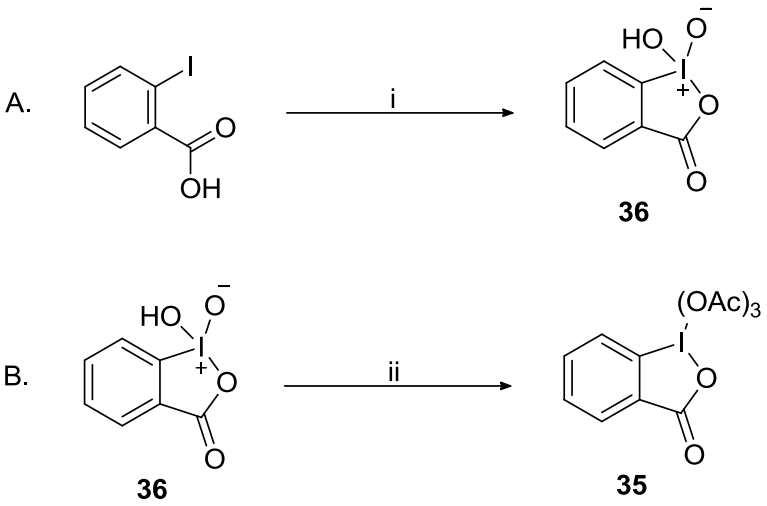

Scheme 22: Reagents and conditions: i. $KBrO_3$, 2.0 M H_2SO_4, 65 °C, 2.5 h, 81%; ii. Ac_2O, *p*-TSA, 85°C – r.t., 2 h, 77%

TLC analysis of the reaction mixture indicated the formation of a new spot with an R_f value very similar to that of the starting material **16a**. The reaction mixture was purified by silica gel column chromatography. The isolated organic material was submitted for ^{1}H NMR spectroscopic characterisation and from the ^{1}H NMR spectrum we observed a prominent singlet integrating for two protons at δ 4.21 which was characteristic of H-3 of **15a**. Unfortunately, the aldehyde **15a** was not the only compound observed from the ^{1}H NMR spectrum: we also observed the DMP by-product. The reaction was repeated following the same procedure to see if the same results would be obtained and we still isolated a mixture of compound **15a** and DMP by-product. Various other attempts were made to try and get pure **15a**, but they unfortunately all led to the same undesirable results. These results contradicted what was reported in literature, which indicates that DMP oxidation by-products can be easily removed by simple workup procedures.

Our next attempt to carry out the oxidation reaction was done using pyridinium chlorochromate (PCC) (Scheme 23, **37**) as the oxidising agent. PCC **37** is a widely used oxidant for the oxidation of alcohols one step up the oxidation ladder: primary alcohols to aldehydes and secondary alcohols to ketones. Like DMP, PCC **37** is also known for its great advantage of not further oxidising the aldehydes to carboxylic acids.[65] For this synthesis we added compound **16a** and PCC **37** into a flask containing molecular sieves in DCM. The reaction mixture was stirred at room temperature overnight. The observed crude material looked like messy black tar. TLC analysis of the mixture did not indicate the presence of either the starting material **16a**, the product **15a** or any other newly formed organic compound.

The mechanism through which the oxidation of primary alcohols to aldehydes by PCC takes place is outlined in Scheme 23. Briefly, the chlorine atom on the chromium (IV) atom is displaced by the coordination of the hydroxy group. The chlorine atom then acts as a Brønsted base abstracting a proton from the newly formed chromate ester **38**. That results in the formation of an aldehyde and the reduction of chromium(VI) to chromium(IV).

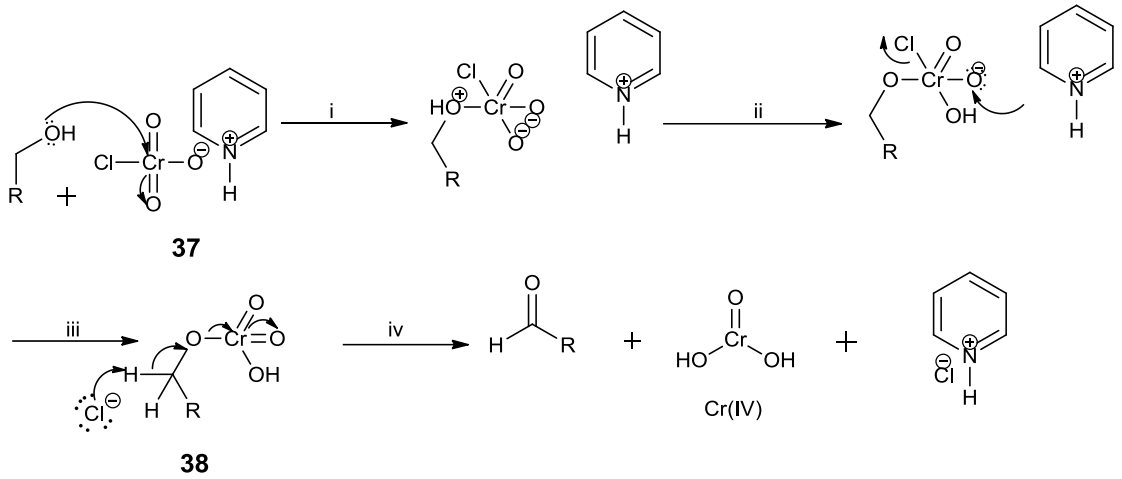

Scheme 23: Oxidation of primary alcohols to aldehydes using PCC

After unsuccessful oxidation of our alcohol **16a** we then hypothesised that any of the oxygen and nitrogen atoms in our compound **16a** could coordinate to chromium(IV) in step (i) of the PCC oxidation. We hypothesised that our compound could then get locked into that complex such that no further reaction occur. No detailed investigation was conducted to validate this hypothesis but to escape the toxicity and messy workup linked to chromium we then decided to investigate other oxidation methods.

For the next attempt we used a method described by Omura *et al.* where DMSO and trifluoroacetic anhydride (TFAA) are used as reagents for the oxidation of alcohols to aldehydes at temperatures lower than -50°C.[66] We added TFAA in DCM dropwise to a solution of DMSO in DCM at -78°C. The reaction mixture was stirred for 30 min at -78°C, whereafter compound **16a** was added and the yellow reaction mixture was stirred for a further 30 min. Triethylamine (TEA) was then added and the mixture was warmed to room temperature and stirred for 30 min. An interesting observation was that after TEA addition the colour of the reaction mixture turned from yellow to clear. This was a hopeful observation as the addition of TEA is supposed to give the desired aldehyde product. However, after stirring for about 15 min the reaction mixture became yellow again. The crude material was characterised by NMR spectroscopy. Although Omura *et al.* reported successful and high yielding oxidation of alcohols to aldehydes using this method, we unfortunately recovered starting material **16a**. This was seen from the ^{1}H NMR spectrum of the crude material where

we did not observe the significant aldehyde peak. Based on the observed colour changes, we speculated that the reaction may have reversed within the given time. The reaction was repeated to assess the effect of the reaction time and confirm the reversibility of the reaction. With regard to the observed colour changes the results were not reproducible: after TEA was added the reaction mixture remained yellow. ^{1}H NMR spectroscopic analysis of the crude material clearly indicated the presence of starting material **16a**.

At this point we decided to investigate an oxidant that was easier to prepare and required simpler reaction conditions. For this investigation we used 2-iodoxybenzoic acid (IBX) **36** as an oxidant. IBX **36** is the precursor used for the preparation of DMP **35** (Scheme 22A), hence it has the same oxidising properties as DMP **35**. IBX **36** has also been found to be effective when oxidising primary and secondary alcohols to their corresponding carbonyl compounds.[64] IBX **36** was easily prepared from 2-iodobenzoic acid in the presence of potassium bromate and sulfuric acid. We used a procedure described by Boeckman *et al.* [63]: they reported a yield of 98% while we obtained an isolated yield of 81% (Scheme 22A). The main drawback observed with IBX **36** is its limited solubility as it is insoluble in most organic solvents but it readily dissolves in DMSO.[63,64]

IBX was added to a solution of **16a** in DMSO and the reaction was stirred at room temperature. Upon TLC analysis a very small R_f shift was observed between the product and the starting material, which made it unclear whether the reaction had taken place or not. Despite the uncertainty the reaction was added to DCM and was washed three times with water and once with brine to yield **15a** as an orange solid in 86% yield. The most prominent evidence of the formation of product **15a** was observed in its ^{1}H and ^{13}C NMR spectra. The most significant change was the appearance of a singlet at δ 4.18 which integrated for two protons due to H-3. Furthermore, in the ^{13}C NMR spectrum a prominent aldehyde peak was observed at δ 200.4. This confirmed that the oxidation of the alcohol to an aldehyde had indeed taken place. The IR spectrum also indicated the absence of the OH group at 3378 cm^{-1} and a new C=O stretch was observed at 1606 cm^{-1} which was characteristic of the aldehyde. Conclusive evidence was then obtained from the HRMS of **15a** where a molecular ion peak was observed at m/z 352.0291 which was in agreement with the calculated $[M+H]^+$ for $C_{14}H_{15}BrN_3O_3$ of 352.0281. We then synthesised five other analogues **15b-f** using IBX as an oxidant (Scheme 24) and, as expected, the NMR spectra were very similar. Compounds **16g & h** were unfortunately isolated in very low yields, hence we could not oxidise them to their aldehyde analogues **15g & h**. The key diagnostic signals of the aldehyde analogues **15a-f** are tabulated in Tables 3 and 4 below.

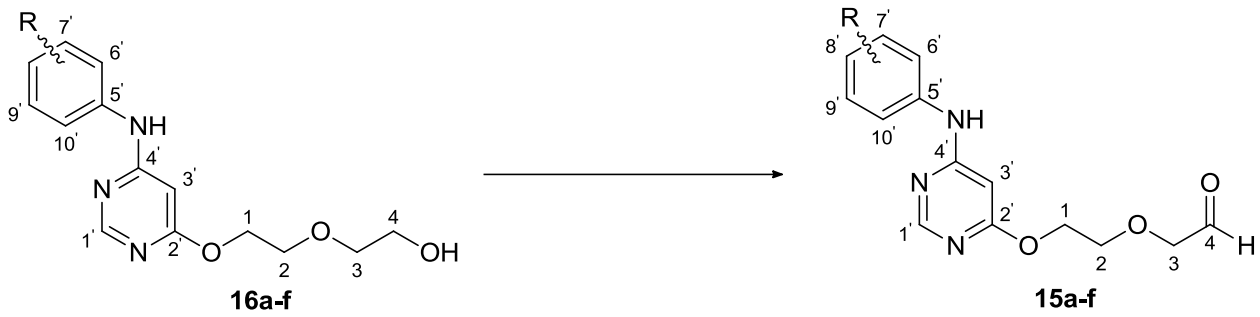

15b: R = H, 66%

15c: = 3-chloro-4-fluoro, 86%

15d: = 3-ethynyl, 62%

15e: = 3,5-dimethoxy, 61%

15f: = 3,4-difluoro, 90%

Scheme 24: Reagents and conditions: IBX, DMSO, r.t., overnight

From the isolated yields we observed that the reaction favoured substrates with electron deficient anilines. The highest isolated yield of 90% was obtained with the most electron deficient 3,4-difluoroaniline and the lowest isolated yield of 61% was obtained with the most electron rich 3,4-dimethoxyaniline.

Table 3: Key signals in the ^{1}H NMR spectra of the anilino-pyrimidine aldehydes **15a-f**

Compound	H-4 (ppm)	H-3 (ppm)
15a	9.74 (s)	4.19 (s)
15b	9.73 (s)	4.16 (s)
15c	9.72 (s)	4.18 (s)
15d	9.73 (s)	4.18 (s)
15e	9.73 (s)	4.18 (s)
15f	9.73 (s)	4.18 (s)

Table 4: Key signals in the ^{13}C NMR spectra of the anilino-pyrimidine aldehydes **15a-f**

Compound	C-4 (ppm)	C-3 (ppm)
15a	200.3	76.7
15b	200.4	76.6
15c	200.3	76.7
15d	200.3	77.6
15e	200.7	76.7
15f	200.3	76.7

The ^{1}H and ^{13}C NMR spectroscopic analysis (Tables 3 and 4) indicated that the aniline substituents had no significant effect on the key signals. The observed chemical shifts were similar for all compounds.

2.1.5. The synthesis of 2-hydroxy-*N*-isopropyl-3-{2-[4-(3-bromophenylamino)pyrimidin-6-yloxy]ethoxy}propanamide 14a and analogues

Multicomponent coupling reactions (MCRs) have been widely applied in organic chemistry and more specifically in medicinal chemistry. The Passerini reaction is one of the influential MCRs that were discovered decades ago.[67] The Passerini reaction is also the first member of the isocyanide-based MCRs; it is a three component MCR that makes use of an aldehyde/ketone, a carboxylic acid and an isocyanide to form α-acyloxy-carboxamides.[67,68] The α-acyloxy-carboxamides can then be hydrolysed to give the useful α-hydroxyamides like compound **14a** (Scheme 25).

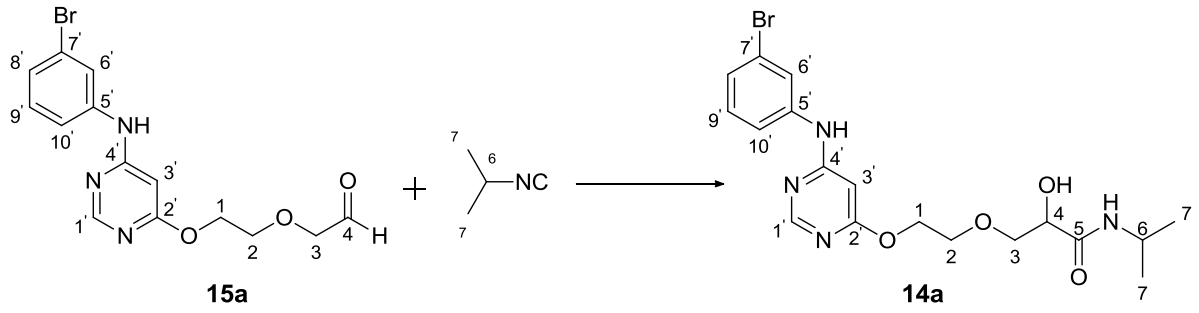

Scheme 25: Reagents and conditions: AcOH, EtOAc/DCM, r.t., 24 h. K_2CO_3, MeOH/H_2O, r.t., 3 h, 59%

For this synthesis we applied the Passerini reaction to give the α-acyloxy-carboxamide adduct **39a** (Scheme 26) which was then hydrolysed under basic conditions to give the desired product **14a**. Initially compound **15a** was dissolved in DCM and diluted with EtOAc, AcOH and isopropyl isocyanide were then added and the reaction mixture was stirred at room temperature for 24 h. Scheme 26 outlines the mechanism through which the reaction occurrs to form **39a** based on the mechanism that was proposed by Ugi.[67]

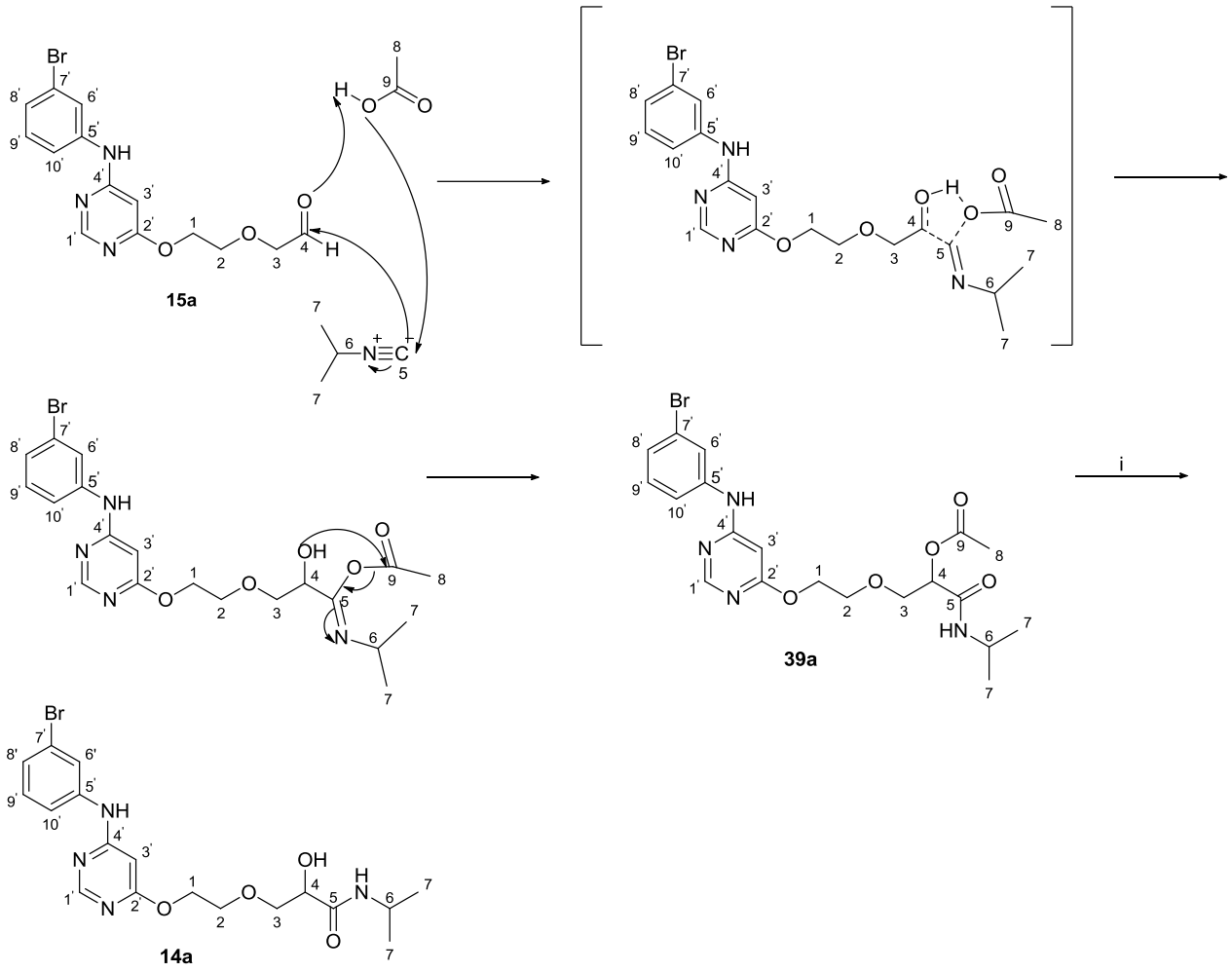

Scheme 26: Reagents and conditions: i. K_2CO_3, MeOH/H_2O, r.t., 3 h, 59%

The reaction is believed to proceed through a cyclic transition state which can either be five-membered or seven-membered depending on which oxygen atom of the carboxylic acid participates.[67] From Scheme 26 we only indicated the five-membered transition state where the hydroxyl oxygen participates, the seven-membered transition state would form when the carbonyl oxygen is participating. After stirring for 24 h we had afforded the α-acyloxy-carboxamide intermediate **39a**. Intermediate **39a** was not isolated, it was hydrolysed by dissolving in methanol in the presence of a solution of potassium carbonate (K_2CO_3) in water to afford the desired product **14a** in 59% yield.

Successful synthesis of compound **14a** was confirmed by NMR spectroscopic and HRMS analysis. In addition to the absence of an aldehyde peak from the ^{1}H NMR spectrum of **14a**, there were four main characteristic signals that differentiated it from the ^{1}H NMR spectrum of the starting material **15a**. The first one was the presence of two doublets at δ 1.16 and δ 1.13 that in total integrated for six protons. This was characteristic of H-7, where each methyl group coupled to H-6. Another characteristic peak was a multiplet, which closely resembled a septet, at δ 4.11 – 4.02 integrating for one proton. This signal was characteristic of H-6: it closely resembled a septet because it was coupled to the six methyl protons. One other characteristic peak was a triplet integrating for one proton at δ 4.22 and that was characteristic of H-4. Finally, the presence of a new NH signal at δ 6.68 confirmed that the reaction had indeed afforded the desired product **14a**. Further confirmation was obtained from the ^{13}C NMR spectrum. Firstly, no aldehyde signal was observed; instead there was a new signal at δ 170.6 that coupled to H-4 as shown by the HMBC experiment, hence it was assigned to C-5. We also observed C-4 at δ 70.3, C-6 at δ 41.2 and C-7 at δ 22.7. We obtained conclusive confirmation from the HRMS spectrum of **14a**, as a molecular ion peak was observed at m/z 439.0975, which was in good agreement with the calculated $[M+H]^{+}$ for $C_{18}H_{24}BrN_4O_4$ of 439.0963. Five other analogues **14b-f** were synthesised using this method (Scheme 27) and Tables 5 and 6 summarise the characteristic signals of the α-hydroxyamides **14a-f**. As can be seen from these tables the aniline substituents did not have any significant effect on the chemical shifts of the α-hydroxyamide group.

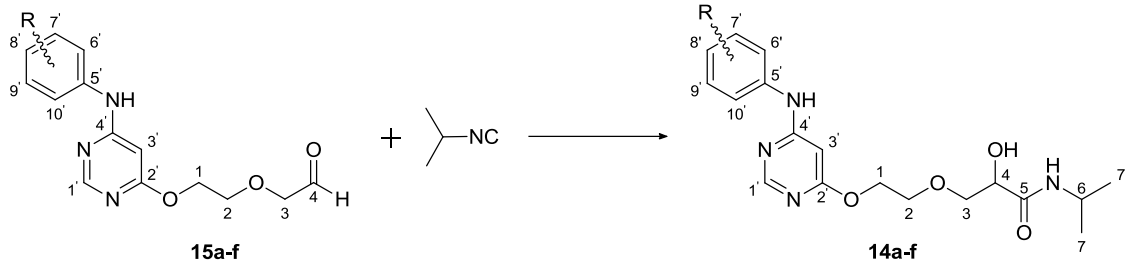

15a-f **14a-f**

14b: R = H, 36%

14c: = 3-chloro-4-fluoro, 60%

14d: = 3-ethynyl, 39%

14e: = 3,5-dimethoxy, 37%

14f: = 3,4-difluoro, 34%

Scheme 27: Reagents and conditions: AcOH, EtOAc/DCM, r.t., 24 h. K_2CO_3, MeOH/H_2O, r.t., 3 h

Table 5: Key signals in the ^{1}H NMR spectra of the α-hydroxyamides **14a-f**

Compound	NH (ppm)	H-4 (ppm)	H-6 (ppm)	H-7 (ppm)
14a	6.68 (d)	4.22 (t)	4.11 – 4.02 (m)	1.15 (d) and 1.13 (d)
14b	6.63 (s)	4.19 (t)	4.11 – 4.02 (m)	1.14 (d) and 1.12 (d)
14c	6.59 (d)	4.18 (t)	4.12 – 4.02 (m)	1.16 (d) and 1.14 (d)
14d	6.66 (d)	4.23 – 4.13 (m)	4.10 – 4.03 (m)	1.15 (d) and 1.13 (d)
14e	6.60 (d)	4.18 (t)	4.11 – 4.03 (m)	1.15 (d) and 1.13 (d)
14f	6.66 (d)	4.18 (t)	4.11 – 4.03 (m)	1.15 (d) and 1.13 (d)

Table 6: Key signals in the ^{13}C NMR spectra of the α-hydroxyamides **14a-f**

Compound	C-5 (ppm)	C-4 (ppm)	C-6 (ppm)	C-7 (ppm)
14a	170.5	70.3	41.2	22.7
14b	170.5	70.1	41.1	22.6
14c	170.4	70.2	41.2	22.6
14d	170.5	70.3	41.2	22.7
14e	170.4	70.1	41.2	22.6
14f	170.5	70.4	41.2	22.7

The pH of the reaction mixture when doing the hydrolysis step was found to be crucial for successful synthesis of **14a**. In instances where some AcOH hadn't reacted with K_2CO_3, both compounds **14a** and **39a** were isolated. For successful hydrolysis the pH had to be basic. In instances where compound **39a** was isolated, from the ^{1}H NMR spectrum it was characterised by a prominent singlet at δ 2.16 integrating for three protons. Initially the signal had been thought to be due to the presence of washing acetone. However, from the low resolution mass spectrum of **39a** two significant signals were observed at m/z 483.3 and 481.3; those were in agreement with the calculated $[M+H]^+$ for the two bromine isotopes of $C_{20}H_{26}BrN_4O_5$. After this analysis the signal was then assigned to H-8. One other significant change observed was the downfield shift of the H-4 triplet from δ 4.22 to δ 5.28 when

comparing compounds **14a** and **39a**. The carbonyl group in conjugation with the oxygen atom reduced the electron donation effect of the oxygen by withdrawing electrons from it. Hence the observed downfield shift of H-4 in compound **14a** when compared to **39a**.

2.1.6. The synthesis of 2-oxo-*N*-isopropyl-3-{2-[4-(3-bromophenylamino)pyrimidin-6-yloxy]ethoxy}propanamide 13a and analogues

The final step towards the synthesis of pyrimidine ketoamides was the oxidation of the α-hydroxy amides **14a-f** using IBX in DMSO (Scheme 28). As per the procedure described in **2.1.4**, IBX was added to a solution of compound **14f** in DMSO (Scheme 29A). The reaction mixture was stirred at room temperature overnight. The ^{1}H NMR spectrum of the crude material clearly confirmed that the oxidation had occurred. This was demonstrated by the presence of a singlet that integrated for two protons at δ 4.91; this signal was being characteristic of H-3.

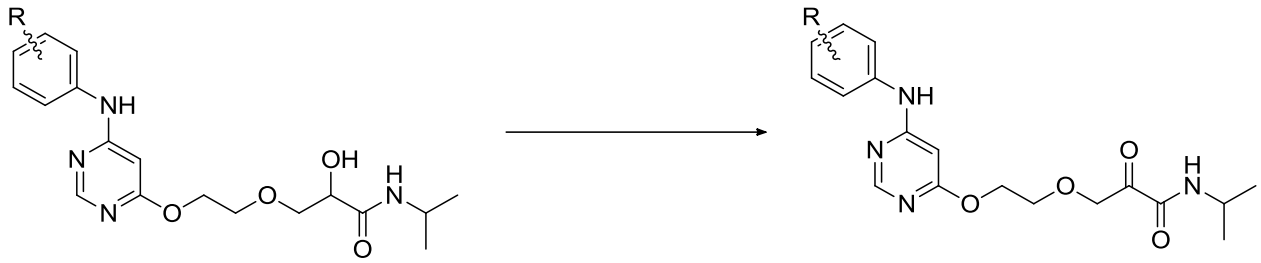

13a: R = 3-bromo

13b: = H, 70%

13c: = 3-chloro-4-fluoro, 84%

13d: = 3-ethynyl, 76%

13e: = 3,5-dimethoxy, 78%

13f: = 3,4-difluoro

Scheme 28: Reagents and conditions: IBX, DMSO, r.t., overnight

From the ^{1}H NMR spectrum of the crude material, we could see that the compound was not pure, as some unknown minor signals were observed. TLC analysis of the crude material indicated three well separated spots of equal quantity, judging from the intensity of the spots. The crude material was then purified by silica gel chromatography and the collected spots

were submitted for ^{1}H NMR spectroscopic characterization. The ^{1}H NMR spectra indicated that the first and the third spots appeared to be the same compound and no insightful information could be deduced from the middle spot.

Interestingly, the ^{1}H NMR spectra of the first and third spot did not indicate the presence of the desired product **13f**, instead they indicated the presence of an unknown compound. First of all, the singlet at δ 4.91 that was assigned to H-3 was no longer observed. Two other signals that were no longer observed were: the multiplet at δ 4.12 – 3.96 assigned to H-6 and the doublet at δ 1.20 assigned to H-7. This observation suggested that the desired product had decomposed. We hypothesised that chain cleavage had occurred to yield compound **40** (Scheme 29B).

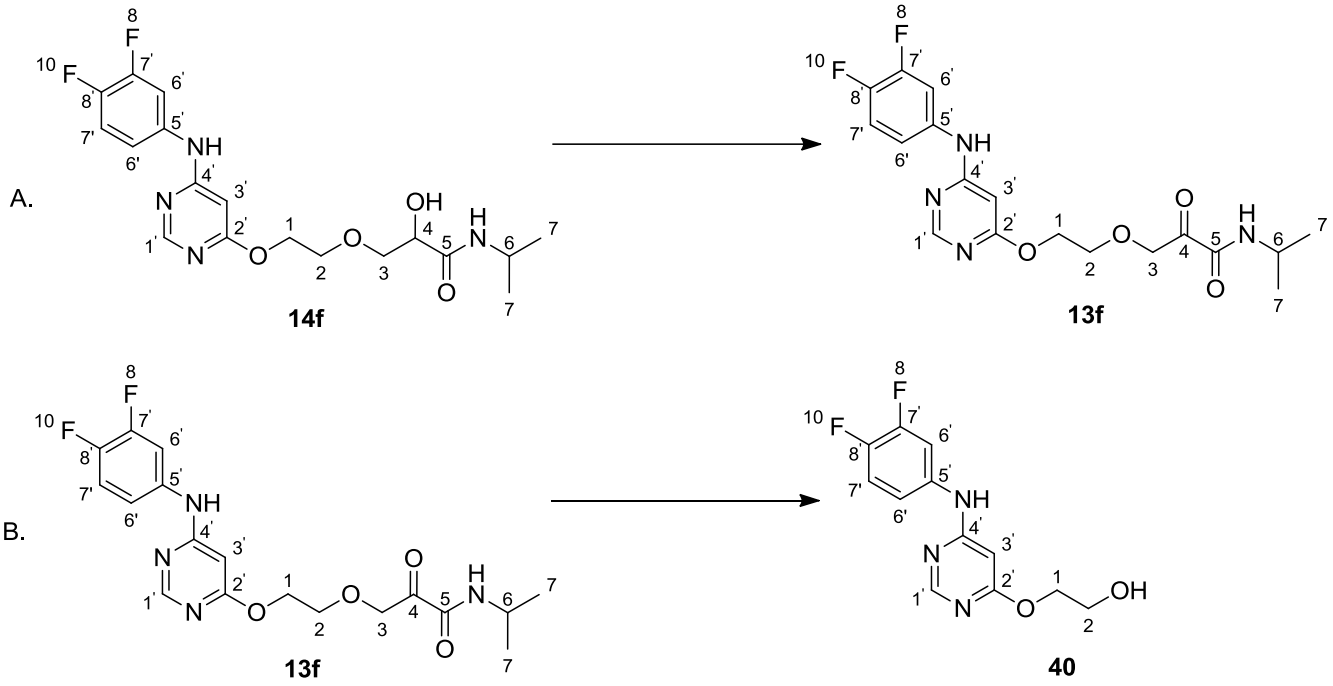

Scheme 29: Pyrimidine ketoamide cleavage

Although not clearly resolved, the ^{1}H NMR spectrum of the cleavage product had signals very similar to those of the expected product **13f** in the aromatic region. The significant difference was observed in the aliphatic region: multiplets each integrating for two protons were observed at δ 4.45 – 4.43 and δ 3.99 – 3.84. The two signals were assigned to H-1 and H-2, respectively. The observed ^{1}H NMR spectrum was in good agreement with the proposed structure of the cleavage product.

In an effort to investigate the decomposition, the reaction was repeated and the crude material was submitted for ^{1}H NMR spectroscopic analysis. The ^{1}H NMR spectrum (Figure 2.2) indicated a singlet at δ 4.90 characteristic of H-3 which confirmed that the oxidation had

taken place. Other observed signals that will be important for this discussion were: the multiplets each integrating for two protons at δ 4.56 – 4.52 and δ 3.90 – 3.85 characteristic of H-1 and H-2, respectively; and another multiplet also integrating for two protons at δ 4.09 – 3.99 which was characteristic of H-6. Since this was a crude sample, there were minor unknown signals that were observed in the spectrum and they were thought to be due to impurities.

The sample was then kept in the NMR tube at room temperature. After 24 h the sample was resubmitted for ^{1}H NMR spectroscopic analysis and not much change was observed from the original spectrum. We then left the sample in the NMR tube at room temperature for a further eight days and upon ^{1}H NMR spectroscopic analysis of the sample we observed that there was a reaction/decomposition occurring. The decomposition was suggested by the progressive increase in intensity of the minor peaks surrounding the two multiplets at δ 4.56 – 4.52 and δ 3.90 – 3.85 (Figure 2.3). We then left the sample for a further eleven days and it was clearly evident that a reaction/decomposition was taking place (Figure 2.4).

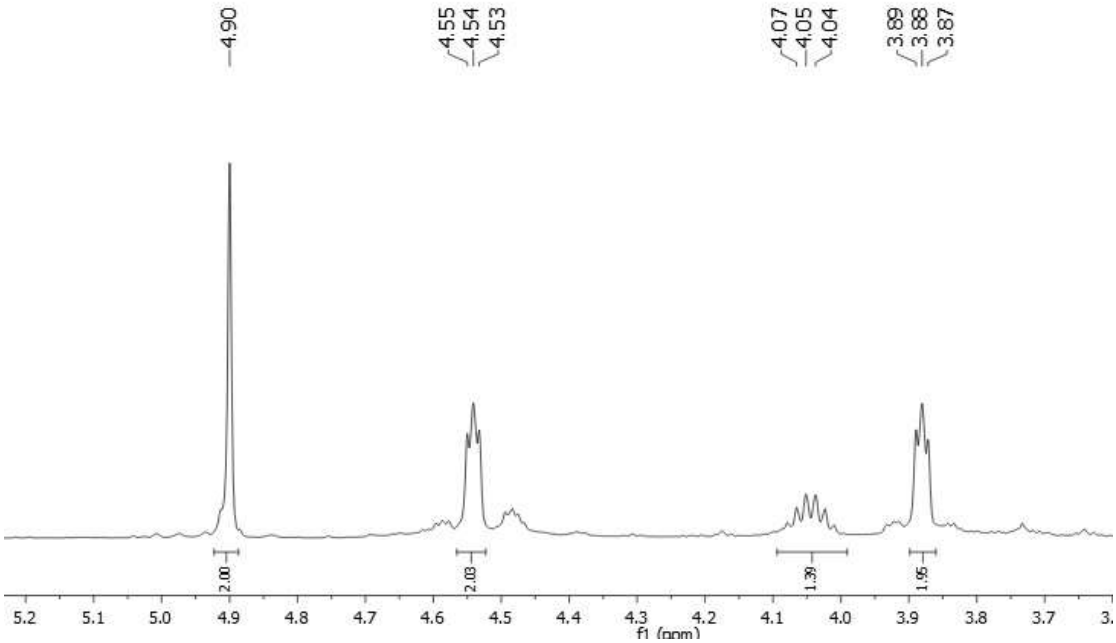

Figure 2.2: Initial ^{1}H NMR spectrum of the crude product containing **13f**

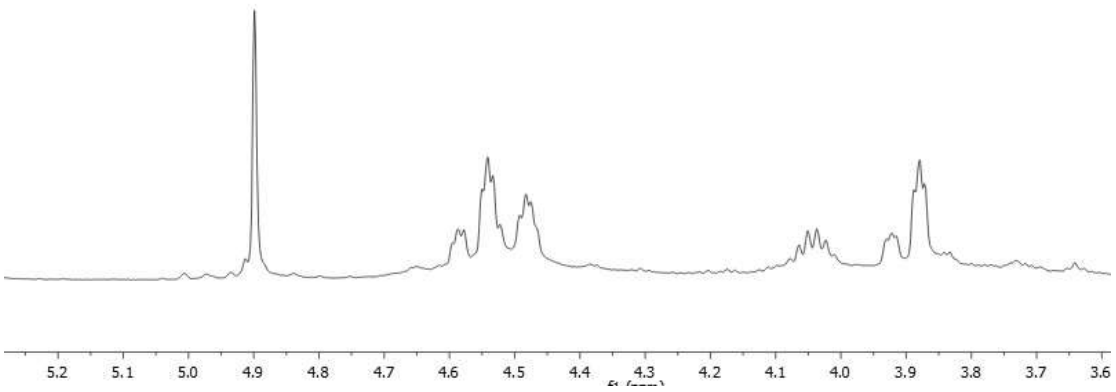

Figure 2.3: ^{1}H NMR spectrum of the crude mixture of **13f** and **40** forming after nine days

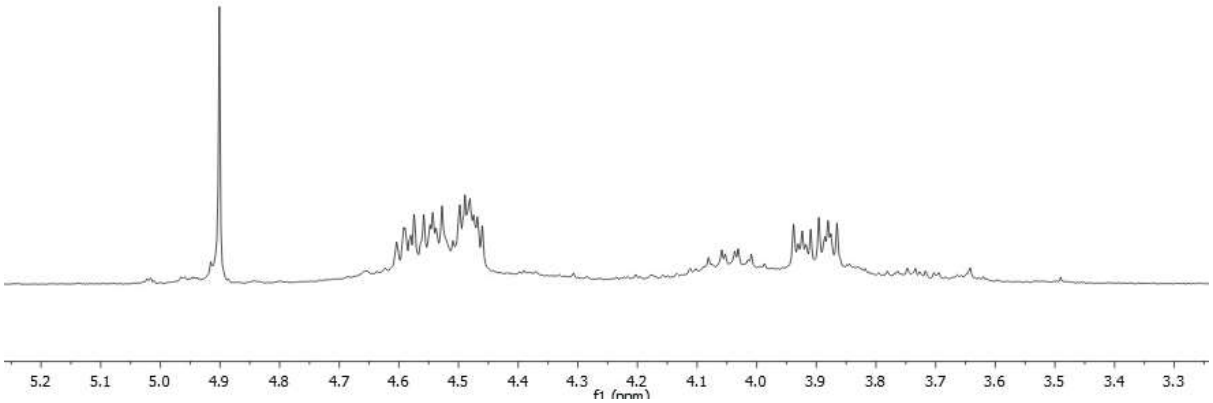

Figure 2.4: ^{1}H NMR spectrum of the crude mixture of **13f** and **40** forming after twenty days

The main observation to be made from these figures is how the minor peaks intensify over time. The fact that the compound decomposed only very slowly upon standing at room temperature gave us the idea that silica gel might be catalysing the decomposition reaction during purification. This theory was supported by the fact that we were not able to isolate the desired product **13f** when purifying our material by silica gel chromatography. The exact mechanism by which the decomposition took place was not fully investigated. Other purification methods like recrystallization and trituration were tried, but none of them resulted in the pure compound **13f**. Taking into account the very small amount of sample available, we were unable to test numerous purification methods.

Five other analogues **13a-e** were synthesised using this method (Scheme 28). After the observation that the desired compound was cleaved upon purification by silica gel column chromatography, compounds **13b-e** were fully characterised without further purification. The yields reported in Scheme 28 are for the crude product. Successful synthesis of the compounds was first confirmed by NMR spectroscopic analysis. A singlet integrating for two protons was observed at δ 4.90 for all products and this was the most significant signal

characteristic of H-3. Further confirmation was obtained from HRMS analysis. The calculated and the observed molecular ion peak masses (m/z) are tabulated in Table 7.

Table 7: Calculated and observed masses (m/z) for compounds **13b-e**

Compound	$[M+H]^+$	Calculated mass (m/z)	Observed mass (m/z)
13b	$C_{18}H_{23}N_4O_4$	359.1709	359.1714
13c	$C_{18}H_{21}ClFN_4O_4$	411.1222	411.1230
13d	$C_{20}H_{23}N_4O_4$	383.1700	383.1714
13e	$C_{20}H_{27}N_4O_6$	419.1907	419.1925

In an attempt to avoid the cleavage reaction seemingly caused by silica gel, an alternative purification of compound **13a** by high performance liquid chromatography (HPLC) using a C18 reversed phase column was tested. A mobile phase consisting of acetonitrile and water was used for the analysis which gave two broad, well-resolved peaks for our crude product. The two compounds were collected after separation by HPLC and were characterised by ^{1}H NMR spectroscopy.

No significant information could be obtained from the ^{1}H NMR spectrum of the less polar compound. From the ^{1}H NMR spectrum of the more polar compound, significant changes were only observed in the aliphatic region: two multiplets each integrating for two protons were observed at δ 4.51 – 4.44 and δ 3.96 – 3.89. To our surprise, these results revealed that the more polar compound was similar to the undesired cleaved compound **40**. In light of the observation that purification by either silica gel or C18-bonded silica led to the isolation of the cleaved product, it became clear that the cleavage reaction was not due only to silica gel. Unfortunately, we could not investigate this reaction any further due to time constraints.

2.1.7. Preliminary biological evaluation of pyrimidine ketoamides

A selection of the anilino-pyrimidine compounds that contained an electrophilic carbon atom, **13-16**, were evaluated for preliminary anticancer activity in an *in vitro* MTT assay on five different cancer cell lines. The assays were done by Dr Leonie Harmse (Wits School of Pharmacy and Pharmacology). The preliminary evaluation was done on the Caco-2 (colorectal cancer), MCF7 (breast cancer), SF268 (glioblastoma), A549 (lung cancer) and H1975 (lung cancer) cell lines. All the cells were exposed to 5 and 50 μM of our test compounds to determine those with cell viability of less than 50% after 48 h exposure. Four

repeat experiments were done for each cell assay and no activity was observed for the colorectal cancer, A549 and H1975 lung cancer cell lines.

Of all the compounds tested for *in vitro* anticancer activity, compounds **15a** and **15c** (Figure 2.5) were found to be the most active. However, these compounds were only active at high concentrations (50 µM) on the MCF7 breast cancer and SF268 glioblastoma cell lines (Figures 2.6 and 2.7).

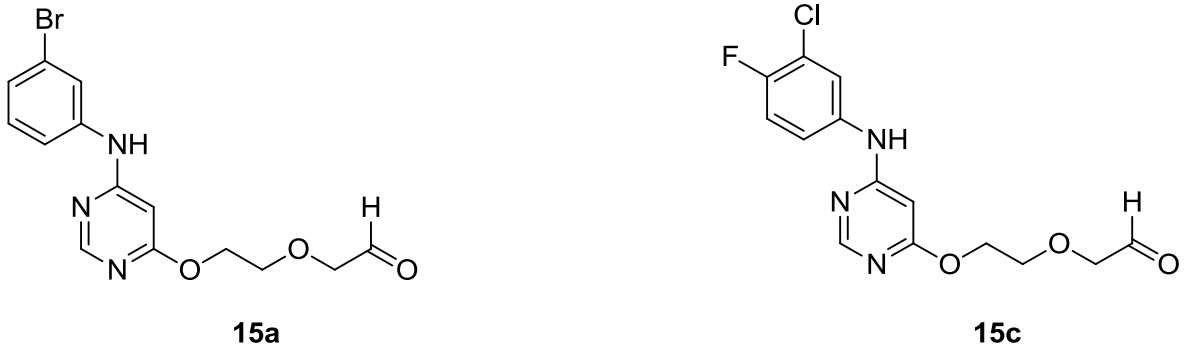

Figure 2.5: Anilino-pyrimidine analogues that displayed preliminary activity against the MCF7 breast cancer and glioblastoma cell lines.

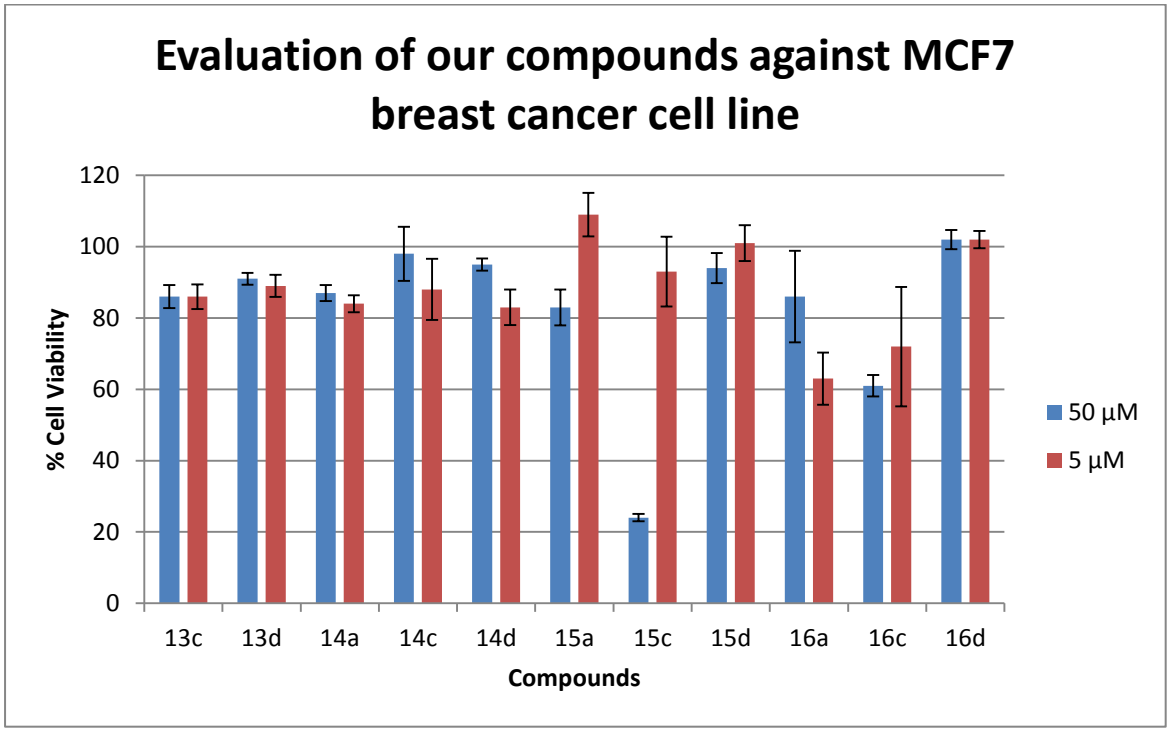

Figure 2.6: Evaluation of our test compounds against MCF7 breast cancer cell line

As can be seen in Figure 2.6, compound **15c** was found to be the most active against the MCF7 breast cancer cell line, and the IC_{50} value of this compound was determined to be 48.74 μM.

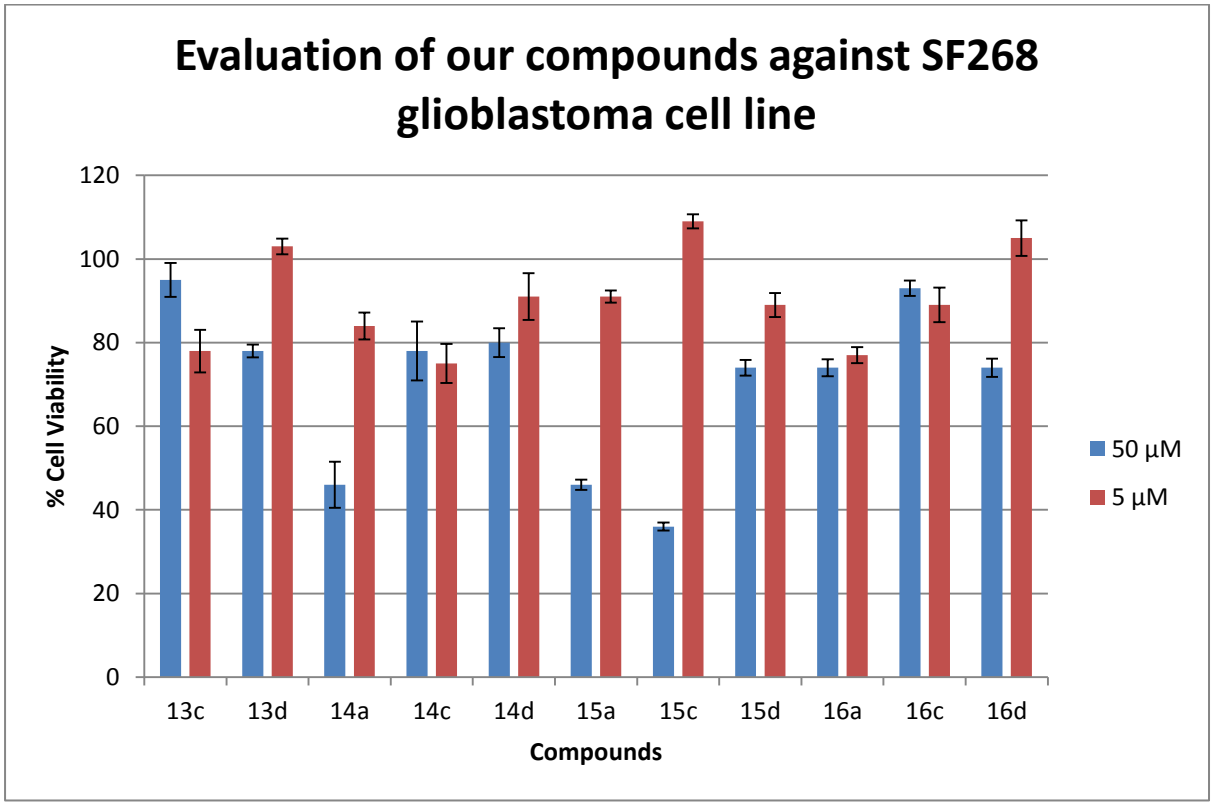

Figure 2.7: Evaluation of our test compounds against the glioblastoma cell line

Figure 2.7 indicates that compounds **15a** and **15c** were active against the glioblastoma cell line. The most active test compound was found to be **15c** and an IC_{50} value of 30.75 μM was determined.

Therefore, from our series of compounds the aldehyde warhead was the one that proved to be the most active. This could be due to the fact that aldehydes can also participate in reversible binding with the cysteine thiol in a similar mechanism to the one described in Scheme 2 (Chapter 1) for the ketoamide warhead. Overall, the results indicated that our compounds were not very active against the cancer cell lines tested. Even though compounds **15a** and **15c** showed some activity in the cell-based assays, the mode of inhibition of cell growth has not been tested. To determine whether or not they are active against EGFR, their activity in an enzymatic (EGFR) inhibition assay would need to be evaluated.

2.2. Attempted synthesis of pyrimidine ketoesters

In another aspect of this project we attempted the synthesis of pyrimidine ketoesters. Based on literature results we realised that we could access the ketoester functional group from our already synthesised aldehydes **15a-b**. Scheme 5 in **1.5.2** outlined the retrosynthetic strategy towards the desired ketoester molecules. Scheme 30 below outlines the synthetic plan. The synthesis began with the preparation of cyanohydrins **22a-b**. These compounds were then subjected to hydrolysis and esterification conditions in an attempt to obtain the desired α-hydroxy esters **21a-b**. The final step was planned to be the oxidation of the α-hydroxy ester compounds **21a-b** to yield the final ketoesters **20a-b**.

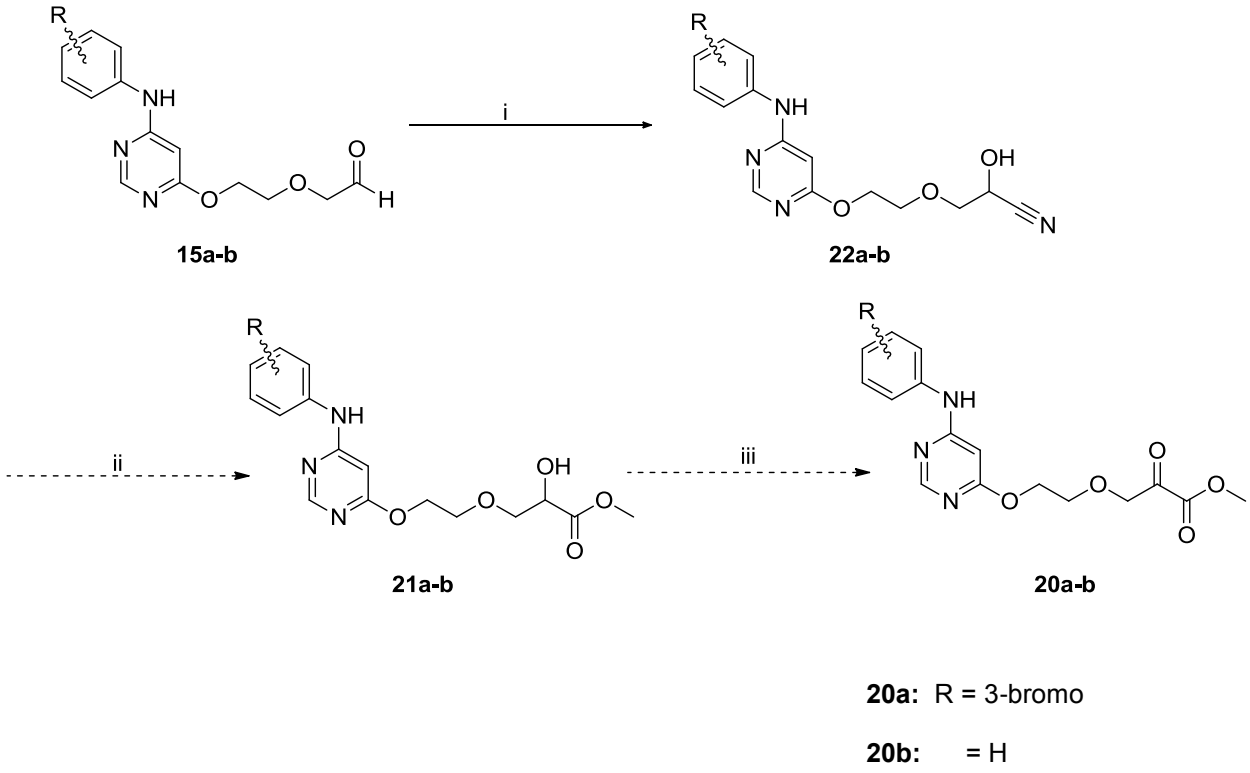

20a: R = 3-bromo

20b: = H

Scheme 30: Outline of the proposed synthetic route towards pyrimidine ketoesters **20a-b**

2.2.1. The synthesis of 2-hydroxy-3-{2-[4-(3-bromophenylamino)pyrimidin-6-yloxy]ethoxy}propanenitrile 22a and analogue

The attempt towards synthesis of α-ketoesters began with the synthesis of cyanohydrin **22a** (Scheme 31). Cyanohydrins have been identified as useful intermediates for the synthesis of α-hydroxy aldehydes, ketones and esters. Cyanohydrins can be prepared by a reaction which involves an aldehyde or a ketone, sodium bisulfite ($NaHSO_3$) and excess amounts of sodium cyanide (NaCN) or potassium cyanide (KCN).[68] We preferred this method as it does not use the hazardous hydrogen cyanide.

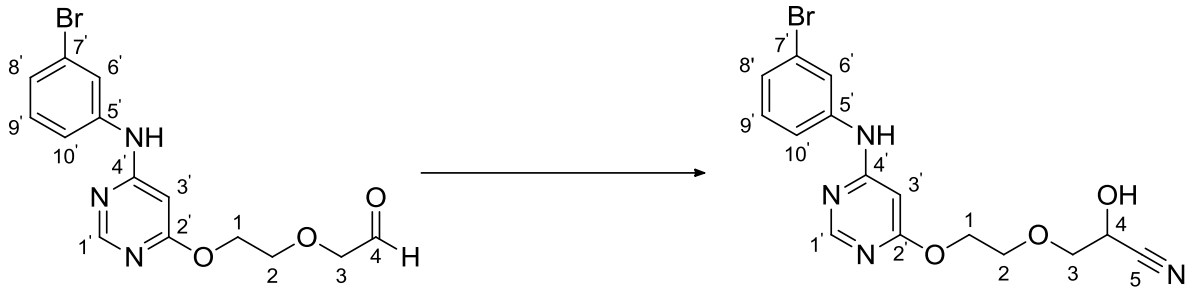

Scheme 31: Reagents and conditions: $NaHSO_3$, $MeOH/H_2O$, 0°C, 2 h. KCN, H_2O, r.t., overnight, 19%

The reaction is believed to proceed by the mechanism postulated in Scheme 32. The first step of this reaction is the formation of the bisulfite addition product. This reaction is reversible and addition of KCN reverses the formation of the bisulfite adduct regenerating the aldehyde **15a**. The cyanide anion attacks the carbonyl carbon to give the cyanohydrin anion, which abstracts a proton from the bisulfite compound to give the desired cyanohydrin **22a**. In order to carry out the reaction, a solution of aldehyde **15a** in MeOH was added to a solution of $NaHSO_3$ in H_2O at 0°C. The isolated yield of product **22a** was very low, only 19% and this was postulated to be due to the reversible nature of the cyanohydrin formation reaction.

The synthesis of compound **22a** was confirmed by NMR spectroscopy and HRMS. The ^1H NMR spectrum of **22a** did not show the aldehyde signal. A singlet integrating for one proton was observed at δ 4.69 and this was characteristic of OH. One other characteristic signal was a triplet integrating for one proton at δ 4.60 and from the COSY experiment this signal was coupled to H-3. This signal was then assigned to H-4. Clear evidence of the formation of the desired product was obtained from the ^{13}C NMR spectrum where a signal at δ 118.2 was observed. This signal was characteristic of a nitrile carbon atom, hence it was assigned to C-5. The signal characteristic of C-4 was observed at δ 60.8. Conclusive confirmation was obtained from HRMS as a molecular ion peak was observed at m/z 379.0400 which was in good agreement with the calculated $[M+H]^+$ for $C_{15}H_{16}BrN_4O_3$ of 379.0390.

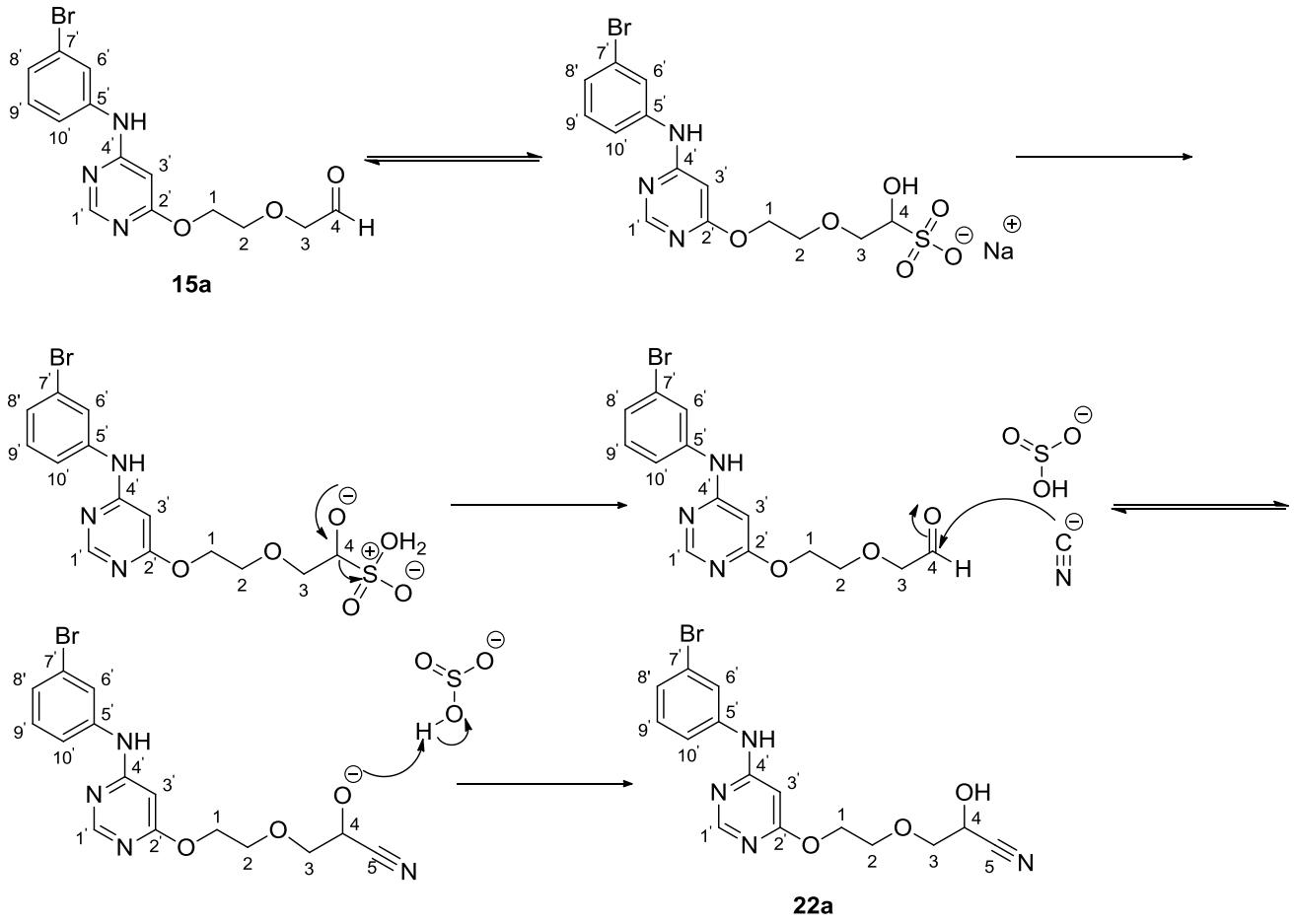

Scheme 32: Proposed mechanism for the formation of cyanohydrin **22a**

Despite the low isolated yield, one other analogue **22b** was successfully synthesised using the procedure (Scheme 33). Similar to compound **22a**, the most significant change in the ^{1}H NMR spectrum of cyanohydrin **22b** was the formation of a multiplet at δ 3.95 – 3.83 which was due to the hydroxyl proton. H-4 was observed as a triplet at δ 4.60. The prominent nitrile carbon atom C-5 was observed as a signal at δ 118.4 in the ^{13}C NMR spectrum. The C-4 signal was observed at δ 60.7. From HRMS, we observed a molecular ion peak at m/z 301.1295 which corresponded with the calculated $[M+H]^+$ for $C_{15}H_{17}N_4O_3$ of 301.1295.

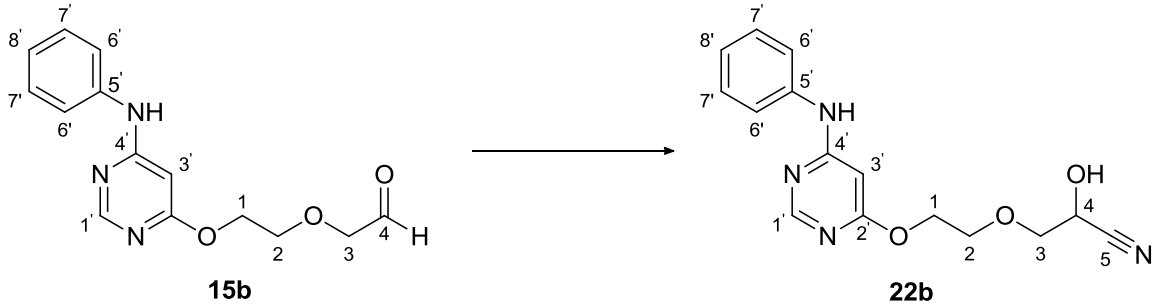

Scheme 33: Reagents and conditions: $NaHSO_3$, $MeOH/H_2O$, 0°C, 2 h. KCN, H_2O, r.t., overnight, 24%

2.2.2. The attempted synthesis of methyl 2-hydroxy-3-{2-[4-(3-bromophenylamino)pyrimidin-6-yloxy]ethoxy}propanoate 21a and 21b

The next step towards ketoester synthesis was the conversion of the nitrile group to an ester by hydrolysis followed by doing an esterification reaction to afford the desired product. A variety of hydrolysis and esterification procedures have been described in the literature. We followed a procedure that was described by Matsuda *et al.*,[70] mainly because they reported high yields when doing this hydrolysis followed by esterification reaction and the substrates they were working on were similar to ours.

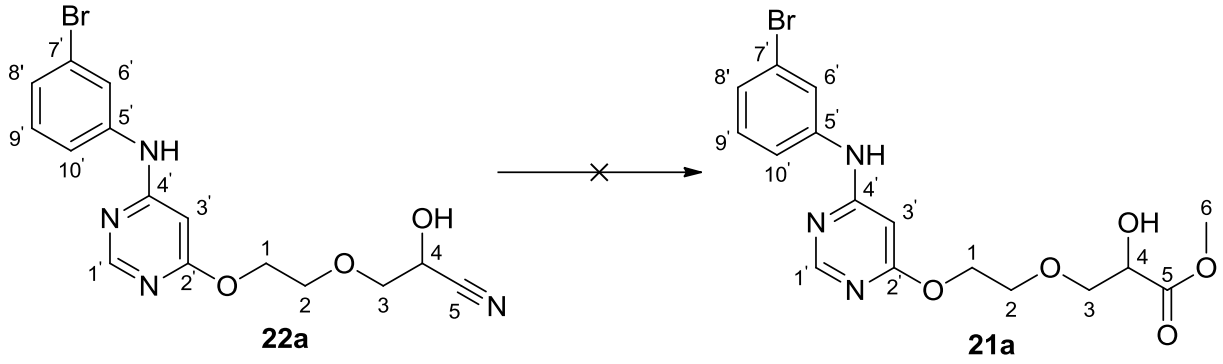

Scheme 34: Reagents and conditions: H_2SO_4, MeOH/H_2O, 60 – 70°C, 4 h. MeOH, reflux, overnight.

For this synthesis; a solution of compound **22a** (Scheme 34) in MeOH/H_2O was added dropwise to a round bottomed flask containing 98% sulfuric acid. This mixture was heated for 1 h at 60°C, thereafter it was heated at 70°C for a further 3 h. At this point we assumed that the hydrolysis reaction to afford the carboxylic acid derivative of compound **21a** was complete. We did not attempt to isolate the carboxylic acid but proceeded directly to the next step. Excess MeOH was added and the reaction was refluxed overnight in an attempt to carry out the esterification reaction. The product was isolated as a light yellow solid in 12% yield.

The isolated yield was very low compared to the reported literature yield of 88%.[70] Various factors could contribute to the very low isolated yields, but one interesting observation that was made was that upon purification some of aldehyde **15a** was recovered. Starting material **22a** was purified prior to doing this reaction, and the presence of the aldehyde **15a** in the final reaction mixture suggested that our reaction conditions were reversing cyanohydrin formation to give the aldehyde **15a**.

The isolated product was characterised by NMR spectroscopy. From the ^{1}H NMR spectrum the main difference observed was the presence of a singlet at δ 3.39 integrating for six protons. This was not in correspondence with the expected results of the desired product

21a: for compound **21a** the singlet would have to integrate for three protons and it would be characteristic of H-6. No major shift was observed for the signal characteristic of H-4, it was observed as a triplet at δ 4.52. From the ^{13}C NMR spectrum it was clear that the nitrile group had reacted as the nitrile carbon signal at δ 118.2 was no longer observed. Interestingly, however, it was observed from the HSQC experiment that the C-4 signal had shifted to a region characteristic of an acetal functional group. The signal was observed at δ 102.8 and it led to the hypothesis that under our reaction conditions we had formed an acetal instead of the α-hydroxy ester.

Scheme 35 outlines the proposed mechanism for the formation of the acetal compound **41a**. It appears that under our reaction conditions the cyanohydrin **22a** eliminates CN^- to form the aldehyde **15a**. This explains why we recovered aldehyde **15a** during purification by silica gel chromatography. In the presence of an acid and methanol, the aldehyde then undergoes functional group interconversion to form an acetal as shown in Scheme 35.

This theory was supported by the HRMS analysis of compound **41a** as a molecular ion peak was observed at 398.0710 which was in good agreement with the calculated $[M+H]^+$ for $C_{16}H_{21}BrN_3O_4$ of 398.0708.

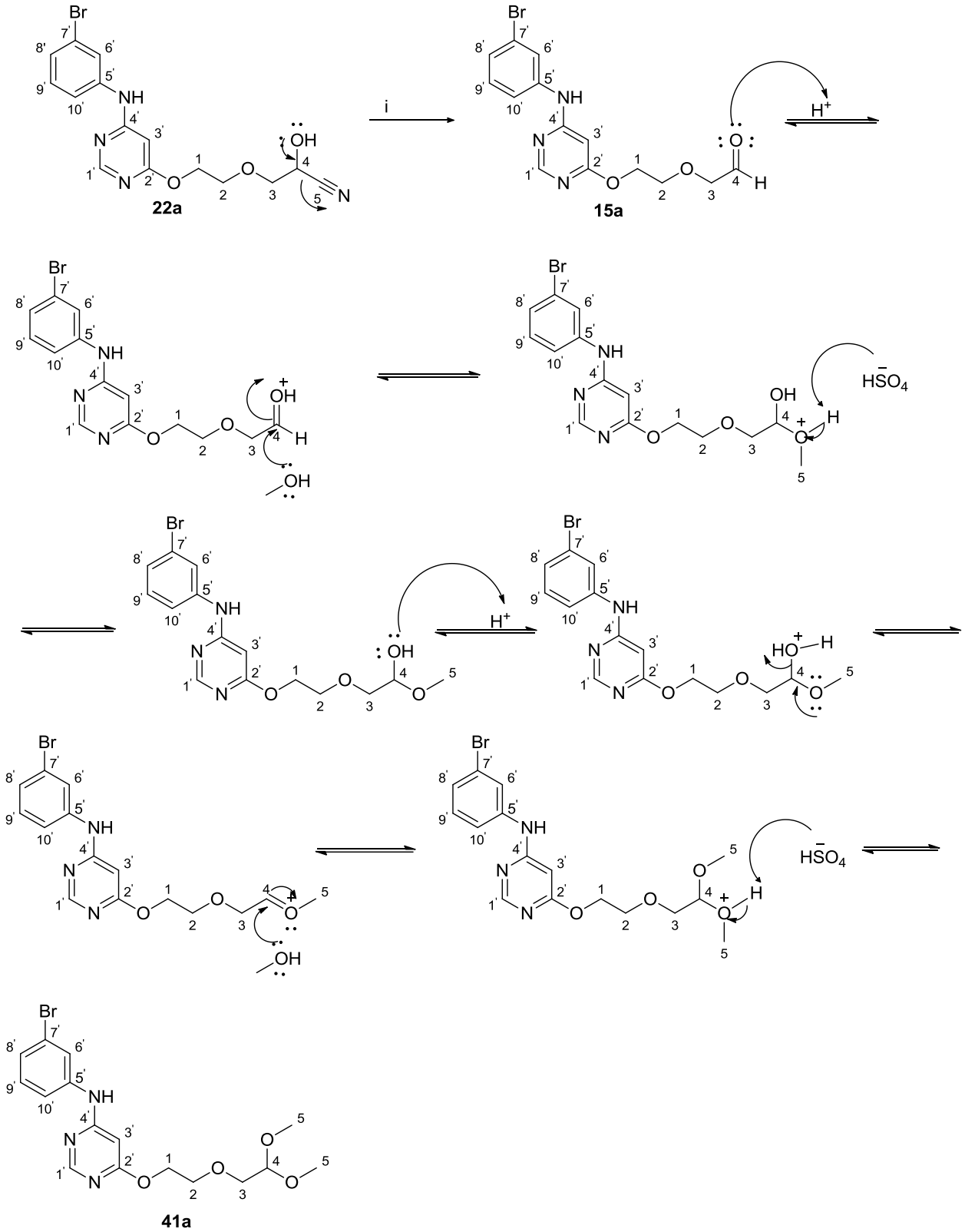

Scheme 35: Proposed mechanism for the formation of acetal **41a**

Compound **22b** was subjected to the same reaction conditions and the same results were observed (Scheme 36). The formation of the acetal **41b** was confirmed by NMR spectroscopy and HRMS. From the ^{1}H NMR spectrum H-5 was observed at δ 3.39 as a singlet integrating for six protons. From the ^{13}C NMR spectrum the significant acetal carbon atom, C-4, was observed at δ 103.3. Conclusive confirmation was obtained from HRMS, where we observed a molecular ion peak at m/z 320.1605 which corresponded with the calculated $[M+H]^{+}$ for $C_{16}H_{22}N_3O_4$ of 320.1608.

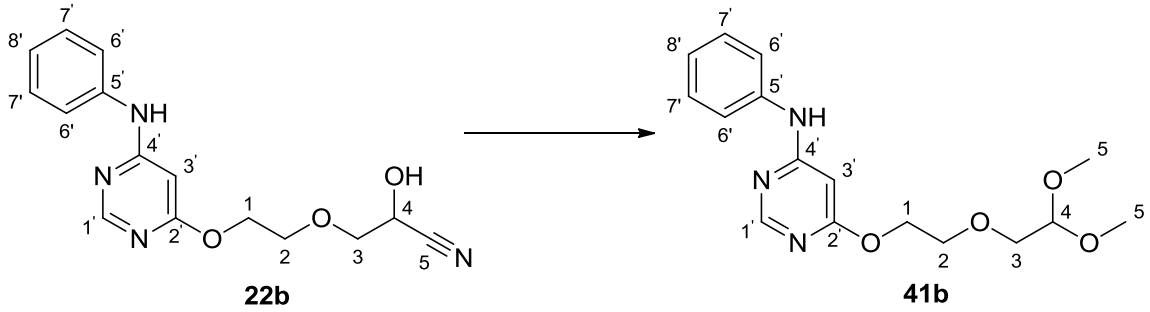

Scheme 36: Reagents and conditions: H_2SO_4, $MeOH/H_2O$, 60 – 70°C, 4 h. MeOH, reflux, overnight, 25%

Alternative reactions would have to be investigated for successful synthesis of compounds **21a-b**. We were, unfortunately, unable to investigate other reactions due to time constraints. Hence, the oxidation of compounds **21a-b** to give the target pyrimidine ketoesters **20a-b** could not be carried out (Scheme 30).

CHAPTER 3: CONCLUSIONS AND FUTURE WORK

The primary aim of this project was to synthesise potential covalent-reversible EGFR-TKIs for anticancer treatment. As a novel class of EGFR-TKIs we chose to synthesise pyrimidine ketoamide and ketoester molecules. The synthesis of the pyrimidine ketoamide compounds began with the protection of one hydroxy group of diethylene glycol using tetrahydropyran. The resultant product was coupled with 4,6-dichloropyrimidine to afford 4-chloro-6-{2-[2-(tetrahydro-2*H*-pyran-2-yloxy)ethoxy]ethoxy}pyrimidine **31** in 54% yield.

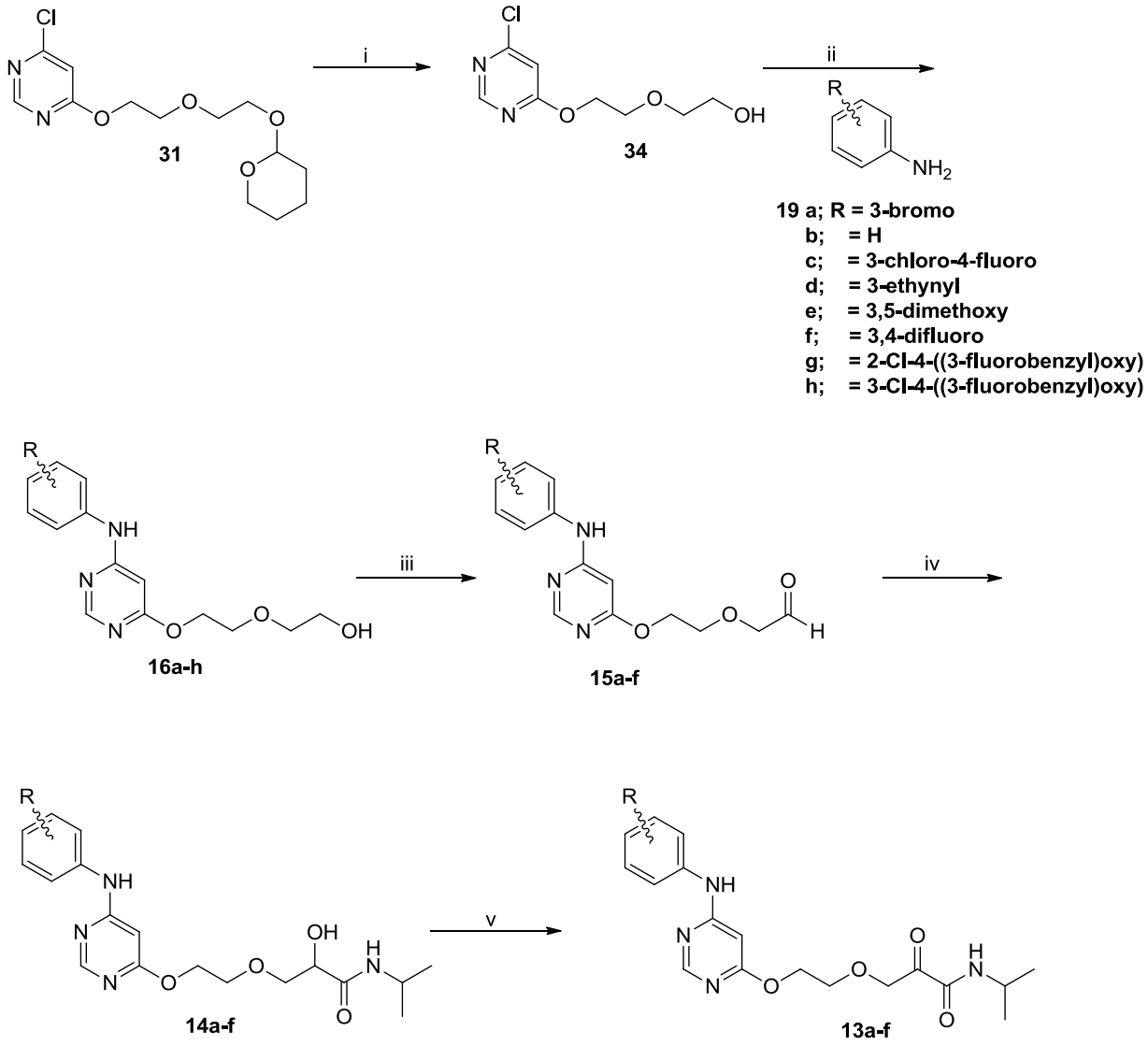

Scheme 37: Reagents and conditions: (i) conc. HCl, 2-propanol, reflux, overnight; (ii) conc. HCl, 2-propanol, reflux, 48 h; (iii) IBX, DMSO, r.t., overnight; (iv) AcOH, EtOAc/DCM, r.t., 24 h. K_2CO_3, MeOH/H_2O, r.t., 3 h; (v) IBX, DMSO, r.t., overnight.

Initially, the deprotection step (i) and amination reaction in step (ii) were done over one step under acidic conditions. The deprotection of THP-protected alcohols under acidic conditions is a well-known reaction, but it was quite interesting to observe that the acid catalysed the cross-coupling reaction in the exact mechanism. This approach was an advantage as we could do two reactions over step, however, the isolated yields were very low. This was due to the various side products that would form when the two transformations were done as one; hence we resorted to doing the deprotection and amination reaction as two separate steps.

The deprotection of the hydroxy group of 4-chloro-6-{2-[2-(tetrahydro-2*H*-pyran-2-yloxy)ethoxy]ethoxy}pyrimidine was done under acidic conditions in step (i) (Scheme 37) producing the desired 2-[2-(4-chloropyrimidin-6-yloxy)ethoxy]ethanol **34** in a fairly good 63% yield. We then did the amination reaction between 2-[2-(4-chloropyrimidin-6-yloxy)ethoxy]ethanol **34** and various aniline substrates **19**, step (ii) (Scheme 37). Various reaction conditions were tried for this coupling reaction: base catalysed, Pd catalysed and acid catalysed amination. To our surprise the acid catalysed amination gave the best yields for almost all anilines (52-75%), with the exception of three anilines. The two sterically hindered anilines 2-chloro-4-((3-fluorobenzyl)oxy)aniline **19g** (13%) and 3-chloro-4-((3-fluorobenzyl)oxy)aniline **19h** (9%) gave very poor yields, this was speculated to be due to steric effects. The amination reaction products **16** were then subjected to oxidation in step (iii) using IBX to yield their aldehyde derivatives **15** in good yields (61-90%). After successful synthesis of the aldehyde derivatives, the Passerini reaction was then employed using the aldehydes **15**, acetic acid and isopropyl isocyanide; to yield the desired α-hydroxy amides **14** (step (iv)). The final step of this synthesis was the oxidation of the α-hydroxy amide system using IBX to afford the targeted α-ketoamides **13**.

In an attempt to purify the α-ketoamide compounds we used a silica gel column, but we unfortunately only isolated an unexpected product **40** (Scheme 38). The observed cleavage reaction was hypothesised to be induced by silica gel, hence we attempted to purify the ketoamide compound using an HPLC C18 column. Unfortunately, we still isolated the unexpected compound **40**. In future, it would be valuable to determine whether the cleavage reaction has anything to do with purification, or if it is self-destruction of the compounds.

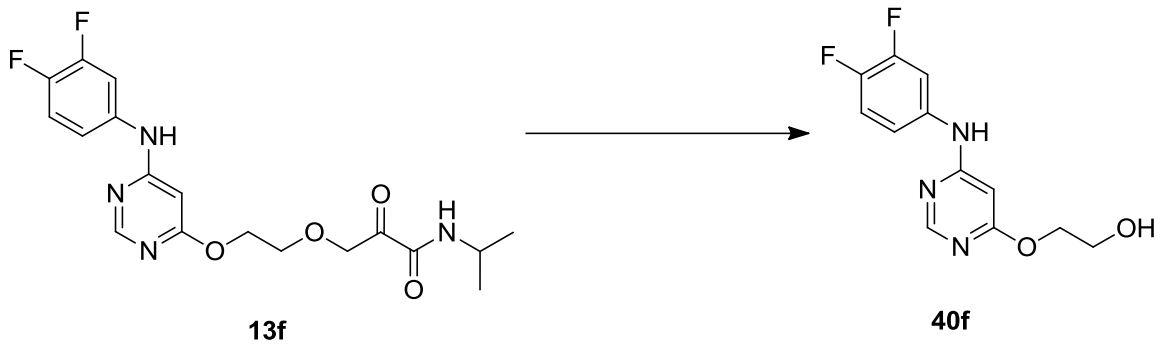

Scheme 38: Pyrimidine ketoamide cleavage reaction

In the second part of this project we attempted to synthesise pyrimidine ketoester compounds (Scheme 39). The synthesis began from the already synthesised aldehyde **15**, which was subjected to functional group conversion in step (i) to give the cyanohydrin **22** using potassium cyanide. In an attempt to produce the α-hydroxy ester **21**, compound **22** was subjected to acidic conditions in methanol in step (ii). Although other researchers have reported success with this kind of reaction in literature, we unfortunately did not get the desired product **21**. Instead, we isolated the acetal **41** of the original aldehyde. This observation was a result of the cyanohydrin **22** undergoing an elimination of cyanide to give the original aldehyde. In the presence of excess methanol and acid the aldehyde was then converted to the acetal **41**. It would be necessary in future to investigate other methods that could successfully produce the α-hydroxy ester compound **21**. Alternatively, biocatalysts such as nitrilase could be used to directly convert the cyanohydrin **22** to the carboxylic acid which, after esterification, would give the targeted α-ketoester **20**, step (iii).

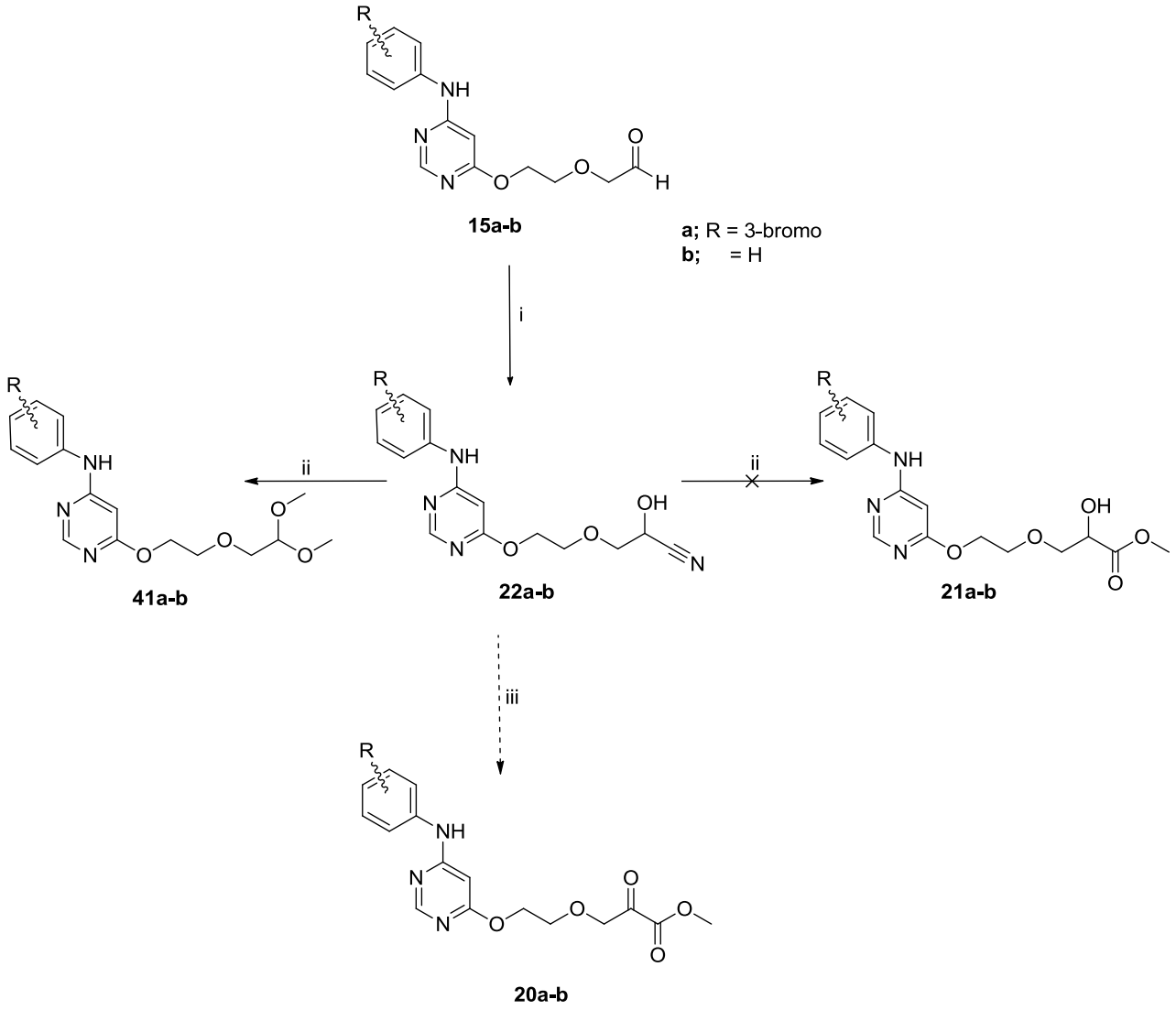

Scheme 39: Reagents and conditions: (i) $NaHSO_3$, $MeOH/H_2O$, 0°C, 2 h. KCN, H_2O, r.t., overnight (ii) H_2SO_4, $MeOH/H_2O$, 60 – 70°C, 4 h. MeOH, reflux, overnight

In a preliminary biological evaluation, a selected number of the anilino-pyrimidine analogues were assessed for anticancer activity in an *in vitro* MTT assay on five different cell lines. In the MCF7 (breast cancer) screen, only the aldehyde **15c** was found to display activity at 50 µM with an IC_{50} = 48.74 µM. In the SF268 (glioblastoma) screen, the aldehydes **15a** and **15c** were found to be active at 50 µM, aldehyde **15c** was found to have an IC_{50} = 30.75 µM. What was interesting was that none of our pyrimidine ketoamide compounds were active; this then brought up the intriguing question of whether the observed poor stability of the ketoamide compounds had an effect on their activity. It would also be advisable that the pyrimidine ketoamide compounds be fully investigated with regards to their stability prior to sending them for biological evaluation.

CHAPTER 4: EXPERIMENTAL SECTION

4.1. General procedures

4.1.1. Solvents and reagents purification

All reagents and solvents used for reactions were purchased from Sigma-Aldrich (South Africa), Merck KGaA (South Africa) and Associated Chemical Enterprises (South Africa); and were used without further purification. When necessary, solvents were distilled over appropriate drying mediums under a nitrogen atmosphere. Tetrahydrofuran (THF) was distilled from sodium wire using benzophenone as an indicator. Dichloromethane (DCM) was distilled from calcium hydride.

Solvents for preparative chromatography and washing acetone were purchased from CC Imelmann (South Africa).

4.1.2. Chromatography

Thin-layer chromatography (TLC) was done on aluminium-backed Merck silica gel 60 F_{254} or Macherey-Nagel silica gel 60 UV_{254}. Preparative TLC was done on glass-backed 1000 µm or 1500 µm Analtech silica gel GF 20 × 20 cm UV_{254} plates. For preparative column chromatography, Sigma-Aldrich silica gel 60 was used as the adsorbent. The mesh particle size was 70 – 230 for conventional gravity chromatography and 230 – 400 for flash chromatography. Dichloromethane and methanol mixtures were used as the mobile phase. High performance liquid chromatography (HPLC) was performed on a Thermo Scientific UHPLC system using a C18 reversed phase column.

4.1.3. Spectroscopic and physical data

Melting points were obtained on a Stuart SMP10 melting point apparatus and are uncorrected.

Hydrogen nuclear magnetic resonance (^{1}H NMR) spectra were acquired on a Bruker 300, 400 or 500 MHz spectrometer in the specified deuterated solvents. For spectra recorded in deuterated chloroform ($CDCl_3$), chemical shifts are reported in parts per million (ppm) relative to the internal tetramethylsilane (TMS) standard. For other deuterated solvents, the residual solvent signal was used as a reference. The ^{1}H NMR spectra chemical shifts are reported as, value (splitting pattern, coupling constant(s) where applicable, number of protons, assignment). Carbon nuclear magnetic resonance (^{13}C NMR) spectra were

acquired on the same instruments in the specified deuterated solvents. Chemical shifts are reported in ppm relative to the residual solvent signal. The ^{13}C NMR spectra chemical shifts are reported as, value (splitting pattern where applicable, coupling constant(s) where applicable, assignment). Coupling constant values are recorded in hertz (Hz). For all experiments the probe temperature was 300K.

Infrared (IR) spectra were obtained on a Bruker Tensor-27 Fourier Transform spectrometer.

High resolution mass spectrometry (HRMS) analysis was performed on a Bruker Compact Q-TOF high resolution mass spectrophotometer. Low resolution mass spectrometry (LRMS) was performed on an Advion expression^{L} compact mass spectrometer.

4.1.4. Other general procedures

For bromine (Br) or chlorine (Cl) containing compounds two molecular ion peaks are observed, the M^+ and the $(M+2)^+$ peaks. The M^+ peak is due to the ^{79}Br or ^{35}Cl isotopes, while the $(M+2)^+$ peak is due to the ^{81}Br or ^{37}Cl isotopes. The m/z values reported in the following sections are for compounds containing the ^{79}Br or ^{35}Cl isotopes.

The numbering on compounds does not follow the official IUPAC rules. The atoms were numbered to allow for simpler characterisation assignments.

4.2. Synthesis of 2-[2-(tetrahydro-2*H*-pyran-2-yloxy)ethoxy]ethanol 17 [59]

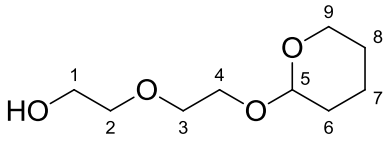

3,4-Dihydro-2*H*-pyran **24** (9.6 g, 0.11 mol) was added over a period of 30 min to a mixture of *p*-toluenesulfonic acid (22 mg, 0.023 mmol) in diethylene glycol **23** (100 g, 0.94 mol) at 0°C. The reaction mixture was stirred for 2 h at 0°C. It was then allowed to warm to room temperature, and was stirred for 1 d. After that, the mixture was poured into 500 mL of 1 M NaOH (aq) and was extracted with DCM (5 × 100 mL). The combined organic layers were dried over $MgSO_4$ overnight. The solvent was removed *in vacuo* to give compound **17** as a colourless oil (19 g, 69%). **^{1}H NMR (300 MHz, $CDCl_3$)** δ 4.69 – 4.61 (m, 1H, H-5), 3.92 – 3.41 (m, 11H, H-1, H-2, H-3, H-4, H-9 & OH), 1.91 – 1.48 (m, 6H, H-6, H-7 & H-8). **^{13}C NMR (75 MHz, $CDCl_3$)** δ 99.1 (C-5), 72.5, 70.3, 66.8, 62.4, 61.6, (C-1, C-2, C-3, C-4 & C-9), 30.5, 25.3 & 19.5 (C-6, C-7 & C-8). **IR (ν_{max}/cm^{-1})** 3405 (OH); 2939, 2869 (-C**-**H); 1121, 1064, 1032 (alkoxy -C**-**O)

4.3. Synthesis of 4,6-dichloropyrimidine 18 [60]

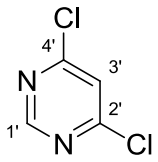

4,6-Dihydroxypyrimidine **25** (25.0 g, 0.220 mol) was mixed with $POCl_3$ (150 mL, 15 eq, 1.60 mol) and refluxed for 3 h. After cooling to room temperature, the reaction mixture was added drop-wise to vigorously stirred ice water (200 mL) in an ice bath. The precipitated product was collected by vacuum filtration to give compound **18** as an orange solid (14.6 g). The filtrate was extracted with EtOAc (5 × 200 mL). The combined organic layers were dried over Na_2SO_4. The solvent was removed *in vacuo* to give an additional 4.82 g of compound **18**, to give a total yield of 19.5 g, 59%. **m.p.** = 68 – 69°C. **^{1}H NMR (500 MHz, DMSO-d_6)** δ 8.97 (s, 1H, H-1'), 8.11 (s, 1H, H-3'). **^{13}C NMR (75 MHz, $CDCl_3$)** δ 162.1 (C-4' and C-2'), 158.8 (C-1'), 121.9 (C-3'). **IR ($\nu_{max.}$/cm^{-1})** 3072, 3040 (=C-H); 1677, 1652 (-C=N); 1585, 1429 (-C=C); 1283 (-C-N)

4.4. Synthesis of 4-chloro-6-{2-[2-(tetrahydro-2*H*-pyran-2-yloxy)ethoxy] ethoxy}pyrimidine 31

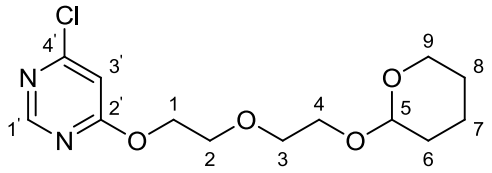

Sodium hydride (4.83 g, 0.120 mol) was flame dried under vacuum and purged with N_2(g) three times, dry THF (150 mL) was added and the suspension was cooled to 0°C. To the suspension, 2-[2-((tetrahydropyranyloxy)ethoxy]ethanol **17** (19.1 g, 0.100 mol) was added over a period of 15 min at 0°C. The reaction was then allowed to warm to room temperature, and was stirred for 40 min. After that, a cold solution of 4,6-dichloropyrimidine **18** (14.9 g, 0.100 mol) in tetrahydrofuran (150 mL) was cannulated to the reaction mixture at 0°C. The reaction mixture was then warmed to room temperature and stirred for 2 d. The mixture was partitioned between EtOAc (300 mL) and H_2O (300 mL), the organic layer was collected and the aqueous layer was extracted with EtOAc (2 × 300 mL). The combined organic layers were dried over Na_2SO_4. The solvent was removed *in vacuo* to give compound **31** as a colourless oil (16.4 g, 54%).**^{1}H NMR (300 MHz, $CDCl_3$)** δ 8.56 (s, 1H, H-1'), 6.83 (s, 1H, H-3'), 4.63 (t, *J* = 3 Hz, 1H, H-5), 4.60 – 4.55 (m, 2H, H-1), 3.92 – 3.82 (m, 4H, H-2, H-4 and H-9), 3.76 – 3.69 (m, 2H, H-3), 3.66 – 3.57 (m, 1H, H-9), 3.54 – 3.46 (m, 1H, H-4),

1.88 – 1.47 (m, 6H, H-6, H-7 and H-8). **^{13}C NMR (75 MHz, $CDCl_3$)** δ 170.1 (C-2'), 160.6 (C-4'), 158.0 (C-1'), 107.9 (C-3'), 98.8 (C-5), 70.6 (C-3), 69.0 (C-2), 66.63 (C-1), 66.60 (C-9), 62.1 (C-4), 30.5, 25.4, 19.4 (C-6, C-7, C-8). **IR ($\nu_{max.}$/cm^{-1})** 2942 (=C-H); 1620 (-C=N); 1565, 1444 (Ar. –C=C); 1136 (phenyl =C-O); 1121, 1078, 1033 (alkoxy -C-O). **ESI-MS (m/z)** calculated $[M+H]^+$ for $C_{13}H_{20}ClN_2O_4$ 303.1103, found 303.1106.

4.5. Synthesis of 2-[2-(4-chloropyrimidin-6-yloxy)ethoxy]ethanol 34

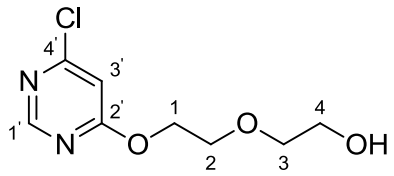

Concentrated HCl (4 mL) was added to a solution of 4-chloro-6-[2-(2-(tetrahydropyranyloxy)ethoxy)ethoxy]pyrimidine **31** (7.0 g, 0.023 mol) in 2-propanol (140 mL). The reaction mixture was stirred at room temperature overnight. After that the solvent was removed *in vacuo* and the crude material was poured into 1 M NaOH (50 mL) and was extracted using DCM (200 mL). The organic layer was dried over Na_2SO_4 and concentrated *in vacuo* to give compound **34** as a pale yellow oil (3.2 g, 63%). **^{1}H NMR (300 MHz, DMSO-d_6)** δ 8.64 (s,1H, H-1'), 7.16 (s, 1H, H-3'), 4.50 – 4.45 (m, 2H, H-1), 3.76 – 3.71 (m, 2H, H-2), 3.55 – 3.52 (m, 2H, H-4), 3.49 – 3.45 (m, 3H, H-3 and OH). **^{13}C NMR (75 MHz, DMSO)** δ 169.8 (C-2'), 159.9 (C-4'), 158.3 (C-1'), 107.5 (C-3'), 72.2 (C-3), 68.1 (C-2), 66.7 (C-1), 60.0 (C-4). **IR ($\nu_{max.}$/cm^{-1})** 3406 (OH), 2872 (=C-H); 1565, 1444 (Ar. –C=C); 1335 (phenyl =C-O); 1129, 1084, 1037 (alkoxy -C-O). **ESI-MS (m/z)** calculated $[M+H]^+$ for $C_8H_{12}ClN_2O_3$ 219.0529, found 219.0531.

4.6. General procedure for the amination to prepare compound 2-{2-[4-(3-bromophenylamino)pyrimidin-6-yloxy]ethoxy}ethanol 16a and analogues

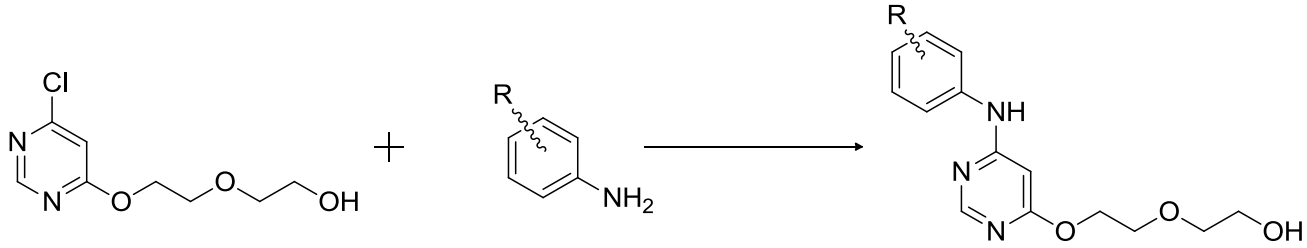

34 **19a-h** **16a-h**

a; R = 3-bromo
b; = H
c; = 3-chloro-4-fluoro
d; = 3-ethynyl
e; = 3,5-dimethoxy
f; = 3,4-difluoro
g; = 2-chloro-4-((3-fluorobenzyl)oxy)
h; = 3-chloro-4-((3-fluorobenzyl)oxy)

The 2-(2-((6-chloropyrimidin-4-yl)oxy)ethoxy)ethanol **34** substrate was dissolved in 2-propanol, subsequently the desired aniline starting material **19** (1-2 eq) and catalytic amount of conc. HCl were added. The reaction mixture was then refluxed for 48 h. After formation of a new product spot, visible by TLC, the reaction was stopped. The reaction mixture was concentrated *in vacuo* and the crude material was poured into 1 M NaOH and was extracted using DCM. The organic layer was dried over Na_2SO_4 and concentrated *in vacuo*. The reaction mixture was purified by column chromatography with DCM/MeOH eluent.

4.6.1. Synthesis of 2-{2-[4-(3-bromophenylamino)pyrimidin-6-yloxy]ethoxy} ethanol 16a

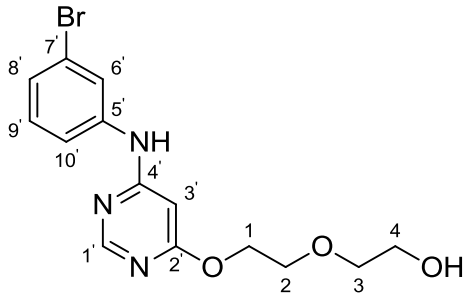

The general procedure was followed using compound **34** (1.00 g, 4.58 mmol) and 3-bromoaniline **19a** (789 mg, 4.58 mmol, 1 eq) in 2-propanol (80 mL). The resulting mixture was purified by column chromatography with 94% DCM/MeOH as an eluent to yield compound **16a** as a light yellow solid (672 mg, 41%). **m.p.** = 130 – 132°C. **^{1}H NMR (300 MHz, DMSO-d_6)** δ 9.58 (s, 1H, NH), 8.42 (s, 1H, H-1'), 8.02 (t, *J* = 2.0 Hz, 1H, H-6'), 7.50 (ddd, *J* = 8.1, 2.2, 1.1 Hz, 1H, H-8'), 7.26 (t, *J* = 8.1 Hz, 1H, H-9'), 7.16 (ddd, *J* = 7.9, 2.0, 1.0 Hz, 1H, H-10'), 6.10 (s, 1H, H-3'), 4.61 (t, *J* = 5.3 Hz, 1H, OH), 4.42 – 4.35 (m, 2H, H-1), 3.76 – 3.68 (m, 2H, H-4), 3.55 – 3.44 (m, 4H, H-2 and H-3). **^{13}C NMR (125 MHz, DMSO)** δ 167.9 (C-2'), 161.1 (C-4'), 156.7 (C-1'), 141.0 (C-5'), 130.1 (C-9'), 124.0 (C-8'), 121.2 (C-6'), 121.0 (C-7'), 117.7 (C-10'), 88.1 (C-3'), 71.8 (C-3), 67.9 (C-2), 64.9 (C-1), 59.6 (C-4). **IR ($\nu_{max.}$/cm^{-1})** 3378 (OH); 3058 (NH); 3001 (=C**-**H); 2732 (-C**-**H); 1629 (-C**=**N); 1582 (Ar. –C**=**C); 1253 (=C**-**N). **ESI-MS (m/z)** calculated $[M+H]^+$ for $C_{14}H_{17}BrN_3O_3$ 354.0440, found 354.0448.

4.6.2. Synthesis of 2-{2-[4-(phenylamino)pyrimidin-6-yloxy]ethoxy}ethanol 16b

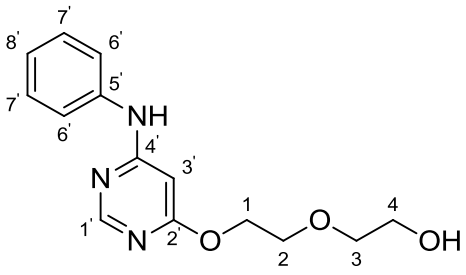

The general procedure was followed using compound **34** (1.39 g, 6.38 mmol) and aniline **19b** (1.19 g, 12.7 mmol, 2 eq) in 2-propanol (112 mL). The resulting mixture was purified by column chromatography with 94% DCM/MeOH as an eluent to yield compound **16b** as a light yellow solid (1.27 g, 73%). **m.p.** = 120 – 121°C **^{1}H NMR (300 MHz, DMSO-d_6)** δ 9.40 (s, 1H, NH), 8.35 (s, 1H, H-1'), 7.57 (d, *J* = 7.7 Hz, 2H, H-6'), 7.31 (t, *J* = 7.9 Hz, 2H, H-7'), 7.01 (t, *J* = 7.3 Hz, 1H, H-8'), 6.08 (s, 1H, H-3'), 4.62 (t, *J* = 5.0 Hz, 1H, OH), 4.40 – 4.34 (m, 2H, H-1), 3.76 – 3.66 (m, 2H, H-2), 3.56 – 3.44 (m, 4H, H-3 and H-4). **^{13}C NMR (75 MHz, DMSO)**

δ168.8 (C-2'), 161.8 (C-4'), 157.6 (C-1'), 139.5 (C-5'), 128.7 (C-7'), 122.5 (C-8'), 119.9 (C-6'), 87.7 (C-3'), 72.1 (C-3), 68.5 (C-2), 65.2 (C-1), 60.0 (C-4). **IR ($\nu_{max.}$/cm^{-1})** 3315 (OH); 3246 (NH); 3081 (=C**-**H); 2943, 2874 (-C**-**H); 1608 (-C**=**N); 1585, 1573 (Ar. –C**=**C); 1252 (=C**-**N). **ESI-MS (m/z)** calculated $[M+H]^+$ for $C_{14}H_{18}N_3O_3$ 276.1343, found 276.1343.

4.6.3. Synthesis of 2-{2-[4-(3-chloro-4-fluorophenylamino)pyrimidin-6-yloxy] ethoxy}ethanol 16c

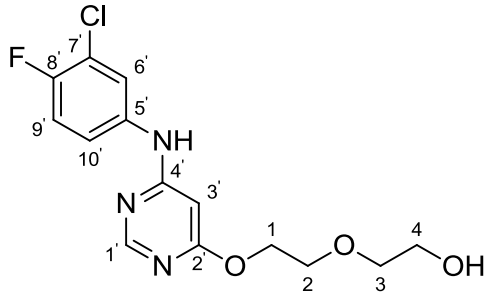

The general procedure was followed using compound **34** (1.94 g, 8.89 mmol) and 3-chloro-4-fluoroaniline **19c** (2.59 g, 17.8 mmol, 2 eq) in 2-propanol (150 mL). The resulting mixture was purified by column chromatography with 94% DCM/MeOH as an eluent to yield compound **16c** as a light brown solid (1.80 g, 62%). **m.p.** = 140 – 142°C. **^{1}H NMR (300 MHz, DMSO-d_6)** δ 9.91 (s, 1H, NH), 8.43 (s, 1H, H-1'), 8.01 (dd, *J* = 6.8, 2.6 Hz, 1H, H-6'), 7.50 (ddd, *J* = 9.0, 4.2, 2.7 Hz, 1H, H-10'), 7.36 (t, *J* = 9.1 Hz, 1H, H-9'), 6.16 (s, 1H, H-3'), 4.82 (s, 1H, OH), 4.46 – 4.37 (m, 2H, H-1), 3.77 – 3.70 (m, 2H, H-2), 3.57 – 3.44 (m, 4H, H-3 and H-4). **^{13}C NMR (75 MHz, DMSO)** δ 168.3 (C-2'), 161.6 (C-4'), 157.1 (C-1'), 152.5 (d, $J_{C\text{-}F}$ = 241.4 Hz, C-8'), 137.2 (d, $J_{C\text{-}F}$ = 2.9 Hz, C-5'), 121.0 (C-6'), 119.9 (d, $J_{C\text{-}F}$ = 6.7 Hz, C-10'), 119.0 (d, $J_{C\text{-}F}$ = 20.0 Hz, C-7'), 116.8 (d, $J_{C\text{-}F}$ = 21.8 Hz, C-9'), 88.4 (C-3'), 72.3 (C-3), 68.5 (C-2), 65.6 (C-1), 60.2 (C-4). **IR ($\nu_{max.}$/cm^{-1})** 3430 (OH); 3040 (NH); 2732 (-C**-**H); 1622 (-C**=**N); 1594 (Ar. –C**=**C); 1259 (=C**-**N). **ESI-MS (m/z)** calculated $[M+H]^+$ for $C_{14}H_{16}ClFN_3O_3$ 328.0888, found 328.0859.

4.6.4. Synthesis of 2-{2-[4-(3-ethynylphenylamino)pyrimidin-6-yloxy]ethoxy} ethanol 16d

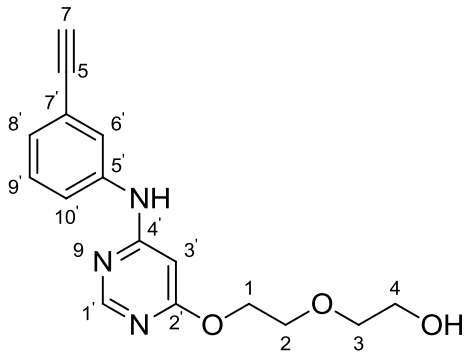

The general procedure was followed using compound **34** (1.00 g, 4.59 mmol) and 3-ethynylaniline **19d** (591 mg, 5.05 mmol, 1.1 eq) in 2-propanol (80 mL). The resulting mixture was purified by column chromatography with 94% DCM/MeOH as an eluent to yield compound **16d** as a yellow-orange solid (400 mg, 29%). **m.p.** = 145 – 147°C. **^{1}H NMR (300 MHz, DMSO-d_6)** δ 9.95 (s, 1H, NH), 8.44 (s, 1H, H-1'), 7.87 – 7.83 (m, 1H, H-6'), 7.63 – 7.56 (m, 1H, H-10'), 7.33 (t, *J* = 7.9 Hz, 1H, H-9'), 7.16 – 7.10 (m, 1H, H-8'), 6.20 (s, 1H, H-3'), 5.40 (s, 1H, OH), 4.43 – 4.36 (m, 2H, H-1), 4.18 (s, 1H, H-7), 3.78 – 3.69 (m, 2H, H-2), 3.54 – 3.44 (m, 4H, H-3 and H-4). **^{13}C NMR (125 MHz, DMSO)** δ 167.5 (C-2'), 162.2 (C-4'), 156.1 (C-1'), 139.6 (C-5'), 129.9 (C-9'), 127.0 (C-8'), 123.6 (C-6'), 122.5 (C-7'), 121.6 (C-10'), 88.2 (C-3'), 83.8 (C-5), 80.9 (C-7), 72.6 (C-3), 68.7 (C-2), 67.2 (C-1), 60.5 (C-4). **IR ($\nu_{max.}$/cm^{-1})** 3352 (OH); 3045 (NH); 3010 (=C-H); 2874 (-C-H); 2210 (-C≡C), 1623 (-C=N); 1580 (Ar. –C=C); 1250 (=C-N). **ESI-MS (m/z)** calculated $[M+H]^+$ for $C_{16}H_{18}N_3O_3$ 300.1344, found 300.1343.

4.6.5. Synthesis of 2-{2-[4-(3,5-dimethoxyphenylamino)pyrimidin-6-yloxy] ethoxy}ethanol 16e

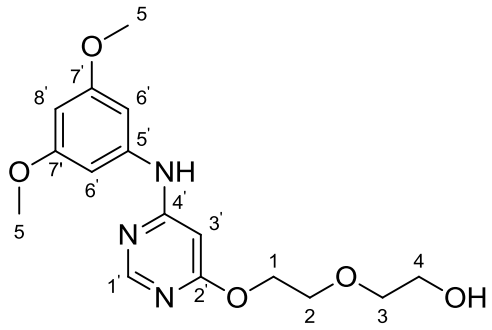

The general procedure was followed using compound **34** (1.42 g, 6.51 mmol) and 3,4-dimethoxyaniline **19e** (1.99 g, 13.0 mmol, 2 eq) in 2-propanol (150 mL). The resulting mixture was purified by column chromatography with 94% DCM/MeOH as an eluent to yield

compound **16e** as a light brown solid (468 mg, 21%). **m.p.** = 102 – 103°C. **^{1}H NMR (500 MHz, DMSO-d_6)** δ 9.36 (s, 1H, NH), 8.37 (s, 1H, H-1'), 6.84 (d, *J* = 2.3 Hz, 2H, H-6'), 6.19 (t, *J* = 2.2 Hz, 1H, H-8'), 6.09 (s, 1H, H-3'), 4.61 (t, *J* = 5.4 Hz, 1H, OH), 4.40 – 4.36 (m, 2H, H-1), 3.74 (s, 6H, H-5), 3.73 – 3.71 (m, 2H, H-2), 3.54 – 3.46 (m, 4H, H-3 and H-4). **^{13}C NMR (125 MHz, DMSO)** δ 169.3 (C-2'), 162.4 (C-4'), 161.1 (C-7'), 158.1 (C-1'), 142.1 (C-5'), 98.6 (C-6'), 94.6 (C-8'), 88.8 (C-3'), 72.9 (C-3), 69.1 (C-2), 65.6 (C-1), 60.7 (C-4), 55.5 (C-5). **IR ($\nu_{max.}$/cm^{-1})** 3380 (OH); 3052 (NH); 2752 (-C-H); 1626 (-C=N); 1574 (Ar. –C=C); 1253 (=C-N); 1085 (C-O). **ESI-MS (m/z)** calculated $[M+H]^+$ for $C_{16}H_{22}N_3O_5$ 336.1547, found 336.1554.

4.6.6. Synthesis of 2-{2-[4-(3,4-difluorophenylamino)pyrimidin-6-yloxy]ethoxy} ethanol 16f

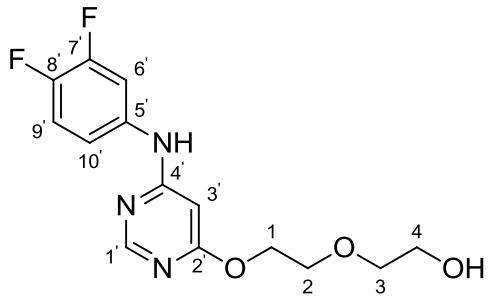

The general procedure was followed using compound **34** (1.46 g, 6.69 mmol) and 3,4-difluoroaniline **19f** (1.73 g, 13.4 mmol, 2 eq) in 2-propanol (120 mL). The resulting mixture was purified by column chromatography with 94% DCM/MeOH as an eluent to yield compound **16f** as a light brown solid (1.07 g, 52%). **m.p.** = 135 – 136°C. **^{1}H NMR (400 MHz, DMSO-d_6)** δ 9.68 (s, 1H, NH), 8.38 (s, 1H, H-1'), 7.85 (ddd, *J* = 13.5, 7.4, 2.6 Hz, 1H, H-6'), 7.39 – 7.30 (m, 1H, H-9'), 7.29 – 7.22 (m, 1H, H-10'), 6.08 (s, 1H, H-3'), 4.39 – 4.34 (m, 2H, H-1), 4.11 (s, 1H, OH), 3.72 – 3.68 (m, 2H, H-2), 3.51 – 3.43 (m, 4H, H-3 and H-4). **^{13}C NMR (125 MHz, DMSO**) δ 167.9 (C-2'), 161.1 (C-4'), 156.6 (C-1'), 148.4 (dd, $J_{C\text{-}F}$ = 243.3, 13.1 Hz, C-7'), 144.1 (dd, $J_{C\text{-}F}$ = 240.8, 12.9 Hz, C-8'), 136.5 (dd, $J_{C\text{-}F}$ = 9.2, 2.5 Hz, C-5'), 116.8 (d, $J_{C\text{-}F}$ = 17.7 Hz, C-9'), 115.3 (dd, $J_{C\text{-}F}$ = 5.7, 3.0 Hz, C-10'), 108.1 (d, $J_{C\text{-}F}$ = 21.4 Hz, C-6'), 87.8 (C-3'), 71.8 (C-4), 68.0 (C-2), 65.0 (C-1), 59.6 (C-3). **IR ($\nu_{max.}$/cm^{-1})** 3456 (OH); 3058 (NH); 2916 (-C-H); 1645 (-C=N); 1584 (Ar. –C=C); 1250 (=C-N). **ESI-MS (m/z)** calculated $[M+H]^+$ for $C_{14}H_{16}F_2N_3O_3$ 312.1149, found 312.1154.

4.6.7. Synthesis of 2-(2-{4-[2-chloro-4-(3-fluorobenzyloxy)phenylamino] pyrimidin-6-yloxy}ethoxy)ethanol 16g

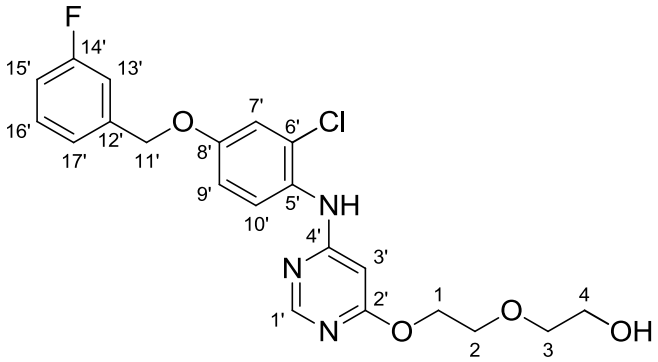

The general procedure was followed using compound **34** (500 mg, 1.66 mmol) and 2-chloro-4-((3-fluorobenzyl)oxy)aniline **19g** (417 mg, 1.66 mmol, 1eq) in 2-propanol (50 mL). The resulting mixture was purified by column chromatography with 94% DCM/MeOH as an eluent to yield compound **16g** as a cream white solid (93 mg, 13%). **m.p.** = 131 – 133°C. **^{1}H NMR (500 MHz, DMSO-d_6)** δ 9.36 (s, 1H, NH), 8.35 (s, 1H, H-1'), 7.81 (d, *J* = 2.6 Hz, 1H, H-10'), 7.49 – 7.44 (m, 1H, H-16'), 7.41 – 7.37 (m, 1H, H-9'), 7.33 – 7.28 (m, 2H, H-13' and H-17'), 7.21 – 7.15 (m, 2H, H-7' and H-15'), 6.00 (s, 1H, H-3'), 5.21 (s, 2H, H-11'), 4.59 (s, 1H, OH), 4.39 – 4.36 (m, 2H, H-1), 3.74 – 3.70 (m, 2H, H-2), 3.54 – 3.49 (m, 2H, H-4), 3.49 – 3.46 (m, 2H, H-3). **^{13}C NMR (125 MHz, DMSO)** δ 169.3 (C-2'), 162.7 (d, $J_{C\text{-}F}$ = 244.4 Hz, C-14'), 162.4 (C-4'), 158.2 (C-1'), 149.2 (C-8'), 140.2 (d, $J_{C\text{-}F}$ = 7.6 Hz, C-12'), 134.7 (C-5'), 130.9 (d, $J_{C\text{-}F}$ = 7.6 Hz, C-16'), 123.8 (d, $J_{C\text{-}F}$ = 2.5 Hz, C-17'), 122.2 (C-10'), 122.0 (C-6'), 120.3 (C-9'), 115.4 (C-7'), 115.1 (d, $J_{C\text{-}F}$ = 21.4 Hz, C-15'), 114.5 (d, $J_{C\text{-}F}$ = 22.7 Hz, C-13'), 88.2 (C-3'), 72.9 (C-3), 70.0 (C-11'), 69.1 (C-2), 65.6 (C-1), 60.7 (C-4). **IR ($\nu_{max.}$/cm^{-1})** 3496 (OH); 3303 (NH); 3115 (=C-H); 2917, 2849 (-C-H); 1623 (-C=N); 1583 (Ar. –C=C); 1352, 1327 (phenyl -C-O); 1246 (=C-N); 1137, 1127, 1048 (alkoxy -C-O). **ESI-MS (m/z)** calculated $[M+H]^+$ for $C_{21}H_{22}ClFN_3O_4$ 434.1261, found 434.1277.

4.6.8. Synthesis of 2-(2-{4-[3-chloro-4-(3-fluorobenzyloxy)phenylamino] pyrimidin-6-yloxy}ethoxy)ethanol 16h

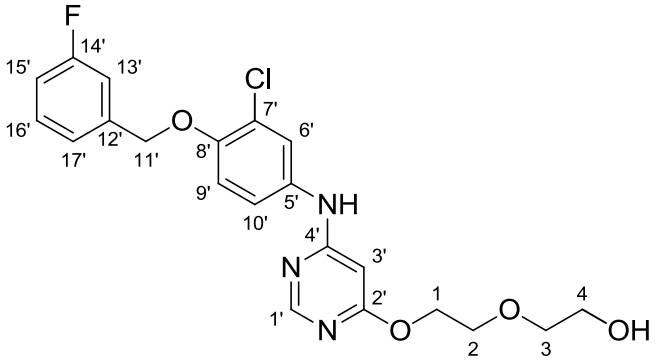

The general procedure was followed using compound **34** (500 mg, 1.66 mmol) and 3-chloro-4-((3-fluorobenzyl)oxy)aniline **19h** (417 mg, 1.66 mmol, 1 eq) in 2-propanol (50 mL). The resulting mixture was purified by column chromatography with 94% DCM/MeOH as an eluent to yield compound **16h** as white solid (65 mg, 9%). **m.p.** = 130 – 131°C. **^{1}H NMR (300 MHz, DMSO-d_6)** δ 9.39 (s, 1H, NH), 8.35 (s, 1H, H-1'), 7.81 (d, *J* = 2.5 Hz, 1H, H-6'), 7.52 – 7.41 (m, 1H, H-16'), 7.38 (dd, *J* = 8.9, 2.6 Hz, 1H, H-10'), 7.34 – 7.25 (m, 2H, H-13' and H-17'), 7.22 – 7.13 (m, 2H, H-9' and H-15'), 5.99 (s, 1H, H-3'), 5.20 (s, 2H, H-11'), 4.62 (t, *J* = 5.2 Hz, 1H, OH), 4.40 – 4.33 (m, 2H, H-1), 3.76 – 3.67 (m, 2H, H-2), 3.52 – 3.46 (m, 4H, H-3 and H-4). **^{13}C NMR (75 MHz, DMSO)** δ 168.8 (C-2'), 162.1 (d, $J_{C\text{-}F}$ = 241.5 Hz, C-14'), 161.8 (C-4'), 157.7 (C-1'), 148.7 (C-8'), 139.7 (d, $J_{C\text{-}F}$ = 7.5 Hz, C-12'), 134.2 (C-5'), 130.5 (d, $J_{C\text{-}F}$ = 8.3 Hz, C-16') 123.3 (d, $J_{C\text{-}F}$ = 3.0 Hz, C-17'), 121.7 (C-10'), 121.5 (C-6'), 119.8 (C-9'), 114.9 (C-7'), 114.6 (d, $J_{C\text{-}F}$ = 21 Hz, C-15'), 114.0 (d, $J_{C\text{-}F}$ = 22.5 Hz, C-13'), 87.7 (C-3'), 72.3 (C-3), 69.5 (C-11'), 68.6 (C-2), 65.1 (C-1), 60.2 (C-4). **IR ($\nu_{max.}$/cm^{-1})** 3494 (OH); 3310 (NH); 3105 (=C**-**H); 2910, 2845 (-C**-**H); 1615 (-C**=**N); 1580 (Ar. –C**=**C); 1350, 1325 (phenyl -C**-**O); 1252 (=C**-**N); 1140, 1137, 1048 (alkoxy -C**-**O). **ESI-MS (m/z)** calculated $[M+H]^+$ for $C_{21}H_{22}ClFN_3O_4$ 434.1267, found 434.1277.

4.7. General procedure to prepare compound 2-{2-[4-(3-bromophenylamino)pyrimidin-6-yloxy]ethoxy}acetaldehyde 15a and analogues

16a-f **15a-f**

a; R = 3-bromo

b; = H

c; = 3-chloro-4-fluoro

d; = 3-ethynyl

e; = 3,5-dimethoxy

f; = 3,4-difluoro

IBX (2 eq.) was added to a solution of compound **16** in DMSO. The reaction mixture was stirred at room temperature overnight. After formation of a new product spot, visible by TLC,

the reaction mixture was stopped. The product was extracted using DCM and washed three times with water and once with brine. The combined organic layers were dried over Na_2SO_4 and concentrated *in vacuo* to give sticky material. The sticky material was put under high vacuum to give a solid, and it was confirmed to be the desired product.

4.7.1. Synthesis of 2-{2-[4-(3-bromophenylamino)pyrimidin-6-yloxy]ethoxy} acetaldehyde 15a

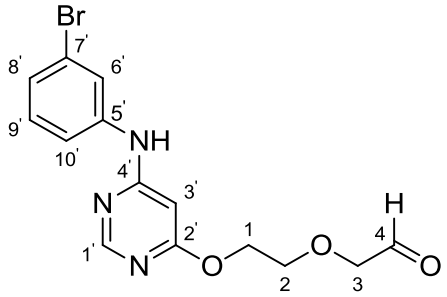

The general procedure was followed using compound **16a** (1.19 g, 3.37 mmol) and IBX (1.88 g, 6.73 mmol, 2 eq) in DMSO (47 mL). The desired compound **15a** was yielded as an orange solid (1.02 g, 86%). **m.p.** = 52 – 53°C. **^{1}H NMR (300 MHz, $CDCl_3$)** δ 9.74 (s, 1H, H-4), 8.34 (s, 1H, H-1'), 7.57 – 7.48 (m, 2H, NH and H-6'), 7.31 – 7.18 (m, 3H, H-8', H-9' and H-10'), 6.16 (s, 1H, H-3'), 4.57 – 4.52 (m, 2H, H-1), 4.19 (s, 2H, H-3), 3.92 – 3.87 (m, 2H, H-2). **^{13}C NMR (75 MHz, $CDCl_3$)** δ 200.3 (C-4), 170.0 (C-2'), 161.9 (C-4'), 157.9 (C-1'), 139.9 (C-5'), 130.7 (C-9'), 127.5 (C-8'), 124.9 (C-6'), 123.0 (C-7'), 120.5 (C-10'), 87.5 (C-3'), 76.7 (C-3), 70.1 (C-2), 65.4 (C-1). **IR ($\nu_{max.}$/cm^{-1})** 3294 (NH); 2923 (=C-H); 2895 (ald. –C-H); 1606 (ald. –C=O); 1576 (Ar. –C=C). **ESI-MS (m/z)** calculated $[M+H]^+$ for $C_{14}H_{15}BrN_3O_3$ 352.0281, found 352.0291.

4.7.2. Synthesis of 2-{2-[4-(phenylamino)pyrimidin-6-yloxy]ethoxy} acetaldehyde 15b

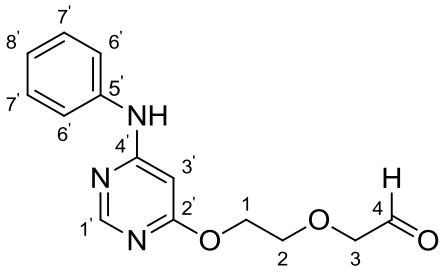

The general procedure was followed using compound **16b** (610 mg, 2.22 mmol) and IBX (1.24 g, 4.44 mmol, 2 eq) in DMSO (15 mL). The desired compound **15b** was yielded as a dark brown solid (400 mg, 66%). **m.p.** = 59 – 61°C. **^{1}H NMR (500 MHz, $CDCl_3$)** δ 9.73 (s,

1H, H-4), 8.32 (s, 1H, H-1'), 7.43 (s, 1H, NH), 7.40 – 7.35 (m, 2H, H-6'), 7.30 – 7.27 (m, 2H, H-7'), 7.20 – 7.14 (m, 1H, H-8'), 6.16 (s, 1H, H-3'), 4.57 – 4.47 (m, 2H, H-1), 4.16 (s, 2H, H-3), 3.93 – 3.83 (m, 2H, H-2). **^{13}C NMR (125 MHz, $CDCl_3$)** δ 200.4 (C-4), 169.9 (C-2'), 162.5 (C-4'), 157.8 (C-1'), 138.2 (C-5'), 129.5 (C-7'), 124.9 (C-8'), 122.6 (C-6'), 86.7 (C-3'), 76.6 (C-3), 70.1 (C-2), 65.2 (C-1). **IR ($\nu_{max.}$/cm^{-1})** 3242 (NH), 2922 (=C**-**H); 2854 (ald. –C**-**H); 1608 (ald. –C**=**O); 1581 (Ar. –C**=**C). **ESI-MS (m/z)** calculated $[M+H]^+$ for $C_{14}H_{16}N_3O_3$ 274.1182, found 274.1186.

4.7.3. Synthesis of 2-{2-[4-(3-chloro-4-fluorophenylamino)pyrimidin-6-yloxy] ethoxy}acetaldehyde 15c

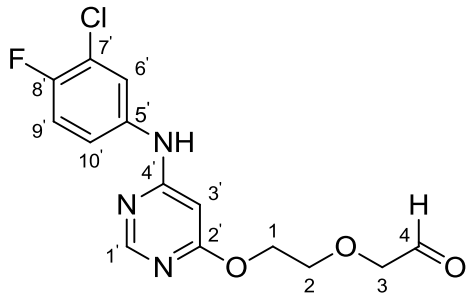

The general procedure was followed using compound **16c** (800 mg, 2.45 mmol) and IBX (1.37 g, 4.89 mmol, 2 eq) in DMSO (25 mL). The desired compound **15c** was yielded as a dark brown solid (683 mg, 86%). **m.p.** = 67 – 69°C. **^{1}H NMR (500 MHz, $CDCl_3$)** δ 9.72 (s, 1H, H-4), 8.29 (s, 1H, H-1'), 7.78 (s, 1H, NH), 7.44 – 7.37 (m, 1H, H-6'), 7.19 – 7.05 (m, 2H, H-9' and H-10'), 6.04 (s, 1H, H-3'), 4.56 – 4.52 (m, 2H, H-1), 4.18 (s, 2H, H-3), 3.91 – 3.86 (m, 2H, H-2). **^{13}C NMR (125 MHz, $CDCl_3$)** δ 200.3 (C-4), 170.0 (C-2'), 162.3 (C-4'), 157.7 (C-1'), 155.3 (d, $J_{C\text{-}F}$ = 252.0 Hz, C-8'), 135.0 (d, $J_{C\text{-}F}$ = 3.8 Hz, C-5'), 124.9 (C-6'), 122.6 (d, $J_{C\text{-}F}$ = 6.3 Hz, C-10'), 121.6 (d, $J_{C\text{-}F}$ = 18.9 Hz, C-7'), 117.2 (d, $J_{C\text{-}F}$ = 22.7 Hz, C-9'), 87.1 (C-3'), 76.7 (C-3), 70.1 (C-2), 65.4 (C-1). **IR ($\nu_{max.}$/cm^{-1})** 3064 (NH); 2923 (=C**-**H); 2853 (ald. –C**-**H); 1702 (ald. –C**=**O); 1585 (Ar. –C**=**C). **ESI-MS (m/z)** calculated $[M+H]^+$ for $C_{14}H_{14}ClFN_3O_3$ 326.0705, found 326.0702.

4.7.4. Synthesis of 2-{2-[4-(3-ethynylphenylamino)pyrimidin-6-yloxy]ethoxy} acetaldehyde 15d

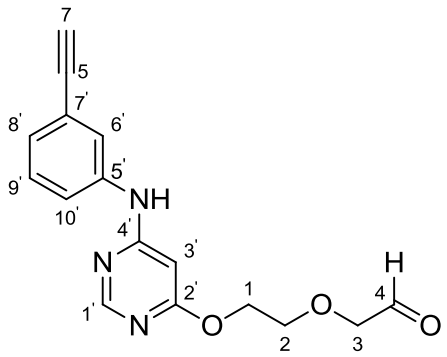

The general procedure was followed using compound **16d** (563 mg, 1.88 mmol) and IBX (1.05 g, 3.77 mmol, 2 eq) in DMSO (22 mL). The desired compound **15d** was yielded as a dark brown solid (349 mg, 62%). **m.p.** = 67 – 68°C. **^{1}H NMR (500 MHz, $CDCl_3$)** δ 9.73 (s, 1H, H-4), 8.34 (s, 1H, H-1'), 7.46 – 7.39 (m, 2H, NH and H-6'), 7.34 – 7.27 (m, 3H, H-8', H-9' and H-10'), 6.15 (s, 1H, H-3'), 4.56 – 4.53 (m, 2H, H-1), 4.18 (s, 2H, H-3), 3.91 – 3.87 (m, 2H, H-2), 3.11 (s, 1H, H-7). **^{13}C NMR (125 MHz, $CDCl_3$)** δ 200.3 (C-4), 169.5 (C-2'), 162.2 (C-4'), 157.7 (C-1'), 139.5 (C-5'), 129.1 (C-9'), 127.1 (C-8'), 124.5 (C-6'), 122.8 (C-7'), 121.8 (C-10'), 88.0 (C-3'), 83.3 (C-5),77.6 (C-7), 76.6 (C-3), 70.1 (C-2), 65.1(C-1). **IR ($\nu_{max.}$/cm^{-1})** 3292 (NH); 2920 (=C-H); 2895 (ald. –C-H); 1610 (ald. –C=O); 1574 (Ar. –C=C). **ESI-MS (m/z)** calculated $[M+H]^+$ for $C_{16}H_{16}N_3O_3$ 298.1184, found 298.1186.

4.7.5. Synthesis of 2-{2-[4-(3,5-dimethoxyphenylamino)pyrimidin-6-yloxy] ethoxy}acetaldehyde 15e

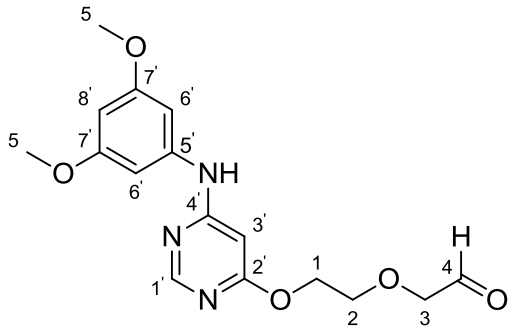

The general procedure was followed using compound **16e** (290 mg, 0.87 mmol) and IBX (484 mg, 1.73 mmol, 2 eq) in DMSO (12 mL). The desired compound **15e** was yielded as a dark brown solid (177 mg, 61%). **m.p.** = 56 – 58°C. **^{1}H NMR (300 MHz, $CDCl_3$)** δ 9.73 (s, 1H, H-4), 8.33 (s, 1H, H-1'), 7.17 (s, 1H, NH), 6.44 (d, *J* = 2.2 Hz, 2H, H-6'), 6.27 (t, *J* = 2.2 Hz, 1H, H-8'), 6.23 (s, 1H, H-3'), 4.56 – 4.50 (m, 2H, H-1), 4.18 (s, 2H, H-3), 3.92 – 3.86 (m, 2H, H-2), 3.79 (s, 6H, H-5). **^{13}C NMR (125 MHz, $CDCl_3$)** δ 200.7 (C-4), 170.0 (C-2'), 162.6

(C-4'), 161.3 (C-7'), 157.7 (C-1'), 140.0 (C-5'), 100.8 (C-6'), 96.7 (C-8'), 87.4 (C-3'), 76.7 (C-3), 70.2 (C-2), 65.3 (C-1), 55.4 (C-5). **IR ($\nu_{max.}$/cm^{-1})** 3068 (NH); 2922 (=C**-**H); 2895 (ald. –C**-**H); 1695 (ald. –C**=**O); 1576 (Ar. –C**=**C). **ESI-MS (m/z)** calculated $[M+H]^+$ for $C_{16}H_{20}N_3O_5$ 334.1393, found 334.1397.

4.7.6. Synthesis of 2-{2-[4-(3,4-difluorophenylamino)pyrimidin-6-yloxy]ethoxy} acetaldehyde 15f

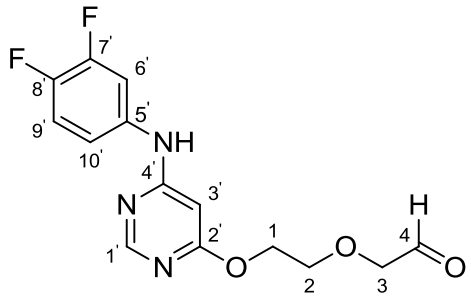

The general procedure was followed using compound **16f** (440 mg, 1.41 mmol) and IBX (792 mg, 28.3 mmol, 2 eq) in DMSO (18 mL). The desired compound **15f** was yielded as a dark brown solid (396 mg, 90%). **m.p.** = 51 – 52°C. **^{1}H NMR (500 MHz, CDCl$_3$)** δ 9.73 (s, 1H, H-4), 8.34 (s, 1H, H-1'), 7.28 – 7.22 (m, 1H, H-6'), 7.20 – 7.10 (m, 1H, H-9'), 7.03 – 6.93 (m, 2H, H-10 and NH), 6.06 (s, 1H, H-3'), 4.58 – 4.51 (m, 2H, H-1), 4.18 (s, 2H, H-3), 3.92 – 3.87 (m, 2H, H-2). **^{13}C NMR (125 MHz, CDCl$_3$)** δ 200.3 (C-4), 170.0 (C-2'), 162.1 (C-4'), 158.0 (C-1'), 150.5 (dd, $J_{C\text{-}F}$ = 249.5, 13.9 Hz, C-7'), 147.5 (dd, $J_{C\text{-}F}$ = 247.0, 12.6 Hz, C-8'), 134.8 (dd, $J_{C\text{-}F}$ = 11.3, 6.3 Hz, C-5'), 118.4 (dd, $J_{C\text{-}F}$ = 6.3, 3.8 Hz, C-10'), 117.8 (dd, $J_{C\text{-}F}$ = 18.1, 1.3 Hz, C-9'), 112.0 (d, $J_{C\text{-}F}$ = 19.7 Hz, C-6'), 87.3 (C-3'), 76.7 (C-3), 70.2 (C-2), 65.4 (C-1). **IR ($\nu_{max.}$/cm^{-1})** 3062 (NH); 2890 (=C**-**H); 2801 (ald. –C**-**H); 1695 (ald. –C**=**O); 1595 (Ar. –C**=**C). **ESI-MS (m/z)** calculated $[M+H]^+$ for $C_{14}H_{14}F_2N_3O_3$ 310.0994, found 310.0998.

4.8. General procedure to prepare 2-hydroxy-*N*-isopropyl-3-{2-[4-(3-bromophenylamino)pyrimidin-6-yloxy]ethoxy}propanamide 14a and analogues

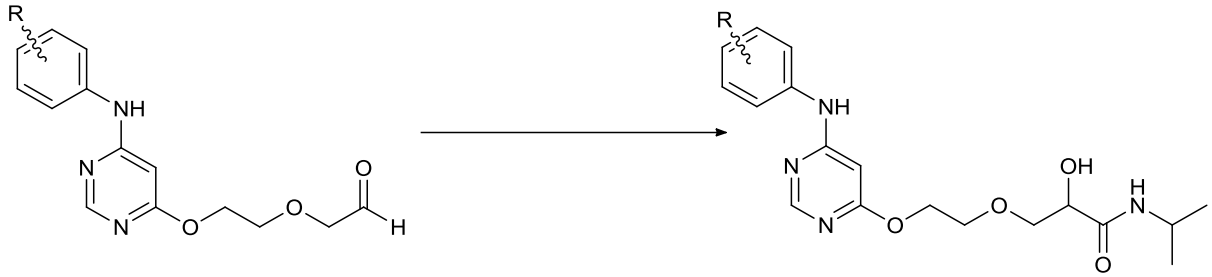

15a-f **14a-f**

a; R = 3-bromo

b; = H

c; = 3-chloro-4-fluoro

d; = 3-ethynyl

e; = 3,5-dimethoxy

f; = 3,4-difluoro

Compound **15** was dissolved in DCM and diluted with EtOAc. AcOH and isopropyl isocyanide were then consecutively added. The reaction mixture was stirred at room temperature for 24 h, after that the mixture was concentrated *in vacuo*. K_2CO_3 in MeOH/H_2O was then added to the concentrate and it was stirred at room temperature for 3 h. The mixture was extracted with DCM and washed with H_2O, the organic layer was collected and the aqueous layer was back-extracted with DCM (× 2). The combined organic layers were dried over Na_2SO_4 and concentrated *in vacuo*. The reaction mixture was purified by column chromatography with 94% DCM/MeOH as an eluent to give the desired product.

4.8.1. Synthesis of 2-hydroxy-*N*-isopropyl-3-{2-[4-(3-bromophenylamino) pyrimidin-6-yloxy]ethoxy}propanamide 14a

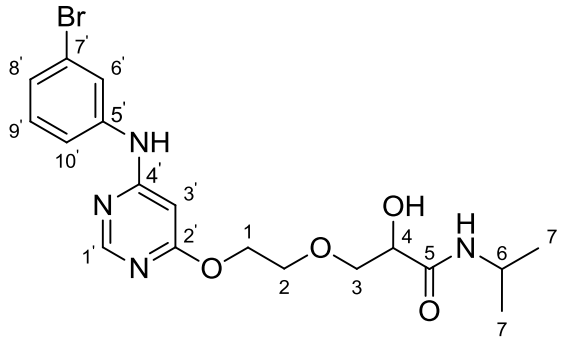

The general procedure was followed using compound **15a** (200 mg, 0.568 mmol) in DCM (7 mL) and EtOAc (14 mL). Isopropyl isocyanide (39 mg, 0.568 mmol), AcOH and K_2CO_3 (173 mg, 1.25 mmol) in MeOH (29 mL) and H_2O (15 mL) were added. The resulting mixture was purified by column chromatography with 94% DCM/MeOH as an eluent to yield compound **14a** as a pale yellow solid (147 mg, 59%). **m.p.** = 103 – 105°C. **^{1}H NMR (500 MHz, $CDCl_3$)** δ 8.31 (s, 1H, H-1'), 7.87 (s, 1H, NH), 7.50 (s, 1H, H-6'), 7.29 – 7.18 (m, 3H, H-8', H-9' and H-10'), 6.68 (d, *J* = 7.8 Hz, 1H, NH), 6.08 (s, 1H, H-3'), 4.52 – 4.41 (m, 2H, H-1), 4.22 (t, *J* = 5.5 Hz, 1H, H-4), 4.11 – 4.02 (m, 1H, H-6), 3.87 – 3.77 (m, 3H, H-2 and H-3), 3.73 (dd, *J* = 9.6, 6.5 Hz, 1H, H-3), 1.15 (d, *J* = 6.7 Hz, 3H, H-7), 1.13 (d, *J* = 6.7 Hz, 3H, H-7). **^{13}C NMR (125 MHz, $CDCl_3$)** δ 170.6 (C-5), 170.0 (C-2'), 161.9 (C-4'), 157.9 (C-1'), 140.0 (C-5'), 130.7 (C-9'), 127.4 (C-8'), 124.8 (C-6'), 122.9 (C-7'), 120.4 (C-10'), 87.4 (C-3'), 72.7 (C-3), 70.3 (C-4), 69.7 (C-2), 65.4 (C-1), 41.2 (C-6), 22.7 (C-7). **IR ($\nu_{max.}$/cm^{-1})** 3298 (OH); 2925 (NH); 1648 (–C**=**O); 1575 (Ar. –C**=**C); 1265, 1296 (alkoxy –C**-**O); 1049 (alcohol –C**-**O).**ESI-MS (m/z)** calculated $[M+H]^+$ for $C_{18}H_{24}BrN_4O_4$ 439.0963, found 439.0975.

4.8.2. Synthesis of 2-hydroxy-*N*-isopropyl-3-{2-[4-(phenylamino)pyrimidin-6-yloxy]ethoxy}propanamide 14b

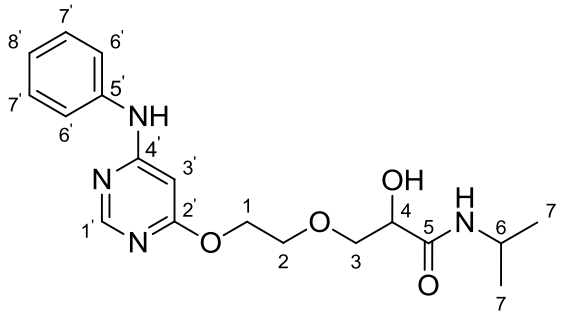

The general procedure was followed using compound **15b** (367 mg, 1.34 mmol) in DCM (14 mL) and EtOAc (28 mL). Isopropyl isocyanide (186 mg, 2.69 mmol), AcOH and K_2CO_3 (408 mg, 2.95 mmol) in MeOH (54 mL) and H_2O (27 mL) were added. Compound **14b** was

yielded as a brown solid (175 mg, 36%). **m.p.** = 104 – 105°C. **^{1}H NMR (500 MHz, $CDCl_3$)** δ 8.30 (s, 1H, H-1'), 7.50 (s, 1H, NH), 7.39 – 7.33 (m, 2H, H-6'), 7.29 – 7.26 (m, 2H, H-7'), 7.19 – 7.14 (m, 1H, H-8'), 6.63 (s, 1H, NH), 6.09 (s, 1H, H-3'), 4.49 – 4.41 (m, 2H, H-1), 4.19 (t, *J* = 5.7 Hz, 1H, H-4), 4.11 – 4.00 (m, 1H, H-6), 3.83 – 3.77 (m, 3H, H-2 and H-3), 3.73 – 3.69 (m, 1H, H-2), 1.14 (d, *J* = 6.6 Hz, 3H, H-7), 1.12 (d, *J* = 6.6 Hz, 3H, H-7). **^{13}C NMR (125 MHz, $CDCl_3$)** δ 170.5 (C-5), 169.9 (C-2'), 162.5 (C-4'), 157.9 (C-1'), 138.2 (C-5'), 129.5 (C-7'), 124.9 (C-8'), 122.5 (C-6'), 86.6 (C-3'), 72.6 (C-3), 70.1 (C-4), 69.7 (C-2), 65.2 (C-1), 41.1 (C-6), 22.6 (C-7). **IR ($\nu_{max.}$/cm^{-1})** 3249 (OH); 3086 (NH); 2974 (=C**-**H); 1610 (–C**=**O); 1587 (Ar. –C**=**C), 1253 ((=C**-**N). **ESI-MS (m/z)** calculated $[M+H]^+$ for $C_{18}H_{25}N_4O_4$ 361.1867, found 361.1870.

4.8.3. Synthesis of 2-hydroxy-*N*-isopropyl-3-{2-[4-(3-chloro-4-fluorophenyl amino)pyrimidin-6-yloxy]ethoxy}propanamide 14c

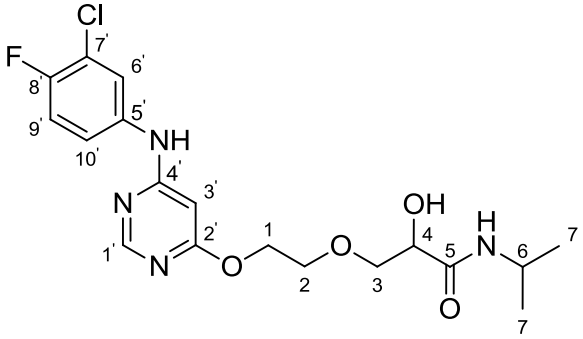

The general procedure was followed using compound **15c** (210 mg, 0.646 mmol) in DCM (9 mL) and EtOAc (16 mL). Isopropyl isocyanide (49 mg, 0.710 mmol), AcOH and K_2CO_3 (250 mg, 1.81 mmol) in MeOH (33 mL) and H_2O (17 mL) were added. The resulting mixture was purified by column chromatography with 94% DCM/MeOH as an eluent to yield compound **14c** as a light brown solid (160 mg, 60%). **m.p.** = 110 – 112°C. **^{1}H NMR (500 MHz, $CDCl_3$)** δ 8.33 (s, 1H, H-1'), 7.42 (dd, *J* = 6.3, 2.1 Hz, 1H, H-6'), 7.19 – 7.09 (m, 3H, NH, H-9' and H-10'), 6.59 (d, *J* = 7.4 Hz, 1H, NH), 5.98 (s, 1H, H-3'), 4.53 – 4.44 (m, 2H, H-1), 4.18 (t, *J* = 5.7 Hz, 1H, H-4), 4.12 – 4.02 (m, 1H, H-6), 3.83 (t, *J* = 4.4 Hz, 2H, H-2), 3.79 (dd, *J* = 9.8, 5.1 Hz, 1H, H-3), 3.72 (dd, *J* = 9.7, 6.4 Hz, 1H, H-3), 1.16 (d, *J* = 6.6 Hz, 3H, H-7), 1.14 (d, *J* = 6.6 Hz, 3H, H-7). **^{13}C NMR (125 MHz, $CDCl_3$)** δ 170.4 (C-5), 170.0 (C-2'), 162.3 (C-4'), 158.0 (C-1'), 155.3 (d, $J_{C\text{-}F}$ = 247.4 Hz, C-8'), 135.0 (d, $J_{C\text{-}F}$ = 3.4 Hz, C-5'), 124.9 (C-6'), 122.5 (d, $J_{C\text{-}F}$ = 6.9 Hz, C-10'), 121.7 (d, $J_{C\text{-}F}$ = 18.9 Hz, C-7'), 117.2 (d, $J_{C\text{-}F}$ = 22.2 Hz, C-9'), 87.2 (C-3'), 72.5 (C-3), 70.2 (C-4), 69.7 (C-2), 65.4 (C-1), 41.2 (C-6), 22.6 (C-7). **IR ($\nu_{max.}$/cm^{-1})** 3304 (OH); 2973 (NH); 1612 (–C**=**O); 1584 (Ar. –C**=**C); 1249, 1298 (alkoxy –C**-**O); 1052 (alcohol –C**-**O). **ESI-MS (m/z)** calculated $[M+H]^+$ for $C_{18}H_{23}ClFN_4O_4$ 413.1378, found 413.1386.

4.8.4. Synthesis of 2-hydroxy-*N*-isopropyl-3-{2-[4-(3-ethynylphenylamino) pyrimidin-6-yloxy]ethoxy}propanamide 14d

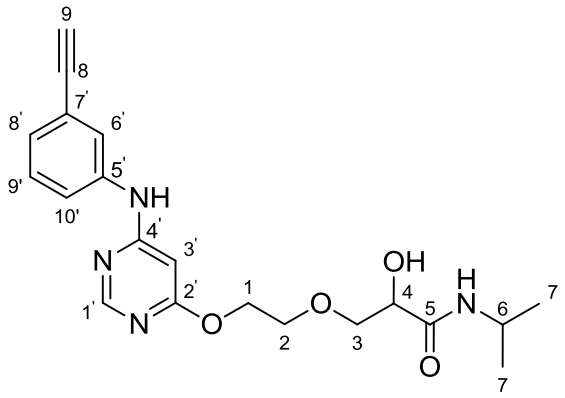

The general procedure was followed using compound **15d** (339 mg, 1.14 mmol) in DCM (14 mL) and EtOAc (28 mL). Isopropyl isocyanide (79 mg, 1.14 mmol, 1 eq.), AcOH and K_2CO_3 (424 mg, 3.07 mmol) in MeOH (57 mL) and H_2O (29 mL) were added. The resulting mixture was purified by column chromatography with 94% DCM/MeOH as an eluent to yield compound **14d** as a cream white solid (170 mg, 39%). **m.p.** =107 – 108°C. **^{1}H NMR (500 MHz, $CDCl_3$)** δ 8.30 (s, 1H, H-1'), 7.71 (s, 1H, NH), 7.42 (s, 1H, H-6'), 7.33 – 7.25 (m, 3H, H-8', H-9' and H-10'), 6.66 (d, *J* = 7.9 Hz, 1H, NH), 6.07 (s, 1H, H-3'), 4.49 – 4.41 (m, 2H, H-1), 4.23 – 4.13 (m, 2H, H-4 and OH), 4.10 – 4.03 (m, 1H, H-6), 3.84 – 3.79 (m, 3H, H-2 and H-3), 3.77 – 3.69 (m, 1H, H-3), 3.11 (s, 1H, H-9), 1.15 (d, *J* = 6.6 Hz, 3H, H-7), 1.13 (d, *J* = 6.6 Hz, 3H, H-7). **^{13}C NMR (125 MHz, $CDCl_3$)** δ 170.5 (C-5), 170.0 (C-2'), 162.2 (C-4'), 157.9 (C-1'), 138.6 (C-5'), 129.5 (C-9'), 128.3 (C-8'), 125.5 (C-6'), 123.4 (C-7'), 122.7 (C-10'), 87.1 (C-3'), 83.0 (C-8), 78.0 (C-9), 72.7 (C-3), 70.3 (C-4), 69.7 (C-2), 65.3 (C-1), 41.2 (C-6), 22.7 (C-7). **IR ($v_{max.}$/cm^{-1})** 3286 (OH); 2926 (NH); 1646 (–C**=**O); 1587 (Ar. –C**=**C); 1253 (alkoxy –C**-**O); 1050 (alcohol –C**-**O). **ESI-MS (m/z)** calculated $[M+H]^+$ for $C_{20}H_{25}N_4O_4$ 385.1863, found 385.1870.

4.8.5. Synthesis of 2-hydroxy-*N*-isopropyl-3-{2-[4-(3,5-dimethoxyphenyl amino)pyrimidin-6-yloxy]ethoxy}propanamide 14e

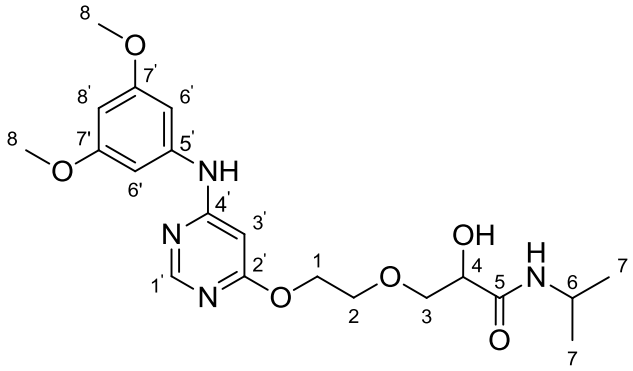

The general procedure was followed using compound **15e** (147 mg, 0.441 mmol) in DCM (6 mL) and EtOAc (12 mL). Isopropyl isocyanide (30.5 mg, 0.710 mmol, 1 eq.), AcOH and K_2CO_3 (163 mg, 1.18 mmol) in MeOH (22 mL) and H_2O (11 mL) were added. The resulting mixture was purified by column chromatography with 94% DCM/MeOH as an eluent to yield compound **14e** as a brown solid (69 mg, 37%). **m.p.** = 98 – 99°C. **^{1}H NMR (500 MHz, $CDCl_3$)** δ 8.31 (s, 1H, H-1'), 7.14 (s, 1H, NH), 6.60 (d, *J* = 7.1 Hz, 1H, NH), 6.43 (d, *J* = 2.1 Hz, 2H, H-6'), 6.27 (t, *J* = 2.0 Hz, 1H, H-8'), 6.18 (s, 1H, H-3'), 4.51 – 4.43 (m, 2H, H-1), 4.18 (t, *J* = 5.7 Hz, 1H, H-4), 4.11 – 4.03 (m, 1H, H-6), 3.83 (t, *J* = 4.5 Hz, 2H, H-2), 3.79 (s, 6H, H-8), 3.72 (dd, *J* = 9.7, 6.3 Hz, 2H, H-3), 1.74 (s, 1H, OH), 1.15 (d, *J* = 6.6 Hz, 3H, H-7), 1.13 (d, *J* = 6.6 Hz, 3H, H-7). **^{13}C NMR (125 MHz, $CDCl_3$)** δ 170.4 (C-5), 170.0 (C-2'), 162.3 (C-4'), 161.5 (C-7'), 157.9(C-1'), 139.9 (C-5'), 100.8 (C-6'), 96.6 (C-8'), 87.3 (C-3'), 72.5 (C-3), 70.1 (C-4), 69.7 (C-2), 65.2 (C-1), 55.4 (C-8), 41.2 (C-6), 22.6 (C-7). **IR ($\nu_{max.}$/cm^{-1})** 3249 (OH); 2935 (NH); 1609 (–C=O); 1584 (Ar. –C=C); 1254 (alkoxy –C-O); 1056 (alcohol –C-O). **ESI-MS (m/z)** calculated $[M+H]^+$ for $C_{20}H_{29}N_4O_6$ 421.2075, found 421.2082.

4.8.6. Synthesis of 2-hydroxy-*N*-isopropyl-3-{2-[4-(3,4-difluorophenylamino) pyrimidin-6-yloxy]ethoxy}propanamide 14f

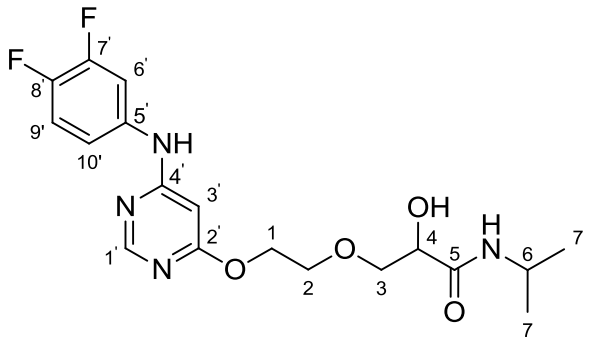

The general procedure was followed using compound **15f** (396 mg, 1.28 mmol) in DCM (15 mL) and EtOAc (30 mL). Isopropyl isocyanide (88.4 mg, 1.28 mmol, 1 eq.), AcOH and K_2CO_3 (440 mg, 3.18 mmol) in MeOH (58 mL) and H_2O (29 mL) were added. The resulting mixture was purified by column chromatography with 94% DCM/MeOH as an eluent to yield compound **14f** as a cream white solid (179 mg, 34%). **m.p.** =122 – 123°C. **^{1}H NMR (500 MHz, $CDCl_3$)** δ 8.30 (s, 1H, H-1'), 7.67 (s, 1H, NH), 7.29 – 7.22 (m, 1H, H-6'), 7.14 (q, *J* = 9.1 Hz, 1H, H-9'), 7.02 – 6.97 (m, 1H, H-10'), 6.66 (d, *J* = 7.7 Hz, 1H, NH), 5.99 (s, 1H, H-3'), 4.50 – 4.42 (m, 2H, H-1), 4.21 (t, *J* = 5.3 Hz, 1H, H-4), 4.12 – 4.03 (m, 2H, H-6 and OH), 3.85 – 3.79 (m, 3H, H-2 and H-3), 3.75 – 3.70 (m, 1H, H-3), 1.15 (d, *J* = 6.8 Hz, 3H, H-7), 1.13 (d, *J* = 6.7 Hz, 3H, H-7). **^{13}C NMR (125 MHz, $CDCl_3$)** δ 170.5 (C-5), 169.9 (C-2'), 162.2 (C-4'), 157.9 (C-1'), 150.4 (dd, $J_{C\text{-}F}$ = 239.4, 13.5 Hz, C-7'), 147.4 (dd, $J_{C\text{-}F}$ = 252.0, 12.7 Hz, C-8'), 135.1 (dd, $J_{C\text{-}F}$ = 8.2, 3.3 Hz, C-5'), 118.2 (dd, $J_{C\text{-}F}$ = 5.9, 3.4 Hz, C-10'), 117.7 (dd, $J_{C\text{-}F}$ = 18.1, 0.8 Hz, C-9'), 111.8 (d, $J_{C\text{-}F}$ = 19.7 Hz, C-6'), 87.2 (C-3'), 72.7 (C-3), 70.4 (C-4), 69.7 (C-2), 65.4 (C-1), 41.2 (C-6), 22.7 (C-7). **IR ($\nu_{max.}$/cm^{-1})** 3304 (OH); 2984 (NH); 1610 (–C=O); 1582 (Ar. –C=C); 1253 (alkoxy –C-O); 1053 (alcohol –C-O). **ESI-MS (m/z)** calculated $[M+H]^+$ for $C_{18}H_{23}F_2N_4O_4$ 397.1676, found 397.1682.

4.9. General procedure to prepare 2-oxo-*N*-isopropyl-3-{2-[4-(phenylamino) pyrimidin-6-yloxy]ethoxy}propanamide 13a and analogues

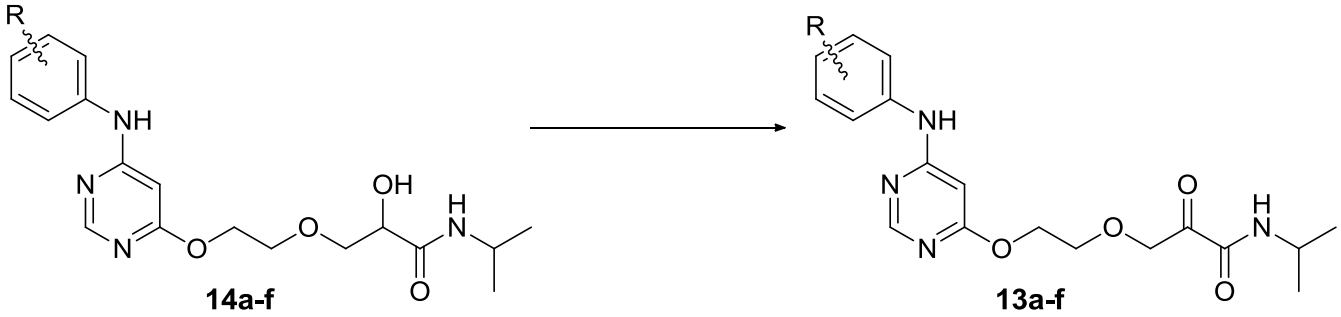

a; R = 3-bromo

b; = H

c; = 3-chloro-4-fluoro

d; = 3-ethynyl

e; = 3,5-dimethoxy

f; = 3,4-difluoro

IBX (2 eq.) was added to a solution of compound **14** in dry DMSO. The reaction mixture was stirred at room temperature overnight. After formation of a new product spot, visible by TLC, the reaction mixture was stopped. The product was extracted using DCM and washed three

times with H_2O and once with brine. The combined organic layers were dried over Na_2SO_4 and concentrated *in vacuo* to give sticky material. The sticky material was put under high vacuum to give a solid, and it was confirmed to be the desired product.

4.9.1. Synthesis of 2-oxo-*N*-isopropyl-3-{2-[4-(phenylamino)pyrimidin-6-yloxy] ethoxy}propanamide 13b

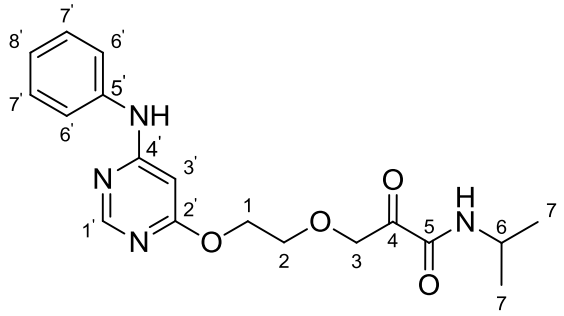

The general procedure was followed using compound **14b** (47 mg, 0.13 mmol) and IBX (73 mg, 0.261 mmol, 2 eq) in DMSO (2 mL). The desired compound **13b** was yielded as a pale yellow solid (33 mg, 70%). **m.p.** = 50 – 51°C. **^{1}H NMR (300 MHz, $CDCl_3$)** δ 8.32 (s, 1H, H-1'), 7.43 (s, 1H, NH), 7.41 – 7.33 (m, 2H, H-6'), 7.30 – 7.26 (m, 2H, H-7'), 7.20 – 7.12 (m, 1H, H-8'), 6.75 (s, 1H, NH), 6.17 (s, 1H, H-3'), 4.90 (s, 2H, H-3), 4.58 – 4.44 (m, 2H, H-1), 4.11 – 3.95 (m, 1H, H-6), 3.93 – 3.81 (m, 2H, H-2), 1.20 (d, *J* = 6.6 Hz, 6H, H-7). **^{13}C NMR (75 MHz, $CDCl_3$)** δ 194.7 (C-4), 169.9 (C-2'), 162.4 (C-4') , 158.3 (C-5), 157.8 (C-1') , 138.2 (C-5'), 129.5 (C-7'), 124.8 (C-8'), 122.5 (C-6'), 86.8 (C-3'), 73.4 (C-3), 69.9 (C-2), 65.3 (C-1), 41.5 (C-6), 22.3 (C-7). **IR ($\nu_{max.}$/cm^{-1})** 3299 (NH); 2925 (=C-H); 1723 (ketone –C=O); 1649 (amide –C=O); 1249 (alkoxy =C-O). **ESI-MS (m/z)** calculated $[M+H]^+$ for $C_{18}H_{23}N_4O_4$ 359.1709, found 359.1714.

4.9.2. Synthesis of 2-oxo-*N*-isopropyl-3-{2-[4-(3-chloro-4-fluorophenylamino) pyrimidin-6-yloxy]ethoxy}propanamide 13c

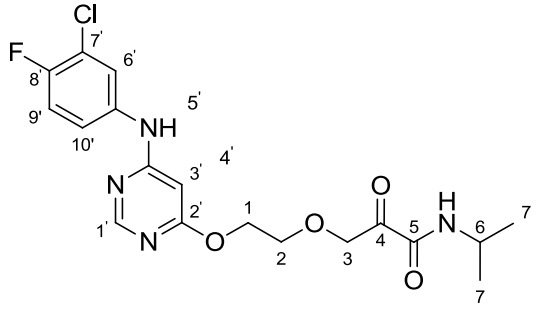

The general procedure was followed using compound **14c** (120 mg, 0.29 mmol) and IBX (163 mg, 0.58 mmol, 2 eq) in DMSO (4 mL). The desired compound **13c** was yielded as a pale yellow solid (100 mg, 84%). **m.p.** = 72 – 73°C. **^{1}H NMR (300 MHz, $CDCl_3$)** δ 8.27 (s, 1H,

H-1'), 7.90 (s, 1H, NH), 7.40 (dd, *J* = 6.4, 2.5 Hz, 1H, H-6'), 7.20 – 7.13 (m, 1H, H-10'), 7.13 – 7.06 (m, 1H, H-9'), 6.77 (d, *J* = 7.8 Hz, 1H, NH), 6.02 (s, 1H, H-3'), 4.88 (s, 2H, H-3), 4.53 – 4.46 (m, 2H, H-1), 4.09 – 3.95 (m, 1H, H-6), 3.88 – 3.82 (m, 2H, H-2), 1.18 (d, *J* = 6.6 Hz, 6H, H-7). **^{13}C NMR (125 MHz, $CDCl_3$)** δ 194.7 (C-4), 169.8 (C-2'), 162.2 (C-4'), 158.4 (C-5), 157.5 (C-1') 156.3 (C-8'), 135.0 (C-5'), 124.8 (C-6'), 122.5 (C-10'), 121.7 (C-7'), 117.2 (C-9'), 87.3 (C-3'), 73.4 (C-3), 69.9 (C-2), 65.5 (C-1), 41.6 (C-6), 22.3 (C-7). **IR ($\nu_{max.}$/cm^{-1})** 3294 (NH); 2921 (=C**-**H); 1646 (amide –C**=**O); 1259 (=C**-**N); 1612 (ketone –C**=**O). **ESI-MS (m/z)** calculated $[M+H]^+$ for $C_{18}H_{21}ClFN_4O_4$ 411.1222, found 411.1230.

4.9.3. Synthesis of 2-oxo-*N*-isopropyl-3-{2-[4-(3-ethynylphenylamino)pyrimidin-6-yloxy]ethoxy}propanamide 13d

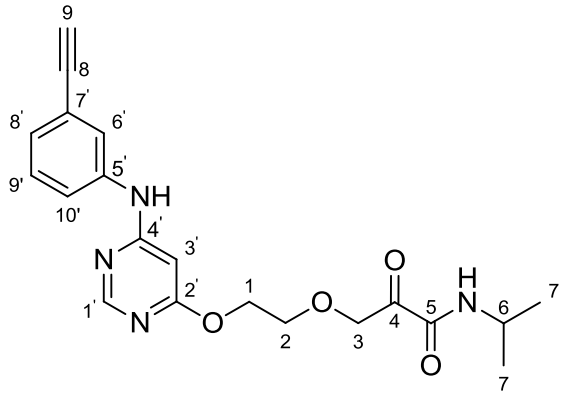

The general procedure was followed using compound **14d** (52 mg, 0.135 mmol) and IBX (76 mg, 0.271 mmol, 2 eq) in DMSO (2 mL). The desired compound **13d** was yielded as a dark brown solid (39 mg, 76%). **^{1}H NMR (500 MHz, $CDCl_3$)** δ 8.32 (s, 1H, H-1'), 7.68 (s, 1H, NH), 7.43 (s, 1H, H-6'), 7.30 (m, 3H, H-8', H-9' and H-10'), 6.77 (d, *J* = 7.1 Hz, 1H, NH), 6.15 (s, 1H, H-3'), 4.90 (s, 2H, H-3), 4.56 – 4.50 (m, 2H, H-1), 4.11 – 3.99 (m, 1H, H-6), 3.91 – 3.86 (m, 2H, H-2), 3.11 (s, 1H, H-9), 1.20 (d, *J* = 6.6 Hz, 6H, H-7). **^{13}C NMR (125 MHz, $CDCl_3$)** δ 194.7 (C-4), 170.0 (C-2'), 162.1 (C-4'), 158.4 (C-5), 157.8 (C-1'), 138.6 (C-5'), 129.5 (C-9'), 128.3 (C-8'), 125.5 (C-6'), 123.4 (C-7'), 122.7 (C-10'), 87.3 (C-3'), 83.0 (C-8), 78.0 (C-9), 73.6 (C-3), 69.9 (C-2), 65.4 (C-1), 41.6 (C-6), 22.3 (C-7). **IR ($\nu_{max.}$/cm^{-1})** 3298 (NH); 2923 (=C**-**H); 1646 (ketone –C**=**O); 1612 (amide –C**=**O); 1259 (=C**-**N). **ESI-MS (m/z)** calculated $[M+H]^+$ for $C_{20}H_{23}N_4O_4$ 383.1700, found 383.1714.

4.9.4. Synthesis of 2-oxo-*N*-isopropyl-3-{2-[4-(3,5-dimethoxyphenylamino) pyrimidin-6-yloxy]ethoxy}propanamide 13e

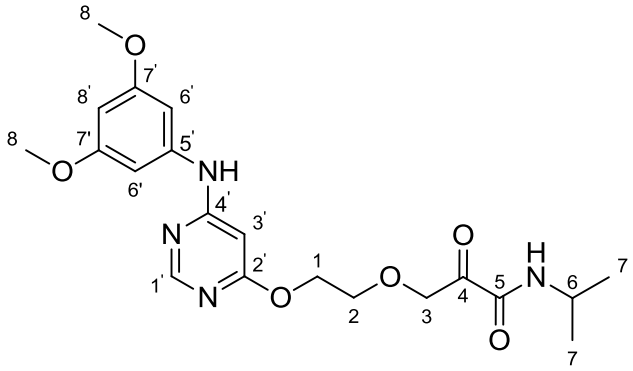

The general procedure was followed using compound **14e** and IBX in DMSO (2 mL). The desired compound **13e** was yielded as a pale yellow solid. **^{1}H NMR (500 MHz, $CDCl_3$)** δ 8.32 (s, 1H, H-1'), 7.34 (s, 1H, NH), 6.74 (d, *J* = 8.3 Hz, 1H, NH), 6.47 – 6.43 (m, 2H, H-6'), 6.29 – 6.26 (m, 1H, H-8'), 6.24 – 6.22 (m, 1H, H-3'), 4.90 (s, 2H, H-3), 4.56 – 4.50 (m, 2H, H-1), 4.09 – 4.00 (m, 1H, H-6), 3.94 – 3.84 (m, 2H, H-2), 3.79 (s, 6H, H-8), 1.20 (d, *J* = 6.6 Hz, 6H, H-7). **^{13}C NMR (125 MHz, $CDCl_3$)** δ 194.7 (C-4), 170.1 (C-2), 161.5 (C-4'), 160.7 (C-7'), 158.4 (C-5), 157.5 (C-1'), 139.8 (C-5'), 100.8 (C-6'), 96.8 (C-8'), 87.4 (C-3'), 73.4 (C-3), 69.9 (C-2), 65.4 (C-1), 55.4 (C-8), 41.6 (C-6), 22.4 (C-7). **IR ($\nu_{max.}$/cm^{-1})** 3358 (NH); 2974 (=C-H); 1721 (ketone –C=O); 1649 (amide –C=O); 1249 (=C-N). **ESI-MS (m/z)** calculated $[M+H]^+$ for $C_{20}H_{27}N_4O_6$ 419.1907, found 419.1925.

4.10. General procedure to prepare 2-hydroxy-3-{2-[4-(3-bromophenylamino) pyrimidin-6-yloxy]ethoxy}propanenitriles 22a and 22b

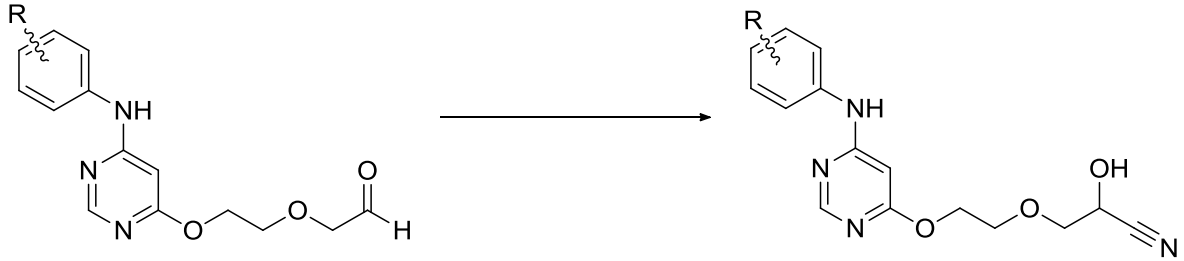

15a-b **22a-b**

a; R = 3-bromo

b; = H

To a round bottomed flask was added a solution of $NaHSO_3$ in water, the flask was then cooled in an ice bath. A solution of compound **15** in MeOH was then added and the reaction mixture was stirred in an ice bath for 2 h. After that a solution of KCN in water was added

and the reaction was left to stir at room temperature overnight. The mixture was extracted with DCM and washed with H_2O and the organic layer was collected and dried over Na_2SO_4 and concentrated *in vacuo*. The reaction mixture was purified by preparative thin layer chromatography with 97% DCM/MeOH as an eluent to give the desired product.

4.10.1. Synthesis of 2-hydroxy-3-{2-[4-(3-bromophenylamino)pyrimidin-6-yloxy]ethoxy}propanenitrile 22a

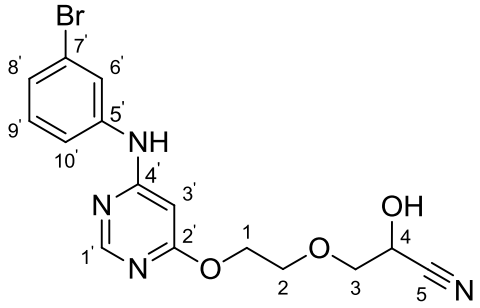

The general procedure was followed using $NaHSO_3$ (64.9 mg, 0.63 mmol, 1.1 eq.) in H_2O (2 mL), compound **15a** (200 mg, 0.57 mmol, 1 eq.) in MeOH (3 mL) and KCN (40.1 mg, 0.63 mmol, 1.1 eq.) in H_2O (2 mL). Compound **22a** was yielded as a pale yellow sticky solid (41.2 mg, 19%).**^{1}H NMR (500 MHz, $CDCl_3$)** δ 8.32 (s, 1H, H-1'), 7.49 (s, 1H, H-6'), 7.29 – 7.27 (m, 1H, NH), 7.25 – 7.17 (m, 3H, H-8', H-9' and H-10'), 6.07 (s, 1H, H-3'), 4.69 (s, 1H, OH), 4.60 (t, *J* = 4.2 Hz, 1H, H-4), 4.52 – 4.47 (m, 2H, H-1), 3.99 – 3.86 (m, 2H, H-2), 3.84 – 3.79 (m, 2H, H-3). **^{13}C NMR (125 MHz, $CDCl_3$)** δ 169.9 (C-2'), 161.9 (C-4'), 157.9 (C-1'), 139.7 (C-5'), 130.7 (C-9'), 127.7 (C-8'), 125.0 (C-6'), 123.0 (C-7'), 120.6 (C-10'), 118.2 (C-5), 87.5 (C-3'), 72.4 (C-3), 70.5 (C-2), 65.4 (C-1), 60.8 (C-4). **IR ($\nu_{max.}$/cm^{-1})** 3105 (OH); 3058 (NH); 2984 (-C-H); 2215 (-C≡N); 1296 (alkoxy –C-O). **ESI-MS (m/z)** calculated $[M+H]^+$ for $C_{15}H_{16}BrN_4O_3$ 379.0390, found 379.0400.

4.10.2. Synthesis of 2-hydroxy-3-{2-[4-(phenylamino)pyrimidin-6-yloxy] ethoxy}propanenitrile 22b

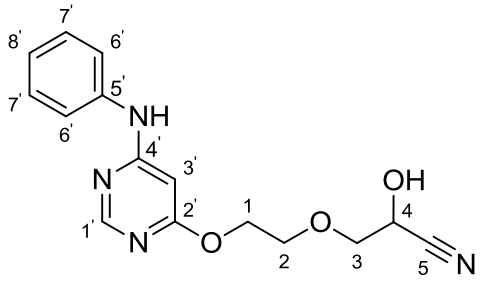

The general procedure was followed using $NaHSO_3$ (209 mg, 2.01 mmol, 1.1 eq.) in H_2O (2 mL), compound **15b** (500 mg, 1.83 mmol, 1 eq.) in MeOH (3 mL) and KCN (131 mg, 2.01 mmol, 1.1 eq.) in H_2O (2 mL). Compound **22b** was yielded as a pale yellow sticky solid (131 mg, 24%). **^{1}H NMR (500 MHz, $CDCl_3$)** δ 8.28 (s, 1H, H-1'), 7.51 (s, 1H, NH), 7.35 (t, *J* = 7.6 Hz, 2H, H-6'), 7.25 – 7.23 (m, 2H, H-7'), 7.15 (t, *J* = 7.4 Hz, 1H, H-8'), 6.07 (s, 1H, H-3'), 4.60 (t, *J* = 4.3 Hz, 1H, H-4), 4.45 (t, *J* = 4.4 Hz, 2H, H-1), 3.95 – 3.83 (m, 3H, H-2 and OH), 3.80 (d, *J* = 4.2 Hz, 2H, H-3). **^{13}C NMR (125 MHz, $CDCl_3$)** δ 169.9 (C-2'), 162.5 (C-4'), 157.8 (C-1'), 138.1 (C-5'), 129.5 (C-7'), 125.0 (C-8'), 122.6 (C-6'), 118.4 (C-5'), 86.6 (C-3'), 72.5 (C-3), 70.4 (C-2), 65.3 (C-1), 60.7 (C-4). **IR ($\nu_{max.}$/cm^{-1})** 3250 (OH); 3086 (NH); 2989 (-C-H); 2220 (-C≡N); 1252 (alkoxy –C-O). **ESI-MS (m/z)** calculated $[M+H]^+$ for $C_{15}H_{17}N_4O_3$ 301.1295, found 301.1295.

4.11. General procedure for the attempted preparation of methyl-3-{2-[4-(3-bromophenylamino)pyrimidin-6-yloxy]ethoxy}-2-hydroxypropanoate 21 which yielded methyl *N*-3-bromophenyl-6-[2-(2,2-dimethoxyethoxy) ethoxy]pyrimidin-4-amine 41a and 41b

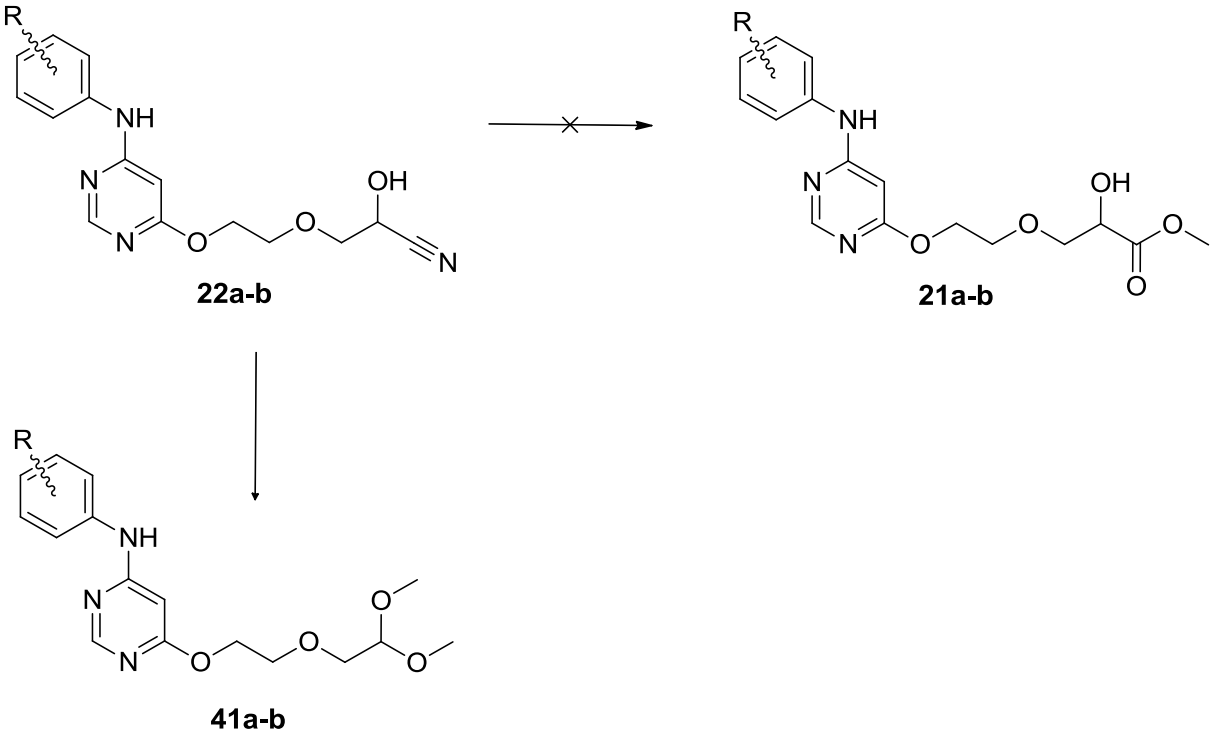

a; R = 3-bromo

b; = H

To a round bottomed flask was added 98% sulfuric acid (H_2SO_4) and subsequently compound **22** in MeOH/H_2O was added dropwise, while maintaining the temperature at 43°C. After complete addition the mixture was heated at 60°C for 1 h, thereafter it was heated at 70°C for 3 h. Excess MeOH was then added and the reaction mixture was refluxed for 6 h. The mixture was cooled in ice cold water, neutralised with 25% NH_3, extracted with DCM and washed with H_2O. The aqueous layer was then back extracted with DCM (× 3). The collected organic layers were dried over Na_2SO_4 and concentrated *in vacuo.* The crude material was purified by preparative thin layer chromatography with 95% DCM/MeOH as an eluent to give the desired product.

4.11.1. Synthesis of *N*-3-bromophenyl-6-[2-(2,2-dimethoxyethoxy)ethoxy] pyrimidin-4-amine 41a

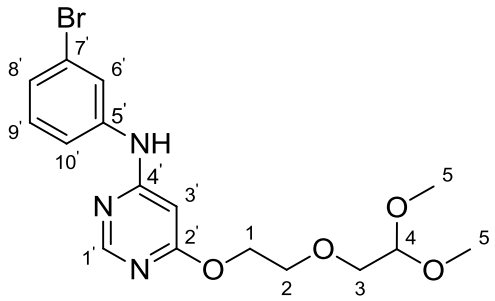

The general procedure was followed using H_2SO_4 and compound **22a** (87 mg, 0.229 mmol) in MeOH (3 mL) and H_2O (1 mL). Thereafter MeOH (6 mL) was added. The crude material was purified by preparative thin layer chromatography with 95% DCM/MeOH as an eluent to yield compound **41a** as a cream white solid (11.8 mg, 12%). **m.p.** = 100 – 101°C. **^{1}H NMR (500 MHz, $CDCl_3$)** δ 8.35 (s, 1H, H-1'), 7.51 (s, 1H, H-6'), 7.24 – 7.20 (m, 3H, H-8', H-9' and H-10'), 6.93 (s, 1H, NH), 6.15 (s, 1H, H-3'), 4.52 (t, *J* = 5.2 Hz, 1H, H-4), 4.51 – 4.48 (m, 2H, H-1), 3.85 – 3.81 (m, 2H, H-2), 3.58 (d, *J* = 5.2 Hz, 2H, H-3), 3.39 (s, 6H, H-5). **^{13}C NMR (125 MHz, $CDCl_3$)** δ 170.2 (C-2'), 161.7 (C-4'), 158.0 (C-1'), 139.9 (C-5'), 130.7 (C-9'), 127.4 (C-8'), 124.7 (C-6'), 123.0 (C-7'), 120.4 (C-10'), 102.8 (C-4), 87.7 (C-3'), 71.0 (C-3), 69.8 (C-2), 65.5 (C-1), 54.1 (C-5). **IR ($\nu_{max.}$/cm^{-1})** 3316 (OH); 3242 (NH); 3081 (=C**-**H); 2742 (-C**-**H); 1610 (–C**=**N); 1252 (=C**-**N); 1244 (alkoxy C**-**O). **ESI-MS (m/z)** calculated $[M+H]^+$ for $C_{16}H_{21}BrN_3O_4$ 398.0708, found 398.0710.

4.11.2. Synthesis of *N*-phenyl-6-[2-(2,2-dimethoxyethoxy)ethoxy] pyrimidin-4-amine 41b

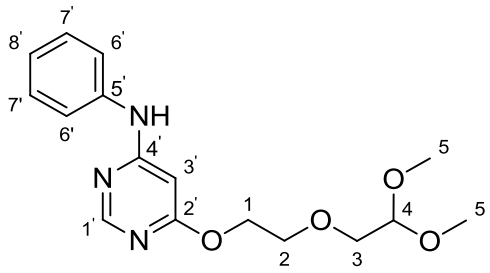

The general procedure was followed using H_2SO_4 and compound **22b** (100 mg, 0.333 mmol) in MeOH (3 mL) and H_2O (1 mL). Thereafter MeOH (6 mL) was added. The crude material was purified by preparative thin layer chromatography with 95% DCM/MeOH as an eluent to yield compound **41b** as a cream white solid (27.8 mg, 25%). **m.p.** = 103 – 104°C. **^{1}H NMR (400 MHz, $CDCl_3$)** δ 8.33 (s, 1H, H-1'), 7.37 (t, *J* = 7.8 Hz, 2H, H-6'), 7.29 – 7.27 (m, 2H, H-7'), 7.16 (t, *J* = 7.4 Hz, 1H, H-8'), 6.80 (s, 1H, NH), 6.15 (s, 1H, H-3'), 4.51 (t, *J* = 5.2 Hz, 1H, H-4), 4.50 – 4.45 (m, 2H, H-1), 3.84 – 3.80 (m, 2H, H-2), 3.57 (d, *J* = 5.2 Hz, 2H, H-3), 3.39 (s, 6H, H-5). **^{13}C NMR (100 MHz, $CDCl_3$)** δ 170.6 (C-2'), 162.8 (C-4'), 158.5 (C-1'), 137.9 (C-5'), 129.9 (C-7'), 125.3 (C-8'), 122.9 (C-6'), 103.3 (C-4), 87.4 (C-3'), 71.5 (C-3), 70.3 (C-2), 65.8 (C-1), 54.5 (C-5). **IR ($\nu_{max.}$/cm^{-1})** 3376 (OH); 3024 (NH); 2923 (=C**-**H); 2732 (-C**-**H); 1625 (–C**=**N); 1248 (=C**-**N); 1235 (alkoxy C**-**O). **ESI-MS (m/z)** calculated $[M+H]^+$ for $C_{16}H_{22}N_3O_4$ 320.1608, found 320.1605.

4.12. Synthesis of 6-chloro-4-(3-bromophenylamino)pyrimidine 26a

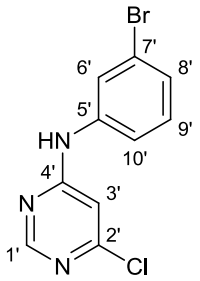

Ethanol (100 mL), 3-bromoaniline **19a** (6.9 g, 0.040 mol, 1 eq.) and triethylamine (5.6 mL, 0.040 mol, 1 eq.) were sequentially added to a round bottomed flask containing 4,6-dichloropyrimidine **18** (6.0 g, 0.040 mol, 1 eq.). The reaction was refluxed at 80°C for 18 h. After that the reaction was dissolved in EtOAc (50 mL) and consecutively washed with H_2O (50 mL), saturated NH_4Cl (50 mL) and brine (50 mL). The organic layer was dried over Na_2SO_4 and concentrated *in vacuo* to give compound **26a** as a yellow solid (6.3 g, 55%). **^{1}H NMR (500 MHz, DMSO-d_6)** δ 10.03 (s, 1H, NH), 8.55 (s, 1H, H-1'), 8.06 (s, 1H, H-6'), 7.57 –

7.51 (m, 1H, H-8'), 7.31 (t, *J* = 8.0 Hz, 1H, H-9'), 7.27 – 7.23 (m, 1H, H-10'), 6.84 (s, 1H, H-3'). **^{13}C NMR (75 MHz, DMSO)** δ 160.9 (C-2'), 158.4 (C-4'), 158.0 (C-1'), 140.7 (C-5'), 130.7 (C-9'), 125.5 (C-8'), 122.2 (C-6'), 121.6 (C-7'), 118.8 (C-10'), 105.7 (C-3').

4.13. Synthesis of 4-(3-bromophenylamino)-6-{2-[2-(tetrahydro-2H-pyran-2-yloxy)ethoxy] ethoxy}pyrimidine 29a

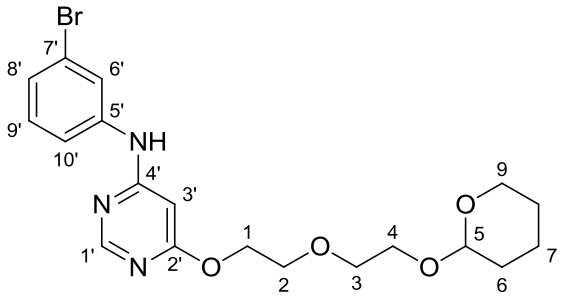

Method 1

Sodium hydride (845 mg, 2.11 mmol, 1.2 eq.) was flame dried under vacuum and purged with N_2 (g) three times. Dry DMF (4 mL) and 2-[2-((tetrahydropyranyloxy)ethoxy]ethanol **17** (330 mg, 1.76 mmol, 1 eq.) were added and the reaction mixture was stirred for 40 min. After that, a solution of 6-chloro-4-(3-bromophenylamino)pyrimidine **26a** (500 mg, 1.76 mmol, 1 eq.) in DMF (4 mL) was cannulated to the reaction mixture. The reaction mixture was then stirred at 150°C for 24 h. The product was extracted using DCM (100 mL) and washed three times with water (50 mL) and once with brine (50 mL). The combined organic layers were dried over Na_2SO_4. The solvent was removed *in vacuo* and the crude material was purified by silica gel column chromatography with 95% DCM/MeOH as an eluent to give compound **29a** as a yellow solid (~30 mg, 3.9%).

Method 2

Alternatively, method 1 was followed using DMSO as a solvent to give compound **29a** as a yellow solid (123 mg, 16%).

Method 3

Alternatively, $Pd_2(dba)_3$ (242 mg, 4 mol%) and (*rac*)-BINAP (494 mg, 12 mol%) were added to a round bottomed flask containing DMSO (15 mL). The flask was sealed and stirred at 80°C for 10 min under nitrogen purge. 4-chloro-6-{2-[2-(tetrahydro-2*H*-pyran-2-yloxy)ethoxy] ethoxy}pyrimidine **31** (2.00 g, 6.62 mmol, 1 eq.), 3-bromoaniline **19a** (2.27 g, 13.3 mmol, 2 eq.) and K_2CO_3 (915 mg, 6.62 mmol, 1 eq.) were then consecutively added and the reaction was stirred at 80°C overnight. The reaction mixture was dissolved in chloroform (200 mL) and washed twice with water (100 mL). The combined organic layers were dried over

Na_2SO_4. The solvent was removed *in vacuo* and the crude reddish-brown oil was purified by silica gel column chromatography with 50% EtOAc/Hex as an eluent to yield compound **29a** as a yellow solid (580 mg, 20%).

Method 4

Method 3 was repeated using $Pd_2(dba)_3$ (54.0 mg, 2 mol%) and (*rac*)-BINAP (112 mg, 6 mol%) which were added to a round bottomed flask containing DMSO (5 mL). Thereafter 4-chloro-6-{2-[2-(tetrahydro-2*H*-pyran-2-yloxy)ethoxy]ethoxy}pyrimidine **31** (906 mg, 3.00 mmol, 1 eq.), 3-bromoaniline **19a** (1.03 g, 6.00 mmol, 2 eq.) and K_2CO_3 (415 mg, 3.00 mmol, 1 eq.) were then consecutively added and the reaction was stirred at 80°C overnight. The crude reddish-brown oil was purified by silica gel column chromatography with 50% EtOAc/Hex as an eluent to yield compound **29a** as a yellow solid (638 mg, 22%). **^{1}H NMR (300 MHz, $CDCl_3$)** δ 8.35 (s, 1H, H-1'), 7.51 (s, 1H, H-6'), 7.23 – 7.21 (m, 3H, H-8', H-9' and H-10'), 6.16 (s, 1H, H-3'), 4.66 – 4.60 (m, 1H, H-5), 4.52 – 4.46 (m, 2H, H-1), 3.93 – 3.80 (m, 4H, H-2, H-4 and H-9), 3.76 – 3.69 (m, 2H, H-3), 3.67 – 3.58 (m, 1H, H-9), 3.53 – 3.44 (m, 1H, H-4), 1.87 – 1.44 (m, 6H, H-6, H-7 and H-8).

4.14. Synthesis of 4-(3-bromophenylamino)-6-dimethylaminopyrimidine 30a

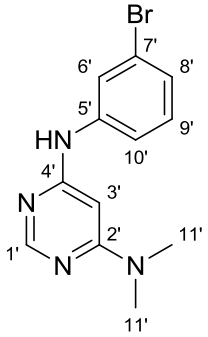

Sodium hydride (845 mg, 2.11 mmol, 1.2 eq.) was flame dried under vacuum and purged with N_2(g) three times. Dry DMF (4 mL) and 2-[2-((tetrahydropyranyloxy)ethoxy]ethanol **17** (330 mg, 1.76 mmol, 1 eq.) was added and the reaction mixture was stirred for 40 min. After that, a solution of 6-chloro-4-(3-bromophenylamino)pyrimidine **26a** (500 mg, 1.76 mmol, 1 eq.) in DMF (4 mL) was cannulated to the reaction mixture. The reaction mixture was then stirred at 150°C for 24 h. The product was extracted using DCM (100 mL) and washed three times with water (50 mL) and once with brine (50 mL). The combined organic layers were dried over Na_2SO_4. The solvent was removed *in vacuo* and crude material was purified by silica gel column chromatography with 95% DCM/MeOH as an eluent give compound **30a** as a pale yellow solid (268 mg, 52%). **^{1}H NMR (300 MHz, $CDCl_3$)** δ 8.26 (s, 1H, H-1'), 7.78 (s, 1H, NH), 7.53 (s, 1H, H-6'), 7.26 – 7.16 (m, 3H, H-8', H-9' and H-10'), 5.83 (s, 1H, H-3'), 3.05 (s, 6H, H-11').

4.15. Synthesis of 4-chloro-6-isopropoxypyrimidine 32

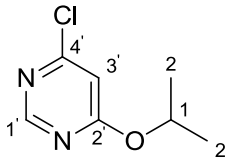

Potassium bis(trimethylsilyl)amide (KHMDS) (5 mL) was added to a solution of 4-chloro-6-{2-[2-(tetrahydro-2*H*-pyran-2-yloxy)ethoxy] ethoxy}pyrimidine **31** (1.00 g, 3.31 mmol, 1 eq.) in 2-propanol (80 mL). 3-Bromoaniline (854 mg, 4.97 mmol, 1.5 eq.) was then added and the reaction mixture was refluxed overnight. The solvent was removed *in vacuo* and crude material was purified by silica gel column chromatography with 94% DCM/MeOH as an eluent to give compound **32** as a white solid (170 mg, 30%). **^{1}H NMR (300 MHz, $CDCl_3$)** δ 8.55 (s, 1H, H-1'), 6.71 (s, 1H, H-3'), 5.39 (hept, *J* = 6.3 Hz, 1H, H-1), 1.36 (d, *J* = 6.3 Hz, 6H, H-2). **^{13}C NMR (75 MHz, $CDCl_3$)** δ 169.9 (C-2'), 160.6 (C-4'), 158.2 (C-1'), 108.2 (C-3'), 70.7 (C-1), 21.8 (C-2).

4.16. Synthesis of 4-dimethylamino-6-{2-[2-(tetrahydro-2H-pyran-2-yloxy) ethoxy]ethoxy}pyrimidine 33

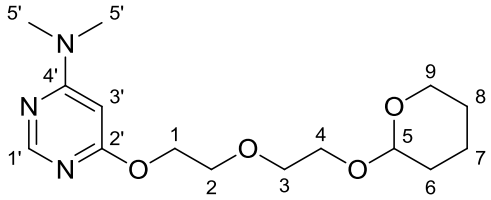

Potassium bis(trimethylsilyl)amide (KHMDS) (2.5 mL) was added to a solution of 4-chloro-6-{2-[2-(tetrahydro-2*H*-pyran-2-yloxy)ethoxy] ethoxy}pyrimidine **31** (500 mg, 1.66 mmol, 1 eq.) in DMF (15 mL). 3-Bromoaniline (185 mg, 1.99 mmol, 1.2 eq.) was then added and the reaction mixture was stirred at 80°C overnight. The product was extracted using DCM (100 mL) and washed three times with water (50 mL) and once with brine (50 mL). The combined organic layers were dried over Na_2SO_4. The solvent was removed *in vacuo* and crude material was purified by silica gel column chromatography with 50% EtOAc/Hex as an eluent give compound **33** as a clear oil (274 mg, 46%). **^{1}H NMR (300 MHz, $CDCl_3$)** δ 8.28 (s, 1H, H-1'), 5.77 (s, 1H, H-3'), 4.66 – 4.62 (m, 1H, H-5), 4.49 – 4.45 (m, 2H, H-1), 3.93 – 3.81 (m, 4H, H-2, H-4 and H-9), 3.76 – 3.69 (m, 2H, H-3), 3.66 – 3.58 (m, 1H, H-9), 3.53 – 3.45 (m, 1H, H-4), 3.06 (s, 6H, H-5'), 1.91 – 1.45 (m, 6H, H-6, H-7 and H-8).

References

1. Encyclopedia Britannica. “Enzyme.” Encyclopedia Britannica, 04 June 2015. Web. (accessed 24 August 2017)
2. Noonberg, B., Benz, C. C., *Drugs*, **2000**, 59, 753-767.
3. Matthews, D. J., Gerritsen, M. E., *Targeting protein kinases for cancer therapy*, John Wiley & Sons, **2011**.
4. Veale, D., Ashcroft, T., Marsh, C., Gibson, G. J., Harris, A. L., *Br. J. Cancer*, **1987**, 55, 513-516.
5. Zahorowska, B., Crowe, P. J., Yang, J. L., *J. Cancer Res. Clin. Oncol.*, **2009**, 135, 1137-1148.
6. ACS. https://www.cancer.org/cancer/non-small-cell-lung-cancer.html (accessed 25 August 2017)
7. Stewart, B. W., Kleihues, P., World Cancer Report, **2003**.
8. Bethune, G., Bethune, D., Ridgway, N., Xu, Z., *J. Thorac. Dis.*, **2010**, 2, 48-51.
9. Joshi, M., Rizvi, S. M., Belani, C. P., *Cancer Manag. Res.*, **2015**, 7, 75-82.
10. World Health Organization. Cancer Fact Sheet. **2017**.
11. Sherwin, S. A., Minna, J. D., Gazdar, A. F., Todaro, G. J., *Cancer Res.*, **1981**, 41, 3538-3542.
12. Yarden, Y., Ullrich, A., *Annu. Rev. Biochem.*, **1988** , 57, 443-478.
13. Jorissen, R. N., Walker, F., Pouliot, N., Garrett, T. P., Ward, C. W., Burgess, A. W., *Exp. Cell Res.*, **2003**, 284, 31-53.
14. Jorge, S. E. D. C., Kobayashi, S. S., Costa, D. B., *Braz. J. Med. Biol. Res.*, **2014**, 47, 929-939.
15. Paul, M. K., Mukhopadhyay, A. K., *Int. J. Med. Sci.*, **2004**, 1, 101-115.
16. Sasaki, H., Endo, K., Okuda, K., Kawano, O., Kitahara, N., Tanaka, H., Kawaguchi, T., *J. Canc. Res. Clin. Oncol.*, **2008**, 134, 569-577.
17. Riely, G. J., *J. Thorac. Oncol.*, **2008**, 3, 146-149.
18. Bareschino, M. A., Schettino, C., Troiani, T., Martinelli, E., Morgillo, F., Ciardiello, F., *Ann. Oncol.*, **2007**, 18, 35-41.
19. Wakeling, A. E., Guy, S. P., Woodburn, J. R., Ashton, S. E., Curry, B. J., Barker, A. J., Gibson, K. H., *Cancer Res.*, **2002**, 62, 5749-5754.
20. Noble, M. E., Endicott, J. A., Johnson, L. N., *Science*, **2004**, 303, 1800-1805.
21. Saijo, N., Kenmotsu, H., *Intern. Med.*, **2010**, 49, 1923-1934.
22. Zwick, E., Bange, J., Ullrich, A., *Trends Mol. Med.*, **2002**, 8, 17-23.
23. Nelson, V., Ziehr, J., Agulnik, M., Johnson, M., *Onco. Targets Ther.*, **2013**, 6, 135-143.
24. Engelman, J. A., Jänne, P. A., *Clin. Cancer Res.*, **2008**, 14, 2895-2899.

25. Kazandjian, D., Blumenthal, G. M., Yuan, W., He, K., Keegan, P., Pazdur, R., *Clin. Cancer Res.,* **2016**, 22, 1307-1312.
26. Thatcher, N., Chang, A., Parikh, P., Pereira, J. R., Ciuleanu, T., von Pawel, J., Carroll, K., *Lancet*, **2005**, 366, 1527-1537.
27. Douillard, J. Y., Shepherd, F. A., Hirsh, V., Mok, T., Socinski, M. A., Gervais, R., Watkins, C. L., *J. Clin. Oncol.*, **2009**, 28, 744-752.
28. Shepherd, F. A., Rodrigues Pereira, J., Ciuleanu, T., Tan, E. H., Hirsh, V., Thongprasert, S., van Kooten, M., *N. Engl. J. Med.*, **2005**, 353, 123-132.
29. Kawaguchi, T., Ando, M., Asami, K., Okano, Y., Fukuda, M., Nakagawa, H., Kamimura, M., *J. Clin. Oncol.*, **2014**, 32, 1902-1908.
30. Kalemkerian, G. P., Akerley, W., Bogner, P., Borghaei, H., Chow, L. Q., Downey, R. J., Hayman, J., *J. Natl. Compr. Cancer*, **2013**, 11, 78-98.
31. Cohen, M. H., Johnson, J. R., Chen, Y. F., Sridhara, R., Pazdur, R., O*ncologist*, **2005**, 10, 461-466.
32. Tang, J., Salama, R., Gadgeel, S. M., Sarkar, F. H., Ahmad, A., *Front. Pharmacol.*, **2013**, 4, 1-9.
33. Rosell, R., Carcereny, E., Gervais, R., Vergnenegre, A., Massuti, B., Felip, E., Porta, R., *Lancet Oncol.*, **2012**, 13, 239-246.
34. Yun, C. H., Mengwasser, K. E., Toms, A. V., Woo, M. S., Greulich, H., Wong, K. K., Eck, M. J., *Proc. Natl. Acad. Sci. U.S.A.*, **2008**, 105, 2070-2075.
35. Spicer, J. F., Rudman, S. M., *Target. Oncol.*, **2010**, 5, 245-255.
36. Solca, F., Dahl, G., Zoephel, A., Bader, G., Sanderson, M., Klein, C., Adolf, G. R., *J. Pharmacol. Exp. Ther.*, **2012**, 343, 342-350.
37. Camidge, D. R., Pao, W., Sequist, L. V., *Nat. Rev. Clin. Oncol.*, **2014**, 11, 473-481.
38. Han, W., Du, Y., *Chem. Biodivers.*, **2017**, 14, 1-21.
39. Patel, H., Pawara, R., Ansari, A., Surana, S., *Eur. J. Med. Chem.*, **2017**, 142, 32-47.
40. Wang, S., Cang, S., Liu, D., *J. Hematol. Oncol.*, **2016**, 9, 34.
41. Goss, G., Tsai, C. M., Shepherd, F. A., Bazhenova, L., Lee, J. S., Chang, G. C., Han, J. Y., *Lancet Oncol.*, **2016**, 17, 1643-1652.
42. Zhang, H., *Onco. Targets Ther.*, **2016**, 9, 5489-5493.
43. Niederst, M. J., Hu, H., Mulvey, H. E., Lockerman, E. L., Garcia, A. R., Piotrowska, Z., Engelman, J. A., *Clin. Cancer Res.*, **2015**, 21, 3924-3933.
44. Thress, K. S., Paweletz, C. P., Felip, E., Cho, B. C., Stetson, D., Dougherty, B., Ercan, D., *Nat. Med.*, **2015**, 21, 560-562.
45. Basu, D., Richters, A., Rauh, D., *Bioorganic Med. Chem.*, **2015**, 23, 2767-2780.
46. Wang, S., Song, Y., Liu, D., *Cancer Lett.*, **2017**, 385, 51-54.

47. Cross, D. A., Ashton, S. E., Ghiorghiu, S., Eberlein, C., Nebhan, C. A., Spitzler, P. J., Hughes, G., *Cancer Discov.*, **2014**, 4, 1046-1061.
48. Zhou, W., Ercan, D., Jänne, P. A., Gray, N. S., *Bioorganic Med. Chem. Lett.*, **2011**, 21, 638-643.
49. Yun, C. H., Boggon, T. J., Li, Y., Woo, M. S., Greulich, H., Meyerson, M., Eck, M. J., *Cancer Cell*, **2007**, 11, 217-227.
50. Stamos, J., Sliwkowski, M. X., Eigenbrot, C., *J. Biol. Chem.*, **2002**, 277, 46265-46272.
51. De Cesco, S., Kurian, J., Dufresne, C., Mittermaier, A., Moitessier, N., *Eur. J. Med. Chem.*, **2017**, 138, 96-114.
52. Smith, S., Keul, M., Engel, J., Basu, D., Eppmann, S., Rauh, D., *ACS Omega*, **2017**, 2, 1563-1575.
53. Schwartz, P. A., Kuzmic, P., Solowiej, J., Bergqvist, S., Bolanos, B., Almaden, C., Kath, J. C., *Proc. Natl. Acad. Sci. U.S.A.*, **2014**, 111, 173-178.
54. Copeland, R. A., Pompliano, D. L., Meek, T. D., *Nat. Rev. Drug Discov.*, **2006**, 5, 730-739.
55. Duplan, V., Hoshino, M., Li, W., Honda, T., Fujita, M., *Angew. Chem. Int. Ed.*, **2016**, 55, 4919-4923.
56. Barf, T., Kaptein, A., *J. Med. Chem*, **2012**, 55, 6243-6262.
57. Lescop, C., Herzner, H., Siendt, H., Bolliger, R., Henneböhle, M., Weyermann, P., Meier, T., *Bioorganic Med. Chem. Lett.*, **2005**, 15, 5176-5181.
58. Lee, C. U., Grossmann, T. N., *Angew. Chem. Int. Ed.*, **2012**, 51, 8699-8700.
59. Tian, Z., Chen, C., Allcock, H. R., *Macromolecules*, **2014**, 47, 1065-1072.
60. McCluskey, A., Keller, P. A., Morgan, J., Garner, J., *Org. Biomol. Chem.*, **2003**, 1, 3353-3361.
61. Changunda, C. R., Basson, A. E., van Vuuren, S. F., Rousseau, A. L., Bode, M. L., *Tetrahedron*, **2017**, 73, 137-147.
62. Brown, D. J., *The Pyrimidines Supplement II*, John Wiley & Sons, **2009**, 16.
63. Boeckman, R. K., Shao, P., Mullins, J. J., *Org. Synth.*, **2000**, 77, 141.
64. Frigerio, M., Santagostino, M., Sputore, S., Palmisano, G., *J. Org. Chem.*, **1995**, 60, 7272-7276.
65. Corey, E. J., Schmidt, G., *Tetrahedron Lett.*, **1979**, 20, 399-402.
66. Omura, K., Sharma, A. K., Swern, D., *J. Org. Chem.*, **1976**, 41, 957-962.
67. Banfi, L., Riva, R., *Org. React.*, **2005**, 65, 1-140.
68. Fatiadi, A. J., *Preparation and synthetic applications of cyano compounds,* John Wiley & Sons: New York, **1983**, 2, 1057-1303.
69. Omura, K., Swern, D., *Tetrahedron*, **1978**, 34, 1651-1660.
70. Matsuda, Hideki; Okabe, Fumihiko; Tamai, Hiroyuki, Japan Patent 2004346022, **2004**.

71. Zhou, W., Ercan, D., Chen, L., Yun, C. H., Li, D., Capelletti, M., Engen, J. R., *Nature*, **2009**, 462, 1070-1074.
72. Holohan, C., Van Schaeybroeck, S., Longley, D. B., Johnston, P. G, *Nat. Rev. Canc.*, **2013**, 13, 714-726.
73. Nicolaou, K. C., Mathison, C. J., Montagnon, T., *Angew. Chem.*, **2003,** 115, 4211-4216.
74. Singh, J., Petter, R. C., Baillie, T. A., Whitty, A., *Nat. Rev. Drug Discov.*, **2011**, 10, 307-317.
75. Singh, J., Petter, R. C., Kluge, A. F., *Curr. Opin. Chem. Biol.*, **2010**, 14, 475-480.
76. Belani, C. P., *Cancer Invest.*, **2010**, 28, 413-423.
77. Li, D., Ambrogio, L., Shimamura, T., Kubo, S., Takahashi, M., Chirieac, L. R., Rettig, W. J., *Oncogene*, **2008**, 27, 4702-4711.
78. Heuckmann, J. M., Rauh, D., Thomas, R. K., *J. Clin. Oncol.*, **2012**, 30, 3417-3420.
79. Oxnard, G. R., Thress, K. S., Alden, R. S., Lawrance, R., Paweletz, C. P., Cantarini, M., Jänne, P. A., *J. Clin. Oncol.*, **2016**, 34, 3375-3382.
80. Mok, T. S., Wu, Y. L., Ahn, M. J., Garassino, M. C., Kim, H. R., Ramalingam, S. S., Lee, C. K., *N. Engl. J. Med.*, **2017**, 376, 629-640.

APPENDIX

A1. Docking protocol

In order to investigate the potential binding modes that our pyrimidine ketoamides could have with wild type and T790M mutated EGFR, computational docking was done using CDOCKER (Discovery Studio 4.0). The protein X-ray crystal structure of the T790M mutated EGFR (PDB code: 4I24) was downloaded from the protein data bank (PDB). The protein PDB file was prepared for docking by firstly checking and adjusting the tautomeric state of each Histidine residue to maximize H-bonding, and H-bonds added to the rigid model followed by protein minimization. Minimization was performed on the protein model using the CHARMm force field Smart Minimizer algorithm. This was done by performing 20000 steps of steepest decent (with RMS gradient tolerance of 0.01 kcal/mol) in a Generalized Born with a simple Switching (GBSW) implicit solvent model (pH 7.4). This was followed by a conjugate Gradient minimization step.

The reliability of the CDOCKER protocol and parameters was first verified by docking the X-ray crystal structure ligands erlotinib and dacomitanib back into the active site of the T790M (PDB: 4I24) EGFR. Encouragingly, the top ranked docked poses for each ligand compared favorably with the X-ray crystal bound structures suggesting the docking parameters used were reliable. We then proceeded to dock our proposed pyrimidine ketoamide library with the T790M EGFR. The pyrimidine ketoamides were built in ChemDraw 12 and subsequently exported into Discovery Studio (DS) for docking. They were first prepared for docking using the prepare ligand protocol and then energy minimized using DS.

A2. Selected ^{1}H and ^{13}C NMR spectra

A2.1. Compound 17

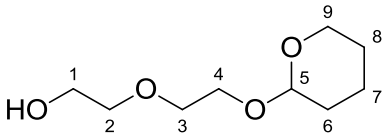

^{1}H NMR spectrum

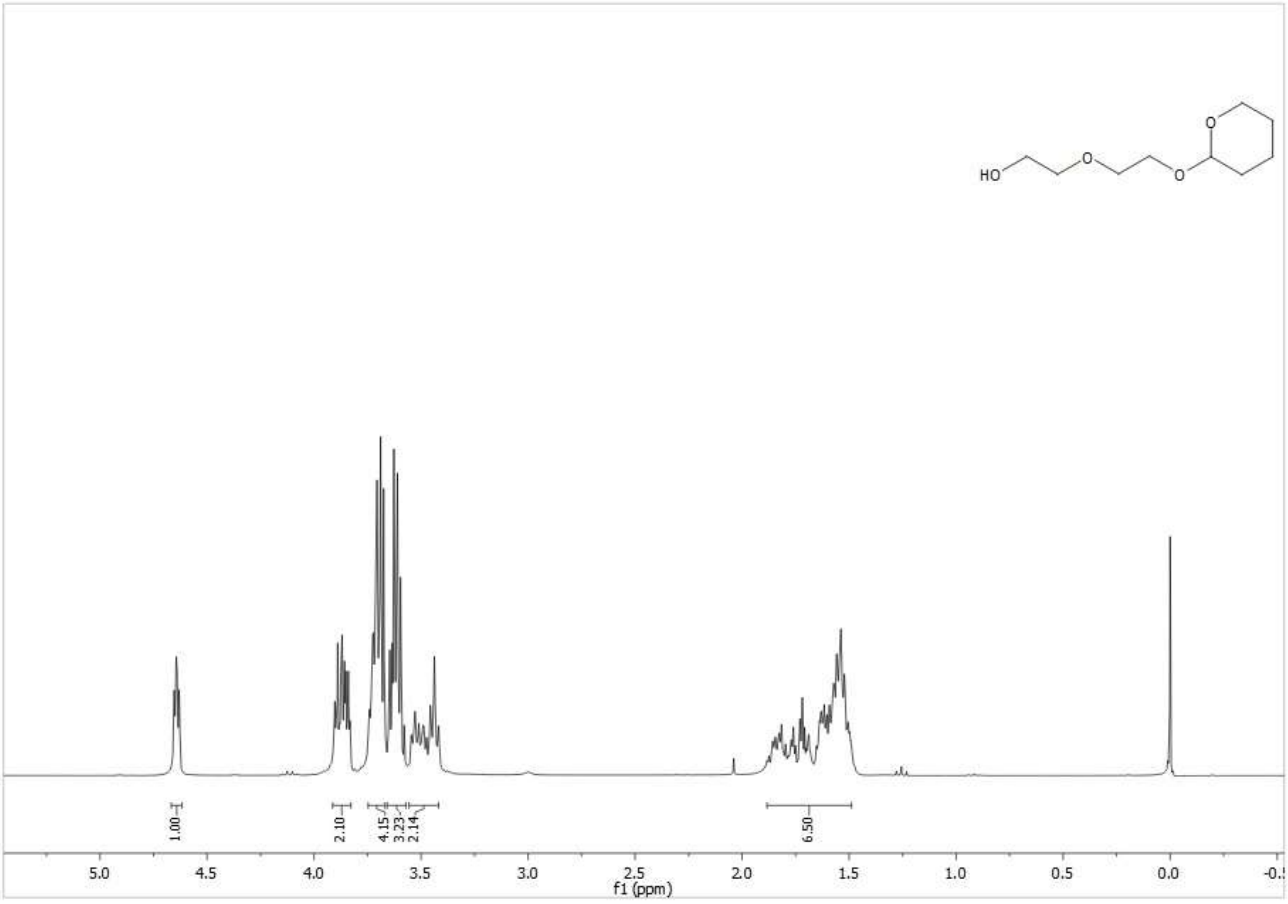

^{13}C NMR spectrum

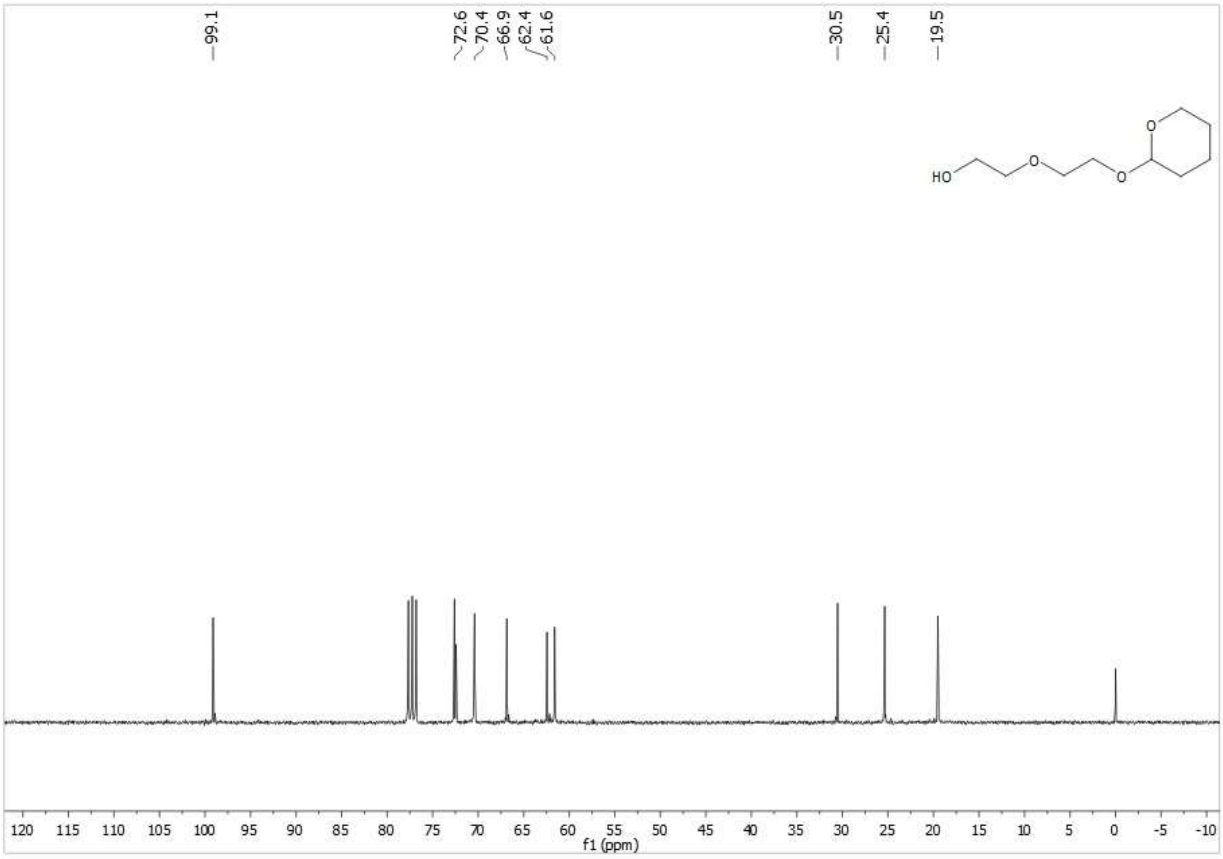

A2.2. Compound 18

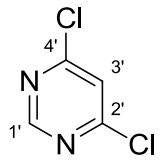

^{1}H NMR spectrum

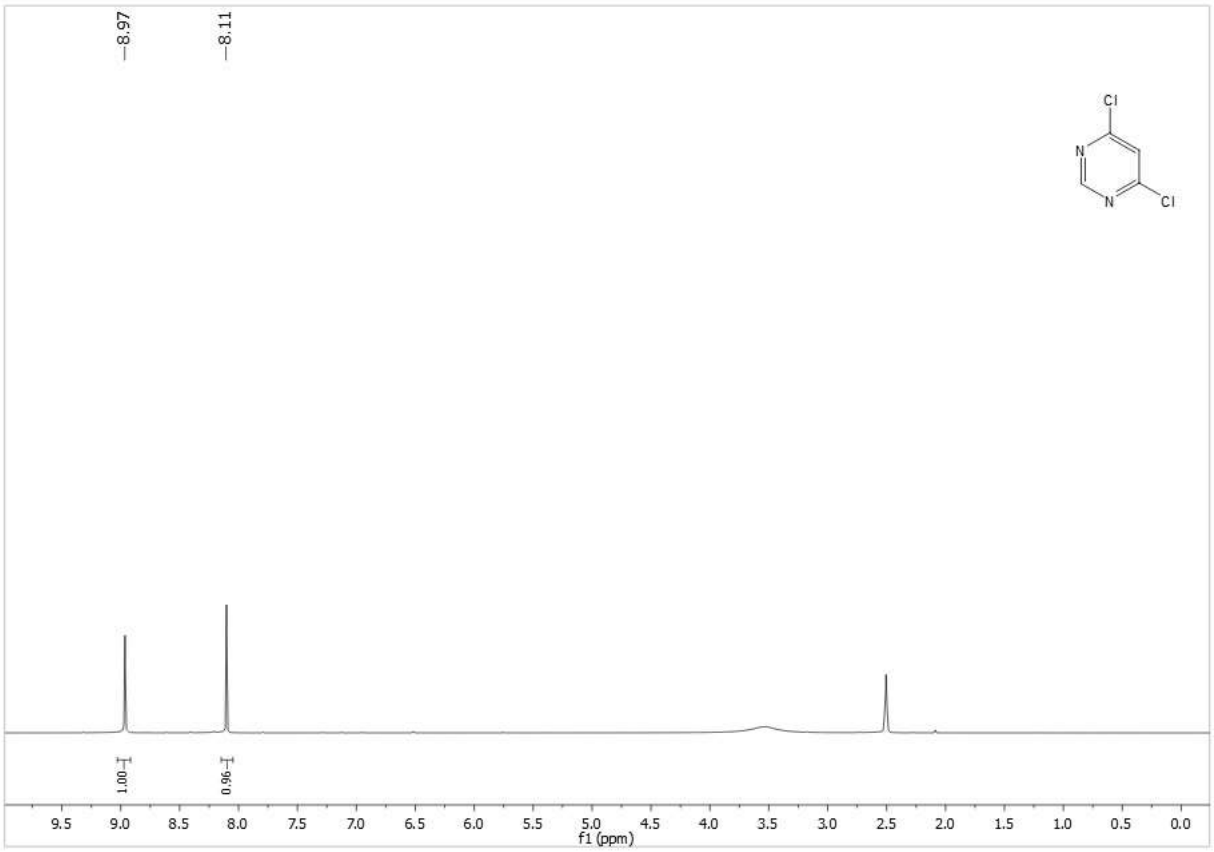

^{13}C NMR spectrum

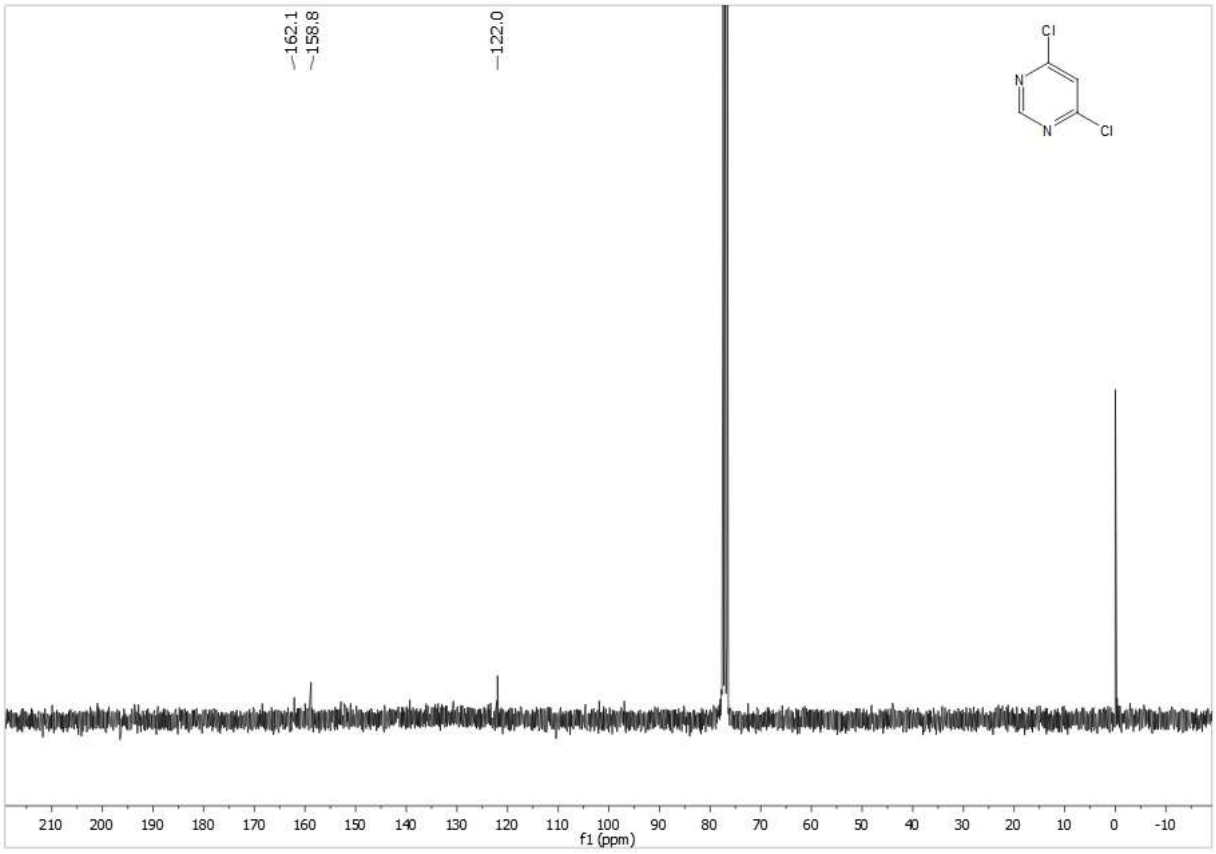

A2.3. Compound 31

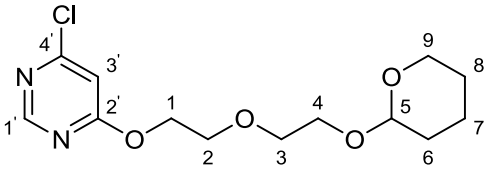

^{1}H NMR spectrum

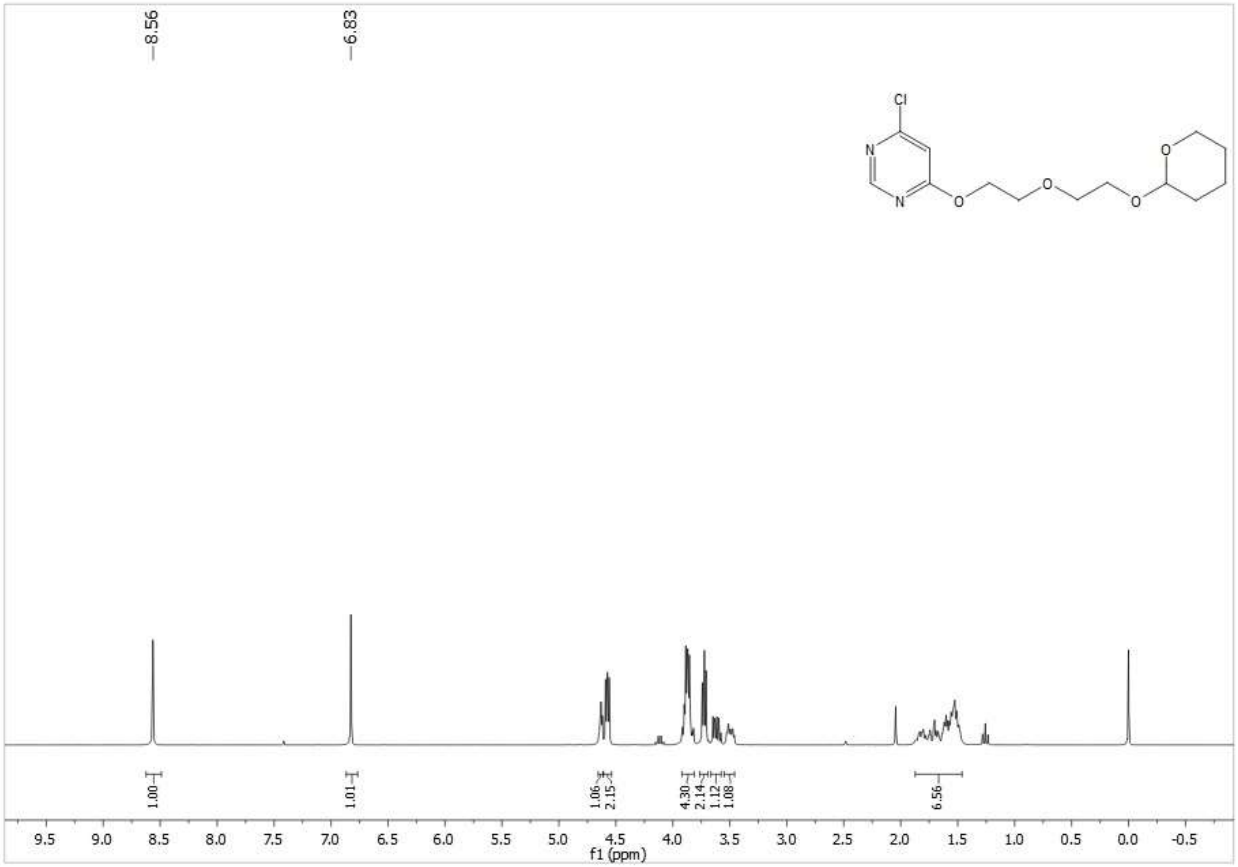

^{13}C NMR spectrum

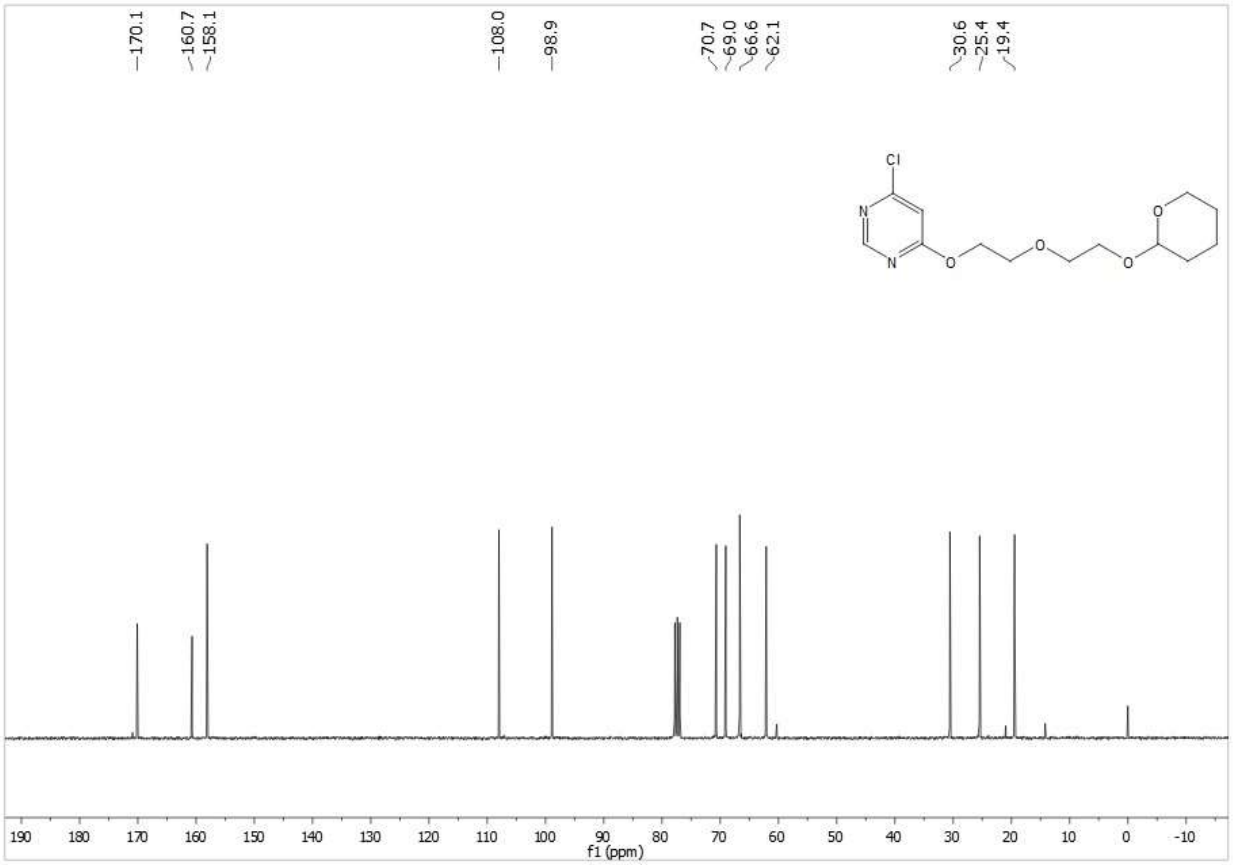

A2.4. Compound 34

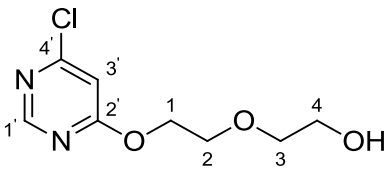

^{1}H NMR spectrum

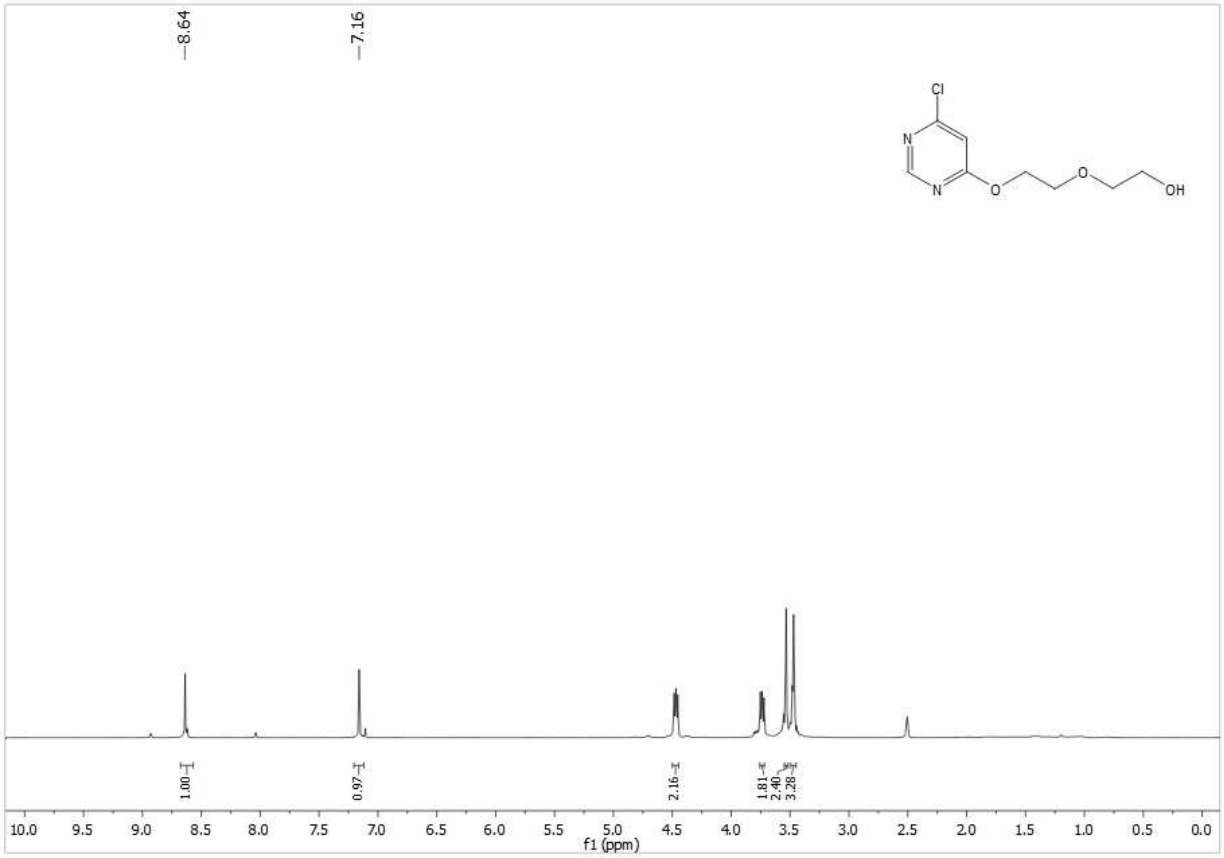

^{13}C NMR spectrum

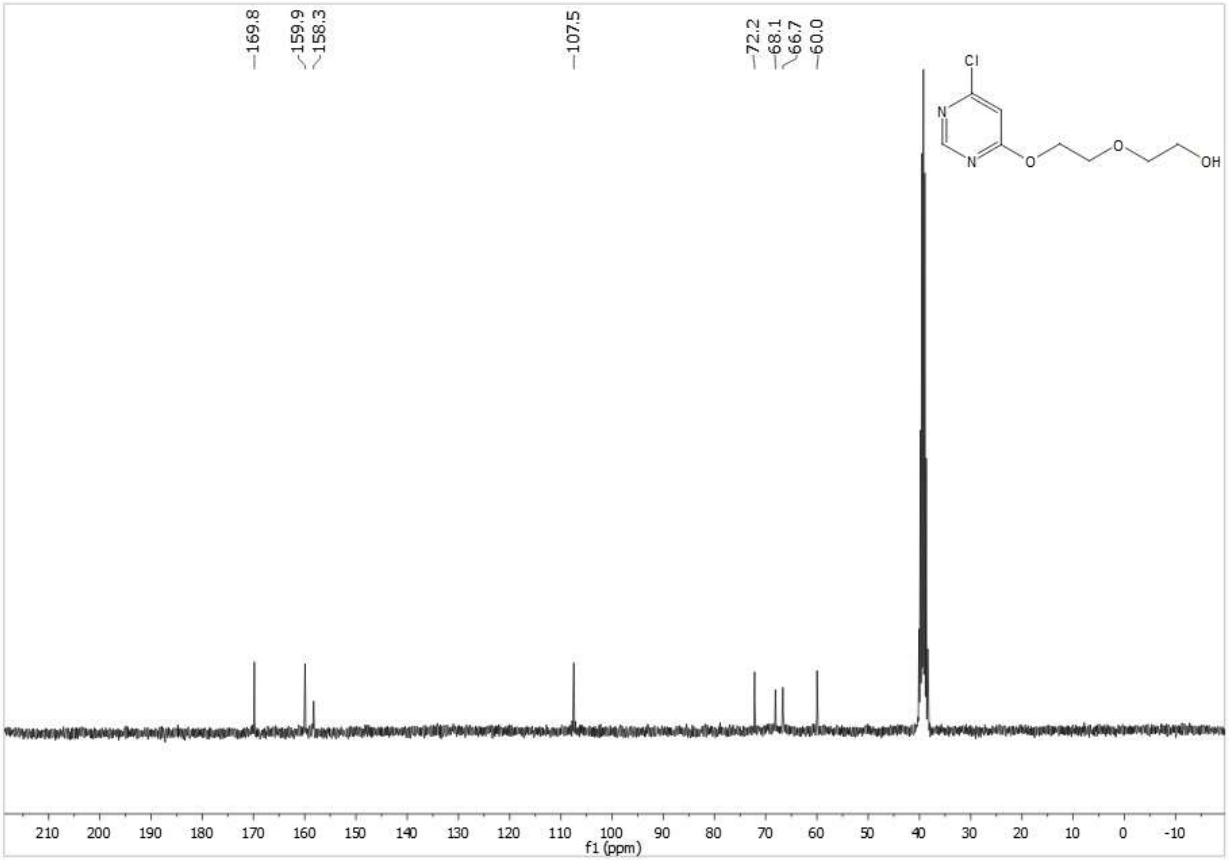

A2.5. Compound 26a

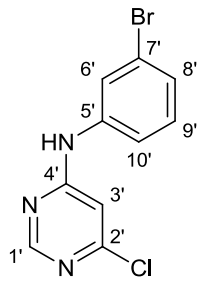

^{1}H NMR spectrum

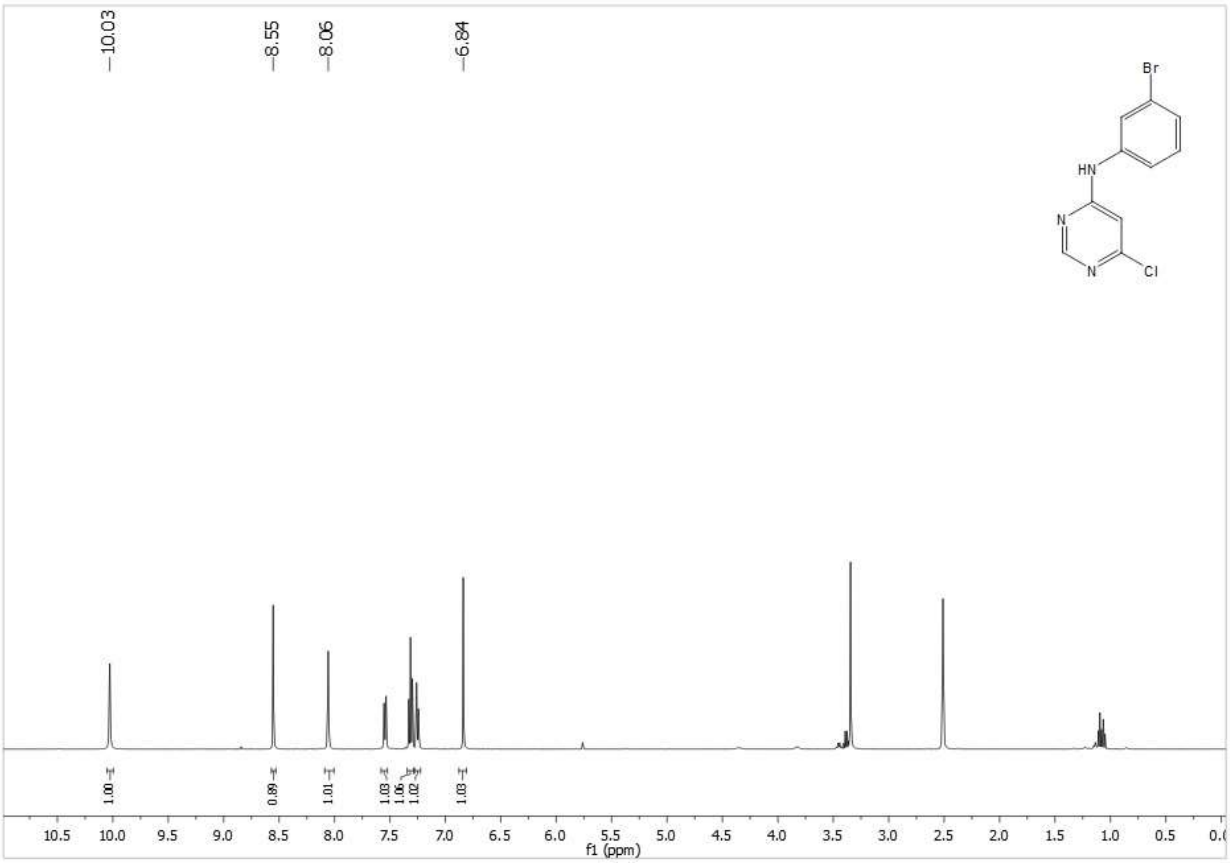

^{13}C NMR spectrum

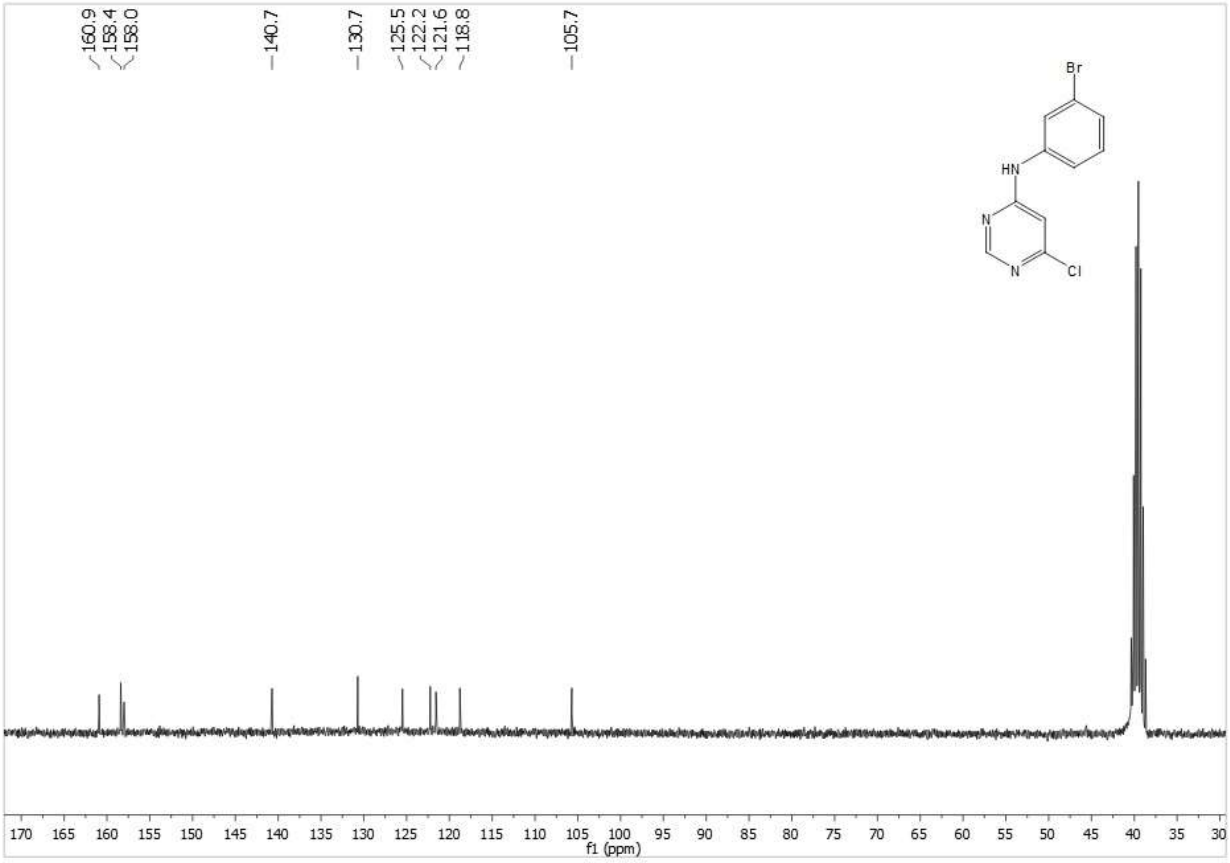

A2.6. Compound 16e

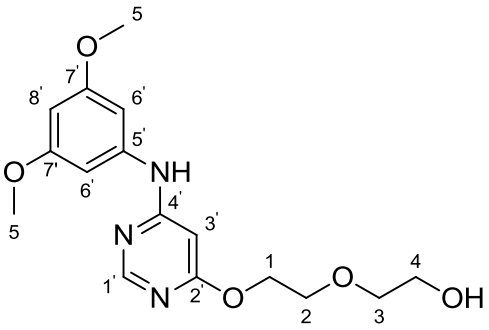

^{1}H NMR spectrum

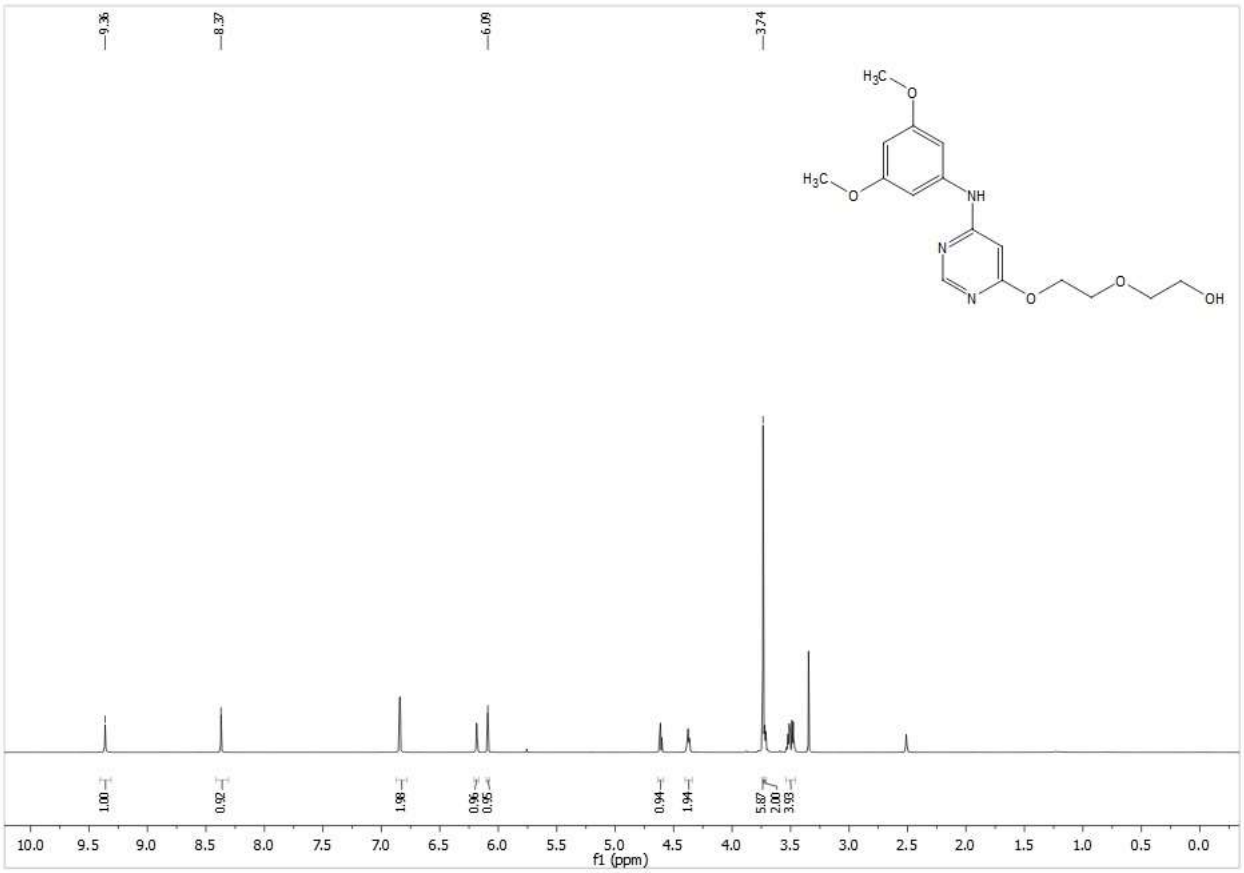

^{13}C NMR spectrum

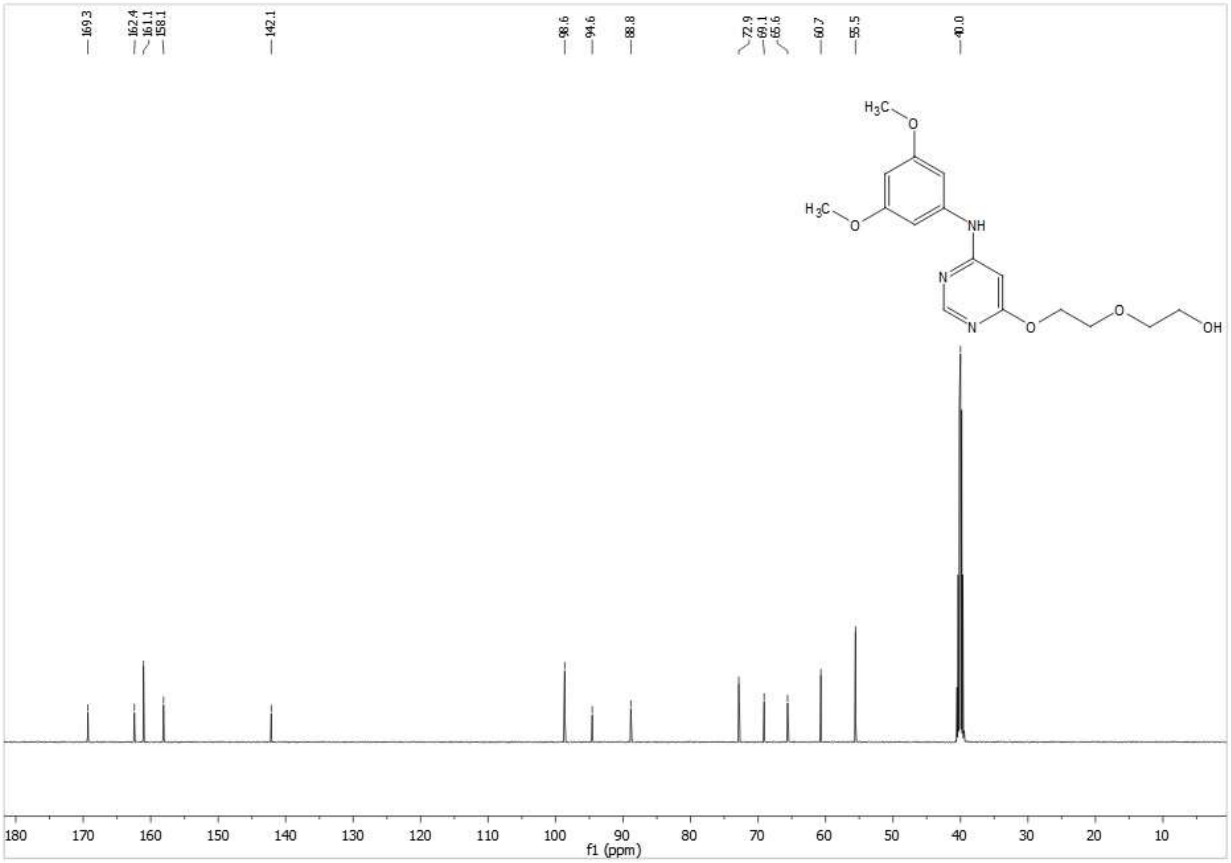

A2.7. Compound 16f

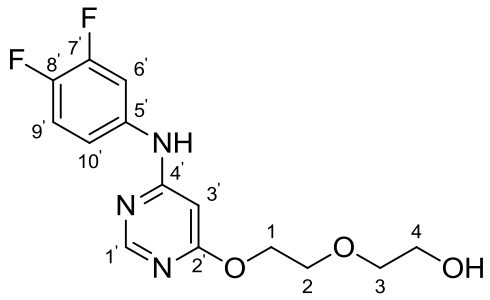

^{1}H NMR spectrum

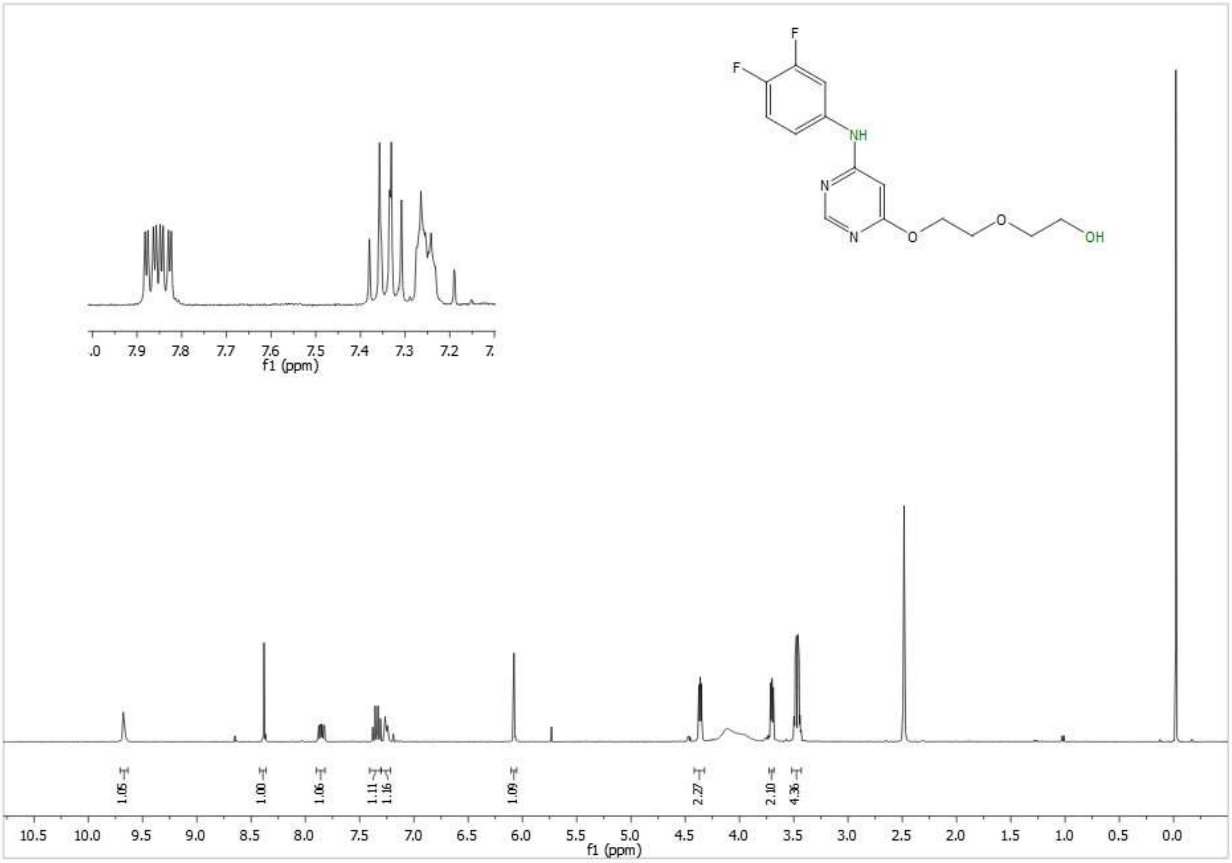

^{13}C NMR spectrum

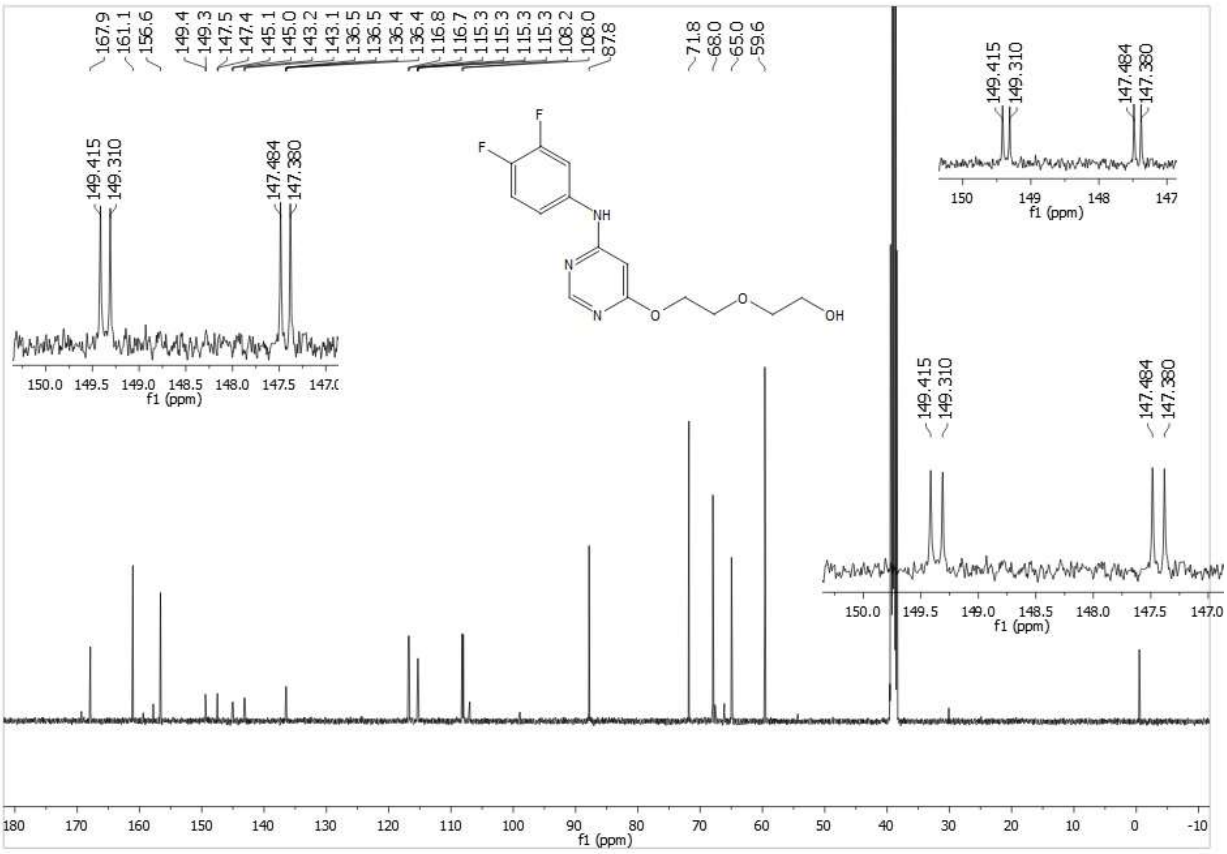

A2.8. Compound 15e

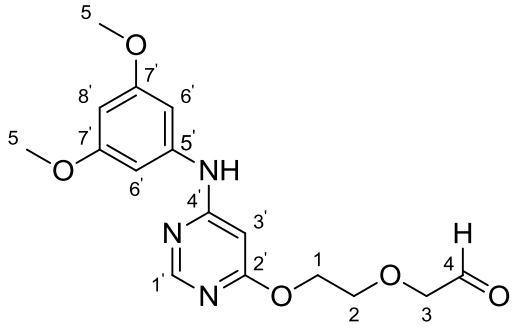

^{1}H NMR spectrum

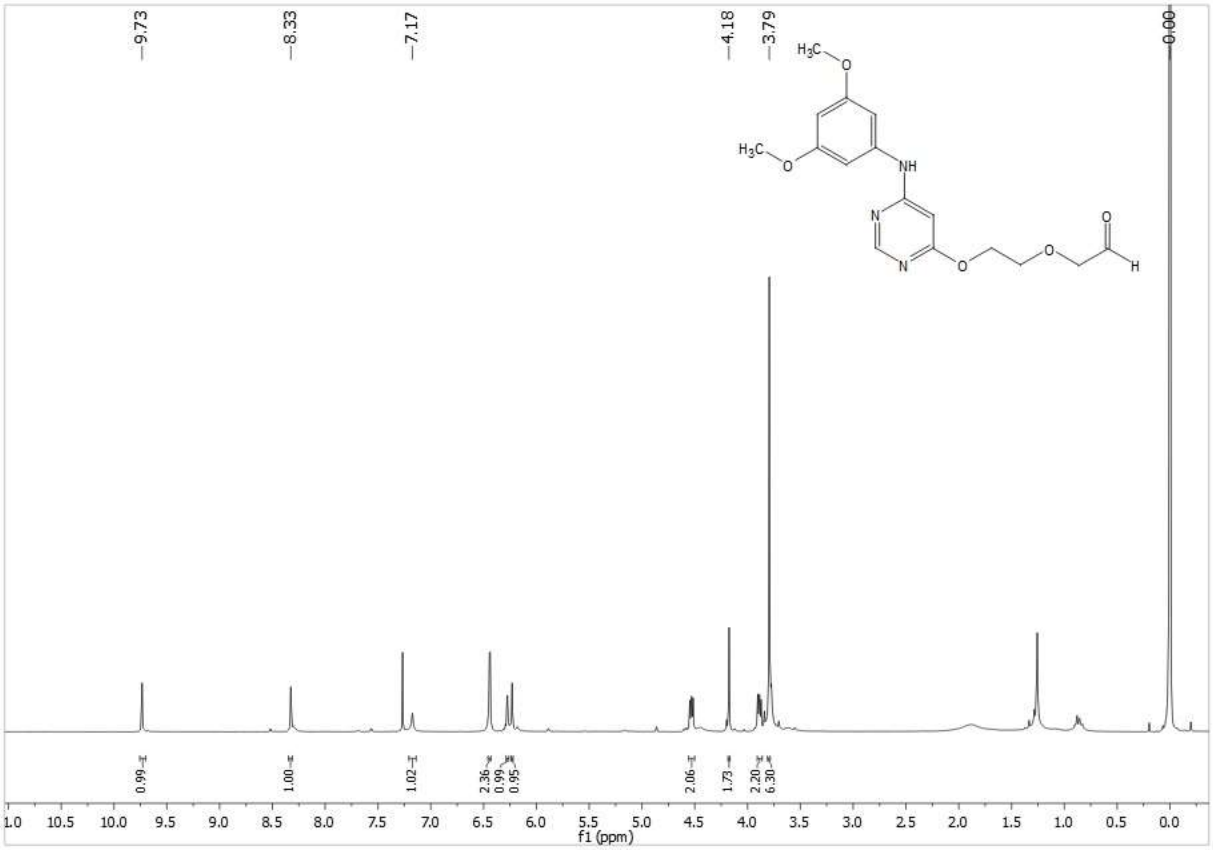

^{13}C NMR spectrum

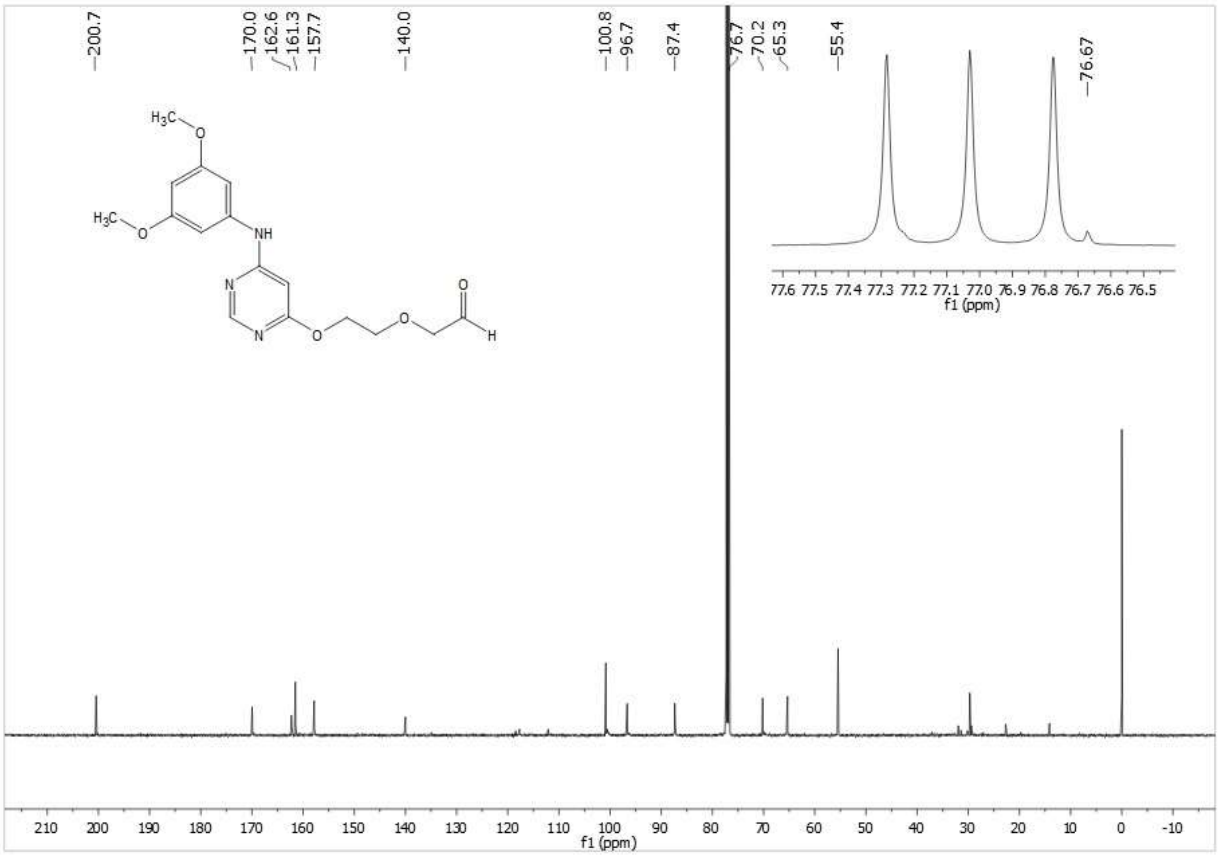

A2.9. Compound 14e

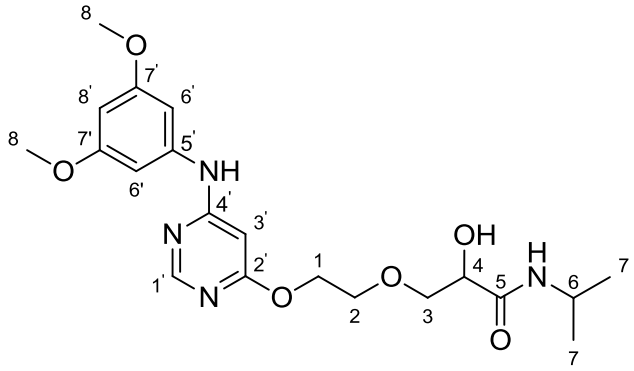

^{1}H NMR spectrum

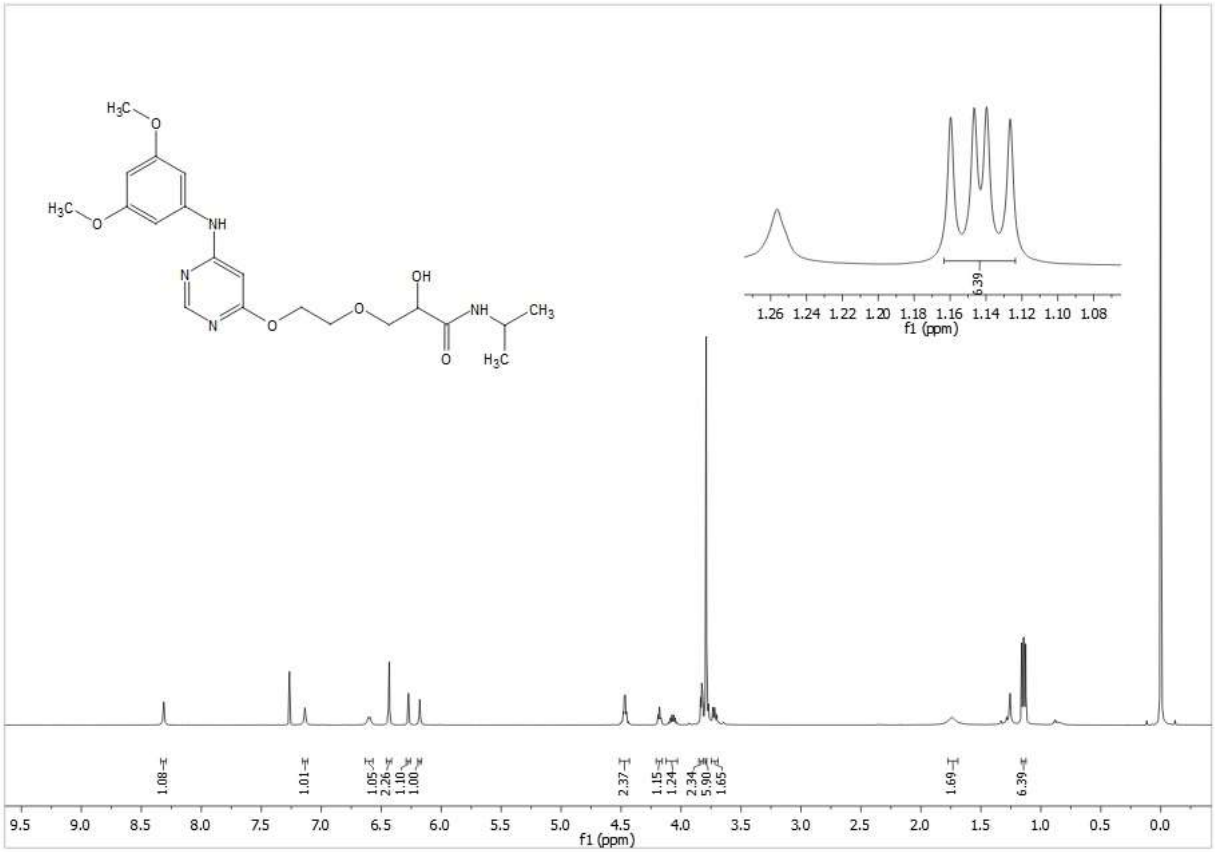

^{13}C NMR spectrum

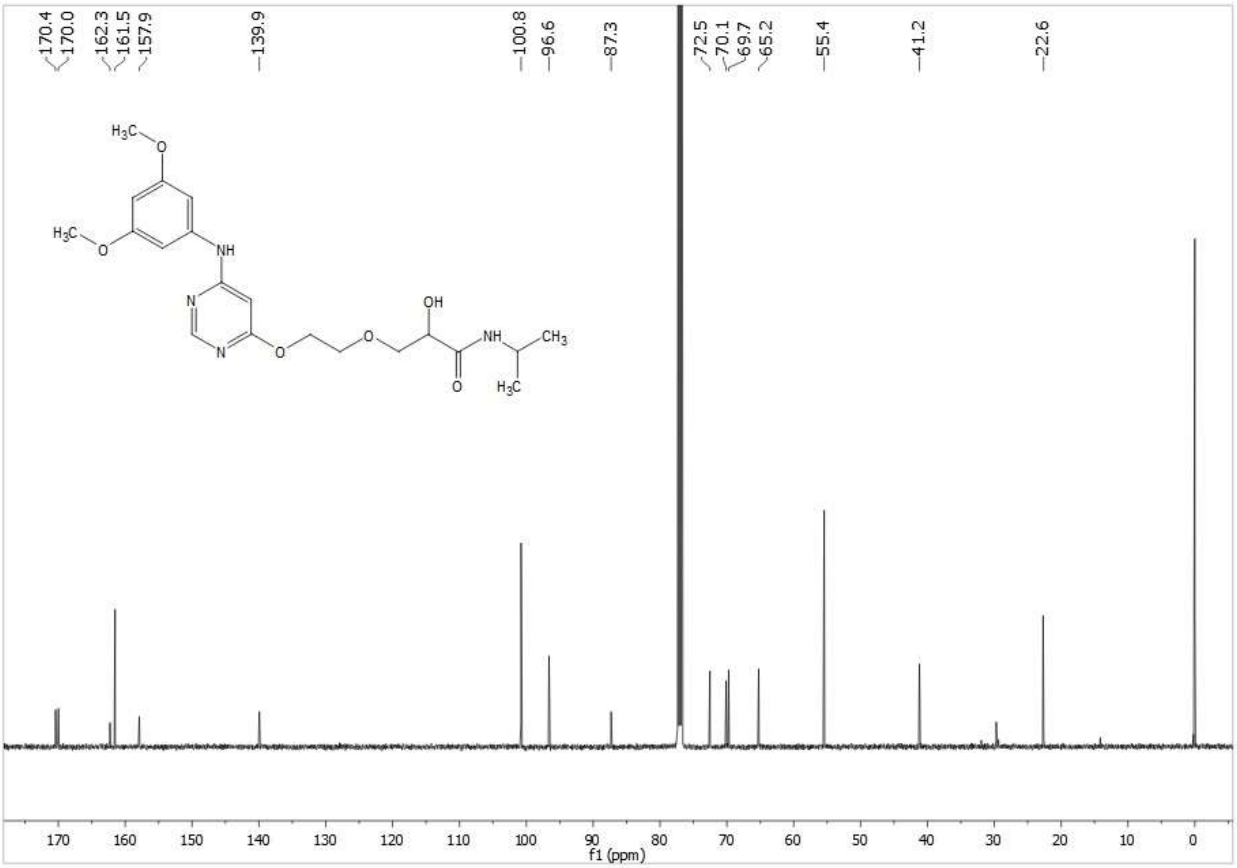

A2.10. Compound 13b

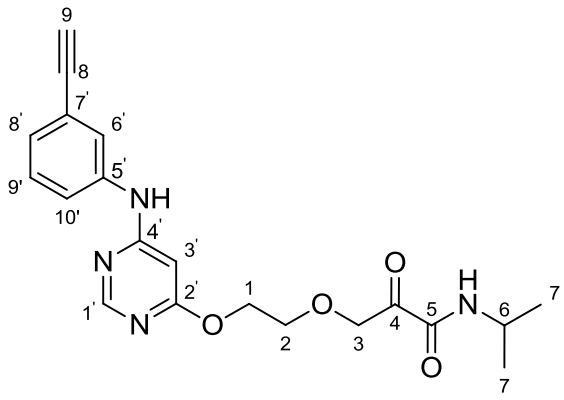

^{1}H NMR spectrum

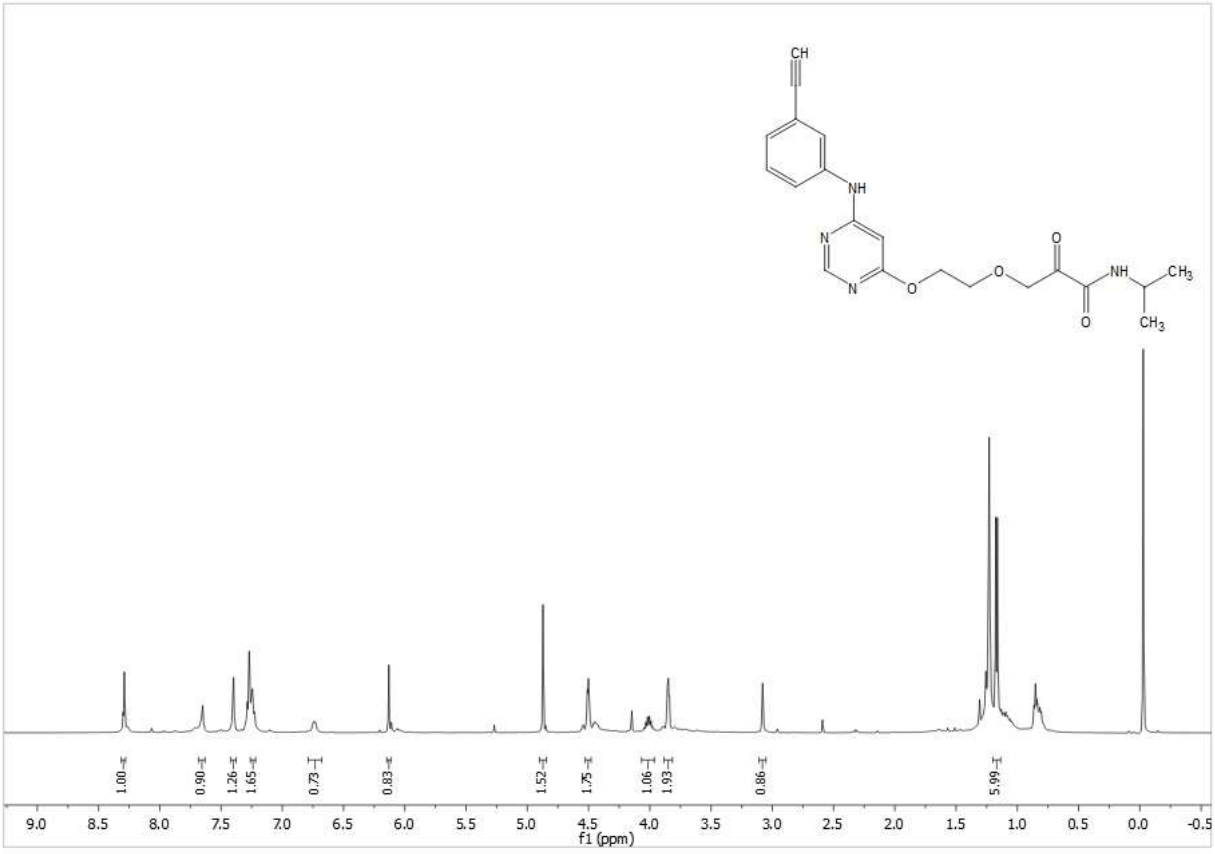

^{13}C NMR spectrum

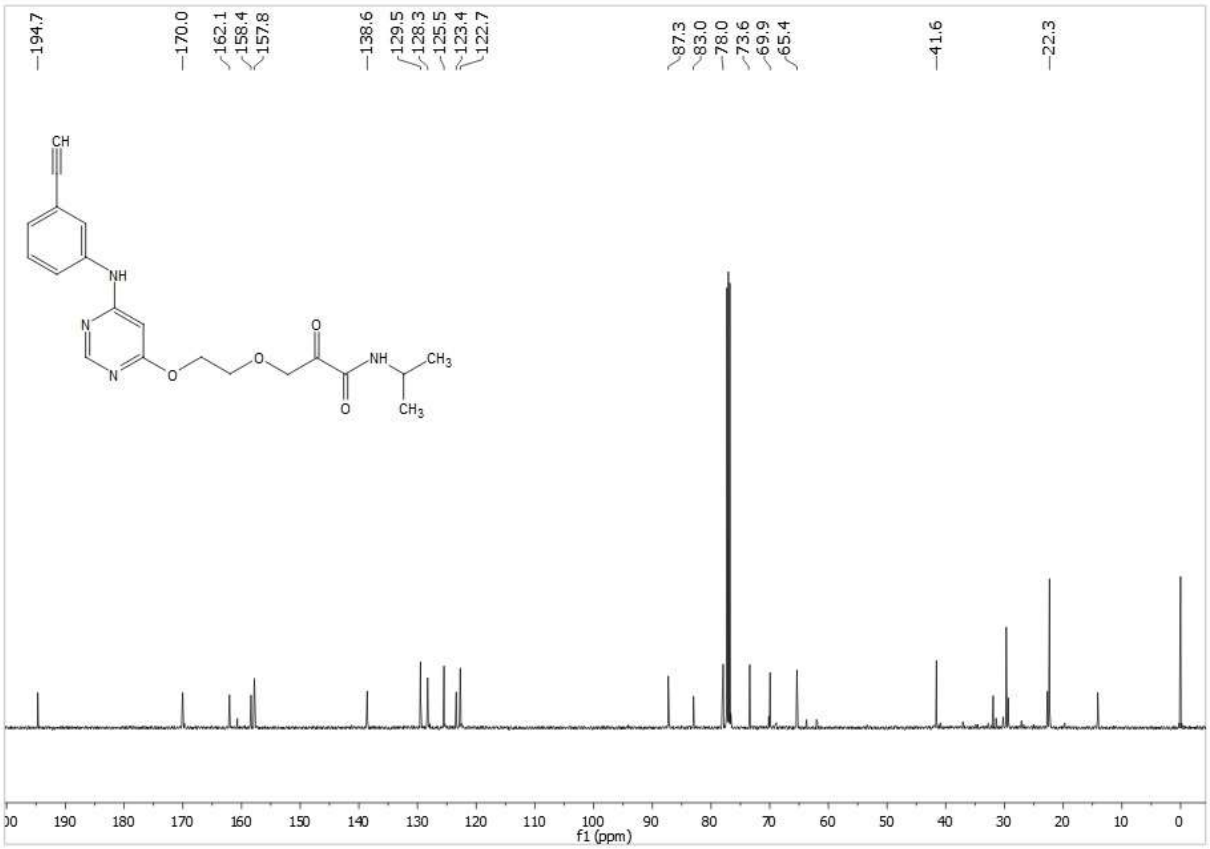

A2.11. Compound 22a

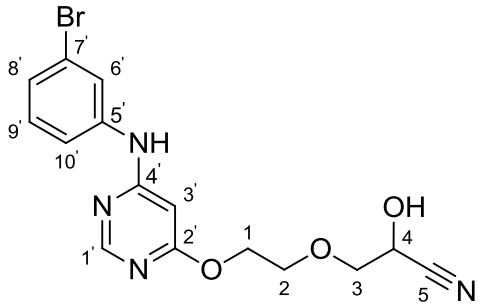

^{1}H NMR spectrum

^{13}C NMR spectrum

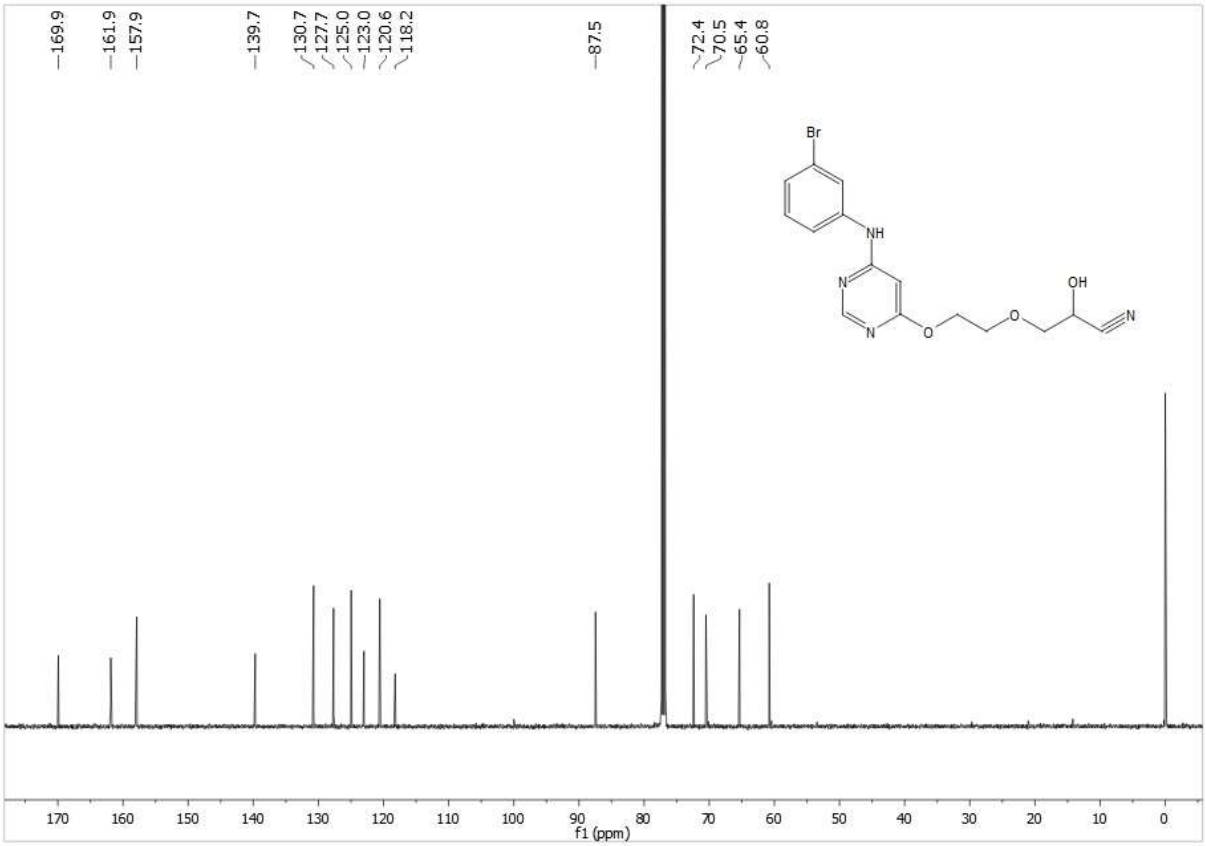

A2.12. Compound 41b

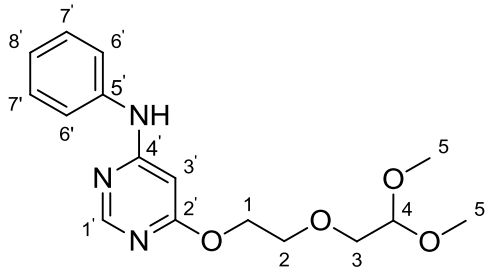

^{1}H NMR spectrum

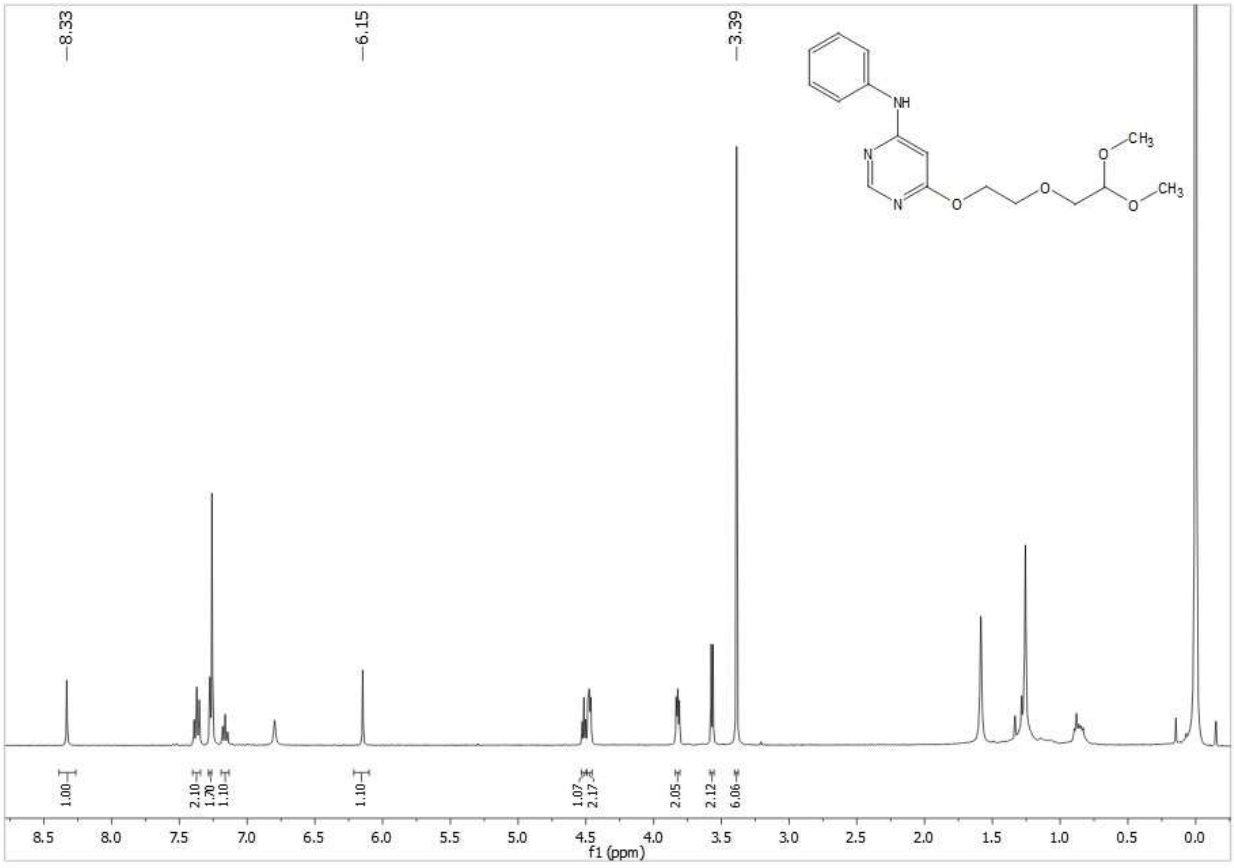

^{13}C NMR spectrum